STP 1452

Tissue

ENGINEERED MEDICAL PRODUCTS (TEMPs)

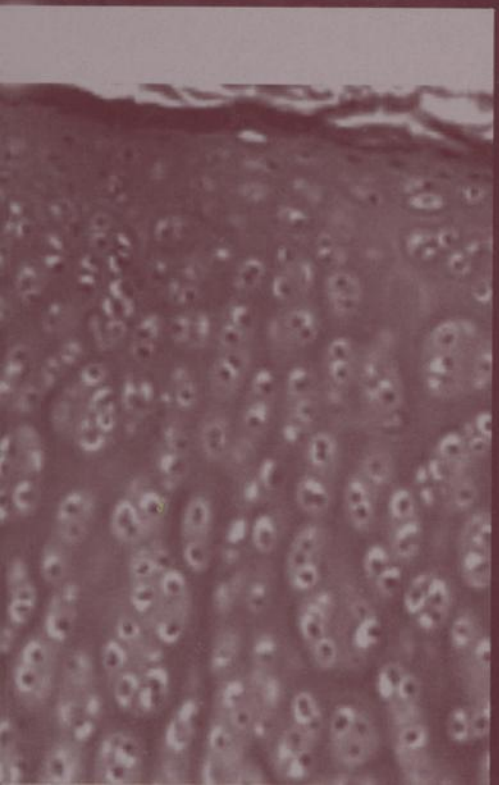

TECHNICAL EDITORS:
Eliane Schutte,
David S. Kaplan,
and Grace L. Picciolo

ASTM INTERNATIONAL
Standards Worldwide

STP 1452

Tissue Engineered Medical Products (TEMPs)

Eliane Schutte, Grace L. Picciolo, and David Kaplan, editors

ASTM Stock Number: STP1452

ASTM
100 Barr Harbor Drive
PO Box C700
West Conshohocken, PA 19428-2959

Printed in the U.S.A.

Library of Congress Cataloging-in-Publication Data

Tissue engineered medical products (TEMPs) / Eliane Schutte, Grace L. Picciolo, and David Kaplan, editors.
p. ; cm. -- (STP ; 1452)
"ASTM Stock Number: STP1452."
Papers presented at a symposium held in Miami Beach, Florida, on 4-5 November, 2002.
Includes bibliographical references and indexes.
ISBN 0-8031-3471-1 (alk. paper)
1. Tissue engineering--Standards--Congresses. 2. Medical protocols--Congresses. I. Schutte, Eliane, 1970- II. Picciolo, Grace Lee. III. Kaplan, David S., 1957- IV. ASTM special technical publication ; 1452.
[DNLM: 1. Tissue Engineering--standards--Congresses. 2. Biocompatible Materials--standards--Congresses. QT 37 T6153 2004]
R857.T55T545 2004
610'.28--dc22

2004043760

Photocopy Rights

Peer Review Policy

Each paper published in this volume was evaluated by two peer reviewers and at least one editor. The authors addressed all of the reviewers' comments to the satisfaction of both the technical editor(s) and the ASTM International Committee on Publications.

To make technical information available as quickly as possible, the peer-reviewed papers in this publication were prepared "camera-ready" as submitted by the authors.

The quality of the papers in this publication reflects not only the obvious efforts of the authors and the technical editor(s), but also the work of the peer reviewers. In keeping with long-standing publication practices, ASTM International maintains the anonymity of the peer reviewers. The ASTM International Committee on Publications acknowledges with appreciation their dedication and contribution of time and effort on behalf of ASTM International.

Printed in Saline, MI
2004

Foreword

This publication, *Tissue Engineered Medical Products (TEMPs)*, contains papers presented at the symposium of the same name held in Miami Beach, Florida, on 4-5 November, 2002. The symposium was sponsored by the ASTM International Committee F4 on Medical and Surgical Materials and Devices and its Division IV on Tissue Engineered Medical Products, in cooperation with Biomat.net, The Society for Biomaterials and The Tissue Engineering Society. The symposium co-chairpersons were Eliane Schutte, IsoTis BV, The Netherlands, Grace L. Picciolo, USFDA (Retired), Rockville, MD., and David S. Kaplan, FDA/CDRH, Rockville, MD.

Contents

What Technology Do We Have and How Is It Doing?

Paul Tomlins,[1] Paul Grant,[1] Sergey Mikhalovsky,[2] Stuart James,[2] and Lyuba Mikhalovska[2]

Measurement of Pore Size and Porosity of Tissue Scaffolds

Reference: Tomlins, P., Grant, P., Mikhalovsky, S., James, S., and Mikhalovska, L., **"Measurement of Pore Size and Porosity of Tissue Scaffolds,"** *Tissue Engineered Medical Products (TEMPs), ASTM STP 1452,* E. Schutte, G. L. Picciolo, and D. S. Kaplan, Eds., ASTM International, West Conshohocken, PA, 2004.

Abstract: Tissue engineering involves seeding the patient's cells on to a three-dimensional temporary scaffold. It is becoming increasingly obvious that cells used to seed the scaffold have very specific requirements concerning the morphology and chemistry of the surface of the scaffold and its interconnectivity. A range of techniques has been examined in relation to key measurements such as pore size and porosity. Since capillary flow porometry measures a pore solely at its most constricted point, the method is unable to provide characterisation of other aspects of the pore.
Scanning Electron Microscopy is limited to examining surface pores in 'stiff' scaffolds. Although cryo-SEM reduces the amount of ice-induced damage generated in 'soft' scaffolds upon freezing, the technique is limited to the same constraints. Images produced via scanning confocal microscopy are probably more representative of the true structure of the scaffold than that implied by cryo-SEM, although due to the diffuse nature of the image it is difficult to measure pore sizes.

Keywords: tissue engineering, tissue scaffolds, characterisation, pore size, porosity

Introduction

The cost of maintaining the increasingly aging population of the Western world where individuals are living for longer periods of time and expect a high quality of life is a serious concern to providers of health services. These factors coupled with the increased difficulty of obtaining donor organs to replace diseased or 'worn out' organs and concern over transmissible diseases such as HIV makes tissue engineering an extremely attractive proposition. The ability to repair damaged or diseased tissues

[1]Materials Centre, National Physical Laboratory, Queens Road, Teddington, Middlesex, UK TW11 0LW.
[2]School of Pharmacy and Biomolecular Science, University of Brighton, UK.

for relatively low costs using cells derived from the patient not only obviates the need to wait for donor organs to become available but also offers a cost saving because immunosuppressent drugs are not required. Typically tissue engineering involves seeding the patient's cells on to a three-dimensional temporary scaffold. The seeded cells are then cultured in a bioreactor to form a block of functional tissue that can then be implanted into the patient. In the majority of cases the tissue scaffold subsequently degrades to leave biological tissue that is similar to the native tissue that it has replaced.

Most scaffolds, with the exception of those used to repair hard tissues such as bone are manufactured from polymers. Hard tissue scaffolds tend to be produced from ceramics, bioglass, bovine bone or coral. Fabricating polymers to form a stable scaffold can be achieved in a variety of ways including melt spinning and the production of stable foams with open cells. Scaffolds manufactured by these routes are well-defined structures and are made from relatively stiff materials. However, more supple and less easily defined scaffold structures are available for use in the repair of soft tissue, ranging from a loose knit array of fibres such as collagen to hydrogels possessing a very high water content (typically >90%).

It is becoming increasingly obvious that cells used to seed the scaffold have very specific requirements concerning the morphology and chemistry of the surface of the scaffold and its interconnectivity. The latter is not only important for cellular migration but also to ensure that the supply of nutrients and removal of waste products is maintained. To optimise the conditions for cell growth requires knowledge of the pore size distribution and levels of interconnectivity.

Experimental

Figure 1, which summarises the effective range of a variety of pore characterisation techniques shows that no single technique can be used to measure the broad range of nanoscale to sub-millimetre pore sizes found in tissue scaffolds. The techniques described in Figure 1 can be used on relatively stiff materials such as metal, ceramic or polymer foams that have a structure that is not influenced by the presence of water. However, the data generated by these different measurement methods need to be treated with some caution. Figures 2 and 3 show scanning electron micrographs of a polycaprolactone (PCL) scaffold (supplied by the National Institute of Standards and Technology, USA).

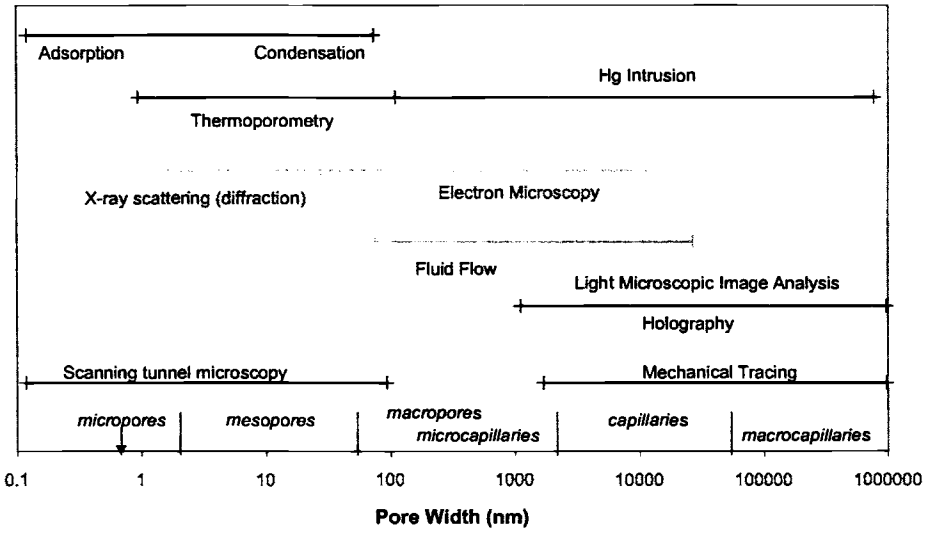

Figure 1 – *Techniques available to characterise 'stiff' porous materials* [*1*].

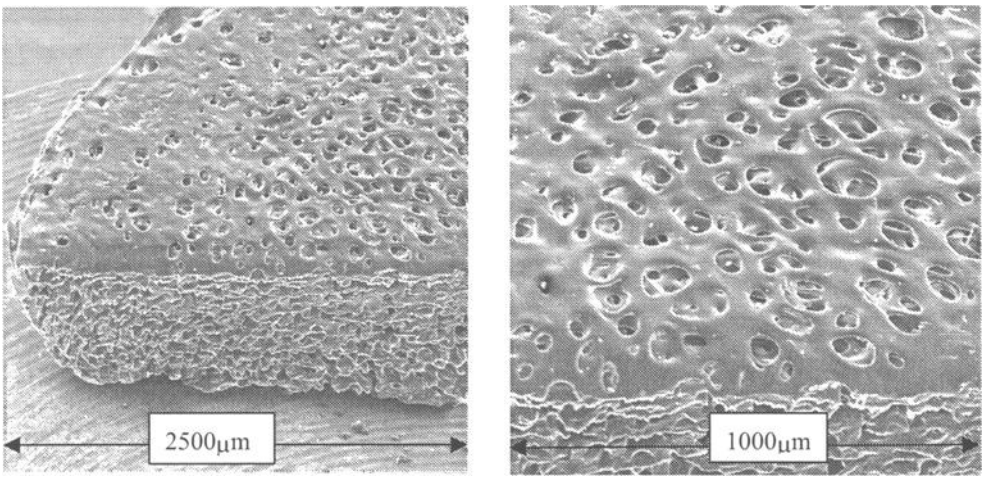

Figure 2 – *Scanning electron micrographs of PCL at approximate magnifications of x35 and x70.*

The PCL scaffold appears to have a reasonable evenly spaced distribution of pores over its surface away from the edge. At higher magnifications some of the complicated inner structure of the scaffold is revealed, as shown in Figure 3. Images of the scaffold obtained by light or scanning electron microscopy (SEM) can be analysed to give an estimate of the pore size distribution at the surface or within the scaffold itself.

Measurements of pore sizes within the scaffold are usually obtained from fracture surfaces that may contain artefacts introduced during sample preparation.

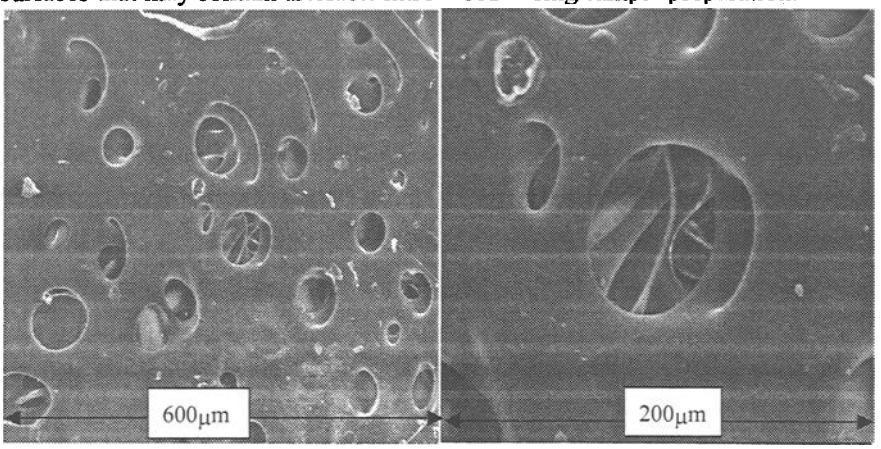

Figure 3 – *Scanning electron micrographs of PCL at approximate magnifications of x100 and x350.*

An alternative approach to SEM for assessing pore size is to use indirect methods such as porometry and porosimetry. In capillary flow porometry, the sample is placed in a sealed chamber and then brought into contact with a wetting fluid, which fills the pores in the sample. Gas is then introduced into the chamber behind the sample. When the gas pressure exceeds the force retaining the water due to capillarity, bubbles begin to form on the front face of the sample. These nascent bubbles identify the position of the largest pores. The gas pressure is continually increased and the flow of gas through the sample monitored until all pores are purged of water and the sample is considered 'dry'.

The pressure to displace liquid at a location in the pore is given by the Washburn equation [*2*]

$$D = (4\gamma \cos\theta)/p \tag{1}$$

where

D = the diameter of a pore (assuming it to be cylindrical)
γ = the surface tension of the wetting liquid on the scaffold material
θ = the contact angle of the wetting liquid on the scaffold material
p = the differential gas pressure across the sample.

The pore size distribution is calculated via the following expressions:

$$F = 100\left(\frac{Wf}{Df}\right) \tag{2}$$

$$F_i = F_c - F_p \tag{3}$$

$$P_D = \frac{F_i}{D_p - D_{c\,i}} \tag{4}$$

where

F = filter flow (%)
F_i = incremental filter flow (%)
F_p = filter flow of previous pore
F_c = filter flow of current pore
W_f = wet flow (litres/min)
D_f = dry Flow (litres/min)
D_p = pore diameter of previous pore
D_p = pore diameter of current pore
P_D = pore distribution.

Figure 4 shows the distribution of pores calculated for PCL 30.

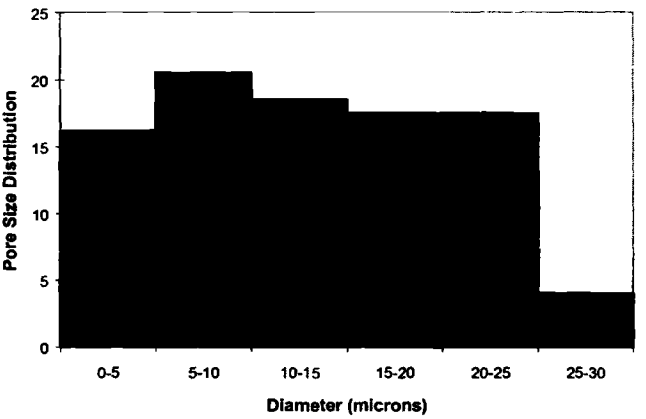

Figure 4 – *Pore size distribution for PCL 30 derived from capillary porometry data.*

Table 1 shows a comparison of pore measurements derived from different types of microscopy and capillary flow porometry. As expected there is some agreement for data derived from microscopic images, but there is a significant disparity between microscopy and capillary porometry. This is not surprising since flow porometry measures the diameter of the pore at its narrowest section [*3*].

Table 1 – *A comparison of pore dimensions as measured by flow porometry and microscopy.*

Material	Technique	Largest pore diameter observed (μm)	Mean pore diameter (μm)
PCL	Light Microscopy	190	130*
	SEM	150	100*
	Capillary Flow Porometry	26	13

* Values are approximate as very small pores are not seen

While the data generated by porometry techniques can be used to assess the size and frequency of pores connecting to the opposite side, these methods remain insensitive to blind-end pores and enclosed cells. Techniques that involve filling the porous structure with a liquid, e.g., mercury porosimetry can help to overcome these limitations by measuring the volume of accessible pores. This includes through pores and blind-end ones. Neither technique can determine the percentage volume or size distribution of enclosed voids.

Figure 5a shows a micrograph of a collagen matrix. This specimen was prepared by sputter coating of the material with gold. The image shows a complex structure, which is not easily interpreted in terms of a 'pore' size distribution or a degree of interconnectivity. The sample used to generate the image shown in Figure 5b was frozen in slush nitrogen. The use of semi-solid nitrogen produces faster cooling than liquid nitrogen producing a more delicate, detailed structure. However these improvements in detail, which are significant in providing additional scaffold structure visualization do not help with solving the problem of how to describe the structure in terms of its porosity.

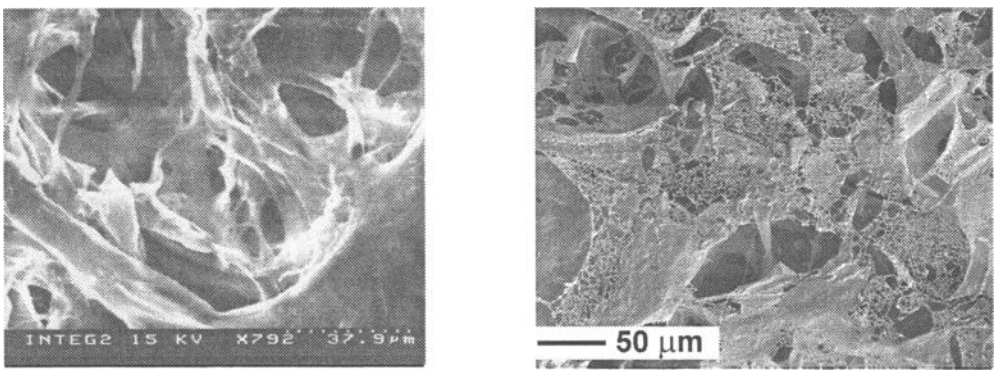

Figure 5 – *A comparison of the structure of a loose collagen matrix a) sputtered with gold and b) frozen in slush nitrogen.*

It has already been stated that the techniques shown in Figure 1 can be used to investigate 'stiff' materials, such as metallic and ceramic foams. Some polymer foams can also be examined by these techniques providing that: they are resilient enough to withstand the intrusion of mercury or a gas pressure or have sufficient contrast or be

amenable to electron microscopical preparation. 'Stiff' scaffold materials will be used to replace hard tissues. However much of the current research into tissue engineering is concerned with developing scaffolds for soft tissue replacement. These scaffolds range from 'soft' air filled foams to hydrogels. These classes of material represent significant measurement challenges.

In terms of the techniques shown in Figure 1, the point at which errors due to deformation of 'soft' air filled foams becomes significant is unclear when using porosimetry or porometry techniques. The preparation of high water content gels for microscopical investigation by freeze-drying tends to alter significantly what is usually a complex and intricate structure (Although it may be possible to overcome this limitation using environmental SEM). Confocal light microscopy has been used to study soft materials such as the collagen matrix shown in Figure 5. The images generated by this technique do not show the clear, sharp boundaries present in, say, the light microscopy sections, but are probably a better representation of the true structure of the gel, as implied by cryo-SEM. Whilst image analysis can be used to improve the sharpness of the images and then generate a measure of tortuosity it is by no means clear what the value of such information will be. Light microscopy is limited in its ability to record sub-micron detail and in its ability to penetrate deep within a scaffold. The resultant data will therefore reflect the surface structure above a cut-off size scale.

Techniques that measure the movement of probes through soft polymeric foam or hydrogel scaffolds can potentially generate more meaningful information than methods that can distort or disrupt the native scaffold. The identity of the probe may range from a small molecule including dissolved gases to proteins. Figure 6 shows the time dependence of simple diffusion of a small molecule (paracetamol) compared with a protein (albumin) through a collagen matrix. This approach to measurement of the permeability of scaffolds to materials can be expanded to include diffusion of charged molecules to explore the surface charge within the scaffold. Diffusion can be also be accelerated by applying a potential difference across the gel (electrophoresis).

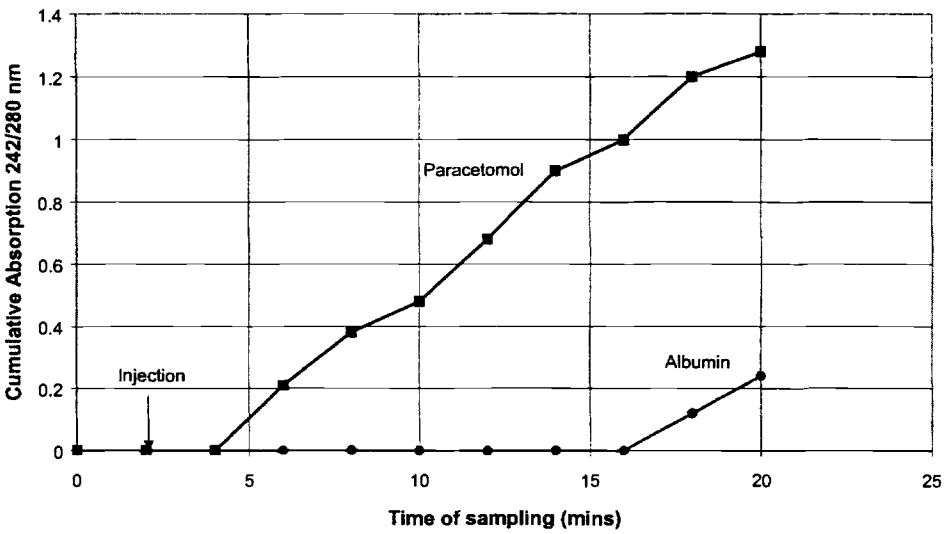

Figure 6 – *Diffusion of paracetomol and albumin through collagen-GAG matrix.*

The properties of highly hydrated scaffolds can also be investigated by monitoring the behaviour of the water contained within them. Techniques such as differential scanning calorimetry can be used to measure the percentage of bound water in porous materials, water located in very narrow pores will freeze or boil off at temperatures below or in excess of those required to induce the same effect in 'free' water in large pores. Again the value and usefulness of this information needs to be discussed in order to appreciate its value and limitations.

Conclusions

- Since capillary flow porometry measures a pore solely at its most constricted point the method is unable to provide characterisation of other aspects of the pore.
- Scanning electron microscopy (SEM) is a suitable technique for examining pores located in the surface of 'stiff' scaffolds such as polymer foams. However there are limitations to using the technique: samples need to be plasma sprayed prior to being studied and the data obtained is only applicable to an exposed surface.
- SEM of high water content materials is prone to generating artifacts. Freezing in liquid nitrogen tends to generate ice crystals that damage the delicate structures typically found in 'soft' scaffolds. Faster freezing using slush nitrogen (cryo-SEM) substantially reduces the amount of ice-induced damage. However the technique is subject to the same constraints as SEM of 'hard' scaffolds.
- Scanning confocal microscopy of highly hydrated samples does not show clear, sharp boundaries that are typically seen in microtomed, sectioned scaffolds investigated by light microscopy. The diffuse structure seen by the confocal microscope is probably a more representative of the true structure of the scaffold

than implied by cryo-SEM. Due to the diffuse nature of the image it is difficult to measure pore sizes.

- Differential scanning calorimetry appears to be a useful technique for detecting bound water in scaffolds and could be of value in identifying nanopores in scaffolds. However further work needs to be done in this area to establish its usefulness, i.e., on the interpretation of the data.

References

[1] Meyer, K., Lorenz, P., Bohl-Kuhn, B., and Klobes, P., "Porous Solids and their Characterisation," *Cryst. Res. Tech.*, 29 (7), pp. 903-930, 1994

[2] Jena, A., Sanders, H., Miller, J., and Wimberly, R., "*Comparison of Mercury Porosimetry and Flow Porometry for the Testing of Battery Separator Materials,*" Amerace Microporous Products Technical Article

[3] Stillwell, C.R., "*Recent Advances in Porometry and Porosimetry: The Microflow Porometer and the Aquapore Porosimeter,*" PMI Technical Article, 1999

Daniel N. Galbraith,[1] Terry Collins,[1] John Black,[1] Barbara McManus,[1] Donna McMutrie,[1] and Archie Lovatt[1]

Development and Validation of a Detection Method for a Broad Range of Human Papillomavirus Types

Reference: Galbraith, D. N., Collins, T., Black, J., McManus, B., McMutrie, D., and Lovatt, A., **"Development and Validation of a Detection Method for a Broad Range of Human Papillomavirus Types,"** *Tissue Engineered Medical Products (Temps), ASTM STP 1452,* E. Schutte, G.L. Picciolo, and D.S. Kaplan, Eds., ASTM International, West Conshohocken, PA, 2004.

Abstract: Human papillomaviruses (HPVs) are viruses that are almost unique in their tropism for human skin cells; they also have the potential to cause severe pathology. These viruses present a significant risk to contaminate tissue engineered skin replacement products that use human-derived skin cells as part of their manufacture. Eight pairs of primers and appropriate DNA oligonucleotide probes were designed from a relatively conserved region of the L1 open reading frame of HPV. TaqMan® PCR using these primer/probe sets was found to be capable of detecting HPV-DNA in a background of cellular material likely to be present in skin replacement products. The assay is more sensitive than any currently described in the scientific literature and can be completed in a single working day making it suitable for testing the short shelf life that many of these products have.

Keywords: Safety, Artificial skin, Human papillomavirus, PCR

Introduction

With the introduction of tissue engineered products that are designed to treat or replace human skin, the use of human skin-derived cells, such as those from the epithelium or dermis, has dramatically increased [1]. The skin products that are available today are varied in nature and production techniques, and a number are in widespread clinical trials or are already marketed products both in the United States and Europe. The prospects for these treatments will expand as there is a large patient population who require these types of treatment. The microbiological safety of these products is a major consideration not only for the manufacturers but also for the regulatory agencies approving the trials or the licensed products. The characteristics of these engineered skin products are unique in biotechnology, being made up of unusual living cell types and a biologically derived scaffolding material. In some

[1] Director of Technical Services and Regulatory Affairs, Project Manager, Laboratory Manager, Study Director, Study Director and Director of Development respectively. Q-One Biotech Ltd., Todd Campus, West of Scotland Science Park, Glasgow G20 0XA, United Kingdom.

cases these materials are regulated as a device or a medicinal product (biologic). The microbiological and virologic safety concerns still require to be evaluated in some cases.

The source of the skin cells used for many of these products can be autologous, however, some cells are allogenic. In either case the cells are harvested and may be cultured for a number of days or weeks before being finally used as a product or laid down in a cell bank for future production. The harvested skin cells present microbiological concerns regarding their safety, these cells can harbour viruses that are unique to the skin cells and are not present in other cell types. A virus of particular concern in the cells of the skin is *Human Papillomavirus* (HPV). There are approximately 70 types of HPV described in the literature and a number have been associated with benign and malignant cancers [2]. A number of types of HPV, including 5, 6, 8, 11, 16 and 18 as well as others, have been linked to malignancies of the skin [3,4]. Papillomaviruses have a specific tropism for squamous epithelial cells and replication of the virus is linked to the differentiation of the cells [5]. The basal cells of the epithelium are the target cells for HPV infection. Late gene expression and formation of the virus particle occurs only in terminally differentiating squamous epithelial cells. Many second-generation engineered skin products make use of both stem cells and epithelial cells in the products, and therefore have the potential to harbour viruses and may support the production of virions.

HPV is a risk in skin derived cells and its detection is hampered by a number of factors. As the virus will only grow in very specific cell types, there is no useful in vitro cell culture system that can be applied to detect the virus. In addition, the virus when in basal cells can be present in very low copy numbers, which makes detection difficult. This, coupled with the numerous types of virus, complicates the design of an effective assay. Previous studies, describing detection systems for HPV, have the disadvantages of using degenerate primer sets or nested Polymerase Chain Reaction (PCR) [3,4]. With many skin replacement products there is a very limited shelf life, consequently any assay applied to detect viruses will be required to be completed in a timely manner to allow for successful delivery of the product. In the present study we have designed and evaluated a multiple primer PCR technique using the TaqMan®[2] technology [6].

Methods

Primer Design

The purpose of this study was to develop a general assay to detect the most frequently observed types of HPV that may pose a risk of infection to tissue engineered products. The conserved region of the L1 Open Reading Frame (ORF) was chosen to design primers for the detection of the virus. Eight pairs of primers

[2] AmpliTaq Gold, TaqMan and AmpErase are registered trademarks of Roche Molecular Systems, Inc., CA, USA.

were designed based on HPV 6, 11, 16, 18, 31, 33, 52 and 58 to give a broad spectrum of detection of HPV sequences.

The HPV type 6 primer/probe set used was designed to detect the following Genbank accessions: #NC_001668, #NC_000904, #AF092932, #L41216, #NC_001355, and #X00203. The HPV type 11 primer/probe set was designed to detect the following Genbank accessions: #NC_001525, and #M14119. The HPV type 16 primer/probe set was designed to detect the following Genbank accessions: #NC_001526, #AF125673, #AF001599, #U89348 and #K02178. The HPV type 18 primer/probe set was designed to detect the following Genbank accessions: #NC_001357, #M20325, #U89349, #X05015 and #NC_001590. The HPV type 31 primer/probe set was designed to detect the following Genbank accessions: #NC_001527 and #J04353. The HPV type 33 primer/probe set was designed to detect the following Genbank accessions: #NC_001528 and #M12732. The HPV type 52 primer/probe set was designed to detect the following Genbank accessions: #NC_001592 and #X74481. The HPV type 58 primer/probe set was designed to detect the following Genbank accessions: #NC_001443 and #D90400.

PCR Reaction Conditions

Closed optical capped PCR reactions are analysed and discarded, therefore, chances of contamination by PCR carryover product is greatly reduced. Amplification is carried out in the presence of dUTP instead of dTTP and AmpErase® Uracil N'-glycosylase (UNG) is used. AmpErase® UNG acts on single and double stranded dU-containing DNA and prevents re-amplification of any PCR carryover products [7].

The sensitivity of PCR assays is dependent on extraction procedures and the absence of substances in the test material, which interfere with the PCR reaction and the release of nucleic acids during sample processing. Therefore, extraction and amplification of nucleic acid from a test article are assessed. To ensure that DNA can be extracted and amplified from each test article, the test material is spiked with an appropriate internal positive control DNA prior to extraction. The percentage recovery of this internal control DNA is assessed by quantitative polymerase chain reaction (Q-PCR), and controls for DNA recovery within each individual test sample DNA extraction.

In all PCR master mixes, TaqMan® exogenous internal positive control (IPC) reagents are included. The IPC reagents are included in all reactions to establish that negative PCR results are truly negative amplifications and are not due to PCR inhibition from the test article or failed amplification.

The PCR reactions are carried out in separate single wells of 96-well or 384-well reaction plates. TaqMan® Universal PCR master mix (containing TaqMan® buffer A, Mg^{2+}, dNTPs, AmpErase® UNG, AmpliTaq Gold® DNA polymerase, target specific primers and fluorescent probe) is placed into each reaction. Each HPV primer set was used separately for each test. DNA equivalent to approximately 10^5 from each test material is added to each reaction mix. Each test material is tested in triplicate reactions. The reaction plate is placed into the ABI 7900HT instrument where

AmpErase® incubation, AmpliTaq® activation and amplification reactions are performed.

The AmpErase® reaction is performed at 50°C for 2 minutes followed by an AmpliTaq Gold® activation step at 95°C for 10 minutes. The PCR reaction conditions are as follows: 40 cycles consisting of denaturation at 95°C for 15 seconds and annealing/extension at 60°C for 1 minute.

C_T, or threshold cycle, is calculated in real time and represents the PCR cycle at which an increase in reporter fluorescence above the baseline signal can first be detected. After cycling is complete, data is analysed in real time and the C_T values of each replicate observed and recorded. The standard deviations and confidence intervals of C_T values of the replicates are also recorded to detect similarities and significant differences between groups of replicates.

Assay Specificity - Specificity is the ability to assess unequivocally the analyte, in this case HPV, in the presence of components that may be expected to be present. Typically these might include other viruses, bacteria, impurities, degradants, matrix, etc. The assay must be shown to discriminate between negative and positive samples. In order to demonstrate this ability, a range of negative samples of similar origin were screened. To demonstrate the assay's ability to detect target sequences a range of positive target control samples were tested.

D*etection Limit (DL)* -Q-PCR assay DL was determined as the lowest amount of genome equivalents that produce amplification signals in 100% of the replicated reactions with two operators. Assay DL was determined initially over eight replicates. The coefficient of variation (CV) at the limit of detection was determined for operators to assess intra-assay precision. The combined data of operators for each target was used to determine intermediate precision of the assay at the DL. The assay positive reactions were used to generate a standard curve and measure linearity.

Assay Repeatability - Two operators assessed repeatability and accuracy of the Q-PCR assay over 24 replicates at, above and below the previously determined DL. The percentage of positive target sequences present at each level was assessed. The combined data of operators was used to determine variability within the values generated at the DL.

Test Materials Submitted for Analysis -A number of cell banks and other biological samples used in the production of human biologicals were submitted by manufacturers for analysis by HPV PCR.

Results

The assay could detect HPV in a background of typical cellular materials that may be found in tissue engineered products. With regard to specificity, no amplification signals were detected in the cellular genomic DNA tested. The DNA polymerase

(AmpliTaq Gold®) used in the amplification stage of the PCR reaction is likely to have aided in yielding the specific results with no observable amplification from non-HPV targets. DNA extracted from HeLa (Human cervical carcinoma cell line, known to be positive for HPV sequences) cells were tested and shown to be positive. Amplification of the exogenous positive controls were demonstrated in each PCR reaction indicating that all negative results generated were true and not due to PCR failure. Limit of detection, linearity and repeatability were all determined for the assay and found to be adequate for the purpose of the test. The combined data of each operator was used to define the limit of detection of each target. HPV 6: DL defined as 10^4genome equivalent (g.e.) per reaction, HPV 11, 16, 18, 31, 33, 52 and 58: DL defined as 10^3g.e. per 10^5 cells. The assay was linear over a range from the detection limit to 6 $\log_{10}$ increments for each assay. The standard curves generated by both operators with each assay target demonstrated a linear correlation coefficient (r^2) that suggests a significant positive correlation and implies a direct relationship between the C_T value generated and the number of genome equivalents present (Table 1).

Table 1 - *Assay Linearity Results*

	Operator 1			Operator 2		
	R^2	Slope	Y-Intercept	R^2	Slope	Y-Intercept
HPV 6	0.965	-3.53	52.02	0.995	-3.84	47.03
HPV 11	0.980	-3.23	42.92	0.986	-3.49	45.04
HPV 16	0.986	-3.06	42.59	0.976	-3.26	44.47
HPV 18	0.954	-3.37	43.93	0.991	-3.30	44.55
HPV 31	0.967	-3.17	41.48	0.987	-3.25	42.79
HPV 33	0.981	-3.29	41.67	0.978	-3.35	43.38
HPV 52	0.971	-3.27	42.00	0.967	-3.41	45.03
HPV 58	0.989	-3.63	47.15	0.996	-3.53	44.46

The repeatability of the assay was assessed; the degree of spread within the values generated was low, as determined by the mean ± S.D (Standard Deviation), however the overall DL did vary between operators. Differences in assay DL for each operator are not uncommon and reflect the variance that can be encountered within the assay on a day to day basis when using different reagents, positive control dilutions and operators. In this instance the data set generating the highest DL between the operators was chosen to define the DL of the assay.

HPV Findings of Biological Samples used in human therapies have been submitted for analysis (Table 2). There have been 14 samples of human origin submitted for analysis for HPV sequences (the lists of types of samples are made in table below). In none of the samples were there any detectable HPV sequences using the assay as described.

Table 2 – *Sample types analysed by HPV-PCR*

Sample Types examined	Number
Human Foreskin cells	4
Human Keratinocytes	5
Human Epithelial cells	2
Human Dermal cells	2

Discussion

In the present study we have developed a PCR assay that can detect a wide range of HPV types. Multiple sets of primers and a TaqMan® amplification platform were used, which is in contrast to that previously described [3, 4, 7, 8]. These previous studies also used the L1 ORF as the target for detection but used degenerate primers as a means of broadening the specificity of the assay. These studies used conventional PCR amplification, gel electrophoresis and DNA hybridisation for detection. The main disadvantage of using degenerate primers was the reduced sensitivity and specificity of these assays. In these studies the sensitivity of the assays was given as 10-100 virus copies per cell [3]. In our results we express the sensitivity as 10^3 -10^4 viral copies per reaction. Given that every reaction normally includes DNA from approximately 10^5 cells, it can be seen that our method is considerably more sensitive than those already published. Perhaps of more concern is the lack of specificity seen with previous studies. There are instances where amplification products have been reported that are significantly larger in nucleotide length than would be predicted products. When these were investigated they were shown to be repetitive sequences of cellular origin and not HPV derived. In addition, sequences from a control DNA (lambda phage) were also shown to yield a positive signal. The consequences of these erroneous results in a clinical setting would be of concern. In addition, the manufacturer of the tissue-engineered products showing these non-specific reactives would suffer economic loss since the product would have to be discarded. In the present method the high specificity of the "hotstart" Taq polymerase coupled with the primer probe arrangement allowed by the TaqMan® technology resulted in an assay that was very specific to the target sequence (no non-specific reactives were observed).

In a number of published clinical studies, a correlation has been made between skin samples positive for HPV and various skin tumours. Interestingly, in these studies a number of apparently normal skin tissues yielded positive results from the described assays. The suggestion has been made that some skin cells may act as a reservoir for virus. This may also indicate there is the possibility to detect these viruses, at least before there is clinical evidence of infection in the samples. Increased sensitivity of the assay detection may improve detection rates of these low level viral sequences and thus improve safety. All of the samples analysed in this study were found to be negative for the presence of virus. This may be due to the cell type assayed as many of the cells used for the manufacture of tissue engineered skin products are from human neonatal foreskins. These neonatal samples have a very low risk of infection with

human papilloma virus. The literature indicates that infection with HPV is age dependent and virus is frequently absent from neonates. Therefore, it is expected that these samples should be negative. However, other types of tissue engineered products make use of different sources of cells that can be autologous. In these cases the cells are harvested from adults, where the risk of HPV is much greater. HPV has been found in high frequency in hairs plucked from normal skin, suggesting a subclinical infection of individuals [9]. The cell culture conditions used to produce the products almost exactly replicate those used for the propagation of HPV *in vitro* [5] and therefore present a significant risk of increasing the titre of these viruses in the product. Infection of product with HPV can go unnoticed as infection is exhibited only by small morphological changes to the infected cells; these may be overlooked during production. The risk from HPV contaminated product may be heightened as these products are used to treat damaged skin where the immune system may be impaired. These conditions may allow introduced HPV to multiply and cause serious pathology.

The role of HPV in human pathology clearly requires some further investigation, however, from a tissue engineering safety viewpoint these viruses are clearly of concern. It may be that, in the future, mandatory tests are used to eliminate the possibility of these viruses from being present in these products. At present there are no guidelines for these particular products and there is no requirement for manufacturers to ensure their products are free from these viruses before use. Assays such as the one described here may be a way that manufacturers can improve the safety profile of their products and increase the public confidence in such treatments.

References

[1] Pearson, R.G., Bhandari, R., Quirk, R.A. and Shakesheff, K.M. "Recent Advances in Tissue Engineering: An Invited Review," *Journal of Long Term Effects of Medical Implants*, Vol. 12, No. 1, 2002, pp.1-33.

[2] De Jong-Tieben, L.M., Berkhout, R.J., Smits, H.L., Bouwes Bavinck, J.N., Vermeer, B.J., van der Woude, F.J. and ter Schegget, J., "High Frequency of Detection of Epidermodysplasia Verruciformis-Associated Human Papillomavirus DNA in Biopsies from Malignant and Premalignant Skin Lesions from Renal Transplant Recipients," *Journal of Investigative Dermatology*, Vol. 105, 1995, pp. 367-371.

[3] Forslund, O., Antonsson, A., Nordin, P., Stenquist, B. and Hansson, B.G., "A Broad Range of Human Papillomaviruses Detected with a General PCR Method Suitable for Analysis of Cutaneous Tumours and Normal Skin," *Journal of General Virology*, Vol. 80, 1999, pp. 2437-2443.

[4] Shamanin, V., Delius, H. and de Villiers, E.M., "Development of a Broad Spectrum PCR Assay for Papillomaviruses and its Application in Screening Lung Cancer Biopsies," *Journal of General Virology* Vol. 75, 1994, pp. 1149-1156.

[5] Howley, P.M. and Lowy, D.R., "Papillomaviruses and their replication," *Fields Virology,* Editors in chief, Knipe, D.M. and Howley, P.M., 4th Ed., Lippincott Williams and Wilkins, pp.2197-2264.

[6] Lee, L.G., Connell, C.R. and Bloch,.W., "Allelic Discrimination by Nick-Translation PCR with Fluorgenic Probes," *Nucleic Acids Research*, Vol. 21, 1993, pp. 3761-3766.

[7] Perkin Elmer Applied Biosystems, "Relative Quantitation of Gene Expression," *User Bulletin # 2 ABI PRISM 7700 Sequence Detection System*, 1997.

[8] Pizzighella, S., Pisoni, G., Bevilacqua, F., Vaona, A. and Palu, G., "Simultaneous Polymerase Chain Reaction Detection and Restriction Typing for the Diagnosis of Human Genital Papillomavirus Infection," *Journal of Virological Methods*, Vol. 55, 1995, pp. 245-256.

[9] Boxman, I.L., Berkhout, R.J., Mulder, L.H., Wolkers, M.C., Bouwes Bavinck, J.N., Vermeer, B.J. and ter Schegget, J., "Nested PCR Approach for the Detection and Typing of Epidermodysplasia Verruciformis-Associated Human Papillomavirus Types in Cutaneous Cancers from Renal Transplant Recipients," *Journal of Clinical Microbiolog*, Vol. 33, 1997, pp. 690-695.

Edward P. Ingenito,[1] Larry Tsai, [2] Robert L. Berger,[3] and Andrew Hoffman[4]

Bronchoscopic Lung Volume Reduction – A Novel Tissue Engineering Treatment for Advanced Emphysema

Reference: Ingenito, E. P., Tsai, L., Berger, R. L., and Hoffman, A., **"Bronchoscopic Lung Volume Reduction – A Novel Tissue Engineering Treatment for Advanced Emphysema,"** *Tissue Engineering Medical Products (TEMPs) ASTM STP 1452*, E. Schutte, G. L. Picciolo, and D. S. Kaplan, Eds., ASTM International, West Conshohocken, PA, 2004.

Abstract: Emphysema is a progressive, disabling pulmonary disease characterized by destruction of elastic lung tissue. It results in hyperinflation, and loss of recoil, and medical therapies are of limited benefit. Lung volume reduction surgery (LVRS) has recently emerged as an effective therapy for emphysema. LVRS involves surgical resection of diseased lung, allowing more space within the chest cavity for the remaining lung to expand and function. Unfortunately, LVRS is associated with substantial mortality (5-10%), morbidity (20-40%) and cost ($25-35,000 per operation). We have recently developed a safer, effective, and less costly approach to lung volume reduction therapy based on tissue engineering principles that can be administered through a bronchoscope. Testing of this procedure required the development of a large animal model that accurately reproduces the physiology of emphysema. This report summarizes the development and validation of such a model, and the testing of our approach, known as Bronchoscopic Lung Volume Reduction (BLVR). The model has facilitated refinement of the procedure in preparation for clinical trials.

Keywords: emphysema, tissue engineering, hydrogel, fibrin gels, volume reduction therapy

---

[1] Assistant Professor of Medicine, Harvard Medical School, Boston Ma, 02115, and President Bistech Inc, 10A Roessler Rd, Woburn, MA, 01801.
[2] Vice President of Research and Development, Bistech Inc, 10A Roessler Rd, Woburn, MA, 01801.
[3] Professor of Cardiovascular Surgery, Boston University, and Senior Medical Consultant, Bistech Inc, 10A Roessler Rd, Woburn, MA, 01801.
[4] Assistant Professor of Veterinary Medicine, Tufts University Medical Center, 200 Westboro Rd, Grafton, MA, 01563.

Introduction

Overview

Tissue engineering-based therapies for advanced forms of human disease are being developed as alternatives to organ transplantation and complex surgery. By their very nature, these types of therapies cannot be adequately evaluated in vitro, or in simple cell and tissue culture systems. Evaluation of therapeutic effectiveness and safety requires development of stable, reproducible animal models to look at organ level and systemic responses. This manuscript summarizes the development and characterization of a sheep model of emphysema for the evaluation of bronchoscopic lung volume reduction, a novel tissue engineering based, minimally invasive approach designed to replace surgical lung volume reduction. The model displays those key features of emphysema that are important determinants of physiological limitation, and are altered by volume reduction therapy so as to cause lung function to improve.

Target Disease

Emphysema is a form of chronic obstructive pulmonary disease (COPD) that affects between 1.5 and 2 millions Americans, and three to four times that number of patients worldwide [1-3]. Patients with emphysema experience progressive destruction of lung tissue, and loss of function over time. Tissue destruction is caused by the release of enzymes from inflammatory cells recruited into the airways and alveoli as a consequence of exposure to irritants, most commonly cigarette smoke [4]. These enzymes, known as proteases, are released from neutrophils and macrophages, and digest the collagen and elastin fibers that provide the lung with structural integrity and elasticity [5]. The structural changes are irreversible, cumulative, and associated with loss of lung function such that eventually, patients are left with little or no respiratory reserve.

In contrast to other common forms of chronic lung disease such as asthma and chronic bronchitis, medical treatment for emphysema is of limited utility [1]. This is because the site and nature of the pathologic abnormalities in asthma and chronic bronchitis are different from emphysema, even though each of these diseases compromises breathing and limits airflow. Asthma and chronic bronchitis are characterized by flow obstruction due to smooth muscle constriction and mucus secretion affecting the airways. Pharmacologic agents that relax airway smooth muscle, and loosen accumulated secretions are therefore effective at improving breathing function and relieving symptoms. These include beta-agonist and anti-cholinergic inhalers, oral theophylline preparations, leukotriene antagonists, steroids, and mucolytic agents. By contrast, airflow limitation in emphysema is due to loss of tissue elastic recoil that limits expiration, and leads to gas trapping and hyper-inflation [6]. While bronchodilators, anti-inflammatory agents, and mucolytic agents are frequently prescribed by physicians for patients with emphysema, their clinical utility is generally

limited because none of these agents directly address the physiological basis for dysfunction.

Volume Reduction Therapy

A non-medical therapy that does address the physiologic dysfunction in emphysema has recently emerged, and has been shown to be effective. This treatment is lung volume reduction surgery (LVRS). LVRS was originally proposed in the late 1950s by Otto Brantigan as a surgical remedy for emphysema based on clinical observations that the lung frequently bellowed out of the confines of the chest cavity when performing thoracic surgery on such patients [7]. Brantigan concluded that the emphysema lung had become too large for the rigid chest cavity, and that resection of lung tissue would help re-size the lung and improve its ability to function. Unfortunately, failure to provide objective outcome measures of improvement, coupled with a 16% operative mortality, led to LVRS being temporarily abandoned as a therapeutic intervention.

LVRS became a clinical reality in 1995 when Joel Cooper re-examined the theories put forth by Brantigan, and applied more stringent preoperative evaluation criteria and modern post-operative management schemes to these same high risk patients [8]. He reported dramatic improvements in lung function and exercise capacity among a cohort of 20 patients with advanced emphysema who had undergone this procedure. There were no deaths at 90-day follow-up, and physiological and functional improvements were markedly better than had been achieved with medical therapy alone.

The benefits of volume reduction have been confirmed in numerous cohort studies, as well as several recently-completed randomized clinical trials [9-12]. On average, 75-80% of patients have experienced a beneficial clinical response to LVRS (generally defined as a 15% or greater improvement in forced expiratory volume in 1 second (FEV_1) at 3 month follow-up) [13]. The peak responses generally occur at between 3 and 6 months post-operatively, and benefits have persisted for between 2-5 years, depending upon the rate of progression of the underlying disease in any given patient [14, 15].

The mechanistic basis for improvement in lung function following volume reduction therapy is embodied in the pressure-volume diagram representation of emphysema (Figure 1) presented by Fessler et al in 1998. This diagram summarizes the relationship between the rigid chest wall and the lung. In the normal lung, the level of trapped gas is small (RV1). When inflated by the bellows action of the chest, the normal lung inflates along a compliance curve described by the pressure-volume trajectory A to B. When fully inflated, the lung reaches a maximal volume equal to TLC1.

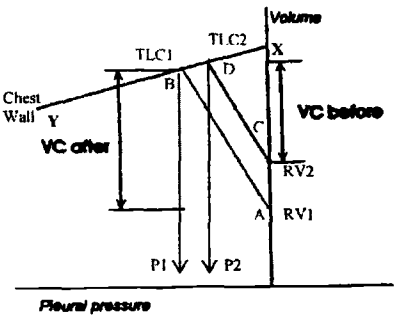

Figure 1—*(Taken from Fessler and Permutt) - The chest wall inflation pressure-volume relationship is described by the line X-Y. The normal lung P-V relationship is described by the line A-B, with a lung capacity = TLC1, trapped gas volume = RV1, and recoil pressure = P1. The emphysema P-V relationship is described by the line C-D with a lung capacity of TLC2, trapped gas volume = RV2, and recoil pressure of P2. The major defect in the emphysema lung is the increase from RV1 to RV2.*

Contrast this with the emphysema lung. In emphysema, the pressure-volume relationship of the chest wall is normal (YX). However, that of the lung is markedly altered (AB to CD). The level of trapped gas is increased from RV1 to RV2. As the lung inflates under the bellows action of the chest, volume increases from point C to D. The vital capacity (VC) of the normal lung, which is equal to the difference between TLC1 and RV1, is significantly larger than the vital capacity of the emphysema lung, which is equal to the volume difference between TLC2 and RV2. As shown in this figure, the primary abnormality in emphysema is an increase in trapped gas (RV1 to RV2). This increase causes a reduction in recoil pressure from P1 to P2 at full lung inflation, and a reduction in FEV_1 that is proportional to the reduction in vital capacity. Fessler et al. go on to argue that the principal effect of volume reduction therapy is to reduce gas trapping, resulting in a shift in the lung compliance relationship from line CD to line AB. Subsequent measurements in patients with emphysema have confirmed the Fessler model, and shown the primary physiological effect of volume reduction therapy is to increase vital capacity [16].

While volume reduction therapy is beneficial for many patients with emphysema, it is not without risk. At present, volume reduction therapy requires that major thoracic surgery be performed on patients with pre-existing advanced lung disease. Many of these patients have co-morbid conditions that increase the risk of general anesthesia and

thoracic surgery. It is therefore not surprising that LVRS is associated with a 5-15% 30 day postoperative mortality. Significant morbidity is also extremely common (40-50%) and includes a high incidence of prolonged post-operative air-leaks, respiratory failure, pneumonia, cardiac arrhythmia, and gastrointestinal complications [17]. Furthermore, the cost of LVRS is between $30000 and $50000, and making this procedure available to potential recipients could pose a significant financial burden to the American Health Care System [18]. Clearly, less invasive, and less expensive alternatives for achieving volume reduction therapy are desirable.

The beneficial effects of lung volume reduction relate specifically to the elimination of regions of hyper-inflated, dysfunctional lung. While this has until now been achieved surgically, we hypothesized that volume reduction therapy can be achieved non-surgically with the use of biocompatible reagents to stimulate localized, controlled scar tissue formation. The scar replaces and shrinks the hyperinflated areas of lung targeted for treatment, and thus reduces the overall volume of the remaining pulmonary parenchyma. The structure and character of the organized scar that replaces the hyperinflated lung are similar to those found in tissues generated during the ordinary wound healing process. This therapy can be administered through a bronchoscope positioned under direct visual guidance into selected target areas of lung, and thus does not require surgery. It is known as bronchoscopic lung volume reduction therapy (BLVR). BLVR is a tissue-engineering based therapy that initiates a complex, controlled biological response to produce a beneficial physiological effect over a period of several weeks to months. It is best evaluated by performing serial measurements in vivo in an animal model that closely replicates the human condition. In this communication we describe the development of a reproducible large animal model of emphysema, and testing of our tissue engineering approach to lung volume reduction in this model.

Methods/Procedures

Rationale for Developing a Large Animal Model of Emphysema

Emphysema can present clinically with two anatomic patterns. Tissue damage uniformly distributed throughout the lung is known as homogeneous disease. Alternatively, damage localized predominantly to selected areas of lung is known as heterogeneous disease. Distinguishing between these two forms generally requires imaging studies, such as CT scanning, since medical history, clinical signs and symptoms, and lung function tests cannot reliably do so.

The distinction between heterogeneous and homogeneous disease is of particular importance in the context of lung volume reduction therapy. Experience with surgical volume reduction has demonstrated that this procedure has different effects in the two patient groups [19]. To understand how new therapies, such as BLVR, that are designed to replace surgical volume might affect patients with a clinical diagnosis of emphysema, models for both homogeneous and heterogeneous subtypes of the disease must be tested.

We considered using several animal models, including rodent (rat, guinea pig, and mouse), canine, swine, and ovine (sheep) models. Based on anatomic, physiologic, and biologic considerations, we chose the ovine model for development. Sheep lung

anatomy, including overall lung size, airway dimensions, and airway branching patterns, is quite similar to that of the human lung [20]. Physiology, including baseline airway resistance, elastance, and diffusing capacity values, are also similar [21]. Furthermore, the sheep model allows testing of the BLVR system using protocols and equipment that are very similar to those that would be used in humans. Finally, procedural safety and effectiveness can be evaluated at selected time points using a protocol design that directly parallels human trials.

Protocol Overview

Model development and BLVR testing were conducted in accordance with a protocol approved by the Tufts University Veterinary Medical Center Institutional Animal Care and Use Committee. All interventions and physiologic measurements were performed under light anesthesia while mechanical ventilation was administered through an endotracheal tube. Anesthesia was induced with intravenous ketamine (Ketaset, Fort Dodge Pharmaceuticals, Fort Dodge, Iowa, 7 mg/kg) and diazepam (Valium, 0.25 mg/kg), and maintained with continuous intravenous propofol (0.5-1.0 mg/kg/hr; Propoflo, Abbott Labs). A 10 mm diameter endotracheal tube was inserted under fiberoptic guidance and attached to a mechanical ventilator. An esophageal balloon was introduced through the nares, and the desired position was verified by observing trans-pulmonary (P_{tp}) and trans-respiratory system pressures, and cardiac oscillations on P_{tp} profiles. Heart rate and arterial oxygen saturation were continuously monitored using an oximeter and tongue probe.

Detailed respiratory physiologic measurements were performed and CT scans of the chest were obtained at baseline (BAS), two weeks after receiving a full course of papain upon development of experimental emphysema but just prior to BLVR (EMPH), and approximately one and three months after BLVR (BLVR-1 and BLVR-2, respectively). Clinical status including activity levels, body weights and vital signs were monitored. Upon completion of the BLVR-2 studies, the animals were sacrificed and autopsied. Gross and microscopic examinations were performed and representative photographic documentation was obtained.

Development of Large Animal Model of Homogeneous Emphysema

A model for severe homogeneous emphysema was developed in six female sheep. Seven animals were initially evaluated. Under light anesthesia and controlled mechanical ventilation, Albuterol (five puffs) was administered through an in-line metered dose inhaler (MDI) device to prevent bronchospasm and to provide uniform distribution of the papain (Sigma Chemical, St. Louis, MO) used to produce emphysema. The papain (75U/kg) was delivered over 15-20 minutes using a parallel system of dual nebulizers (Pari LC Plus, Pari Respiratory Equipment, Midlothian, VA) connected to the positive pressure ventilator circuit through a series of one-way valves. Tidal volume was set at 12ml/kg, rate at 12 breaths/min, and inspired oxygen content of 60%. Each animal received four doses of nebulized papain at weekly intervals. One of the seven in the initial group of animals developed pulmonary hemorrhage after the

second dose and was euthanized. The remaining six animals were included in the study protocol.

Development of Large Animal Model of Heterogeneous Emphysema

Seven additional sheep received papain (1.5 U/kg) administered in bolus form through a catheter positioned under bronchoscopic guidance. Each animal also received nebulized papain 75 U/kg once per week for three weeks. This combination of treatments was used successfully to generate heterogeneous emphysema. Of these seven animals, one died of pulmonary hemorrhage. The remaining six animals were included in the study protocol.

Tissue Engineering Approach to BLVR - Reagent Mode of Action

BLVR therapy using a tissue-engineering approach requires three components:

1. A buffered, enzymatic *Primer solution*.
2. A *Washout solution*.
3. A biocompatible, bioabsorbable *hydrogel*.

The active component of the Primer Solution is trypsin, a serine proteinase, which performs two important functions at the epithelial boundary of the target area within the lung: 1) it loosens epithelial cells from their attachments to the underlying basement membrane, and 2) it promotes localized collapse by cleaving and inactivating surfactant proteins, rendering surfactant dysfunctional. Loosening of epithelial cells is accomplished through the cleavage of cellular integrins, trans-membrane attachment proteins, which anchor cells to binding sites located on protein components of the extracellular matrix. The primary cell-matrix interaction targeted by trypsin is that between lung epithelial cells, and the Type IV collagen and laminin of the basement membrane. [22] By removing epithelial cells, fibroblasts from the underlying interstitial space can migrate to the bronchial and alveolar surface, and begin the process of scar formation. Cleave and inactivation of surfactant proteins also results from the proteolytic effects of trypsin. Loss of surfactant proteins leads to surfactant inactivation, and mechanical destabilization and collapse of alveoli and small airways at sites of treatment. The resulting collapse reduces the volume of hydrogel needed to produce effective coating of the target area, and inhibits re-expansion.

The Washout solution is composed of RPMI 1640 culture media, an isotonic, buffered, growth media commonly used to maintain mammalian cells in culture. Administration of the Washout solution: 1) rinses out epithelial cells previously loosened by Primer solution, from the treatment site, and 2) removes, and dilutes, residual trypsin preventing ongoing, unregulated cell detachment and surfactant inactivation.

The hydrogel is fibrin-based, and is generated by delivering fibrinogen solution and thrombin solution simultaneous through a dual lumen catheter at a predetermined treatment site within the lung. Gel formation results from the polymerization of fibrin monomer, formed by the pharmacological action of thrombin on fibrinogen. Neither thrombin nor fibrinogen is intended to exert a direct pharmacological effect, however. The primary function of the hydrogel is to provide a scaffold that immobilizes

components needed to initiate a localized biological response that leads to volume reduction through scar formation and contraction.

The hydrogel contains two active components that promote localized scar formation in the absence of inflammation. These are:

1. Chondroitin-6-sulfate (CS), a naturally occurring glycosaminoglycan used in tissue engineering applications to foster skin and nerve regeneration [23-25];
2. Poly-L-lysine (PLL), a synthetic cationic polyamine that promotes cell adhesion [26-28].

In combination, CS and PLL, incorporated in the fibrin scaffold and immobilized at the target site, facilitate fibroblast attachment, proliferation, and collagen expression. Without these two components, fibrin hydrogels are cleared from the lung within 4 weeks, and do not promote scarring or lung volume reduction.

The hydrogel also contains RPMI-1640, the cell culture media used in the Washout solution. This provides fibroblasts at treatment sites with nutrient support so that they can proliferate efficiently. To prevent bacterial contamination of the hydrogel, tetracycline (1.5 mg/ml) has been incorporated into the fibrinogen solution. Tetracycline is one of several antibiotics that are both water soluble and compatible with fibrinogen. Once formed, the scaffold provided by the hydrogel directs site-specific scar formation and tissue contraction by resident fibroblasts, resulting in effective volume reduction over a 1 to 2 month period.

BLVR Protocol

The procedure was performed as follows: A fiberoptic endoscope (Olympus Corporation, GIF-n30 pediatric gastroscope, Tokyo, Japan) with 5 mm outside diameter and 90 cm working length was introduced through the indwelling endotracheal tube and advanced sequentially to subsegmental bronchi (three in the left lung, and three in the right lung) supplying the targeted pulmonary territory. At each site, the endoscope was advanced as distally as possible under direct visualization, a position referred to as the *wedge position.* Positioning the scope in this manner ensures that injected reagents cannot leak back into the airways or spill into adjacent non-targeted areas. The Primer solution and Washout solution were then delivered sequentially through the endoscope. Following suctioning, the catheter was placed into the same region and the hydrogel injected. The endoscope was then withdrawn, the site was inspected, and the endoscope repositioned into the next target site.

Each BLVR treatment required approximately 5 to 7 minutes to complete, and the total procedure (treatment at six different sites) took approximately 45 minutes. Upon completion of BLVR, anesthesia was discontinued and animals were monitored closely during recovery. Once observed to be clinically stable, each animal was returned to its stall.

Physiologic measurements

Responses to papain treatment and BLVR were assessed by monitoring lung function. The tests chosen are identical to those currently used in clinical practice for

evaluating responses to surgical volume reduction therapy in patients with emphysema. Lung volume (functional residual capacity (FRC)) was measured by whole body plethysmography during spontaneous breathing (Buxco Instruments, Marlboro, MA.). Pleural pressure was obtained during inspiratory efforts against a closed shutter at FRC and FRC + 1.5 liters, to characterize the pressure-volume relationship for the chest wall during respiratory muscle contraction (referred to as CW_{act}). The maximum inspiratory effort generated during a 60-90 second occlusion was recorded as the maximal inspiratory pleural pressure at the corresponding lung volume. The deflation pressure volume relationship (PV) for the lung measured from 30 cm H_2O P_{tp} distending pressure was determined by intermittent occlusion. Airway resistance (R_{aw}), tissue resistance, and dynamic elastance measurements were determined to characterize the dynamic properties of the lung using a computer-controlled pneumatic large animal ventilator [29]. Single breath diffusing capacity (D_{Lco}) was measured using an airtight three-way valve system, a calibrated carbon monoxide and helium meter (Morgan Transfer factor system, Morgan Scientific, MA), a source of calibrated tracer gas, and a 3-liter syringe.

Chest CT scans were performed at BAS, EMPH, BLVR-1, and BLVR-2 time points at FRC and at full lung inflation (TLC).

Analysis of Physiological Data

Plethysmography data was used to calculate FRC via the method of Dubois based on Boyle's law [30]. Pleural pressure deflections measured during inspiratory efforts against the closed shutter at FRC, and at FRC + 1.5 L were used to construct an "active chest wall" compliance relationship that was assumed to be linear between TLC and RV. Static PV data for the lungs were fit to the exponential equation of Salazaar and Knowles, in which lung volume was expressed as a function of pressure according to the equation

$$V(P) = V_{max} - Ae^{-kP}$$

where V is volume, P pressure, V_{max} the volume attained at "infinite" distending pressure, $A = (V_{max} - V_{min})$, V_{min} is the volume at zero distending pressure (equivalent to residual volume (RV)), and k is a parameter describing the shape of the exponential relationship between pressure and volume (the shape factor) [31]. Results are expressed in terms of the parameters V_{max}, V_{min}, and k. TLC is determined as the volume intercept of the active chest wall pressure-volume relationship and the passive lung pressure-volume relationship. The corresponding pressure at this point of intercept is the recoil pressure at TLC (P_{TLC}) [6].

Dynamic lung function measurements obtained using the OVW technique were interpreted by fitting frequency domain expressions for pressure, volume, and flow data to the constant phase impedance model

$$P(\omega)/V(\omega) = R_{aw} + \{(G-Hj)/\omega^{\alpha}\}$$

where P is pressure, V is flow, ω is angular frequency in radians/sec, j is the imaginary number $\sqrt{-1}$, and other terms are as previously defined. Results are summarized in

terms of airway resistance (R_{aw}), tissue resistance (expressed as the dissipative modulus G) and dynamic elastance (expressed as the elastic modulus H) [29].

Pathologic Anatomy and Histopathology

Following study completion (BLVR-2), the animals were euthanized with intravenous pentobarbital (100 mg/kg) and autopsied. The lungs were removed, fully inflated, and the pulmonary circulation was flushed with 2.5 liters of normal saline 20 cm H_2O pressure. Sites of BLVR treatments were readily detected by visual inspection and manual palpation, and were photographically documented. The lungs were sliced serially into 2 – 2.5 cm axial sections and further inspected for signs of scar formation, or other gross changes. Samples from all BVR treatment sites and representative samples from untreated sites were fixed in 15% buffered formalin, and stained with hemotoxylin and eosin (H&E).

Outcome Variables and Statistical Analysis

Treatment responses were summarized using three groups of outcome variables: 1) incidence of clinical complications following the procedure; 2) static and dynamic lung physiology in the intact animals at baseline, post-emphysema, and post-BLVR; 3) lung histology and anatomy assessed at necropsy.

Clinical complications were defined according to the following list: 1) hypoxemia (determined by tongue oximetry measurements) requiring oxygen supplementation (Sao_2 < 85% for longer than 5 minutes); 2) pneumonia diagnosed by clinical symptoms and chest radiography; 3) fever > 1.5 °C above baseline; 4) respiratory distress requiring re-intubation or euthanasia; 5) progressive weight loss of greater than 10% body mass.

Static lung physiology, expressed in terms of k, V_{max}, and V_{min} values, and dynamic lung function, expressed in terms of R_{aw}, G (the tissue dissipation modulus), and H (the tissue elastic modulus) were compared at different time points among different treatment groups by one way analysis of variance (ANOVA). Differences between specific groups were identified using Duncan's post hoc analysis test. Statistical significance was defined as a P value of < 0.05.

CT scans were analyzed by computerized densitometry. Representative values for a given animal at each time point were obtained by averaging cross-sectional readings 10 cm below the apex, at the carina, and 10 cm above the diaphragm.

Histology was evaluated for:

1. The extent and severity of emphysema present;
2. The presence of scar formation;
3. Presence of foreign body material;
4. Cellular dysplasia or anaplasia;
5. Evidence of pneumonia or abscess formation;
6. Granuloma formation;
7. Vasculitic or allergic changes.

Results

Lung and Chest Wall Physiology

Both homogeneous and heterogeneous emphysema models displayed gas trapping and hyperinflation, which are the key determinants of physiological dysfunction in emphysema. Comparisons of lung and chest wall physiology before and after papain exposure are summarized for both models in Figure 2. Results are presented in the form of Campbell diagrams analogous to the approach used by Fessler et al. to describe physiological responses to volume reduction therapy in humans. This approach was chosen because it depicts, in a single figure, how changes in the interaction between the chest wall and lung determine gas trapping and hyperinflation, and how volume reduction therapy benefits lung function by improving the mechanics of this interaction. Both models demonstrate a similar pattern of hyper-inflation: the volume of trapped gas, reflected by a greater change in residual volume (RV) than the overall increase in lung volume (TLC). As a result, functional lung volume, equal to vital capacity, the difference between TLC and RV, is decreased. In the homogenous

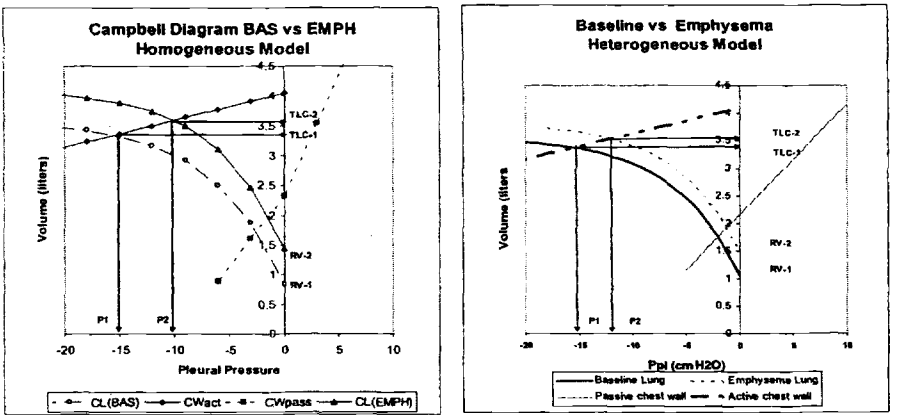

Figure 2 — *Papain treatment caused increases in gas trapping (RV-1 to RV-2) in both homogeneous and heterogeneous models by altering the static pressure volume relationship of the lung. Active chest wall compliance (CWact) was unaffected by papain exposure. In both homogeneous and heterogeneous models, the upward shift in the pressure-volume relationship of the lung prevented full inflation by the inspiratory muscles. As a result, recoil pressure decreased from P1 to P2.*

emphysema model, TLC increased from 3.36 ± 0.36 to 3.63 ± 0.42 L (p=0.09), Functional Residual Capacity (FRC) increased from 1.72 ± 0.23 to 2.04 ± 0.27 (p=0.003), and RV increased from 0.86 ± 41 to 1.43 ± 0.48 (p=0.009). In the heterogeneous model, similar changes were observed. TLC increased from 3.34 ± 0.34 L to 3.56 ± 0.33 L (p = NS), FRC increased from 1.81 ± 0.44to 1.89 ± 0.50 L (p= NS), and RV increased from 1.15 ± 0.52 L to 1.51 ± 0.47 L emphysema, (p=0.001). In

neither instance was respiratory muscle function affected. That is, the ability of the respiratory muscles to generate active pressure at any given lung volume was the same before and after papain. However, following papain, the lung developed hyper-inflation and gas trapping. As a result, full expansion within the chest cavity was limited, not by a loss of muscle strength, but rather by a loss of space within the chest cavity for the lung to inflate. This pattern of physiological alterations parallel those observed in patients with advanced emphysema [6, 16].

Volume reduction therapy in both homogeneous and heterogeneous emphysema was effective in reducing gas trapping, increasing lung recoil pressure, and increasing vital capacity by providing more space within the chest cavity into which the lung can expand. Measurements performed at 1 and 3 months following BLVR are summarized in Figure 3. In animals with homogeneous emphysema, BLVR produced a sustained reduction in TLC, FRC and RV that was associated with a 6% improvement in vital capacity. Similarly, in animals with heterogeneous emphysema, BLVR produced changes in TLC, FRC, and RV that were associated with a 22% improvement in vital capacity.

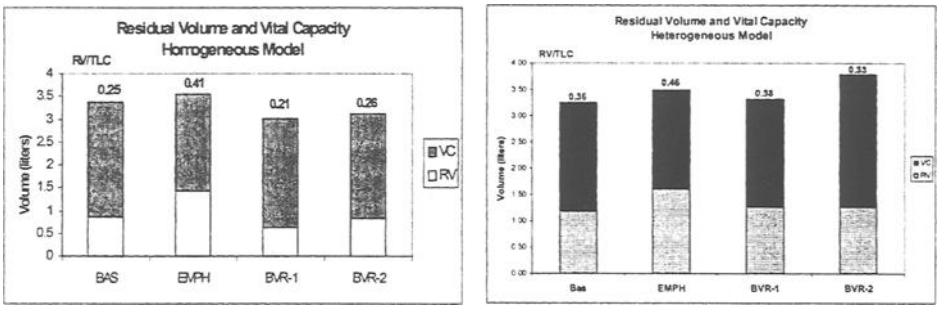

Figure 3— *The effects of papain exposure and subsequent BLVR on lung volumes are summarized in homogeneous and heterogeneous emphysema sheep models. Both groups demonstrate hyper-inflation, reflected as an increase in total lung volume, and gas trapping reflected as an increase in residual volume (RV) and reduction in vital capacity (VC) at the EMPH time point. BLVR was effective in reducing lung volumes, eliminating gas trapping, and increasing vital capacity at BVR-1 and BVR-2 follow-up time points.*

Lung Resistance and Dynamic Elastance Measurements

In addition to altering static lung mechanics and causing lung hyperinflation, papain exposure also caused changes in dynamic lung behavior. In homogeneous animals, R_{aw} increased significantly (0.45 ±0.31 to 0.79 ± 0.27 cm H_2O/l/sec, p = 0.035), and smaller but not statistically significant increases in tissue resistance (i.e. G = tissue resistance: 2.3 ± 0.6 to 2.8 ± 0.5 cm H_2O/L, p = NS and H (16.9 ± 4.2 to 19.6 ± 3.4 cm H_2O/L, p = NS) were observed. These physiological measurements indicate that the emphysema truly behaves in a homogeneous manner, with relatively uniform changes in resistance to airflow, and little frequency dependence in lung resistance (reflected by a change in G) or dynamic lung elastance (reflected by a change in H).

In sheep with heterogeneous emphysema, there were significant increases in tissue resistance (G = 2.12 ± 0.48 vs 3.26 ± 0.63 cm H_2O/L, p=0.025) rather than in airway resistance. Substantial changes in H were also observed (15.6 ± 2.2 vs 21.9 ± 4.5 cm H_2O/L, p=0.066). This type of exposure causes changes in the tissue resistance parameter G and dynamic elastance parameter H because it produces tissue injury that is more severe at specific sites within the lung, resulting in differences in dynamic time constants for filling and emptying. Thus, as breathing frequency changes, different regions of lung fill and empty, altering dynamic properties. This frequency-dependent behavior, indicative of physiological heterogeneity, corresponded closely with anatomic heterogeneity observed by CT scan.

Despite the differences in dynamic lung physiology observed between heterogeneous and homogeneous disease, BLVR had beneficial effects on lung function in both groups. Segmental BLVR treatment was performed at six sites uniformly distributed throughout the lung in homogeneous animals, while treatment was directed specifically to the six papain injection sites in heterogeneous animals. Raw, G, and H values are summarized in Table 1. In both groups, BLVR was associated with normalization of physiological parameters to pre-emphysema baseline values at the BVR-2 follow-up time points.

Table 1— *Summary of dynamic lung function.*

Time point	Homogeneous			Heterogeneous		
	Raw (cmH_2O/L/sec)	G (cmH_2O/L)	H (cmH_2O/L)	Raw	G	H
BAS	0.45 ± 0.31	2.3 ± 0.6	16.9 ± 4.2	0.79 ± 0.16	2.1 ± 0.5	15.6 ± 2.2
EMPH	0.79 ± 0.27	2.8 ± 0.5	19.6 ± 3.4	0.54 ± 0.19	3.3 ± 0.6	21.9 ± 4.5
BVR-2	0.54 ± 0.29	2.2 ± 0.6	18.7 ± 4.2	0.41 ± 0.12	1.9 ± 0.4	11.7 ± 3.1

Diffusing capacity

To evaluate the effectiveness of gas exchange at the alveolar level, diffusing capacity was measured in both groups of animals. Results show that papain exposure caused significant reductions in diffusing capacity, which improved following BLVR treatment (Figure 4). In animals with both homogeneous and heterogeneous emphysema, D_{Lco} values measured following development of emphysema (EMPH) were significantly less than at baseline (BAS), indicating a loss of surface area for gas exchange after papain exposure. At the BVR-2 time points, D_{Lco} had increased in both emphysema groups, and was not significantly different from baseline.

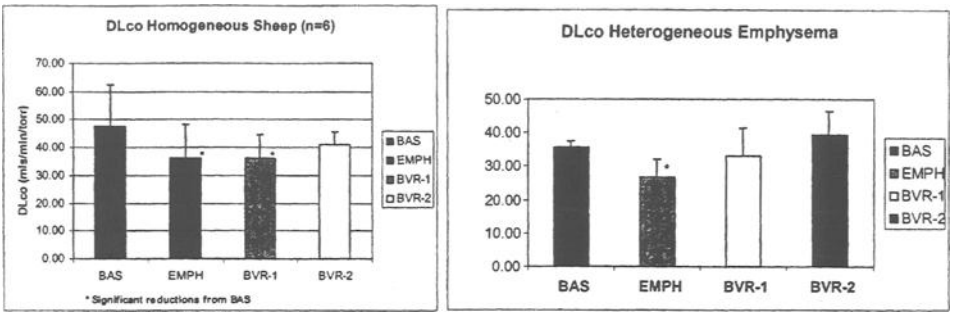

Figure 4 — *D_{Lco} decreased significantly following papain exposure (EMPH) but returned towards baseline (BAS) in both groups after BLVR therapy. At BVR-2 values were not different from baseline.*

CT imaging studies

Densitometry measurements on CT images at TLC were recorded at baseline (BAS), and following papain exposure (EMPH) to further document the development of emphysema. Decreases in tissue density have been shown to correlate with destruction of tissue in vivo [32]. Results for homogeneous and heterogeneous animal models are summarized in Figure 5. In both models, papain exposure was associated with reductions in tissue density expressed in terms of Houndsfield units.

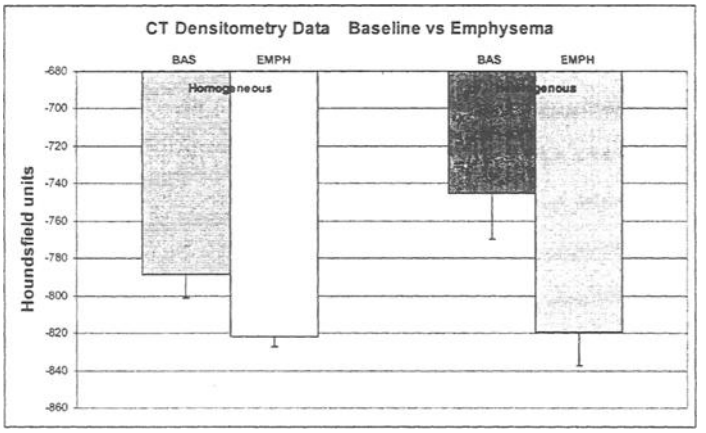

Figure 5 — *Papain exposure caused a decrease in overall lung tissue density measured in terms of Houndsfield units in both homogenous and heterogeneous emphysema models, confirming the presence of loss of tissue density for the lung as a whole.*

In selected animals, serial CT measurements were performed to evaluate the anatomical progression in response to BLVR. Treatment sites in homogeneous and

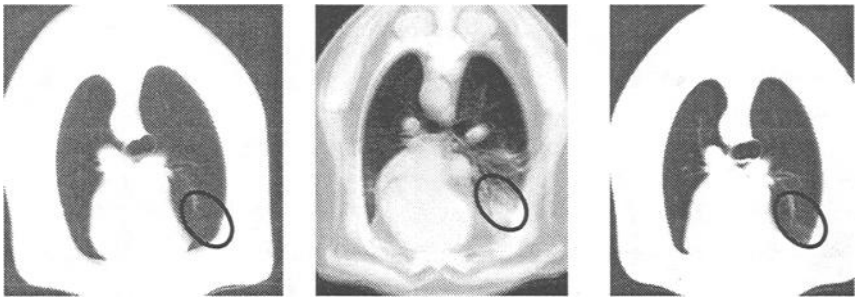

Figure 6 - *Serial CT images showing EMPH pre-treatment (left), EMPH immediately post treatment (center), and three months post BLVR (right). BLVR caused an immediate infiltrate at the treatment site due to injection of materials, and the ensuing collapse. At the BVR-2 follow-up time point, an organized peripheral scar is shown.*

heterogeneous animals prior to, immediately after, and three months following treatment are summarized in figures 6 and 7. In both instances, immediately following BLVR therapy, a localized infiltrate was detected at the site of treatment, confirming the ability to identify treatment sites, and provide localized therapy without spillover of materials outside the target area. In both examples, treatment resulted in the formation of a

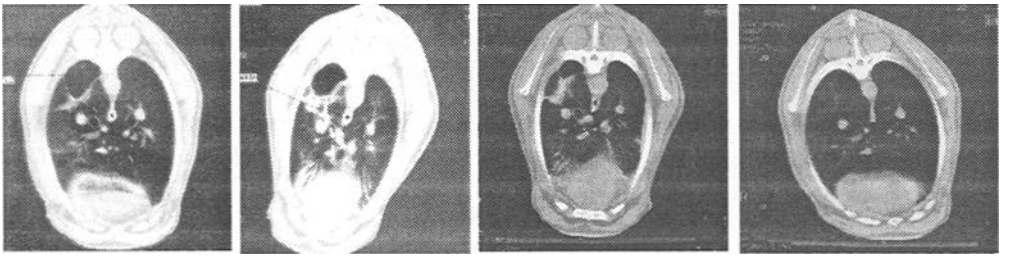

Figure 7 — *Serial CT images showing the lung at the EMPH time point pre-treatment (left), at the time of treatment (image 2), at BVR-1 (image 3), and at BVR-2 (right). The images document the progression of change from a 5 cm bulla to a collapsed scar over three months.*

linear density which, at autopsy was shown to be organized scar tissue. Figure 7 shows a striking example of how a large bulla gradually involutes after BLVR. At one month post BLVR (Image 3) the lesion is reduced in volume by 78%. By three months, the lesion is reduced to a linear density consistent with scar tissue.

Assessment of Safety Parameters

Arterial blood saturations levels measured prior to and immediately following completion of BLVR in both homogeneous and heterogeneous sheep were unaffected by treatment. None of the animals developed respiratory distress or failure that required resumption of ventilator support. Two animals in the homogeneous treatment group, and one in the heterogeneous treatment group developed transient fevers following BLVR.

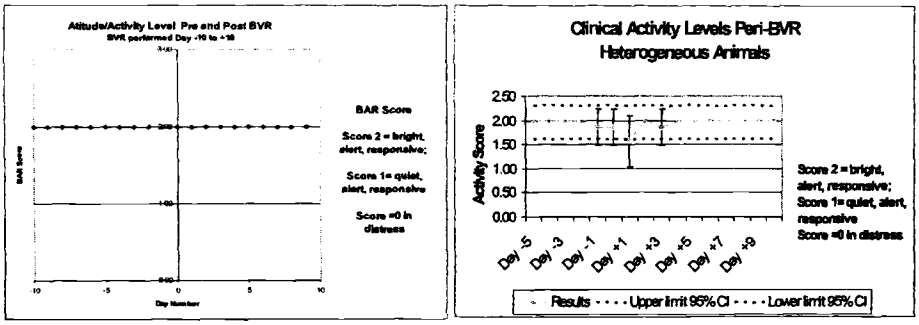

Figure 8 — *Activity levels recorded prior to BLVR (minus days) and following BLVR (plus days) are shown. Activity levels of 1 or 2 are normal. Values of 0 indicate clinical evidence of distress. None of the animals in either group demonstrated evidence of distress following the procedure.*

None required treatment, as the temperatures returned to baseline within 48 hours. Food consumption and body weight remained stable in all animals throughout the course of the study.

Clinical activity scores assessed by the veterinary staff (Tufts University Medical Center) using the conventional Attitude and Activity Scoring System are summarized in Figure 8. Activity levels were within normal limits following BLVR therapy in both groups.

Hematology and blood chemistry studies were performed in heterogeneous BLVR sheep, and results compared to a control group of sheep that did not receive treatment. Results showed that BLVR was not associated with any changes in blood hematology or chemistry profiles. Specifically, there were no changes in white blood cell count to suggest either infection or bone marrow toxicity, or with any changes in hematocrit to suggested decreased RBC production or hemolysis. Differential cell counts further indicate that BLVR treatment was not associated with eosinophilia to suggest an allergic reaction. Serum blood urea nitrogen (BUN), serum creatinine (Cr), serum levels of gamma glutamyl transferase (GGT), and serum levels of aspartate amino transferase (AST) were within normal limits at both time points, and were similar to controls. Furthermore, BLVR did not produce hyper-gammaglobulinemia that could have suggested chronic infection or inflammation.

Necropsy and histopathology findings

Representative lung sites from both homogeneous and heterogeneous treatment groups are shown in Figures 9, 10, and 11. Figure 9 shows treatment sites three months following BLVR. Peripheral scarring, and tissue contraction are visible at target sites in lungs with both types of emphysema.

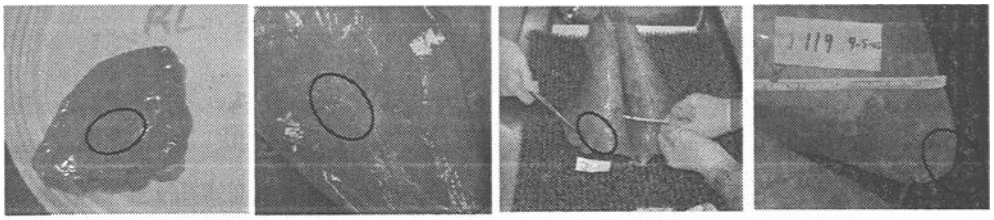

Homogeneous Emphysema BLVR Sites Heterogeneous Emphysema BLVR Sites

Figure 9 - Necropsy examination demonstrates evidence of peripheral scar formation at target sites in both homogeneous and heterogeneous emphysema animals. Photos of heterogeneous samples demonstrate contraction that limits inflation.

Photomicrographs of tissue from areas of experimentally-induced emphysematous lung show that papain exposure caused significant tissue destruction, and disruption of normal architecture compared to control tissue (Figure 10).

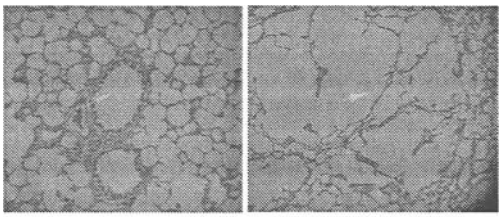

Control Emphysema

Figure 10 - Control tissue in the left panel shows normal alveolar architecture and airway structure. Tissue from papain treated lungs shows marked destruction of alveolar architecture with airspace enlargement.

Photomicrographs of tissue samples from BLVR treatment sites shown that treatment

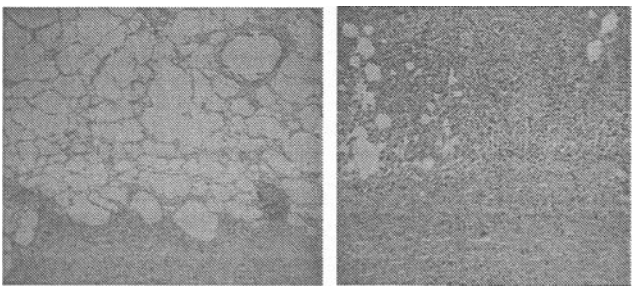

Figure 11 — *BLVR treatment sites are shown. The left hand panel shows emphysema lung adjacent to an organizing scar. The right hand panel shows cellular and tissue elements within the scar. Fibroblasts and collagen have replaced the pre-existing, gas filled lung tissue. It is by this mechanism that volume reduction occurs.*

produces localized formation of scar without infection, inflammation, infarction, or allergic reaction.

Summary and Conclusions

Testing of new tissue engineering therapies for human disease are greatly facilitated by the development of stable, reproducible animals models that permit evaluation of safety and effectiveness. This manuscript summarizes the development and characterization of a sheep model of emphysema that was employed to evaluate bronchoscopic lung volume reduction, a novel tissue-engineering therapy. Our measurements confirm that papain treatments administered either via nebulizer alone (homogeneous model), or via nebulizer combined with catheter-directed intrabronchial administration (heterogeneous model), produce emphysema that is stable, and accurately represents the physiology and pathology of human disease.

Use of this model has allowed us to develop and refine the reagents and techniques necessary for BLVR, and prepared us for clinical trials in humans. The model allowed us to demonstrate that BLVR therapy consistently reduces lung volumes, and improves airway resistance and diffusing capacity at three month follow-up. CT imaging demonstrated progression from atelectasis/consolidation to linear density consistent with scar formation. It is this progression and the associated tissue remodeling that result in tissue contraction and volume reduction. Clinical observations, monitoring, and blood testing, confirmed that the procedure was safe without detectable toxicity. There was no evidence of pneumonia, abscess formation, pulmonary infarction, or allergic reactions at any of the treatment sites. Furthermore, treatment caused no measurable alterations in blood cell counts, or blood chemistry values.

The findings presented suggest that this sheep model can be used to evaluate novel therapies for emphysema, and indicate the safety and effectiveness of BLVR as an alternative to surgical volume reduction in the treatment of this disease.

References

1. Committee, A.T.S.C., "Standards for the diagnosis and care of of patients with chronic obstructive pulmonary disease." *Am J Resp Crit Care Med*, 1995. 152: pp. s78-83.
2. Pauwels, R., et al., "Global strategy for the diagnosis, management, and prevention of chronic obstructive pulmonary disease." *Am J Resp Crit Care Med*, 2001. 163: pp. 1256-1271.
3. Institute., N.H.L.B., "Morbidity and Mortality Data, NIH." *Chartbook on Disease*, 1998.
4. Barnes, P., "Chronic Obstructive Pulmonary Disease." *N Engl J Med*, 2000. 343(4): pp. 269-280.
5. Stockley, R., "Neutrophils and protease/antiprotease imbalance." *Am J Resp Crit Care Med*, 1999. 160: pp. S49-S52.
6. Fessler, H.E. and S. Permutt, "Lung volume reduction surgery and airflow limitation." *Am J Respir Crit Care Med*, 1998. 157(3 Pt 1): pp. 715-22.

7. Brantigan, O. and E. Mueller, "Surgical treatment for pulmonary emphysema." *Am Surg*, 1957. 23: pp. 789-804.
8. Cooper, J.D., et al., "Bilateral pneumonectomy for chornic obstructive pulmonary disease." *J Thorac Cardiovasc Surg*, 1995. 109(106-119).
9. Geddes, D., et al., "Effects of lung volume reduction surgery in patients with emphysema." *N Eng J Med*, 2000. 343: pp. 239-245.
10. Criner, G.J., et al., "Prospective randomized trial comparing bilateral lung volume reduction surgery to pulmonary rehabilitation in severe chronic obstructive pulmonary disease." *Am J Respir Crit Care Med*, 1999. 160(6): pp. 2018-27.
11. Goodnight-White, S., et al., "Prospective randomized controlled trial comparing bilateral volme reduction surgery to medical therapy alone in patients with severe emphysema." *Chest*, 2000. 118(Suppl 4): pp. 102s.
12. Pompeo, E., et al., "Reduction pnuemoplasty versus respiratory rehabilitation in severe emphysema: a randomized study." *Ann Thorac Surg*, 2000. 2000(70): pp. 948-954.
13. Cooper, J.D., et al., "Results of 150 consectutive lung volume reduction procedures in patients with severe emphysema." *J Thor Cardiovasc Surg*, 1996. 112: pp. 1319-1330.
14. Gelb, A.F., et al., "Lung function 4 years after lung volume reduction surgery for emphysema." *Chest*, 1999. 116(6): pp. 1608-15.
15. Cooper, J.D. and S.S. Lefrak, "Lung-reduction surgery: 5 years on." *Lancet*, 1999. 353(Suppl 1): pp. 26-27.
16. Ingenito, E.P., et al., "Interpreting improvement in expiratory flows after lung volume reduction surgery in terms of flow limitation theory." *Am J Respir Crit Care Med*, 2001. 163(5): pp. 1074-80.
17. Swanson, S.J., et al., "No-cut thoracoscopic lung plication: a new technique for lung volume reduction surgery." *J Am Coll Surg*, 1997. 185(1): pp. 25-32.
18. Berger, R.L., et al., "Limitations of randomized clinical trials for evaluating emerging operations: the case of lung volume reduction surgery." *Ann Thorac Surg*, 2001. 72(2): pp. 649-57.
19. McKenna, R.J., Jr., et al., "Patient selection criteria for lung volume reduction surgery." *J Thorac Cardiovasc Surg*, 1997. 114(6): pp. 957-64; discussion 964-7.
20. Hare, W.C.D., "The broncho-pulmonary segments in the sheep." *Anatom Record*, 1953. 89: pp. 387-402.
21. Robinson, N.E., "Some functional conseqeunces of species differences in lung anatomy." *Adv Vet Sci Comp Med*, 1982. 26: pp. 1-33.
22. Forbes, B., *Pulmonary Epithelial Cell Culture*, in *Epithelial Cell Culture Protocols*, C. Wise, Editor. 2002, Humana Press: Totowa. p. 65-75.
23. Chamberlain, L.J. and I.V. Yannas, *Preparation of Collagen-Glycosaminoglycan Copolymers for Tissue Regeneration.*, in *Tissue Engineering Methods and Protocols*, M.L. Yarmush, Editor. 1999, Humana Press: Totowa. p. 3-18.
24. Bellamkonda, R.V. and R.F. Valenti, *Fabrication and implantation of gel-filled nerve guidance channels.*, in *Tissue Engineering Methods and Protocols*, M.L. Yarmush, Editor. 1999, Humana Press: Totowa.
25. Liverani, H.W. and V.M. Monard, "Deposition of extracellular matrix along the pathways of migrating fibroblasts." *Cell Tissue Res*, 1990. 262(3): pp. 467-481.

26. Chittchang, M., et al., "Poly(L-lysine) as a model drug macromolecule with which to investigate secondary structure and membrane transport, part I: Physicochemical and stability studies." *J Pharm Pharmacol*, 2002. 54(3): pp. 315-23.
27. Lollo, C.P., et al., "Poly-L-lysine-based gene delivery systems. Synthesis, purification, and application." *Methods Mol Med*, 2002. 69: pp. 1-13.
28. Moreau, E., et al., "Biocompatibility of polycations: in vitro agglutination and lysis of red blood cells and in vivo toxicity." *J Drug Target*, 2002. 10(2): pp. 161-73.
29. Kaczka, D.W., E.P. Ingenito, and K.R. Lutchen, "Technique to determine inspiratory impedance during mechanical ventilation: implications for flow limited patients." *Ann Biomed Eng*, 1999. 27(3): pp. 340-55.
30. Ingenito, E.P., et al., "Bronchoscopic volume reduction: a safe and effective alternative to surgical therapy for emphysema." *Am J Respir Crit Care Med*, 2001. 164(2): pp. 295-301.
31. Salazaar, E. and J.H. Knowles, "An analysis of pressure-volume characteristics of the lung." *J APpl Physiol*, 1964. 19(97-104).
32. Ingenito, E.P., et al., "Comparison of physiological and radiological screening for lung volume reduction surgery." *Am J Respir Crit Care Med*, 2001. 163(5): pp. 1068-73.

John A. Tesk[1] and Lisa R. Karam[1]

NIST and Standards for Tissue Engineered Medical Products

Reference: Tesk, J. A., and Karam, L. R., **"NIST and Standards for Tissue Engineered Medical Products,"** *Tissue Engineered Medical Products (TEMPS), ASTM STP 1452,* E. Schutte, G. L. Picciolo, and D. S. Kaplan, Eds., ASTM International, West Conshohocken, PA, 2004.

Abstract: On June 13-14, 2001, the National Institute of Standards and Technology (NIST) convened a workshop of high level representatives from industry, federal agencies, and standards organizations to identify standards-related needs of the biomedical materials and devices industry. There were individual breakout sessions on standards for: Biomaterials, Therapeutic and Drug Delivery Devices, Auditory Diagnostic and Prosthetic Devices, Manufacturing of Prostheses, and Tissue Engineered Medical Products (TEMPs). Cross-cutting issues of Harmonization of Standards, Data, and Sterilization were also addressed. The session on Standards for TEMPs placed its most significant needs on the development of test methods and materials characterization. Action items for NIST to consider were separated into those relative to the Food and Drug Administration (FDA) approval process and those relative to industry needs not directly related to the FDA approval process. This paper summarizes the needs identified for TEMPs and the status of NIST-related activities.

Keywords: standards for tissue engineering, TEMPs, test methods for tissue engineering, measurements for tissue engineering, scaffolds, cell-material interactions, measurement technologies, characterization of surfaces, characterization of materials, characterization of cells, NIST, standard reference materials, SRM, DNA, bioinformatics.

Introduction

TEMPs are products that may use scaffolds, alone or in combination with biological components such as proteins or cells. From the enormous number of issues that had

[1]Senior Technical Advisor, Industrial Liaison Office, Director's Office, National Institute of Standards and Technology (NIST), Gaithersburg, MD, 20899-1005.

evolved from the ongoing ASTM effort on standards for TEMPs, it became apparent that there were many opportunities for NIST to make unique contributions to the standards processes. During the TEMPs breakout session of the 2001 NIST workshop, significant emphasis was placed on the need to develop new test methods and methods for characterizing biomaterials [1]. The group determined that NIST could play a meaningful strategic role and overwhelmingly urged NIST to take a leadership position, working with collaborators in industry, the National Institutes of Health (NIH), FDA, clinicians, and standards organizations. A list of action items was developed and the group suggested appropriate roles for NIST in carrying out those actions. It was, and is, NIST's intent to respond to these calls for action, consistent with its mission and resources. This paper presents current NIST activities that are relevant to the action items that were identified.

Actions Identified for Standards for Tissue Engineered Medical Devices

The following is a complete list of the actions that the medical-device-industry workshop participants identified as those most needed. Detailed elucidation of the roles suggested for NIST and others, the kinds of standards needed (consensus standard, standardized test method, standard practice), priorities, and underlying rationale, is given in the NIST Internal Technical Report, NISTIR 6791 [1].

High-Priority TEMP Action Items Addressing Industry Needs Relative to NIST and the FDA Approval Process

- 1.1 Develop rapid, highly-accurate, phenotypic determination methods (also see 2.1 & 2.2).
- 1.2 Develop methodology to characterize human-animal co-cultured TEMPs, (particularly with respect to determining the percentage (number-fraction) of each cell type).
- 1.3 Develop criteria for assessing the persistence of degradable material.
- 1.4 Develop non-invasive imaging methods.
- 1.5 Pool information useful for facilitating approvals of TEMPs by the FDA.

The High-Priority TEMP Action Items Addressing Industry Needs Relative to NIST

- 2.1 Develop test methods for phenotype analysis and characterization.
- 2.2 Develop stem-cell analysis/characterization methods. (This is a separate, special consideration of action item 2.1.)
- 2.3 Develop consensus test-standards for temporary components of TEMPs; cells, bioactive agents and solid phase materials.
- 2.4 Identify or develop standards for preservation of cells.
- 2.5 Develop biomarkers for the identification of potentially infectious agents or xenogenic cells from co-cultures that are employed in the manufacture of TEMPs
- 2.6 Develop *in vitro* safety and efficacy assays for individual components of a final TEMP.

• 2.7 Develop standard, non cell-based safety and efficacy assays (e.g. *in vitro* calcification model) and reference materials for detecting residuals on TEMPS.
• 2.8 Develop genomic/proteomic assessments.

NIST Activities Relevant to Workshop-Identified Action Items

Research Addressing Action Items 1.1, 2.1 and 2.2

Measurements for Gene Responses to External Signals

Recently, specific genes have been shown to express different responses to the extracellular matrix. These genes produce proteins that guide cellular functions. Ongoing NIST research is directed toward coupling of fluorescent proteins to genes and utilizing fluorescence for specific indications of cell states and responses. These methods may be employed for tracking cellular activity and responses such as apoptosis, state of differentiation, proliferation, and adhesion to surfaces. This research has relevance to items 1.1, 2.1 and 2.2 (contact: Anne Plant, 301-975-3124, anne.plant@nist.gov). In a related activity, NIST is working on the development of measurement models and a concentration standard that consists of fluorescein immobilized on the surface of microspheres (contact Adolfas Gaigalas, 301-975-2873, adolfas.gaigalas@nist.gov).

Actions with Relevance to Action Item 1.5

Pooling of Data for Facilitating FDA Approvals

This action item called for the pooling of information useful for facilitating approvals of TEMPs by the FDA. Pooling of data presents an enormous challenge and involves not only data from biomaterials but also bioinformatics. Interoperability issues are involved that require consistent identifiers (labels or tags) of data along with software systems capable of accessing the data and extracting or exporting it for use in many other applications. Many activities at NIST support these kinds of efforts, but more extensive cooperation among all users in the health care community is needed. On August 1-2, 2002, NIST held a workshop, "Information Technologies for Healthcare: Barriers to Implementation", as the first of a series of workshops aimed at medical informatics (contact Dr. Ram Sriram, 301-975-3507, ram.sriram@nist.gov, or Lisa Carnahan, 301-975- 3362, carnahan@nist.gov). NIST also co-sponsored the September 19-20, 2002, NIH-FDA workshop "Medical Implant Information, Performance, and Policies (NIST contact: John Tesk, 301-975-6799, john.tesk@nist.gov). These workshops are relevant to item 1.5. They are among ongoing efforts across NIST aimed at bringing together stakeholders to address issues that will impact on the entire health care community, including tissue engineering. Details on other action items and issues may be found on pages 29-35 of NISTIR 6791; they are too numerous to be related here.

Research that Addresses Action Item 2.3

Measurements of Cell Responses to Material Surfaces

NIST is currently investigating the use of combinatorial methods for the development of test methods for the rapid assaying of cell responses to material surfaces. Gradients in

material properties and features provide continuously varying physical, chemical, or biological characteristics, which induce varying degrees of cell responses. Both material characterization and cellular response are part of the program. Materials characterizations are carried out in the Polymers Division of NIST (contact Newell Washburn, 301-975-4348, newell.washburn@nist.gov). The cell responses will be assessed within NIST's Biotechnology Division. NIST and ASTM are planning an October 2003 workshop on "Metrology of Cell Signaling and its Impact on Tissue Engineering" (contact: Anne Plant, 301-975-3124, anne.plant@nist.gov). A poster on this effort (Washburn et al.) can be found elsewhere in this symposium.

Imaging of Cells

At the NIST Center for Neutron Research (NCNR) in Gaithersburg, MD, a collaboration of university and government scientists will use super-chilled neutrons to probe the structure and interactions of cell membranes and their components, gathering information that is key to improving disease diagnosis and treatment. Enhanced understanding may help guide the design of new tissue-engineered medical devices. "Neutron probes offer the only realistic hope for many challenges in medicine and biology," says Stephen White, the University of California Irvine (UCI) biophysicist who leads the Cold Neutrons for Biology and Technology (CNBT) partnership. White has organized the CNBT partnership, which includes researchers from UCI, NIST, the University of Pennsylvania, Rice University, Carnegie Mellon University, the Duke University Medical Center and the Los Alamos National Laboratory. The CNBT team is now building a unique instrument with dual capabilities: diffractometry and reflectometry. To be completed in 2003, this instrument will provide cell membrane scientists with access to powerful technologies well beyond those available from the resources of individual researchers. For more information on CNBT, go to www.nist.gov/public_affairs/releases/neutrons.htm. For technical matters contact Stephen White, UC-Irvine, 949-824-7122, SHWhite@uci.edu or Susan Krueger, NIST, 301-975-6734, susan.krueger@nist.gov.

Characterization of Scaffolds

Another research project involves measurement technology for the characterization of porous scaffolds and the development of reference tissue scaffolds. Well-characterized scaffolds (materials composition, structure, surfaces, porosity, and mechanical properties) and the measurement technologies by which they are characterized were requested also by Picciolo et al. in the July 2000 NIST workshop, "Reference Data for the Properties of Biomaterials" [2]. Reference scaffolds can be employed for validating procedures and for providing materials for specific, known cellular responses against which new materials may be checked in the course of development of new TEMPs. For more on this topic refer to a paper earlier in this session from NIST (Washburn et al.) and one from the National Physical Laboratory and University of Brighton, Middlesex, United Kingdom (Mikhalovsky et al.). There is also a relevant poster at this symposium from NIST by Cicerone et al. on functional imaging of cell-material interactions.

Standards and Measurements for Mitochondrial Proteomics

NIST recently (September 17-18, 2002) held a workshop, "Systems Biology Approaches to Health Care: Mitochondrial Proteomics," that addressed underlying proteomic measurement technologies for detection and diagnosis of disease. Because the human mitochondrion is central to basic life functions for the generation of cellular

energy, and as such is the site of key components of the biosynthetic pathways, as well as the cellular decision points leading to apoptosis (i.e., programmed cell death), the underlying measurement technologies have particular relevance to TEMPs. Since the mitochondrion is a discrete subcellular organelle with a non-nuclear genome that is comprised of about 1000 or more different protein species with tissue-specific features, it can be a tangible model system for the development of clinical standards with direct health care implications. The focus of this workshop was to provide: (1) Assessment of the mitochondrion as an integrated model for systems biology studies, (2) Assessment of emerging proteomics technologies, (3) Identification of the standards needs for proteomic applications in the clinical diagnostics industry and, (4) Guidance for determination of appropriate data elements (common data elements, or CDEs) for health care proteomics (contact Peter Barker, 301-975-5402, peter.barker@nist.gov or Gregory Vasquez, 301-975-4195, gregory.vasquez@nist.gov).
The web site is: http://www.cstl.nist.gov/biotech/mito/mitoproteomics.html

Test Methods and Standard Reference Materials for DNA Sequencing

Human mitochondrial DNA (mtDNA) has become an important tool in forensic and medical studies as well as anthropological and evolutionary research. NIST has a long history of working with the medical communities and helping in the development of test methods and Standard Reference Materials (SRMs) to provide quality control and assurance that scientific and testing results are accurate [3]. NIST has available a Standard Reference Material (SRM 2392) to provide quality control for the amplification and sequencing of human mitochondrial DNA (mtDNA) or any DNA [4]. One of the reasons that SRM 2392 was developed is to provide assurance that the diagnoses of mtDNA diseases being conducted by the medical community were correct. The reference material also is useful for assessing the quality of cells and tissues that may be used for TEMPs. NIST also has developed a simple methodology to detect low levels (number fractions of 0.1 % to 20 %) of the single base pair heteroplasmic mutation MELAS (mitochondrial encephalomyopathy, lactic acidosis and stroke-like episodes) (A3243G) in total DNA extracted from blood [5]. This methodology could be useful in the detection of other low frequency hetroplasmic disease mutations. Barbara C. Levin was an organizer and speaker at the Mitochondrial Standards Workshop held in Dallas Texas in June of 2002 (contact Barbara Levin, 301-975-6682, barbara.levin@nist.gov).

Human Serum Proteomics Standards and SRM 1951a

NIST is currently evaluating SRM 1951a with six outside labs as a prototype proteomics standard for human serum. This SRM is available as a lipid reference, but because the processing that was done for producing SRM 1951a was "minimal" as far as affecting other proteins, it is considered as having a protein composition that is very close to that found in human serum. Hence, it is considered as a viable candidate reference standard for other proteins. This is the first "proteomics standard" in actual field trials and will be discussed as a prototype proteomics standard at a meeting in Europe in November 2002. The lead NIST researcher, Peter Barker, chaired the Human Proteomics Standards session at the organizational meeting of the Human Proteome Organization, that was held in September 2002. (contact Peter Barker, 301-975-5402, peter.barker@nist.gov or Michael Welch, 301-975-3100, michael.welch@nist.gov).

Research that Addresses Action Items 2.5, 2.6, and 2.8

Biomarkers for Inflammatory Responses to Polymer Substrates

NIST has research under way aimed at the development of measurement technologies that may be used to assess the cellular mechanism of how cells react to inflammatory stimuli from different polymer matrices. Rodriguez has noted that it is important to have biological safety check points in place during the manufacturing process of TEMPs [6]. NIST researchers are identifying biomarkers that have the ability to reveal oxidative damage to genomic DNA, mitochondrial damage, mutations, and chromosomal loss. Rodriguez has a poster at this symposium that describes NIST research comparing genomic and mitochondrial markers that can be used to detect cellular inflammation in tissue- engineered skin (contact Henry Rodriguez, 301-975-2578, henry.rodriguez@nist.gov).

Heightened Sensitivity to DNA Malignant Cells-NIST researchers Catherine O'Connell and Henry Rodriguez have been working on the detection of cellular mutations so as to identify malignant cells using recent technological advances in mutational scanning and chip technologies. These advances reduce the region of a gene that needs to be sequenced. This is a less time consuming and less costly process than the most commonly utilized method of DNA sequencing across the entire genome (the "gold standard"). At this symposium, a poster entitled "Molecular Biomarkers Used to Detect Cellular Genetic Damage in Tissue-Engineered Skin" describes this work in more detail. (contact Catherine O'Connell, 301-975-3123, catherine.oconnell@nist.gov).

Measurements for Assurance of Disease-Free Cells and Validation of Biomarker Assays

NIST has established an ongoing collaboration with the Cancer Biomarkers Group, Division of Cancer Prevention at the National Cancer Institute. One validation study involves quantification of chromosomal breaks within a specific chromosomal region. In normal peripheral lymphocytes from short-term cultures, induced breaks in this region have been shown to correlate with susceptibility to lung cancer. These validation and other technology evaluation activities support a large collaborative team of 35 discovery laboratories, eight clinical and epidemiological centers, and two other biomarker validation laboratories, all focused on improving early detection of solid tumors in the American public [7]. This work, when extended to other cells and tissues, may find applications for helping to ensure the use of disease-free cells for TEMPs. (contact Peter Barker, 301-975-5402, peter.barker@nist.gov).

Research that Addresses Action Item 2.7

Tissue-engineered Biomaterial Surface Structure Characterizations

NIST has a project underway that utilizes nonlinear and linear optical methods for determining the properties of interfaces and of molecules found at the surfaces of materials. The materials include those that are important to tissue engineering. The measurement methods include vibrationally resonant sum frequency generation (SFG)

spectroscopy. This method can provide surface specific measurements that exclude bulk effects and focus exclusively on the structure of molecules localized at the surface. Hence, this unique tool is a powerful addition to the armamentarium that is needed for making highly tailored surfaces for directing the responses of cells, localizing proteins, or attaching drugs in combinatorial medical devices. (contact Kimberly Briggman, 301-975-2358, kimberly.briggman@nist.gov, John Elliott, 301-975-8551, john.elliott@nist.gov, or John Stephenson, 301-975-2372, john.stephenson@nist.gov).

Summary

The activities described here are standards-related needs/recommendations made at NIST workshops. They represent a small, but significant, fraction of NIST health-care-related research. For more information, the reader is encouraged to visit the NIST Industrial Liaison Office web site: http://www-i.ilo.nist.gov/ and click on"Health Care".

References

[1] Chapekar, M. and Vasquez, G., "Tissue Engineered Medical Devices," *in "Workshop on Standards for Biomedical Materials and Devices", National Institute of Standards and Technology Internal Report 6791*, J.A.Tesk, and D.Hall, eds., September 2001, pp. 22-28. (http://www-i.ilo.nist.gov/).
[2] Tesk, J.A., "Special report: NIST Workshop on Reference Data for the Properties of Biomaterials," *Applied Biomaterials*, Volume 58, Issue 5, 2001, pp. 463-466.
[3] Levin, B. C., Cheng, H., Kline, M. C., Redman, J. W., and Richie, K. L., "A Review of the DNA Standard Reference Materials Developed by the National Institute of Standards and Technology," *Fresenius' J. Anal. Chem.* Volume 370, 2001, pp. 213-219.
[4] B. C. Levin, H. Cheng, and D. J. Reeder, "A Human Mitochondrial DNA Standard Reference Material for Quality Control in Forensic Identification, Medical Diagnosis, and Mutation Detection", *Genomics* Volume 55, 1999, pp.135-146.
[5] D.K. Hancock, F.P. Schwarz, F. Song, L-J.C. Wong and B.C. Levin, "Design and Use of a Peptide Nucleic Acid for the Detection of the Heteroplasmic Low-Frequency MELAS (Mitochondrial Encephalomyopathy, Lactic Acidosis And Stroke-Like Episodes) Mutation in Human Mitochondrial DNA", *Clinical Chemistry*, accepted for publication, 2002.
[6] Rodriguez, H., "Cellular Biomarkers Used to Detect Damage in Tissue-engineered Medical Products," *Biomaterials FORUM*, Volume 24, Issue 33, 2002, p. 12.
[7] Barker, P.E., Atha, D., Hocker, D., Markowitz, M., Srivastava, S., Wang, W., and O'Connell, C.D., "NIST Collaborates with Cancer Biomarkers Group," *Biomaterials FORUM*, Volume 24, Issue 3, 2002, p. 16.

Matthew C. Summitt,[1] Donna M.K. Squillace,[2] and John R. Bianchi[1]

Mechanical Evaluation of Allograft Bone

Reference: Summitt, M. C., Squillace, D. M. K., and Bianchi, J. R., **"Mechanical Evaluation of Allograft Bone,"** *Tissue Engineered Medical Products (TEMPs), ASTM STP 1452*, E. Schutte, G. L. Picciolo, and D. S. Kaplan, Eds., ASTM International, West Conshohocken, PA, 2004.

Abstract: Standard test methods to evaluate the material properties of cortical bone do not exist. A test methodology that accounts for the anisotropy of cortical bone by subjecting the material to multiple modes of loading is proposed. The four test included are axial compression parallel to the longitudinal axis, tensile load perpendicular to the long axis (diametral compression), double lap shear, and three-point bend. These methods provide a means of documenting the biomechanical changes that may occur as a result of unique attributes inherent to a donor or the processes that the donor tissue is exposed. Several examples illustrate how these methodologies demonstrate the relationship between process and mechanical properties.

Keywords: Mechanical properties, material characterization, allograft, cortical bone, mechanical testing

Introduction

While the mechanical properties of cortical bone have been well established in the literature [1, 2], large variations in value appear. One source of these variations is the use of non-standardized testing protocols. In order to effectively evaluate the material properties of cortical bone, standardized testing methods are needed. Due to the numerous factors that affect the mechanical properties of bone - gender, anatomic location, age, processing, storage, and sterilization - an effective testing methodology is vital to properly evaluate donor material.

A testing methodology that included uniform preparation and testing procedures was designed to assess the mechanical properties of cortical bone. The mechanical properties of bone depend on the direction in which load is applied. In order to account for this anisotropic nature of bone, test methods must provide a means to characterize the properties in a variety of directions.

[1]Research engineer and manager, respectively, Technical Services Department, Regeneration Technologies, Inc., 11621 Research Circle, Alachua, FL 32615.

[2]Research engineer, Research Department, Regeneration Technologies, Inc., 11621 Research Circle, Alachua, FL 32615.

The procedure described evaluated specimens under four modes of loading - axial compression parallel to the longitudinal axis, tensile load perpendicular to the long axis (diametral compression), double lap shear, and three-point bend.

Experimental Methods

Specimen Preparation

Specimens are machined from the cortical portion of femoral and tibial shafts. All tissue was maintained submerged in saline during the entire preparation process excluding the actual machining steps. The machined specimens are oriented so that the long axis of the bone coincides with the long axis of the test specimen. All specimens were machined into cylinder to specific dimensions (Table 1).

Table 1 — *Specimen Geometry.*

Test	Diameter (mm)	Length (mm)
Axial	3-6	5-7
Diametral	3-6	5-7
Shear	0.98-2.91[1]	18-23
Three-Point Bend	2.16 ± 0.10[2]	38 + 5

[1] Diameter should not vary more than 0.15 mm along its length
[2] Diameter should not vary more than 0.2 mm along its length

Testing Procedures

Prior to mechanical testing, the length, diameter and mass of the specimens were measured. Axial and diametral compression specimens were placed onto the testing machine in the center of the steel plate (Fig. 1). The specimen was loaded to failure at a rate of 25 mm/min. Failure was determined as a decrease in load of 500 N for axial compression and 200 N for diametral compression. Shear test specimens were secured in the fixture (Fig. 2). The holes in the three plates were aligned to facilitate the placement of the specimen. The specimen was tested to failure at a rate of 19.1 mm/min. The actuator was positioned to move a distance at least twice the specimen diameter. Three-point bend specimen was located on the fixture (Fig. 3) and loaded to failure at a rate of 6.35 mm/min. The actuator was positioned to move a minimum of 2.5 times the diameter of the specimen.

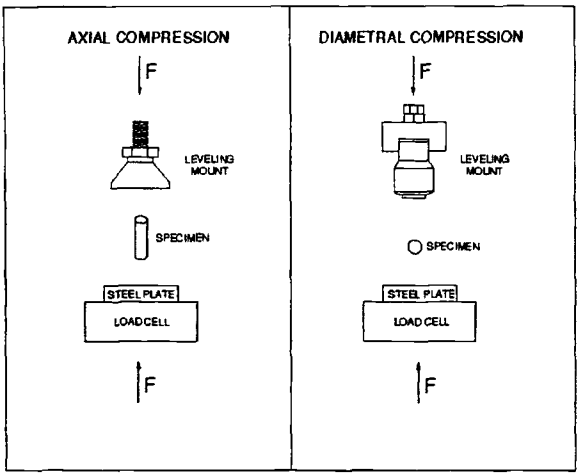

FIG. 1 — *Axial and Diametral Compression Setup.*

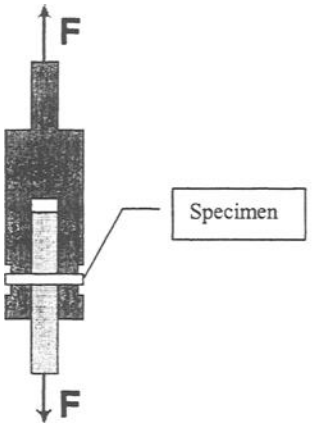

FIG. 2 — *Shear Setup.*

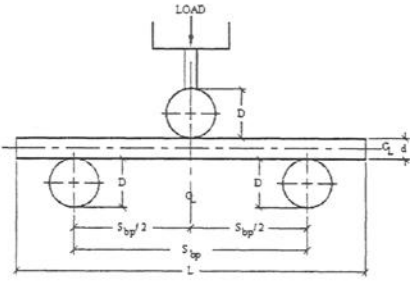

FIG. 3 — *Three-Point Bending Setup.*

Calculation of Results

The density of each specimen is the mass divided by the volume (1)

$$density = \frac{mass}{\pi * (diameter/2)^2} \tag{1}$$

The equations for axial compressive stress, diametral compressive stress, shear stress and bending stress are given in (2-5) respectively

$$Stress = \frac{2 * load}{\pi * (diameter)^2} \tag{2}$$

$$Stress = \frac{2 * load}{\pi * diameter * length} \tag{3}$$

$$Stress = \frac{2 * Load}{\pi * (diameter)^2} \tag{4}$$

$$Stress = \frac{(3/2) * Load * S_{bp}}{(diameter)^3} \tag{5}$$

Results

Testing was performed on cortical bone using the test methods described above and values were comparable to those seen in the literature [1, 2] (Table 2). Furthermore, these testing methods were used to characterize to effects of donor attributes, storage methods, and sterilization techniques on the strength of cortical bone. The following gives examples of where these test methods have been used and results from one test method.

Donor attributes like age and gender can play an important role in the strength of bone. Representative population of donors composed of both males and females between the ages of 18 and 67 years were compared to an elderly female population (70-80 years). Results for diametral compression demonstrated that cortical bone derived from an elderly female population was weaker (Fig. 4).

Freeze-drying or lyophilization is a method of removing moisture from bone to allow it to be stored at room temperature for an extended period of time. To evaluate the effects of lyophilization on cortical bone strength, axial compression of control (frozen, not lyophilized bone), lyophilized bone, and lyophilized and rehydrated bone was tested. Results showed that lyophilization increased the compressive strength of bone; however, after rehydration the compressive strength was similar to that of the control (Fig. 5).

The shear test illustrated how the methodology may be utilized to elucidate the effects of irradiation on cortical bone. The effect of irradiation on the strength of cortical bone at room temperature *versus* bone irradiated while packed in dry ice was evaluated.

The shear results showed a decrease in shear strength after irradiation at room temperature (Fig. 6). Three-point bend testing was performed on specimens treated through a new, low temperature chemical sterilization method and untreated specimens. There was no detectable difference between untreated and treated specimens tested in three point bending (Fig. 7).

Table 2 — *Current results compared to literature values.*

	Strength (MPa)	
Test	Current Testing Results	Literature Values
Axial	193	131-206
Diametral	29	10-56
Shear	63	53-70
3-Point Bend	130	50-300

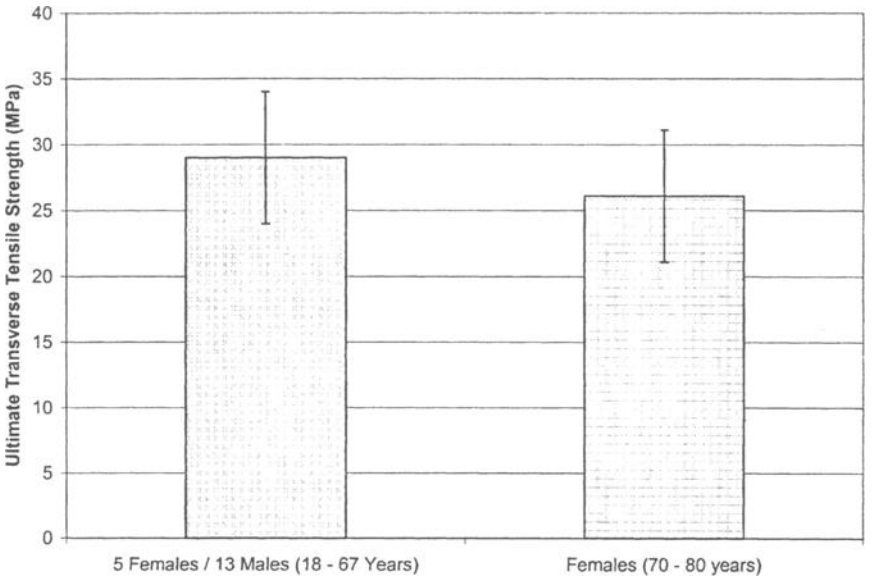

FIG. 4 — *Diametral Compression Results.*

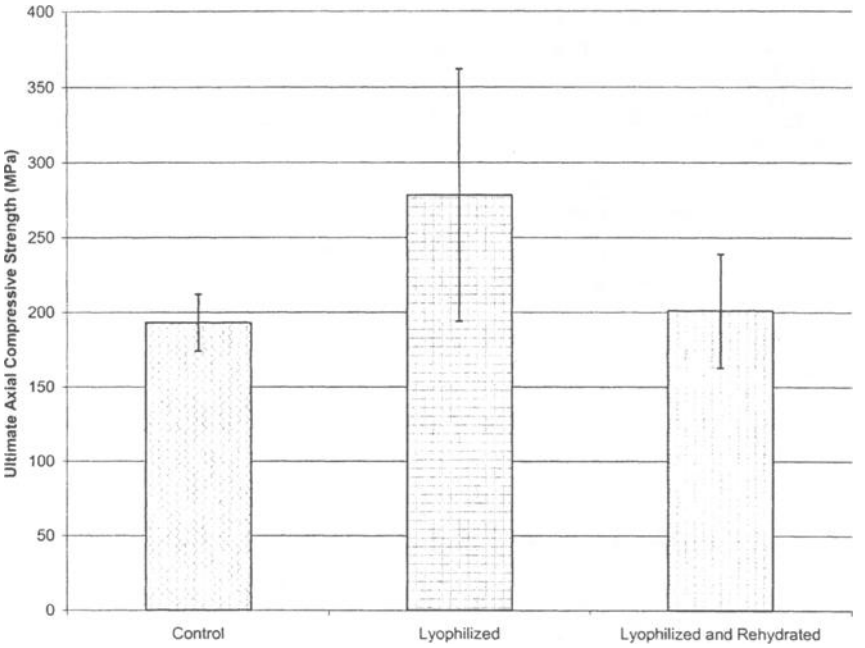

FIG. 5 — *Axial Compression Results.*

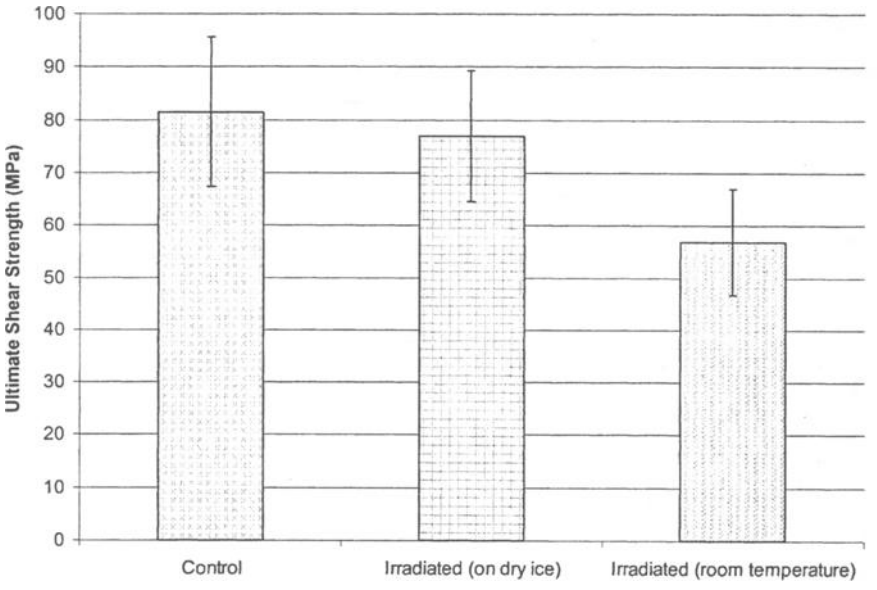

FIG. 6 — *Double Lap Shear Results.*

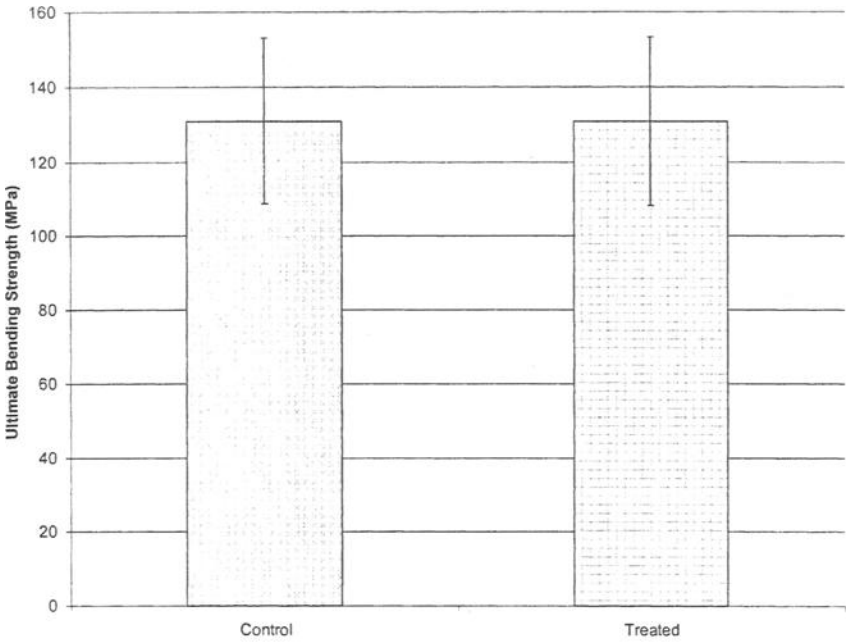

FIG. 7 — *Three Point Bend Results.*

Conclusions

The test methods presented in this paper allow for characterization of the anisotropic properties of cortical bone. This testing methodology may be used to successfully assess the effects that donor characteristics, processing methods and other factors have on the biomechanical properties of bone. While this provides a valuable tool for evaluating material utilized to manufacture grafts for implantation, these tests are not intended to replace evaluation of final product design. Evaluation of a finished graft is always necessary to ensure its safety.

References

[1] Cowin, S. C., *Bone Mechanics*, 1st ed., CTC Press, Boca Raton, FL, 1989, p.313.

[2] Martin, R. B., Burr, D. B., and Sharkey, N. A., *Skeletal Tissue Mechanics*. New York; Springer, 1998, xiv, p.392.

C. Randal Mills,[1] Michael R. Roberts,[1] Jerry Y. Chang,[1] John R. Bianchi,[2] Matthew C. Summitt[2]

Method to Determine Germicidal Inactivation in Allograft Processing

REFERENCE: Mills, C. R., Roberts, M. R., Chang, J. Y., Bianchi, J. R., and Summitt, M. C., "**Method to Determine Germicidal Inactivation in Allograft Processing,**" *Tissue Engineered Medical Products (TEMPs), ASTM STP 1452*, E. Schutte, G. L. Picciolo, and D. S. Kaplan, Eds., ASTM International, West Conshohocken, PA, 2004.

ABSTRACT: Because the risk of disease transmission remains even though stringent requirements for selecting and screening allograft donors have been adopted, processing methods capable of sterilizing tissue are needed. This test method discusses a means of evaluating the efficacy of allograft processing methods to eliminate bacterial contamination within the matrix of cortical bone. A *Bacillus stearothermophilus* biological indicator is inserted into a cavity drilled into the cortex of a long bone and the bone is processed under different treatment methods. A similar set of soft tissue specimens was prepared by inserting the spore strip into the soft tissue matrix and stitching it closed. After treatment the spore strips are aseptically removed and evaluated for growth. This test method allows for the evaluation of sterilization processes of tissue-based products with complex matrices.

KEYWORDS: sterilization, allograft, allograft processing, disease transmission

Introduction

Albeit in very small amounts, the microvasculature of bone and soft tissue can harbor potentially infectious blood-borne agents. Recently, the Centers for Disease Control and Prevention (CDC) investigated and found 26 potential cases of infection due to allograft tissue [1]. For this reason there is a need for developing processing systems that can effectively and reproducibly inactivate microbial contaminants within the matrices of bone and soft tissue. Standard sterilization methods such as gamma irradiation, high temperature thermal treatments, and ethylene oxide have been shown to adversely effect either the biomechanical properties or biocompatibility of tissue products [2-9]. Low temperature chemical germicides and cold sterilants have been shown to be efficacious with regard to antimicrobial capacity, but the issue of complex matrix penetration has been inadequately demonstrated. A testing method is called for to effectively and reproducibly evaluate the elimination of contaminants within the complex matrices of bone and soft tissue.

[1] Vice President of Operations, Manager of Process Research, and Manager of Product Sterilization, respectively, Regeneration Technologies, Inc., 11621 Research Circle, Alachua, FL, 32615.
[2] Manager and research engineer, respectively, Technical Services Department, Regeneration Technologies, Inc., 11621 Research Circle, Alachua, FL, 32615.

The following test method uses *B. stearothermophilus* spore strips (NAMSA® item number STS-06) implanted within the matrices of bone and soft tissue. The spore was chosen because of its well-established resistance to antimicrobial agents [10]. The resistance profile and high concentrations (at least $1x10^6$ CFU/strip) of spores used to test the system are much greater than the types and quantities of microorganisms that would be typically found in contaminated allograft tissue. Cortical bone and tendons were chosen for the study due to their relative density and thickness, providing worst case conditions for aqueous chemical perfusion. Tissue specimens were chosen from a cross section of donors representative of the tissue donor population at large. This is done to control possible differences in perfusion due to demographic variability with respect to relative diaphyseal cortex thickness, bone density, and levels of endogenous blood and lipids that may interfere with sporicidal efficacy.

Experimental Methods

Specimen Preparation

Cortical shafts were derived from cadaveric donors, sectioned into uniform segments, and a 2x15mm longitudinal cavity was drilled into the cortex (Fig. 1). Bone-patellar tendon-bone specimens were derived from cadaveric donors and a lateral incision was created parallel to the tendon fibers approximately 15mm deep (Fig. 2).

Using aseptic handling methods, a biological indicator was removed from its envelope with sterile forceps. The indicator was rolled into a cylinder and placed in the pre-drilled cavity in the cortical bone. A self-tapping stainless steel screw (McMaster-Carr® Part Number 92364A146) was placed into the hole and tightened until the head of the screw was flush with the surface of the bone. The design of the cavity, spore strip length and length of screw were selected to minimize dead space within the insertion cavity. For the bone-tendon-bone samples, the indicator was inserted into the incision between the tendon fibers and the opening was sutured closed.

Treatment

Bone and tendon specimens were separated into two treatment groups. Half of the specimens were processed through a treatment regime that allowed the tissue to soak in sequential solutions of germicides for fixed periods of time in a controlled temperature (48°C) ultrasonic bath (20-40kHz). Germicides tested were hydrogen peroxide, isopropanol, sodium dodecyl sulfate and Triton X-100 (octyl phenol ethoxylate). Germicide concentrations and contact times were based on proprietary formulations. The other half of the specimens saw the same chemicals, temperature, and contact times but with the addition of pressure/vacuum cycling to affect matrix penetration. Specimens were placed into an Erlenmeyer flask fitted with a stopper and tube connected to a vacuum pump. Alternating vacuum and pressure cycles were performed using

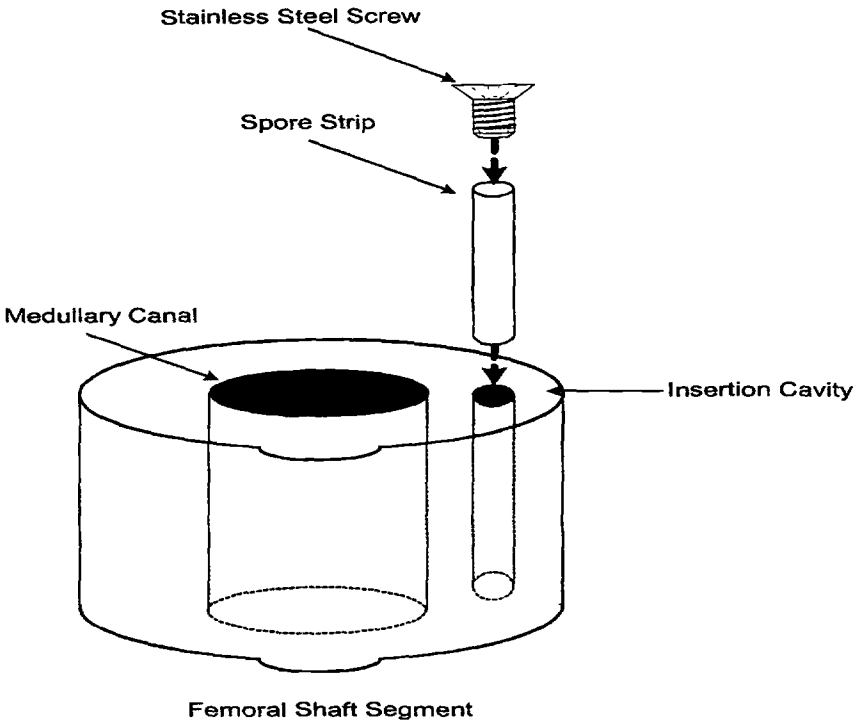

Fig. 1 – *Spore strip inserted into cortical bone.*

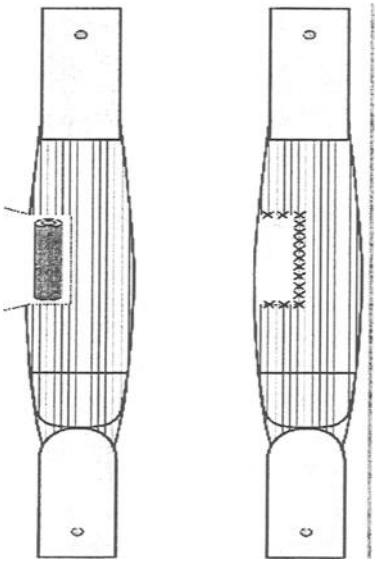

Fig. 2 – *Spore strip inserted into soft tissue.*

proprietary pressure parameters and dwell times. Testing was repeated in triplicate with 12 specimens per group.

Sterility Testing

Upon completion of the treatment the biological indicators were removed from the specimens using aseptic techniques and rinsed with copious amounts of Trypticase Soy Broth culture media. The strips are then placed into fresh TSB media jars, which are then placed in an incubator at 56°C and allowed to incubate for 14 days. After 14 days all specimen were evaluated for growth. Positive results are indicated by media turbidity, and confirmed as *B. stearothermophilus* by subculturing and organism speciation. Positive and negative controls, along with bacteriostasis testing following United States Pharmacopeia (USP) guidelines were performed to confirm the culturing system.

Results

Biological indicators that were subjected to chemical soaking with ultrasonication demonstrated growth of *B. stearothermophilus* while specimens that were subjected to chemicals with the addition of pressure/vacuum cycles were determined not to grow any organism, meeting the criteria for sterilization (Table 1). Negative and positive controls returned appropriate results, and the specimens were determined to have no effect on the validity of the results.

TABLE 1 – *Results of Testing.*

Test Group	Number of Specimens	# Positive	# Negative (no growth)
Ultrasonic Soak #1	12	12	0
Ultrasonic Soak #2	12	12	0
Ultrasonic Soak #3	12	12	0
Pressure Cycling #1	12	0	12
Pressure Cycling #2	12	0	12
Pressure Cycling #3	12	0	12

Conclusions

This test method shows that it is possible to demonstrate the sterilization of tissue-based products with complex matrices. It further demonstrates that liquid chemical germicides can be effective within the tissue environment under the appropriate processing conditions. This method is repeatable when performed using an appropriately controlled protocol to verify test system integrity.

References

[1] CDC. "Update: Allograft-Associated Bacterial Infections --- United States, 2002." *MMWR*: Centers for Disease Control And Prevention; 2002:207-210.

[2] Arizono T, Iwamoto Y, Okuyama K, Sugioka Y. "Ethylene oxide sterilization of bone grafts. Residual gas concentration and fibroblast toxicity." *Acta Orthop Scand.* 1994;65:640-2.

[3] Bianchi JR, Ross K, James E. Keesling J, Mills CR. "The Effect of Preservation/Sterilization Processes on the Shear Strength of Cortical Bone." *Proceedings of the 1999 Bioengineering Conference.* 1999;42:407-408.

[4] Jackson DW, Windler GE, Simon TM. "Intraarticular reaction associated with the use of freeze-dried, ethylene oxide-sterilized bone-patella tendon-bone allografts in the reconstruction of the anterior cruciate ligament." *Am J Sports Med.* 1990;18:1-10; discussion 10-1.

[5] Loty B, Courpied JP, Tomeno B, Postel M, Forest M, Abelanet R. "Bone allografts sterilised by irradiation. Biological properties, procurement and results of 150 massive allografts." *Int Orthop.* 1990;14:237-42.

[6] Rasmussen TJ, Feder SM, Butler DL, Noyes FR. "The effects of 4 Mrad of gamma irradiation on the initial mechanical properties of bone-patellar tendon-bone grafts." *Arthroscopy.* 1994;10:188-97.

[7] Roberts TS, Drez D, Jr., McCarthy W, Paine R. "Anterior cruciate ligament reconstruction using freeze-dried, ethylene oxide-sterilized, bone-patellar tendon-bone allografts. Two year results in thirty-six patients." *Am J Sports Med.* 1991;19:35-41.

[8] Silvaggio VJ, Fu FH, Georgescu HI, Evans CH. "The induction of IL-1 by freeze-dried ethylene oxide-treated bone-patellar tendon-bone allograft wear particles: an in vitro study." *Arthroscopy.* 1993;9:82-6.

[9] Simonian PT, Conrad EU, Chapman JR, Harrington RM, Chansky HA. "Effect of sterilization and storage treatments on screw pullout strength in human allograft bone." *Clin Orthop.* 1994:290-6.

[10] Block SS. *Disinfection, Sterilization, and Preservation.* 5th ed. Philadelphia: Lea & Febiger; 2001.

Marcus T. Cicerone,[1] Joy P. Dunkers,[1] and Newell R. Washburn[1]

Towards *In-Situ* Monitoring of Cell Growth in Tissue Engineering Scaffolds: High Resolution Optical Techniques

Reference: Cicerone, M.T., Dunkers, J.P., and Washburn, N.R., "**Towards *In-Situ* Monitoring of Cell Growth in Tissue Engineering Scaffolds: High Resolution Optical Techniques,**" *Tissue Engineered Medical Products (TEMPs) ASTM STP 1452*, E. Schutte, G.L. Picciolo, and D.S. Kaplan, Eds., ASTM International, West Conshohocken, PA, 2004.

Abstract: Inability to obtain cellular-level information about progress of cell growth in tissue-engineering (TE) scaffolds is a pervasive problem. We demonstrate that a confocal microscope with two collinear contrast mechanisms, optical coherence, and fluorescence, can be used to perform non-destructive imaging of a polymer TE scaffold containing osteoblasts. We show that the combination of the techniques shows promise for *in situ* measurements of cell growth in a bioreactor, even for highly opaque TE scaffolds.

Keywords: coherence microscopy, fluorescence microscopy, morphology, OCT, tissue engineering scaffold

Introduction

It is generally understood that a complex interaction of many variables influences the success of cell infiltration, proliferation, and differentiation within a tissue scaffold (TS). One characteristic that has a large influence on the development of functioning tissue is the three-dimensional (3D) morphology of the scaffold itself [1,2].

[1] Research Scientists, Polymers Division, National Institute of Standards and Technology, 100 Bureau Drive, Mail Stop 8543, Gaithersburg, MD 20899-8543.

Quantification of morphological characteristics of the pores, such as volume, size distribution, connectivity, tortuosity, local curvature and composition, and comparison of those quantities with local cell viability will undoubtedly play an important role understanding the rich interaction between scaffold and cell.

A non-invasive method for scaffold characterization and, ideally, simultaneous cell monitoring, is needed. X-ray computed micro-tomography has been used to yield 3D images of biomaterials at a resolution of 14 μm, [3] and more recently, commercial instruments are available with resolution of (2 to 3) μm, but while this method is innocuous to the scaffold, it has the disadvantage of being potentially damaging to biological tissue, so that *in-situ* imaging is not feasible. NMR [4] has also been used for 3D imaging of biomaterials and tissues, but spatial resolution attainable by NMR methods is typically about 10 μm; insufficient for imaging at the cellular level. Confocal microscopy can give the desired spatial resolution, and is used extensively for cellular imaging in optically "clean" samples. Some work has been reported on scaffold characterization using laser scanning confocal microscopy (LSCM) [5,6], but the image depth is limited to ≈ 80 μm in more opaque systems, such as many TE scaffolds, due to large background signals from scattered light.

Optical coherence tomography (OCT) is a photon time-of-flight method that has both excellent background rejection capability against light scattered out-of-plane, good dynamic range (> 100 dB), and good sensitivity (≈ 1 pW reflected light), making it ideal for obtaining image data deep in highly scattering media. However, without an expensive ultra-broadband light source [7], OCT generally does not give spatial resolution at the ≈ 1 μm level that is desirable for monitoring cells and obtaining structural information of the scaffold. Izatt et al. [8] demonstrated that when an OCT instrument is configured with confocal optics, the instrument response, or point spread function (PSF) is a product of the OCT and confocal PSFs. Thus, a confocal OCT, or optical coherence microscope (OCM) gives the background rejection, sensitivity, and dynamic range of an optical coherence tomography instrument, and also excellent spatial resolution inherent in a confocal microscope. We have taken the additional step of implementing a fluorescence detection channel that is collinear with the OCM channel. In this way we will be able to obtain structural information from the OCM simultaneously with functional information about, e.g. labeled cells, from the fluorescence channel. Beaureparie et al. have implemented a similar marriage previously [9]. They used 830 nm light from a femtosecond laser system to excite two photon fluorescence and simultaneously collected a coherence signal. The system we describe below is significantly less expensive.

In this work we report on nondestructive imaging of a polymeric TE scaffold, demonstrating the improvement in resolution with OCM, as compared to OCT. We also present preliminary data to show the applicability of the OCM / fluorescence combination to *in-situ* cell monitoring, even deep within a TE scaffold.

Experimental

Scaffold Preparation

Poly(ε-caprolactone) (PCL) is blended with poly(ethylene oxide) (PEO) in a twin-screw extruder to form a bicontinuous, two-phase material with micrometer-sized domains. In this work, PCL and PEO were mixed in equal weights. Selective dissolution of the PEO with water results in a porous material, the characteristic pore size of the TE scaffold is controlled by annealing and can reach in excess of 100 μm. The scaffolds in this work were annealed at 75 °C for times in the range of (20 to 30) min. A more detailed description of scaffold preparation is provided elsewhere [10]. The scaffold was immersed in an index matching fluid prior to imaging.

Microscopy Optics and Instrumentation

Figure 1 shows a schematic of our OCM / fluorescence setup. The OCM system consists of a superluminescent diode (SLD) centered at 1.31 μm, in the near infrared (NIR), with a bandwidth of 70 nm (AFC, Hull, Quebec, Canada).[2] The detection system is a fiber-optic optical coherence domain reflectometer built by Optiphase (Van Nuys, CA). The reflectometer is capable of distinguishing reflections with s and p polarization, but in this work, we are monitoring only s reflections. The NIR light is transported by a single mode, polarization-maintaining fiber (0.16 NA), and is launched into a bulk optic system via a 0.55 NA collimating lens. The light then passes through a variable neutral density filter and a cold mirror. A 3:1 expanding

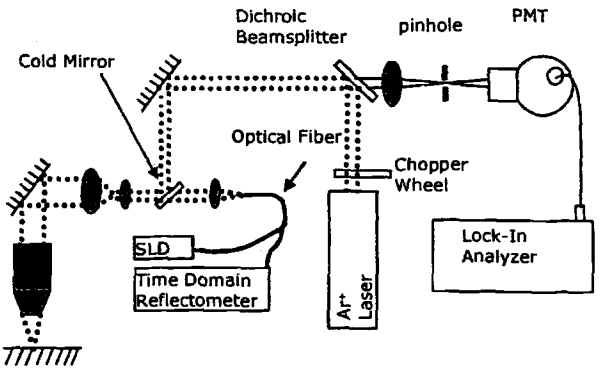

Figure 1 - Experimental configuration of collinear OCM and confocal fluorescence instruments. See text for explanation.

[2] Identification of a commercial product is made only to facilitate experimental reproducibility and to adequately describe experimental procedure. In no case does it imply endorsement by NIST or imply that it is necessarily the best product for the experimental procedure.

telescope is employed to fill the aperture of the objective, an EpiPlan –NEOFLUAR 100X 1.3 NA oil-immersion objective (Zeiss, Germany). The objective has a working distance of 370μm. Reflected light is returned to the single mode fiber, which acts as a confocal aperture for the detection system. The return light has essentially the same ray characteristics as the light delivered (beam diameters, etc.); thus, since the emission and collection aperture are the same, the collection aperture is fixed at 1 Airy unit (AU).

The reference arm of the interferometer is driven by piezoelectric modulators at 300 Hz and filtered at a Doppler frequency of 705 kHz. The dynamic range of the system is 110 dB. In the absence of the high NA objective, (i.e., in OCT mode), this instrument is capable of 19 μm axial resolution, which is slightly degraded from the 12 μm theoretical value for a 70 nm bandwidth source due to group dispersion velocity mismatch in the sample and reference arms. The theoretical values for transverse and axial spatial resolution of the confocal OCM configuration are 0.51 μm and 1.4 μm respectively. The theoretical axial resolution is obtained as the FWHM of the product of the point spread functions of the OCT (Gaussian, with FWHM of 19 μm), and the confocal geometry (Lorentzian with FWHM of 1.5 μm).

A first-surface mirror was moved axially through the focus of the beam, and the OCM response was measured as a function of the axial position of the mirror. The axial resolution of the system was determined to be 1.5±0.3 μm (FWHM of the response function), which is in accord with the theoretical value for a detection pinhole of 1 Airy unit (AU).

Figure 1 also shows the confocal fluorescence system, which is comprised of an air-cooled Omnichrome argon ion laser (Melles Griot, Carlsbad, CA). The 488 nm laser light is sent through a bandpass filter, a dichroic beam splitter, and several turning mirrors before reaching a cold mirror where it becomes collinear with the NIR beam. The fluorescence signal propagates back to the dichroic beam splitter where the excitation line is filtered out. Confocal gating of the fluorescence signal is accomplished by passing the collected light through a 10 μm pinhole that was placed at focus of a 0.15 NA objective. The excitation light was chopped at 1.5 kHz, and the fluorescence signal was detected using a photo-multiplier tube (Oriel, Stratford, CT) and lock-in amplifier (Perkin Elmer, Freemont, CA).

The focal points of the 488 nm

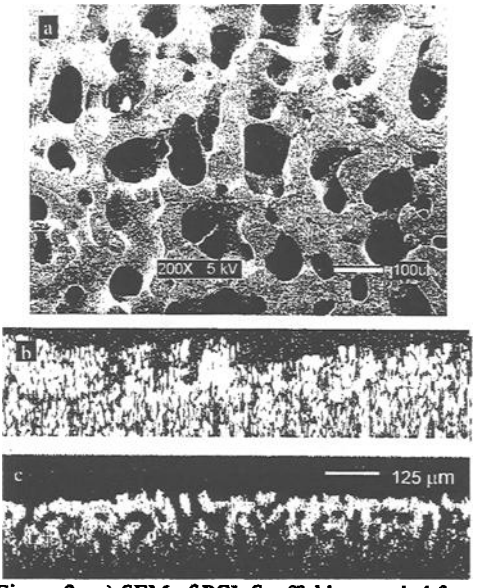

Figure 2 - a) SEM of PCL Scaffold, annealed for 20 min at 75 °C. b) and c) OCT and OCM images (respectively) taken on a similar scaffold to that in a). Imaging conditions for SEM, OCT, and OCM are given in the text.

and NIR beams are separated by (5.8 ± 0.1) μm,[3] with the visible light being focused closer to the objective. This is due to chromatic aberration of the objective. It could be corrected by using a reflective objective, or by delivering a slightly converging NIR beam or slightly diverging visible beam to the objective.

Two-dimensional imaging is performed simultaneously for the OCM and fluorescence channels by repeating a process of scanning the sample in the x direction and subsequently stepping in the y direction. The scanning and stepping are accomplished using motorized stages (Newport, Irvine, CA). After each x-y scan, the sample is moved in the z direction by a motorized stage with a maximum resolution of 100 nm (ASI Inc., Eugene, Oregon). The x-y stages were not designed for high-resolution work; they are specified by the manufacturer to give resolution of 1 μm and repeatability of 5 μm. Our experimental lateral resolution depends on repeatability, and is limited to 5 μm in all OCM / fluorescence images presented here by the x-y stage performance. Experimental axial resolution is limited by the optical arrangement, and is the same as is specified above.

Results and Discussion

Figure 2 shows images of PCL TE scaffolds obtained by SEM, OCT and OCM. Other than contrast scaling adjustments, no post-processing image manipulation routines have been applied. Image a) is an SEM image from a PCL scaffold that was annealed for 20 min at 75 °C. In preparation for data acquisition, the TS was rinsed with methanol, dried under vacuum, and sputter-coated with gold. The SEM image was obtained with a Jeol JL-5300 electron tomograph operating at 5 kV and 50 μA. Images b) and c) are cross-sectional images of PCL scaffolds that were annealed for 30 min at 75 °C, obtained with OCT and OCM respectively. In these images, the white pixels represent volumes from which reflection was detected (i.e. occupied by scaffold matrix material). One sees immediately that without further image manipulation it is impossible to distinguish clearly between pore and matrix from the OCT data, however, the contrast obtained with OCM is sufficient that this distinction can be made easily. The apparent loss of sensitivity at depths greater than 150 μm

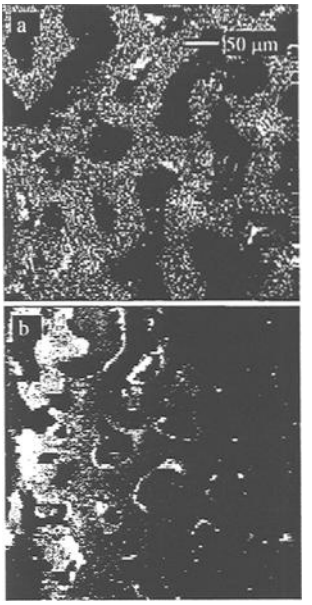

Figure 3 - Dual mode imaging of a PCL scaffold cultured with fluorescently stained osteoblasts. The images were acquired near the scaffold surface. a) confocal OCM image. b) confocal fluorescence image.

[3] All statements of standard uncertainty quoted herein are ± 1 standard deviation.

below the scaffold surface in image c) is due to a sub-optimal optical configuration in place at the time that this data was acquired. Also, due to the optical configuration available at the time, the axial and lateral optical resolution of image c) are 6 μm and 1.5 μm respectively. Better optical quality is obtained and displayed in the images of Figures 3 and 4.

There appears to be a difference in the pore distribution size between images a) and c) in Figure 2; in particular, the pores seem to be smaller in the latter. This apparent difference probably reflects a real difference in the pore sizes. The two scaffolds represented here were made with different batches of PCL. While both batches had a nominal weight average molecular weight of 80 000, the batch from which the scaffold in image a) was made seems to have a slightly lower average molecular weight that the other. This supposition is based on the relative processing characteristics of the two batches, and was not tested quantitatively, but is consistent with the difference in average pore size we see.

Figure 3 shows confocal OCM and fluorescence images from the same TE scaffold in the top and bottom panels, respectively. This scaffold was seeded with primary chick osteoblasts and incubated for six weeks. The cells were then fixed and stained with eosin, so that they could be visualized by fluorescence microscopy.

The dark areas in the OCM image represent pores, and the lighter areas are the scaffold matrix. With the improved spatial resolution that we attain with OCM over OCT, we are able to obtain clear scaffold images with good spatial resolution. It was not our expectation that OCM would give much contrast between the cells and the matrix, but the highly reflective (white) areas in this image appear to be due to cell colonies. This is supported by the fluorescence image (lower panel). The bright areas here represent groups of cells. We notice that the cells are adhered to the scaffold walls, as expected, and that there does not seem to be any strong preference for either high local curvature or flatter surfaces, although these images have not been analyzed quantitatively. We note that the fluorescence data were obtained very near the top of the scaffold, and that the gradual transition from high to low background as you go from left to right in the image is due to a slight tilt of the scaffold with respect to the image plane. In the left side of the image, some intensity was probably due to cells found on the top surface of the scaffold.

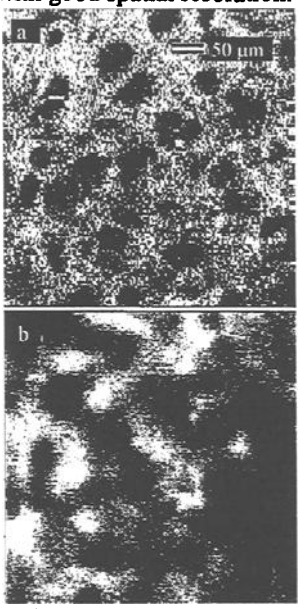

Figure 4 - Dual mode imaging of a PCL scaffold, stained with acridine orange. The images were acquired 180 μm from scaffold surface. a) confocal OCM image. b) confocal fluorescence image.

Differences in the morphology of the scaffold are apparent between the two images in Figure 3. These differences

originate from the fact that image planes are separated by roughly 6 μm, with the OCM image being deeper into the sample, as indicated above. Due to this separation, one gets a sense for the local 3D structure by comparing the differences between the images. We also note that we did not find appreciable cell population in the scaffold imaged in Figure 3. This may have been due to poor perfusion of nutrient, or a "skin" which sometimes forms near the surface during preparation of the scaffold.

Ultimately, one would like to image cells deep in the scaffold, noninvasively, and with high resolution. This is particularly difficult when the scaffold material is highly scattering, as is the case for the polycrystalline PCL scaffolds imaged here; data quality will gradually degrade as one attempts to image deeper into the scaffold. However, due to the background rejection capability of OCM, we are able to obtain structural information even 180 μm into the scaffold, when steps are taken to ameliorate the mismatch of refractive index between the bath and the PCL. We observe that when index-matching oil ($n_D = 1.563$) is used as the bath, imaging with the OCM can be accomplished down to about (175 to 250) μm. If an aqueous solution of ≈ 0.40 mass fraction glycerol is used as the index-matching bath, the imaging range does not suffer significantly and this bath is not likely to be harmful to biological tissues for brief exposure. At present we can scan a single OCM frame in (10 to 15) minutes, so a reasonable volumetric image can be acquired in approximately 1 day. The scan rate could be increased by a factor of five or ten with appropriate scanning stages.

Figure 4 was obtained by staining the surface of the scaffold with acridine orange from a methanol solution, then imbibing the scaffold with immersion oil. The top image was obtained with OCM, and though the contrast suffers with respect to the image taken at the surface, the resolution is still fairly good. Thus, reliable structural information can still be obtained. No cells were seeded into this scaffold, however it is possible that they would give enhanced reflectivity here as they did in the top panel of Figure 3. The bottom image of Figure 4 is a confocal fluorescence image. The spatial resolution is poor, but we are still able to obtain some contrast. This means that we could detect the presence of fluorescently labeled cells, whether stained, or engineered to express a fluorescent protein. Thus, by combining the information obtained by confocal OCM with that obtained by confocal fluorescence, we expect to be able to monitor progress of cell growth, even deep within a TE scaffold. This will be facilitated if we find enhanced reflectivity at the cell surface of NIR light such as that seen in Figure 3 a.

Conclusions

We have obtained high fidelity images of tissue engineering scaffolds using the strengths of two complimentary contrast mechanisms, optical coherence and fluorescence, in a confocal microscope. The coherence technique allows us to obtain images with good spatial resolution, even deep into the scaffold material. Fluorescence detection allows us to detect fluorescent signal equally far into the sample, but with significantly less spatial resolution. When used in parallel, these contrast mechanisms allow us to detect the presence and / or continuing viability of cells that are stained or expressing fluorescent protein deep within a TE scaffold, and to correlate their growth

with local and surrounding scaffold morphology. In principle, such information can be obtained nondestructively, and *in situ*, such that information on a single sample can be obtained throughout the tissue growth process.

References

[1] Ma,T., Li, Y., Yang, S.-T., and Kniss, D., "Effects of Pore Size in 3-D Fibrous Matrix on Human Trophoblast Tissue Development," *Biotechnology and Bioengineering*, Vol. 70, No. 6., 2000, pp. 608-618.
[2] Dillon, G., Yu, X., Sridharan, A., Ranieri, J., and Bellamkonda, R., "The Influence of Physical Structure and Charge on Neurite Extension in a 3D Hydrogel Scaffold," *Journal of. Biomaterial. Science: Polymer Edition.*, Vol. 9, No. 10, 1998, pp. 1049-1069.
[3] Muller, R., Matter, S., Newenschwander, P., Suter, U.W., and Ruegsegger, P., "3D Micro-tomographic Imaging and Quantitative Morphometry for the Nondestructive Evaluation of Porous Biomaterials," *Materials Research Society Symposium Proceedings*, Vol. 461, 1997, pp. 217-222.
[4] Garrido, L., "Non-destructive Evaluation of Synthetic Tissue Scaffolds with NMR", *Materials Research Society Symposium Proceedings*, Vol. 550, 1999, pp 171-176.
[5] Tjia, J. and Moghe, P., "Analysis of 3-D Microstructure of Porous Poly(lactide-glycolide) Matrices using Confocal Microscopy," *Journal of Biomedical Materials Research*, Vol. 43, No. 3, 1998, pp. 291-299.
[6] Birla, R. and Matthew, H. W. T., "3-Dimensional Imaging & Analysis of Smooth Muscle Colonization of Porous Chitosan Scaffolds," *Proceedings of the 1st Joint BMES/EMBS Conference*, 1999, p. 119.
[7] Drexler, W., Morganer, U., Kartner, F., Pitris, C., Boppart, S., Li, X., Ippen, E., and Fujimoto, J., "In vivo ultra-high resolution optical coherence tomography," *Optics Letters*, Vol. 24, No. 17, 1999, pp. 1221-1223.
[8] Wang, H.W., Izatt, J.A., and Kulkarni, D.D., "Optical Coherence Microscopy", *Handbook of Optical Coherence Tomography*, Bouma, B.E. and Tearney, G.J., Eds., Marcel Dekker, Inc. NewYork 2002, pp.275-298.
[9] Beaurepaire, E., Moreau, L., Amblard, F., Mertz, J., "Combined Scanning Optical Coherence and Two-Photon-Excited Fluorescence Microscopy", *Optics Letters*, Vol. 24, No.14, 1999, pp.969-971.
[10] Washburn, N., Simon, C., Tona, A., Elgendy, H., Karim, A. and Amis, E., "Co-extrusion of biocompatible polymers for scaffolds with co-continuous morphology," *Journal of Biomedical Materials Research*, Vol. 60, No. 1, 2002, pp. 20-29.

Darryl D. D'Lima,[1,3] Nicholai Steklov,[1] Arnie Bergula,[1] Peter C. Chen,[1] Clifford W. Colwell,[2] and Martin Lotz[3]

Cartilage Mechanical Properties after Injury

Reference: D'Lima, D. D., Steklov, N., Bergula, A., Chen, P. C., Lotz, M., and Colwell, C. W., **"Cartilage Mechanical Properties after Injury,"** *Tissue Engineered Medical Products (TEMPs), ASTM STP 1452,* E. Schutte, G. L. Picciolo, and D.S. Kaplan, Eds., ASTM International, West Conshohocken, PA, 2004.

Abstract: Cartilage injury often results in matrix degradation and in secondary osteoarthritis. This study was designed to correlate cell death and matrix degradation with biomechanical properties of cartilage. Full-thickness mature bovine femoral articular cartilage was harvested as 5 mm diameter cylindrical disk explants. Explants were divided into three groups: control, injury, and IL-1. The injury group was subjected to mechanical compression of 40% strain for five minutes. The IL-1 group was cultured in media containing 10 ng/mL of IL-1beta. The control group was not injured or exposed to IL-1beta. Chondrocyte viability, glycosaminoglycan release in media, and equilibrium creep were measured ten days after injury. A reduction in cell viability was seen after injury. A significant increase in glycosaminoglycan release and in equilibrium creep was detected in injured explants and in explants exposed to IL-1beta. A correlation was also found between the equilibrium creep and glycosaminoglycan content after injury and IL-1beta stimulation.

Keywords: Chondrocyte, cartilage, injury, viability, biomechanics, biomechanical properties, elastic modulus, glycosaminoglycan, trauma, cartilage repair, cartilage degeneration, cartilage lesion.

[1]Director, Research Associates, and Senior Bioengineer, respectively, Orthopaedic Research Laboratories, Scripps Clinic Center for Orthopaedic Research and Education, 11025 N. Torrey Pines Road, Suite 140, La Jolla, CA 92037.

[2]Director, Scripps Clinic Center for Orthopaedic Research and Education, 11025 N. Torrey Pines Road, Suite 140, La Jolla, CA 92037.

[3]Professor, Division of Arthritis Research, Scripps Research Institute, 10550 N. Torrey Pines Road, MEM161, La Jolla CA 92037.

Introduction

It is well recognized that impact loads can cause cartilage injury resulting in matrix degradation and in subsequent loss of cartilage tissue. The relationship between injury and matrix degeneration is readily apparent when the injury involves the mechanical disruption of the cartilage surface. However, cartilage degradation can also occur in the absence of gross matrix damage. Cell death has been reported after cartilage injury[*1-4*] and can occur in the form of apoptosis[*5-9*]. A correlation between chondrocyte apoptosis and osteoarthritis has been proposed[*10-12*]. Chondrocyte apoptosis has also been detected at significantly higher levels in osteoarthritic cartilage relative to normal cartilage in human subjects[*12*]. However, the link between injury, apoptosis, matrix loss, and loss of mechanical integrity has not been clearly established. The goal of this study was to demonstrate that injury-induced chondrocyte death and glycosaminoglycan release correlated with changes in the mechanical properties of cartilage over time.

Methods

Cartilage Explants

Full-thickness cartilage explants, 5 mm in diameter, were harvested from the weight-bearing region of the femoral condyles of mature fresh bovine joints using a dermal punch. The explants were cultured at 37°C, 5% $C0_2$, and 100% humidity in Dulbecco's Modified Eagle's Medium (DMEM) supplemented with 10% fetal calf serum. Explants were cultured in media for 48 hours before injury to allow glycosaminoglycan release levels to stabilize.

Experimental Design

Explants were divided into three groups: control, injury, and IL-1. The injury group was subjected to mechanical injury as described below. The IL-1 group was stimulated with 10 ng/mL of IL-1beta (interleukin-1 beta). IL-1beta is known to cause matrix degradation. The control group was not subjected to injury or to IL-1beta stimulation. A single experiment used cartilage (n = 4 to 6 explants in each group) harvested from two bovine joints. Each experiment was repeated separately four times.

Mechanical Injury

To simulate mechanical injury, bovine cartilage explants were subjected to 40% compressive strain in radially unconfined compression for five minutes. The injurious compression fell within the range of strain values previously reported to induce apoptosis[*6,8*]. Explants from the control or IL-1 groups were not mechanically injured. After injury, explants were cultured for ten days before analysis.

Cell Viability

Cell viability was quantitated by staining with Calcein-AM[*13*]. Calcein-AM is an uncharged nonfluorescent esterase substrate which diffuses freely into cells. Viable cells containing esterase activity convert Calcein-AM to Calcein, which is a charged, fluorescent green stain, and only retained by cells with an intact plasma membrane. Propidum iodide was used as a counterstain as it reacts with nuclear DNA to produce a red fluorescence. Since propidium iodide is not cell membrane permeable, it cannot stain cells with an intact cell membrane. Cell viability was quantified as the percentage of fluorescent green cells in the explant section at 48 hours after injury.

Glycosaminoglycan Assay

The concentration of glycosaminoglycans released into the media was measured using 1,9-Dimethylene Blue (DMMB) to monitor spectrophotometric changes which occur during the formation of the sulfated GAG dye complex[*14*]. Explants were digested in papain and collagenase, and glycosaminoglycan concentration was determined at ten days after injury.

Mechanical Properties

The elastic modulus of the solid phase was measured on day ten after injury by allowing the explants to creep under a constant load. Explants were placed in a creep chamber and were preloaded with a small tare load. An additional 120 gm of constant load was added and the creep monitored until equilibrium (slope of creep against time was less than $1x10^{-6}$). The equilibrium creep is directly related to the load and to the elastic modulus (E_S) of the cartilage matrix[*15*]. For the same constant load, the equilibrium creep is inversely related to E_S. The confined compression creep test is more widely accepted and was initially chosen to measure the aggregate modulus of the explants. However, injury often changed the shape and the size of the explant, making it difficult to consistently fit the explant in the confined compression chamber.

Statistical Analysis

Multifactor ANOVA (Analysis of Variance) was used to test differences in results between experimental groups. Neuman-Keuls pairwise contrasts was used to test for individual pairwise differences. Linear regression was used to test the association between glycosaminoglycan content and creep. A p value < 0.05 was used to denote statistical significance.

Results

Cell Viability

Figure 1 displays the mean chondrocyte viability (with standard deviation bars) for the different groups, ten days after injury. Cell viability was significantly reduced in the injury group ($p < 0.05$) compared with the control and IL-1 group.

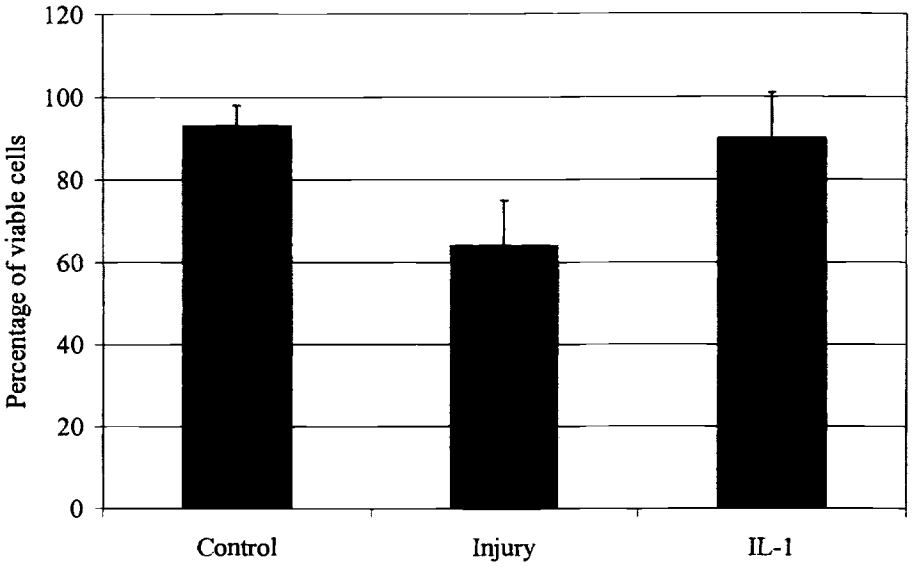

Figure 1 – *Mean Chondrocyte Viability at Ten Days after Injury (n = 24, in 4 separate experiments).*

Glycosaminoglycan Release and Content

The concentration of glycosaminoglycan in culture media from control explants was less than 10 microgm/mL per mg of explant (over ten days of culture). This more than doubled after injury (19.9 microgm/mL/mg, Figure 2, $p < 0.01$). An even higher release of glycosaminoglycan was detected in explants treated with IL-1beta ($p < 0.001$).

A corresponding decrease was noted in glycosaminoglycan content in injury and in IL-1beta explants after ten days in culture (Figure 3). This links the glycosaminoglycan released in media with the glycosaminoglycan content of the explant.

Mechanical Properties

Figure 4 shows the mean equilibrium creep after mechanical testing in unconfined compression with standard deviation bars. At ten days after injury mean equilibrium creep was significantly greater in the injured explants and in the explants cultured in IL-1, relative to control ($p<0.01$). Since the equilibrium creep inversely relates to E_s, this suggests a proportionate reduction in E_s.

A negative correlation was also found between glycosaminoglycan content and equilibrium creep in unconfined compression (Figure 5, $R^2 = 0.3$, $p = 0.03$). This finding links the biomechanical properties with the biochemical changes during the process of matrix degradation.

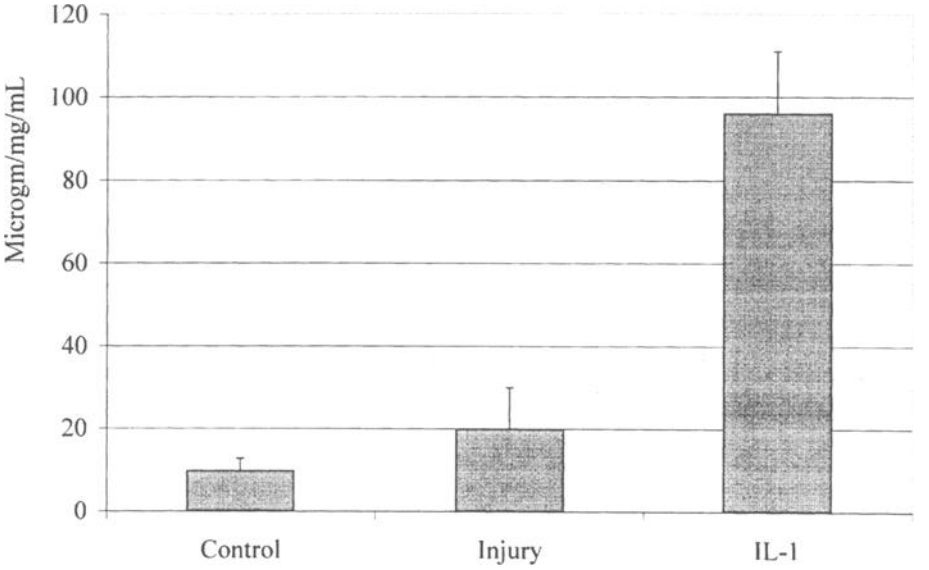

Figure 2 – *Mean Glycosaminoglycan Released in Media Over Ten Days Post Injury (n = 24, in 4 separate experiments).*

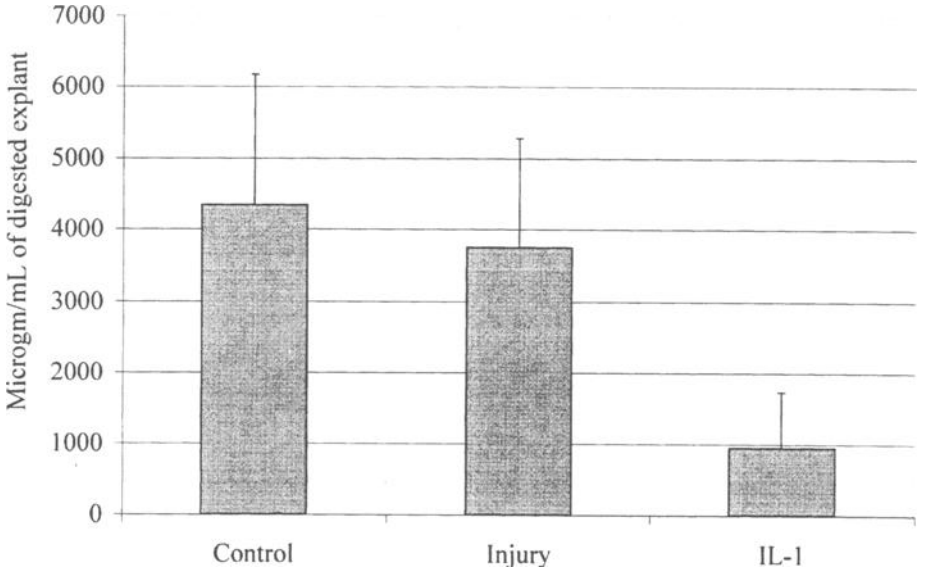

Figure 3 – *Mean Glycosaminoglycan Concentration of Explant Ten Days after Injury (n = 24, in 4 separate experiments).*

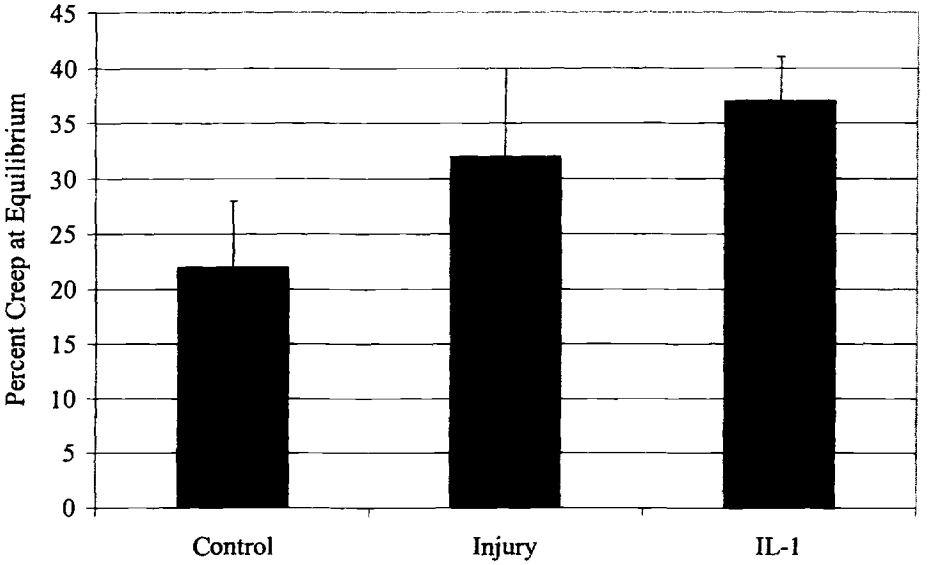

Figure 4 – *Mean Equilibrium Creep at Ten Days after Injury (n = 16, in 4 separate experiments).*

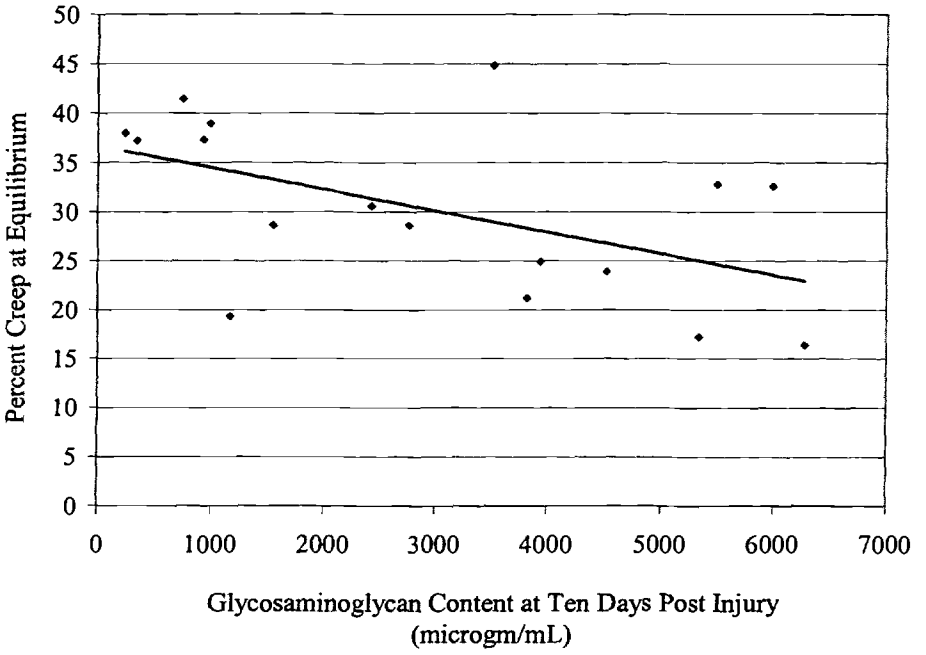

Figure 5 – *Linear Regression of Creep with Glycosaminoglycan Content.*

Discussion

Cartilage injury is a significant contributor to secondary osteoarthritis. Because the inciting event can be easily identified, it is easier to document the progression of cartilage degeneration leading to arthritis compared with primary osteoarthritis or more insidious forms of secondary osteoarthritis. Cartilage injury models are therefore attractive in providing insights in the processes of cartilage degeneration and arthritis. This in vitro model of cartilage injury allows for carefully controlled evaluation of cellular, biochemical, and biomechanical events that may be a significant part of the posttraumatic degenerative process.

In this model, cell viability, matrix loss, and biomechanical strength were found to correlate with each other after injury. Analysis of matrix constituents can serve as valuable surrogate markers of cartilage damage. However, the primary function of articular cartilage is biomechanical support. Hence, the evaluation of biomechanical properties is more important in the context of cartilage degradation and repair. Previous reports have found significant correlations between the elastic modulus of cartilage and the biochemical composition such as glycosaminoglycan and collagen content[*16,17*]. Patwari et al. reported increased swelling of injured calf cartilage explants when placed in hypotonic sodium chloride solution[*18*]. Cartilage swelling is an estimate of damage to the collagen network. Loening et al. also reported a significant reduction in equilibrium modulus of injured calf cartilage explants when tested in unconfined compression immediately after injury[*6*]. The authors attributed this to damage to the collagen network. The present study was also able to correlate the equilibrium creep (which relates inversely to elastic modulus) with the glycosaminoglycan concentration of cartilage explants. This further served to validate surrogate markers of cartilage injury (such as glycosaminoglycan release in media).

This study demonstrated a pattern of cartilage degradation after injury similar to, although less severe than, that seen with IL-1 stimulation. This provides indirect evidence that the posttraumatic degradation may have a significant biochemical component. Other studies have also suggested this by reporting MMP-3 (stromelysin-1) release after similar injurious compression[*18*]. MMP-3 levels in synovial fluid have been reported to rise after clinical joint injury[*19*]. MMP-3 is known to cause degradation of glycosaminoglycan and collagen and therefore can affect both the aggregate modulus and the tensile strength of cartilage.

In early osteoarthritis, there may sometimes be increased synthesis of glycosaminoglycan[*20*]. However, this has been shown to be associated with decreased retention of newly synthesized glycosaminoglycan in matrix[*21*]. This may be attributed to decreased synthesis of link protein, which may have reduced the formation of large aggregates[*22*].

The consequences of cell death are also clinically relevant. There is a constant turnover of the macromolecules (predominantly glycosaminoglycan and type II collagen) that constitute cartilage matrix. Chondrocytes are the sole source of the components of these macromolecules and are therefore primarily responsible for the maintenance, repair, and remodeling of matrix. In mature articular cartilage, a limited pool of chondrocytes is available for this maintenance, and therefore any reduction in this finite pool of cells can result in reduction of net synthesis (leading to progressive degradation).

Coupled with the initial matrix damage, a significant loss in cell viability can lead to accelerated degradation. This opens a novel therapeutic approach through cytoprotection. Preliminary studies suggest that chondrocyte apoptosis can be prevented resulting in increased cell viability after injury[*8,23*]. Whether increased cell viability results in enhanced matrix synthesis, reduction in cartilage degeneration, or improved repair has yet to be demonstrated. A model of cartilage injury that permits accurate analysis of the cellular, biochemical, and biomechanical properties of cartilage can be extremely useful in evaluating such newer therapies.

Acknowledgments

This study was funded in part by OREF Grant #98-052, NIH Grant #AG07996-12, the ALSAM Foundation, and the Skaggs Institute for Research.

Reference List

[1] Repo, R.U. and Finlay, J.B., "Survival of Articular Cartilage After Controlled Impact," *The Journal of bone and joint surgery American volume*, Vol. 59A, 1977, pp. 1068-1076.

[2] Calandruccio, R.A. and Gilmer, W.S., "Proliferation and Repair of Articular Cartilage of Immature Animals," *The Journal of bone and joint surgery American volume*, Vol. 44A, 1962, pp. 431-455.

[3] Mankin, H.J., "Localisation of Tritiated Thymidine in Cartilage. I. Growth in Immature Cartilage," *The Journal of bone and joint surgery American volume*, Vol. 44A, 1962, pp. 682-688.

[4] Bentley, G., Greer, R., "Homotransplantation of Isolated Epiphyseal and Articular Chondrocytes into the Joint Surfaces of Rabbits," *Nature*, Vol. 230, 1971, pp. 385-388.

[5] Tew, S.R., Kwan, A.P., Hann, A., Thomson, B.M., and Archer, C.W., "The Reactions of Articular Cartilage to Experimental Wounding: Role of Apoptosis," *Arthritis and rheumatism*, Vol. 43, 2000, pp. 215-225.

[6] Loening, A.M., James, I.E., Levenston, M.E., Badger, A.M., Frank, E.H., Kurz, B., Nuttall, M.E., Hung, H.H., Blake, S.M., Grodzinsky, A.J., and Lark, M.W., "Injurious Mechanical Compression of Bovine Articular Cartilage Induces Chondrocyte Apoptosis," *Archives of biochemistry and biophysics*, Vol. 381, 2000, pp. 205-212.

[7] D'Lima, D.D., Hashimoto, S., Chen, P.C., Lotz, M., and Colwell Jr, C.W., "Cartilage Injury Induces Chondrocyte Apoptosis," *The Journal of bone and joint surgery American volume*, Vol. 83-A Suppl 2, 2001, pp. 19-21.

[8] D'Lima, D.D., Hashimoto, S., Chen, P.C., Colwell, C.W., Jr., and Lotz, M.K., "Human Chondrocyte Apoptosis in Response to Mechanical Injury," *Osteoarthritis Cartilage*, Vol. 9, 2001, pp. 712-719.

[9] D'Lima, D.D., Hashimoto, S., Chen, P.C., Colwell Jr, C.W., and Lotz, M., "Impact of Mechanical Trauma on Matrix and Cells," *Clinical orthopaedics and related research*, Vol. 391S, 2001, pp. s90-s99.

[10] Hashimoto, S., Ochs, R.L., Rosen, F., Quach, J., McCabe, G., Solan, J., Seegmiller, J.E., Terkeltaub, R., and Lotz, M., "Chondrocyte-Derived Apoptotic Bodies and Calcification of Articular Cartilage," *PROCEEDINGS OF THE NATIONAL ACADEMY OF SCIENCES OF THE UNITED STATES OF AMERICA*, Vol. 95, 1998, pp. 3094-3099.

[11] Hashimoto, S., Takahashi, K., Amiel, D., Coutts, R.D., and Lotz, M., "Chondrocyte Apoptosis and Nitric Oxide Production During Experimentally Induced Osteoarthritis," *Arthritis and rheumatism*, Vol. 41, 1998, pp. 1266-1274.

[12] Hashimoto, S., Ochs, R.L., Komiya, S., and Lotz, M., "Linkage of Chondrocyte Apoptosis and Cartilage Degradation in Human Osteoarthritis," *Arthritis and rheumatism*, Vol. 41, 1998, pp. 1632-1638.

[13] Johnson, I., "Fluorescent Probes for Living Cells," *The Histochemical journal*, Vol. 30, 1998, pp. 123-140.

[14] Farndale, R.W., Buttle, D.J., and Barrett, A.J., "Improved Quantitation and Discrimination of Sulphated Glycosaminoglycans by Use of Dimethylmethylene Blue," *Biochimica et Biophysica Acta*, Vol. 883, 1986, pp. 173-177.

[15] Armstrong, C.G., Lai, W.M., and Mow, V.C., "An Analysis of the Unconfined Compression of Articular Cartilage," *Journal of biomechanical engineering*, Vol. 106, 1984, pp. 165-173.

[16] Armstrong, C.G. and Mow, V.C., "Variations in the Intrinsic Mechanical Properties of Human Articular Cartilage With Age, Degeneration, and Water Content," *The Journal of bone and joint surgery American volume*, Vol. 64A, 1982, pp. 88-94.

[17] Mow, V.C., Holmes, M.H., and Lai, W.M., "Fluid Transport and Mechanical Properties of Articular Cartilage: a Review," *J Biomech*, Vol. 17, 1984, pp. 377-394.

[18] Patwari, P., Fay, J., Cook, M.N., Badger, A.M., Kerin, A.J., Lark, M.W., and Grodzinsky, A.J., "In Vitro Models for Investigation of the Effects of Acute Mechanical Injury on Cartilage," *Clinical orthopaedics and related research*, Vol. 391 Suppl, 2001, pp. S61-S71.

[19] Lohmander, L.S., Hoerrner, L.A., Dahlberg, L., Roos, H., Bjornsson, S., and Lark, M.W., "Stromelysin, Tissue Inhibitor of Metalloproteinases and Proteoglycan Fragments in Human Knee Joint Fluid After Injury," *Journal of Rheumatology*, Vol. 20,1993, pp. 1362-1368.

[20] Mankin, H.J. and Lippiello, L., "Biochemical and Metabolic Abnormalities in Articular Cartilage From Osteo-Arthritic Human Hips," *The Journal of bone and joint surgery American volume*, Vol. 52, 1970, pp. 424-434.

[21] Carney, S.L., Billingham, M.E., Muir, H., and Sandy, J.D., "Demonstration of Increased Proteoglycan Turnover in Cartilage Explants From Dogs With Experimental Osteoarthritis," *Journal of Orthopaedic Research*, Vol. 2, 1984, pp. 201-206.

[22] Sandy, J.D., Barrach, H.J., Flannery, C.R., and Plaas, A.H., "The Biosynthetic Response of the Mature Chondrocyte in Early Osteoarthritis," *Journal of Rheumatology*, Vol. 14 Spec No, 1987, pp. 16-19.

[23] D'Lima, D.D., Hermida, J.C., Hashimoto, S., Chen, P.C., Colwell, C.W., and Lotz, M., "Prevention of Apoptosis Reduces Arthritis in Vivo," *Trans 47th Orthop Res Soc*, Vol. 26, 2001, pp. 659.

Darryl D. D'Lima,[1] Arnie Bergula,[1] Peter C. Chen,[1] Clifford W. Colwell,[2] and Martin Lotz[3]

Age Related Differences in Chondrocyte Viability and Biosynthetic Response to Mechanical Injury

---

Reference: D'Lima, D. D., Bergula, A., Chen, P. C., Colwell, C. W., Lotz, M., "**Age Related Differences in Chondrocyte Viability and Biosynthetic Response to Mechanical Injury,**" *Tissue Engineered Medical Products (TEMPs), ASTM STP 1452,* E. Schutte, G. L. Picciolo, and D. S. Kaplan Eds., ASTM International, West Conshohocken, PA, 2004.

Abstract: Mechanical trauma has been shown to cause chondrocyte death. The response of the surviving cells has not been fully characterized especially with regards to aging. This study investigates the response to injury in aging chondrocytes. Human articular chondrocytes from younger and older donor knees were cultured in agarose gel disks for three weeks. Disks were submitted to a brief 30% compressive insult (injured), or cultured in IL-1beta (IL-1), or served as controls. Glycosaminoglycan biosynthesis was measured by radiolabeled sulfate ($^{35}SO_4$) uptake 48 hours after injury. Chondrocytes from the older group synthesized less glycosaminoglycan as measured by $^{35}SO_4$ uptake. This ranged from a 22% to 61% reduction relative to the younger group. After injury, a further decline in glycosaminoglycan synthesis was noted in both older and younger groups. However, the decline in glycosaminoglycan synthesis was more marked in the older group. While mechanical injury results in chondrocyte death, the surviving cells exhibit the effect of injury by reduced biosynthesis and increased loss of matrix. This suggests that the impact of mechanical injury may progress beyond the traumatic event. With age, fewer cells may survive with a further decrease in biosynthetic response. This has implications in the repair response and may provide insights in the development of chondroprotective measures.

Keywords: Chondrocyte, cartilage, injury, aging, viability, biosynthesis, glycosaminoglycan, trauma, cartilage repair, cartilage degeneration, cartilage lesion.

[1]Director, Research Associates, and Senior Bioengineer, respectively, Orthopaedic Research Laboratories, Scripps Clinic Center for Orthopaedic Research & Education, 11025 N. Torrey Pines Road, Suite 140, La Jolla, CA, 92037.
[2]Director, Scripps Clinic Center for Orthopaedic Research & Education, 11025 N. Torrey Pines Road, Suite 140, La Jolla, CA, 92037.

Introduction

Aging is one of the most significant risk factors associated with cartilage degeneration and osteoarthritis. Studies have shown significant cellular, biochemical, and biomechanical changes in articular cartilage with aging[*1-5*]. Matrix synthesis has also been found to be reduced in cartilage explants from older subjects in rabbits, horses, and humans[*6-10*]. However, the cellular responses of aging cartilage to injury have not been clearly defined. This study compared deoxyribose nucleic acid (DNA) and glycosaminoglycan synthesis in chondrocytes from younger and older donors and evaluated the response to injury.

Methods

Agarose-Chondrocyte Constructs

Cartilage that appeared normal to visual inspection was harvested from the articular cartilage of knee joints (femoral condyles and tibial plateaus) of fresh cadaver donors (within 72 hours of death). The cartilage was diced and digested with pronase and collagenase to release the chondrocytes. Chondrocytes were resuspended at a density of 2 million cells/mL and mixed with an equal volume of 6% low gelling temperature agarose (Fluka 05073, Sigma-Aldrich, Milwaukee, WI). This final suspension (1 million cells/mL in 3% agarose) was gelled at 4° C for 20 minutes in a custom chamber to form a 2 mm thick slab. Cylindrical disks 5 mm in diameter and 2 mm thick were cored from this gel slab using a dermal punch. Approximately 40 explants were obtained from each donor. Each cell-agarose disk construct was then cultured in DMEM (Dulbecco's modified Eagle's medium) supplemented with 10% fetal calf serum for 21 days before being subjected to injury. Each explant was cultured in 1 mL of media, with media changed twice a week.

Experimental Design

Donors were divided into two groups: younger and older. The younger group (n = 5) contained donors who were less than 35 years of age at the time of death. The older group contained donors (n = 5) who were greater than 50 years of age at the time of death and who did not demonstrate significant evidence of degeneration or osteoarthritis (no full thickness lesion). Within each group, explants were divided into control, injury, and IL-1 experimental subgroups. The injury subgroup was subjected to transient mechanical injury (see below). The IL-1 subgroup was stimulated with 10 ng/mL of IL-1beta (interleukin-1 beta). The control subgroup was not subjected to injury or IL-1beta stimulation.

Mechanical Injury

Cell-agarose constructs from the injury group were placed inside the injury chamber and subjected to a 30% unconfined compressive strain for 500 msec using an electromagnetic actuator with a resolution of 1 micron (SMAC, Carlsbad, CA). The magnitude and duration of loading was chosen from previous experiments that produced

a consistent cell death of about 30%. Cell-agarose constructs from the control group were placed in the same chamber but were not subjected to mechanical compression.

Biochemical Analysis

After injury, all groups were incubated for 48 hours in the presence of [^{35}S]-sodium sulfate ($^{35}SO_4$) at a concentration of 20 microcuries/mL (Perkin Elmer, Boston, MA). At the end of 48 hours, the level of $^{35}SO_4$ newly incorporated in the cell-agarose constructs was measured. Cell-agarose constructs were washed five times in ice-cold phosphate-buffered saline (10 minutes per wash), blotted dry, then digested at room temperature for 30 minutes by the addition of Buffer RLT (10 microL per mg, Qiagen, Valencia, CA). The digest was homogenized with Ecoscint (3 mL per sample, National Diagnostics, Manville, NJ) and was placed in a scintillation counter for measurement of total radioactivity. $^{35}SO_4$ incorporation was normalized to explant weight and expressed as coulter counts per minute per mg explant. This served to quantify newly synthesized glycosaminoglycans. Cell-agarose constructs were also incubated in media containing tritiated thymidine (^{3}H -Thymidine) at various time points during the pre-injury culture. The level of ^{3}H -Thymidine in the cell-agarose construct was measured in a similar manner to that described for $^{35}SO_4$. ^{3}H -Thymidine levels served to quantitate DNA synthesis rates.

Statistical Analysis

Multifactor ANOVA (Analysis of Variance) was used to test differences between donor groups and experimental groups. Neuman-Keuls pairwise contrasts was used to test for individual pairwise differences. A p value < 0.05 was assumed to denote statistical significance.

Results

DNA Synthesis

A consistent decrease in ^{3}H -Thymidine uptake was seen in older compared with younger group over the three weeks in culture (Figure 1, $p<0.001$). Cell-agarose constructs were incubated in media containing ^{3}H -Thymidine for 48 hours at each time point. Data shown are means with standard deviation bars from three separate experiments ($n = 6$ explants in each experiment, from each donor). This suggests a significant reduction in DNA synthesis with age even before injury.

Glycosaminoglycan Synthesis

Cell-agarose constructs from the older group also synthesized less glycosaminoglycan as measured by $^{35}SO_4$ uptake. This ranged from a 22% to 61% reduction relative to the younger group, $p<0.01$. After injury, a further decline in glycosaminoglycan synthesis was noted (Figure 2) in both older and younger groups. Data shown are means with standard deviation bars from three separate experiments ($n = 6$ in each experiment). Glycosaminoglycan synthesis is normalized to uninjured control constructs. However, the decline in glycosaminoglycan synthesis after injury was more marked in the older

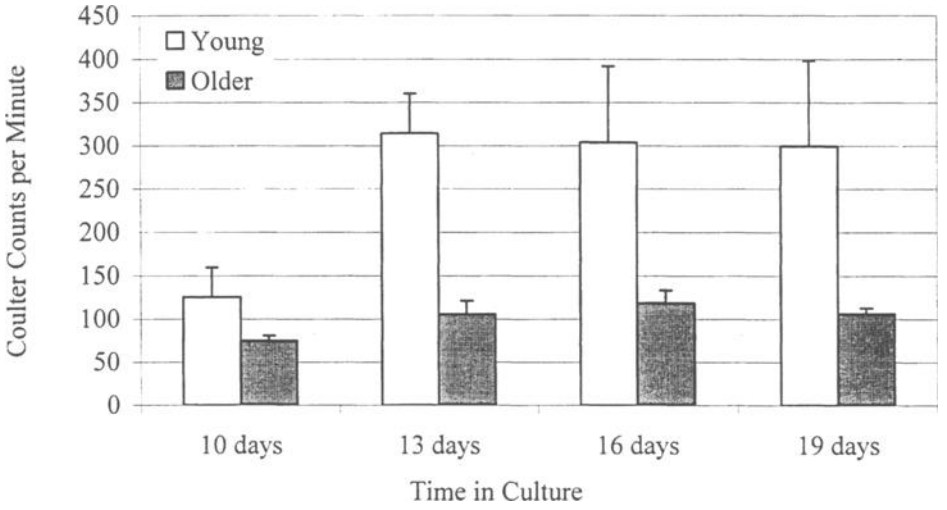

Figure 1 – *DNA Synthesis Over Three Weeks*

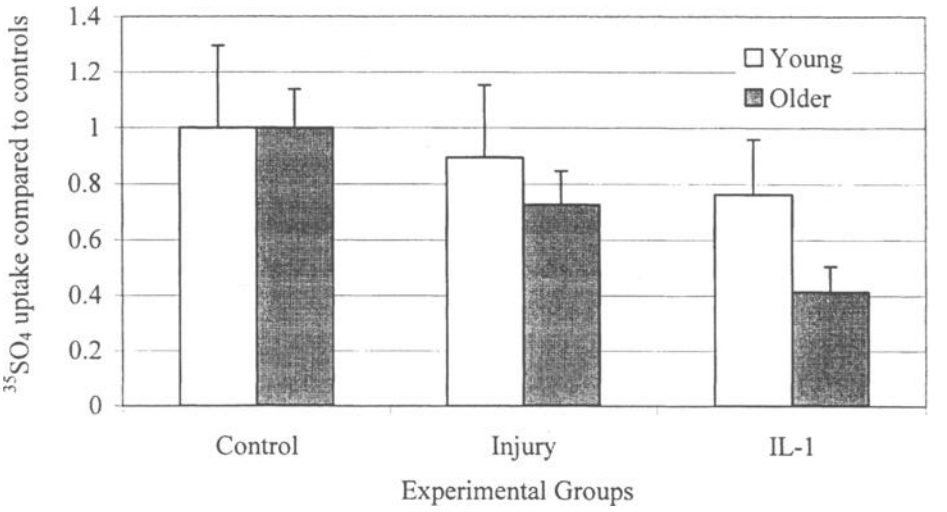

Figure 2 – *Glycosaminoglycan Synthesis After Injury*

group compared to the younger group ($p < 0.05$). Both older and younger groups were sensitive to IL-1 stimulation. This was primarily used as a positive control, however, it of interest to note that IL-1 affected older chondrocytes to a greater degree ($p<0.01$).

Discussion

A strong linear correlation exists between aging and the incidence of significant cartilage degeneration and osteoarthritis. This has been attributed to reduced cellularity, reduction in matrix synthesis, and altered matrix biochemical and biomechanical properties. The response of older chondrocytes to injury, however, has not been fully defined. The agarose gel culture system provides a controlled means of testing altered cellular response by normalizing cell density and removing any effect of a pre-existing altered matrix.

The reduced ^{3}H-Thymidine uptake over three weeks in culture suggests less DNA synthesis in older chondrocytes. The starting cell density was the same for younger and older explants in this study (1 million cells per mL of agarose gel). Verbruggen et al. reported a mean 13.6% decrease in DNA content in the first week of culture (human chondrocytes cultured in 1.5% agarose) but could not correlate the reduced DNA content with age[*11*]. DeGroot et al. have shown that the age-related decrease in glycosaminoglycan synthesis was not related to a decrease in cell density[*8*]. However, a possibility exists that cell density may have changed over time in the cell- agarose constructs containing older chondrocytes. Therefore the $^{35}SO_4$ uptake was compared with controls for each group. This corrected for any systematic change in cell density between groups before injury. A decrease in $^{35}SO_4$ uptake was also noted in older chondrocytes. This was consistent with previous reports of decreased glycosaminoglycan synthesis with increasing age[*8,11*]. In fact, Verbruggen et al. reported an exponential regression of $^{35}SO_4$ uptake with age, which suggests that $^{35}SO_4$ uptake using chondrocytes from 45- and 69-year old subjects is 50% and 25%, respectively, of the uptake using chondroyctes from a 20-year old subject[*11*].

Injury caused a reduction in glycosaminoglycan synthesis. This is consistent with the cell death that has been reported in response to this form of injury[*12-15*]. Older chondrocytes may also be more susceptible to cell death after injury, which can lead to reduced glycosaminoglycan synthesis.

IL-1beta is a known inhibitor of glycosaminoglycan synthesis and was used as a positive control. Glycosaminoglycan synthesis following IL-1 stimulation was even lower than that following injury. Again, older chondrocytes appeared to be more susceptible to IL-1beta effects. Aging chondrocytes have a reduced capacity to assemble a proteoglycan-rich matrix[*10,11*]. This has been attributed to an insufficient synthesis of link protein necessary for the stabilizaton of aggregates. Therefore, matrix loss after injury can be affected not only by a reduction in rate of newly synthesized glycosaminoglycans but also by the decreased ability to retain these newly synthesized glycosaminoglycans in matrix.

A recent study suggested an altered response to mechanical stimulation in chondrocytes from osteoarthritic cartilage[*4*]. Chondrocytes from normal human cartilage expressed higher levels of aggrecan mRNA and lower levels of matrix metalloproteinase-3 (MMP3) after mechanical stimulation. However, chondrocytes from osteoarthritic cartilage did not show these changes, which suggested altered mechanotransduction and signalling. The older chondrocytes tested in this study were obtained from donors without significant cartilage degneration. However, it is entirely possible that some of the donors had early degeneration, and that the reduction in matrix synthesis may be a precursor to or a consequence of early disease.

These data suggest that older cartilage may be more susceptible to the deleterious effects of injury which may partly explain the increased incidence of cartilage lesions with age. In addition, current surgical techniques aimed at cartilage repair that use autologous cells or grafts may not be as successful in older patients since even the host cartilage may demonstrate a compromised repair response.

Acknowledgments

This study was funded in part by OREF Grant #98-052, NIH Grant #AG07996-12, the ALSAM Foundation, and the Skaggs Institute for Research.

References

[1] Plaas, A.H., Sandy, J.D., and Kimura, J.H., "Biosynthesis of Cartilage Proteoglycan and Link Protein by Articular Chondrocytes From Immature and Mature Rabbits," *The Journal of biological chemistry*, 1988, Vol. 263, pp. 7560-7566.

[2] Martin, J.A., Ellerbroek, S.M., and Buckwalter, J.A., "Age-Related Decline in Chondrocyte Response to Insulin-Like Growth Factor-I: The Role of Growth Factor Binding Proteins," *Journal of orthopaedic research*, 1997, Vol. 15, pp. 491-498.

[3] Martin, J.A. and Buckwalter, J.A., "Human Chondrocyte Senescence and Osteoarthritis," *Biorheology*, 2002, Vol. 39, pp. 145-152.

[4] Salter, D.M., Millward-Sadler, S.J., Nuki, G., and Wright, M.O., "Differential Responses of Chondrocytes From Normal and Osteoarthritic Human Articular Cartilage to Mechanical Stimulation," *Biorheology*, 2002, Vol. 39, pp. 97-108.

[5] Armstrong, C.G. and Mow, V.C., "Variations in the Intrinsic Mechanical Properties of Human Articular Cartilage With Age, Degeneration, and Water Content.," *The Journal of bone and joint surgery American volume*, 1982, Vol. 64 A, pp. 88-94.

[6] DeGroot, J., Verzijl, N., Bank, R.A., Lafeber, F.P., Bijlsma, J.W., and TeKoppele, J.M., "Age-Related Decrease in Proteoglycan Synthesis of Human Articular Chondrocytes: the Role of Nonenzymatic Glycation," *Arthritis and rheumatism*, 1999, Vol. 42, pp. 1003-1009.

[7] Maroudas A, Rigler D, and Schneiderman R. Young and Aged Cartilage Differ in their Response to Dynamic Compression as far as the Rate of Glycosaminoglycan Synthesis is Concerned. Trans 45th Orthop Res Soc 24, 170. 1999.
Ref Type: Abstract

[8] Iqbal, J., Dudhia, J., Bird, J.L., and Bayliss, M.T., "Age-Related Effects of TGF-Beta on Proteoglycan Synthesis in Equine Articular Cartilage," *Biochemical and biophysical research communications*, 2000, Vol. 274, pp. 467-471.

[9] Sandy, J.D. and Plaas, A.H., "Age-Related Changes in the Kinetics of Release of Proteoglycans From Normal Rabbit Cartilage Explants," *Journal of orthopaedic research*, 1986, Vol. 4, pp. 263-272.

[10] Sandy, J.D., Barrach, H.J., Flannery, C.R., and Plaas, A.H., "The Biosynthetic Response of the Mature Chondrocyte in Early Osteoarthritis," *The Journal of rheumatology*, 1987, Vol. 14 Spec No, pp. 16-19.

[11] Verbruggen, G., Cornelissen, M., Almqvist, K.F., Wang, L., Elewaut, D., Broddelez, C., de Ridder, L., and Veys, E.M., "Influence of Aging on the Synthesis and Morphology of the Aggrecans Synthesized by Differentiated Human Articular Chondrocytes," *Osteoarthritis Cartilage*, 2000, Vol. 8, pp. 170-179.

[12] Loening, A.M., James, I.E., Levenston, M.E., Badger, A.M., Frank, E.H., Kurz, B., Nuttall, M.E., Hung, H.H., Blake, S.M., Grodzinsky, A.J., and Lark, M.W., "Injurious Mechanical Compression of Bovine Articular Cartilage Induces Chondrocyte Apoptosis," *Archives of biochemistry and biophysics*, 2000, Vol. 381, pp. 205-212.

[13] D'Lima, D.D., Hashimoto, S., Chen, P.C., Lotz, M., and Colwell Jr, C.W., "Cartilage Injury Induces Chondrocyte Apoptosis," *The Journal of bone and joint surgery American volume*, 2001, Vol. 83-A Suppl 2, pp. 19-21.

[14] D'Lima, D.D., Hashimoto, S., Chen, P.C., Colwell, C.W., Jr., and Lotz, M.K., "Human Chondrocyte Apoptosis in Response to Mechanical Injury," *Osteoarthritis Cartilage*, 2001, Vol. 9, pp. 712-719.

[15] D'Lima, D.D., Hashimoto, S., Chen, P.C., Colwell Jr, C.W., and Lotz, M., "Impact of Mechanical Trauma on Matrix and Cells.," *Clinical orthopaedics and related research*, 2001, Vol. 391S, pp. s90-s99.

Henry Rodriguez,[1] Pawel Jaruga,[2] Mustafa Birincioglu,[3] Peter E. Barker,[1] Catherine O'Connell,[1] and Miral Dizdaroglu[1]

A Comparative Study of Biomarkers of Oxidative DNA Damage Used to Detect Free Radical Damage in Tissue-Engineered Skin

Reference: Rodriguez, H., Jaruga, P., Birincioglu, M., Barker, P. E., O'Connell, C., and Dizdaroglu, M., **"A Comparative Study of Biomarkers of Oxidative DNA Damage Used to Detect Free Radical Damage in Tissue-Engineered Skin,"** *Tissue Engineered Medical Products (TEMPs), ASTM STP 1452*, E. Schutte, G. L. Picciolo, and D. S. Kaplan, Eds., ASTM International, West Conshohocken, PA, 2004.

Abstract: The process of tissue engineering often involves the mixing of cells with polymers that may elevate the level of endogenous free radicals and thus cause genetic damage to the cell. In order to assure that such composite materials are free of genetic damage, our laboratory is responding to the need for test methods used to assess the safety and performance of tissue-engineered materials. Specifically, we are identifying cellular biomarkers that could be used to ensure that the cells of tissue-engineered materials have not undergone any oxidative DNA damage from the production of free radicals by oxidative stress during the development, storage or shipment of the product. Using the technique of gas chromatography/mass spectrometry, we have screened for the oxidatively modified DNA base 8-hydroxyguanine in tissue-engineered skin and compared the levels to those in control cells, neonatal fibroblasts and neonatal keratinocytes. No significant level of damage was detected compared to control cells. The technique of liquid chromatography/mass spectrometry was also used in the validation of this biomarker by measuring its nucleoside form. The results obtained with this technique were nearly identical to those obtained with gas chromatography/mass spectrometry. Biomarker programs such as this can provide the basis for an international reference standard of cellular biomarkers that can aid in the development and safety of tissue-engineered medical products.

Keywords: oxidative DNA damage, free radical damage, biomarkers

[1]Staff Scientist, Staff Scientist, Staff Scientist, and Group Leader, respectively, Chemical Science and Technology Laboratory, National Institute of Standards and Technology, 100 Bureau Drive, Mail Stop 831, Gaithersburg, MD 20899-8311.
[2]Guest Researcher, University of Maryland, Baltimore County.
[3]Department of Pharmacology, Medical School, Inönü University, Malatya, Turkey.

Introduction

Tissue engineering is an emerging area of biotechnology that will provide replacement tissues for patients, as well as complex, functional biological systems for research and testing in the pharmaceutical industry. There are two forms of tissue engineering: one in which cells are grown in culture and seeded onto a material, and in the other where an implanted material induces a specific response such as tissue regeneration *in vivo*. The former approach is used to create skin substitutes, while the latter is used to accelerate nerve regeneration as an example.

A new research area of tissue engineering involves the investigation of how living cells interact and respond to synthetic biomaterial surfaces. The clinical development underlying such scientific research includes a number of novel tissue-engineered products that include replacement skin as a synthetic dermal matrix for burn patients and chronic-ulcer patients. The first tissue-engineered organ, which has progressed from lab bench to the first accepted patient care, has been skin. Apligraf is a bilayered living skin analog with appearance and handling characteristics that are similar to normal human skin [1]. TestSkin II (Organogenesis, Inc, Canton, MA) is equivalent to Apligraf and is sold for the purposes of *in vitro* research.

The aim of this program was to help identify cellular biomarkers and measurement technologies that could be used to assure that tissue-engineered skin products are free of genetic changes that could occur during the development, storage and shipment of the product. These biomarkers could possibly help better understand the cellular mechanisms of how cells react to inflammatory stimuli from different matrices. Specifically, we investigated oxidative damage to DNA by free radicals.

Free radicals are produced in living cells by normal metabolism and by exogenous sources such as carcinogenic compounds and ionizing radiations (reviewed in [2]). Of the free radicals, the highly reactive hydroxyl radical (•OH) causes damage to DNA and other biological molecules (reviewed in [2-4]). Scientific studies have shown that free radicals are implicated in many diseases such as cancer, arthritis, cataracts, Alzheimer's disease and Parkinson's disease (reviewed in [2]). It was therefore important to determine if free radical-induced oxidative DNA damage was present in tissue-engineered materials. In this study, tissue-engineered skin (TestSkin II, Organogenesis, Inc, Canton, MA) was used as a representative model. The skin product was obtained and separated into its two cellular layers (Epidermal component consisting of neonatal human keratinocytes and the Dermal component consisting of neonatal human fibroblasts) (Fig. 1).

DNA was isolated and compared to the DNA from neonatal control cells (neonatal human dermal fibroblasts and neonatal human epidermal keratinocytes) and HeLa cells that have not undergone the tissue engineering process. It was also compared to commercial calf thymus DNA (ctDNA).

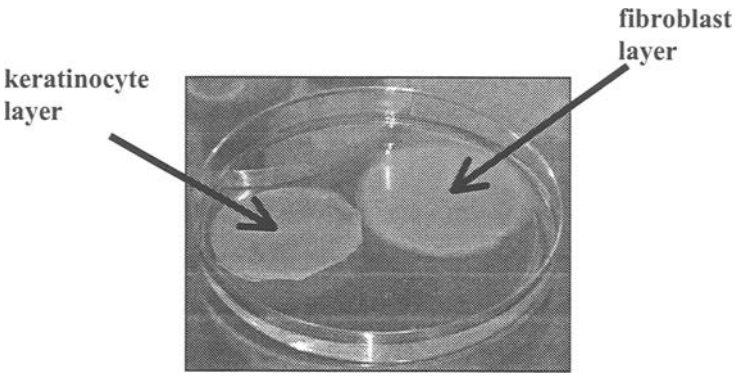

FIG. 1 — *TestSkin II from Organogenesis separated into individual cell layers (neonatal fibroblasts and keratinocytes).*

Experimental Methods[4]

Cell Culture and DNA Isolation

HeLa cells were placed in antibiotic-free Dulbecco's Modified Eagle Medium containing 10% (v/v) fetal bovine serum and grown in 175 cm^2 flasks at 37 °C in a humidified cell culture incubator with 5% CO_2/95% air. Medium was aspirated off and cells were rinsed with 20 mL of 1X Phosphate Buffered Saline (PBS). Cells were detached by adding 3 mL trypsin/EDTA solution. Human dermal neonatal fibroblast cells (HDFn; Cascade Biologics, Portland, Oregon) were cultured in Medium 106 supplemented with Low Serum Growth Supplement (LGGS) in the absence of antibiotics and antimycotics (Cascade Biologics, Portland, Oregon). Medium was aspirated off, and cells were rinsed and detached as above. Trypsin/EDTA solution was immediately removed and an aliquot of 3 mL of Trypsin neutralizer solution (Cascade Biologics, Portland, Oregon) was added to each flask. Human epidermal neonatal keratinocyte cells (HEKn; Cascade Biologics, Portland, Oregon) were cultured in EpiLife medium supplemented with Human Keratinocyte Growth Supplement (HKGS) in the absence of antibiotics and antimycotics (Cascade Biologics, Portland, Oregon) and then treated as above. Calf thymus DNA was purchased from the Sigma Chemical Corporation.

DNA was isolated from cells using a blood and cell culture DNA kit (Qiagen, Valencia, CA). DNA was recovered by spooling, washed once in 70% ethanol, and then air-dried. DNA was dissolved in 10 mM sodium phosphate buffer at a concentration of 0.3 mg/mL and dialyzed against water for 18 h at 4 °C. Water outside the dialysis bags was changed three times during the course of the dialysis. Subsequently, DNA

[4]Certain commercial equipment or materials are identified in this paper in order to specify adequately the experimental procedures. Such identification does not imply recommendation or endorsement by the National Institute of Standards and Technology, nor does it imply that the materials or equipment identified are necessarily the best available for the purpose.

concentration was determined by UV spectroscopy. Aliquots of this solution containing 100 μg of DNA were dried under vacuum in a SpeedVac.

TestSkin II: Fibroblast/Keratinocyte Separation and DNA Isolation

Separating Cell Layers - A TestSkin II disk (Organogenesis, Inc., Canton, MA) was placed in a 150 mm^2 sterile petri dish containing 35 mL 1x PBS and incubated at room temperature for 30 min in a cell culture hood. PBS was removed and replaced with 40 mL protease type X solution (0.5 mg/mL 1x PBS) and incubated at 37 °C for 2 h in a humidified cell culture incubator with 5% CO_2/95% air. Epidermal layer (keratinocytes; gray top layer) was gently separated from the dermal layer (fibroblasts; white bottom layer) using sterile forceps.

Separating Individual Cells and DNA Isolation - Epidermal layer was placed in a 50-mL polypropylene conical tube containing 40 mL trypsin-versene and incubated in a 37 °C water bath for 2 h. The dermal layer was placed in a 175-cm^2 T-flask containing 180 mL collagenase solution [60 mL collagenase (4.17 mg/mL H_2O) and 120 mL collagenase pre-mix (120 ml 1x PBS, 14 mL of 2.5% trypsin solution, 1 mL filtered 0.45% glucose solution)] and incubated at 37 °C in a humidified cell culture incubator with 5% CO_2/95% air for 2 h. Independently, each respective tube was agitated every 15 min. Cells were pelleted by centrifugation (1300 x g/4 °C for 5 min) and rinsed twice with 20 mL 1x PBS with centrifugation (1300 x g/4 °C for 5 min) between each rinse step. Cells were eventually suspended in 4-mL 1x PBS and counted using a cell culture hemocytometer. DNA was isolated from the cells using a blood and cell culture DNA kit (Qiagen, Valencia, CA).

Analysis of Oxidative DNA Damage by Gas Chromatography/Mass Spectrometry and Liquid Chromatography/Mass Spectrometry

The measurement of 8-hydroxyguanine and 8-hydroxy-2′-deoxyguanosine has previously been discussed in detail [5,6]. Statistical values were derived using the ANOVA single factor test.

Results

Oxidative damage to DNA can be measured by a variety of analytical techniques, each of which has its own advantages and drawbacks (reviewed in [7,8]. Most of these techniques measure only a single product with no spectroscopic evidence for identification. Techniques that use mass spectrometry provide unequivocal identification and quantification of DNA damage (reviewed in [8]). For over a decade, gas chromatography/mass spectrometry (GC/MS) has been used for the measurement of DNA base and sugar lesions, and DNA-protein crosslinks in cells and *in vitro* [8]. Recently, liquid chromatography/tandem mass spectrometry (LC/MS/MS) and liquid chromatography/mass spectrometry (LC/MS) emerged as new techniques for the measurement of modified nucleosides in DNA (reviewed in [9]). In the present project,

tissue-engineered skin (TestSkin II) was screened for oxidative DNA damage and compared to control cells: neonatal fibroblasts and neonatal keratinocytes, including cultured HeLa cells and commercially available ctDNA. The biomarkers consisted of 8-hydroxyguanine (a free base) and its nucleoside form (8-hydroxy-2′-deoxyguanosine). GC/MS technology was used to measure the free base while LC/MS was used to measure its nucleoside form.

The results showed that the level of oxidative DNA damage was found to be at background/endogenous levels (less than 10 modified molecules/10^6 DNA bases) (Table 1). No significant level of damage was detected among the samples when compared to control cells using either GC/MS or LC/MS technology. As expected, differences were observed when compared to commercially available ctDNA. Although one sample of tissue engineered skin fibroblasts showed a level of difference between measurement technologies (Table 1, Sample 5), over all no significant difference was observed between the two measurement technologies – GC/MS to measure the modified base 8-hydroxyguanine and LC/MS to measure the modified nucleoside 8-hydroxy-2′-deoxyguanosine.

The National Institute of Standards and Technology is making a concerted effort to identify cellular biomarkers for the field of tissue-engineered medical products. These studies can provide the basis for an international reference standard of cellular biomarkers that can aid in the development and safety of tissue-engineered medical products.

		A	B
	Cell /Tissue	**GC/MS**	**LC/MS**
1	HDFn	8.4 ± 1.4^{a}	8.6 ± 0.9^{b}
2	HEKn	8.6 ± 0.7^{a}	9.1 ± 0.3^{b}
3	TE Skin Fibro (A)	8.1 ± 0.2^{a}	8.0 ± 0.8^{b}
4	TE Skin Kera (A)	5.6 ± 1.3^{a}	8.9 ± 1.1^{b}
5	TE Skin Fibro (B)	$6.9 \pm 0.5^{a,c}$	9.0 ± 0.6^{b}
6	TE Skin Kera (B)	7.2 ± 0.4^{a}	8.0 ± 0.7^{b}
7	HeLa	7.5 ± 1.0^{a}	5.8 ± 0.3^{b}
8	ctDNA	13.9 ± 0.5	14.6 ± 0.6

Table 1 — *Level of 8-hydroxyguanine and 8-hydroxy-2′-deoxyguanosine as measured by GC/MS and LC/MS, respectively. HDFn: Control Human Dermal Fibroblasts neonatal; HEKn: Control Human Epidermal Keratinocytes neonatal; TE Skin Fibro (A & B): Fibroblast cells isolated from TestSkin II products – "A & B" each represent three independent TestSkin fibroblast layers combined into one; TE Skin Kera (A & B); Keratinocyte cells isolated from TestSkin II products – "A & B" each represent three independent TestSkin keratinocyte layers combined into one; HeLa: HeLa DNA isolated from cultured cells; ctDNA: commercially obtained calf thymus DNA . S.D. error values are based on duplicate or triplicate measurement analysis (n=3). [a]Column A: the values of samples 1-7 were statistically different from the value of sample 8 ($p<0.001$); [b]Column B: the values of samples 1-7 were statistically different from the value of sample 8 ($p<0.001$); [c]Value of sample 5 was statistically different between GC/MS and LC/MS ($p<0.05$).*

References

[1] Wilkins, L. M., Watson, S. R., Prosky, S. J., Meunier, S. F., and Parenteau, N. L., "Development of a bilayered living skin construct for clinical applications," *Biotechnology & Bioengineering*, 1994, pp. 747-756.

[2] Halliwell, B. and Gutteridge, J. M. C., 1999, *Free Radicals in Biology and Medicine*, Oxford Science Publishing.

[3] Dizdaroglu, M., "Oxidative damage to DNA in mammalian chromatin," *Mutation Research*, Vol. 275, 1992, pp. 331-342.

[4] Breen, A. P. and Murphy, J. A., "Reactions of oxyl radicals with DNA," *Free Radiccal Biology and Medicine*, Vol. 18, 1995, pp. 1033-1077.

[5] Dizdaroglu, M., Jaruga, P., and Rodriguez, H., "Measurement of 8-hydroxy-2'-deoxyguanosine in DNA by high-performance liquid chromatography-mass spectrometry: comparison with measurement by gas chromatography-mass spectrometry," *Nucleic Acids Research*, Vol. 29, 2001, pp. E12.

[6] Rodriguez, H., Jurado, J., Laval, J., and Dizdaroglu, M., "Comparison of the levels of 8-hydroxyguanine in DNA as measured by gas chromatography mass spectrometry following hydrolysis of DNA by *Escherichia coli* Fpg protein or formic acid," *Nucleic Acids Research*, Vol. 28, 2000, pp. E75.

[7] Collins, A., Cadet, J., Epe, B., and Gedik, C., "Problems in the measurement of 8-oxoguanine in human DNA," *Carcinogenesis*, Vol. 18, 1997, pp. 1833-1836.

[8] Dizdaroglu, M., 1998, "Mechanisms of free radical damage to DNA," *DNA & Free Radicals: Techniques, Mechanisms & Applications*, OICA International.

[9] Dizdaroglu, M., Jaruga, P., Birincioglu, M., and Rodriguez, H., "Free radical-induced damage to DNA: mechanisms and measurement," *Free Radical Biology and Medicine*, Vol. 32, 2002, pp. 1102-1115.

Chuck B. Thomas,[1] Linda Jenkins,[1] James F. Kellam,[2] and Karen J.L. Burg[1]

Endpoint Verification of Bone Demineralization for Tissue Engineering Applications

Reference: Thomas, C. B., Jenkins, L., Kellam J. F., and Burg, K. J. L., "**Endpoint Verification of Bone Demineralization for Tissue Engineering Applications,**" *Tissue Engineered Medical Products (TEMPs), ASTM STP 1452*, E. Schutte and G. L. Picciolo, Eds., ASTM International, West Conshohocken, PA, 2004.

Abstract: Demineralized bone matrix is used in tissue engineering applications due to its ability to promote new bone formation. Numerous processing variables, such as the degree of demineralization, can affect the matrix's bone-forming ability. Several methods exist for determining the extent of demineralization, but each method has disadvantages. This study investigated the potential use of a stereomicroscope in determining the degree of demineralization by comparing the novel technique to two conventional methods. Bone fragments were processed and demineralized using a standard protocol, and their degree of demineralization was characterized over time by the three methods. The results indicate that a stereomicroscopy method is as effective as two established methods in verifying the degree of demineralization.

Keywords: tissue engineering, demineralized bone matrix, stereomicroscope, endpoint determination

Introduction

Demineralized bone matrix (DBM) shows promise in orthopaedic tissue engineering for spinal fusion, craniofacial reconstruction, and for repair of long-bone defects caused by fracture or tumor resection [*1*]. During the mid- to late-1960's, Urist and coworkers explained that the ability of DBM to develop new bone is due to its osteoinductive capacity, that is, its ability to promote bone formation in nonskeletal areas [*2-4*]. Several years later, the inductive factor was identified and named bone morphogenetic protein [*5*]. Harakas [*6*] and Glowacki and Mulliken [*7*] provide a history of research performed on the osteogenesis of DBM. Numerous animal studies have been performed to study the inductive properties of DBM, with promising results [*2-4, 6-11*].

[1] Graduate research assistant, histotechnologist, and assistant professor, respectively, Department of Bioengineering, Clemson University, 501 Rhodes Engineering Research Center, Clemson, SC 29634-0905.

[2] Vice Chairman, Department of Orthopaedic Research, Carolinas Medical Center, P.O. Box 32861, Charlotte, NC 28232-2861.

Clinical studies involving human patients have also been successful. Russell and Block evaluated results from 21 studies that used DBM rather than bone grafts for orthopaedic reconstruction [*1*]. According to their report, more than 80% of the studies resulted in positive outcomes with the use of DBM in humans, even in difficult cases such as resistant nonunions. Despite the promising results, Russell and Block argue that the clinical efficacy of DBM is not widely acknowledged due to variable experimental procedures and processing methods that could have negative effects on graft performance [*1*]. Controlled experimental trials and standardization of processing techniques is therefore imperative for DBM used in Tissue Engineered Medical Products (TEMPs). This study addresses one aspect of DBM processing: determining the degree of demineralization in DBM.

A number of processing variables can affect the osteoinductivity of DBM. The choice of demineralizing agent and its concentration, time spent in the demineralizing agent, usage and amounts of various organic agents, pre- and post-processing storage conditions, and sterilization are just a few of the parameters that can determine the fate of DBM in the body [*1, 6*]. Urist, for example, found that bone decalcified with 0.6 *N* hydrochloric acid (HCl) induced bone growth in at least 90% of rectus abdominus same-species implants in mouse, rat, rabbit, and guinea pig [*2*]. Bone matrix demineralized with 1 *N* ethylenediaminetetraacetic acid (EDTA), 0.6 *N* acetic acid, or a 1 *N* formic-citric acid mixture also induced bone growth, but bone induction only occurred 50% of the time when acetic acid was used. EDTA and the formic-citric acid mixture produced a positive result in 80% and 85% of the cases, respectively. Bone decalcified in 0.6 *N* nitric acid or 0.6 *N* nitrous acid did not induce new bone growth due to protein deamination, and it led to a high degree of inflammation. Results from Urist's study also showed that bone sterilized with β-propriolactone and decalcified with HCl did not induce bone growth [*2*].

In another study, Urist and others researched the effects of numerous processing factors on the bone induction principle [*4*]. Bone decalcified in 0.6 *N* HCl, frozen in liquid nitrogen at -70°C, and lyophilized, produced a higher incidence of bone induction than samples stored at 28°C, 0°C, or -30°C. Cryolysis, produced by freezing and thawing the decalcified bone three times, inhibited bone induction completely. The Urist group also found that cold sterilization of the bone in 70% alcohol did not harm the inductivity. The researchers additionally observed that heat denaturation using modest increases in temperature promoted induction. In this study, as the temperature was increased from 25°C to 50°C, the incidence of bone induction reached a maximum of 90%. At a temperature of 60°C, collagen shrinkage occurred; the incidence of bone induction fell continuously with further increases in temperature, reaching a value of zero at 100°C. As a result, steam sterilization of decalcified bone was deemed inappropriate. Sterilization by ^{60}cobalt radiation at a level of approximately 2 Mrads or greater led to denaturation of the bone and the formation of fibrous tissue. Exposure of decalcified bone to methanol did not prevent bone induction [*4*].

During the demineralization process, hydroxyapatite and tricalcium phosphate are removed when the bone is exposed to an acid such as HCl. An acid-insoluble matrix

of collagen and growth factors, including bone morphogenetic protein, is left behind. Monitoring the degree of demineralization is an important step in the demineralization process that can affect the osteoinductivity of the DBM. Dubuc and Urist reported that surface-decalcified bone allows sufficient inductive cell interactions to form new bone [*12*]. Urist and Strates found that the quantity of new bone formed in the patient is inversely proportional to the amount of mineral remaining in the DBM implant [*13*].

Current methods that exist for evaluating the degree of demineralization include: radiography, timed immersion, mechanical testing, chemical testing, fluoroscopy, flame photometry, and continuous colorimetric analysis [*14, 15*]. Of these methods, radiography or calcium oxalate chemical testing is often chosen for reliability [*14-18*]. The degree and time of demineralization depends on both the demineralization process and the size and shape of the specimen. Complete demineralization (commonly called the endpoint) is generally desired; however, controlling demineralization to obtain specific levels of remaining mineral is useful in varying the biomechanical properties [*19-22*]. Thus, demineralization should be precisely controlled, and standards for monitoring demineralization of DBM used in TEMPs would be beneficial.

This study originated due to an unusual phenomenon that occurred during standard histological processing of what was assumed to be completely demineralized bone fragments. The fragments were unable to be cut during the sectioning process; instead, they were ejected from the embedding medium. Stereomicroscopy of the bone fragments revealed that each fragment exhibited two distinctly different regions: a bright white inner core that appeared opaque, and a dim translucent outer ring that extended completely around the core. From this observation, we postulated that the bone fragments were not completely demineralized. The goal of this study was to determine if a novel stereomicroscopic method could be as effective as conventional radiographic and chemical methods in determining the endpoint of demineralization for small (approximately 1-2 mm) DBM fragments.

Materials and Methods

To compare the stereomicroscopic, chemical, and radiographic methods, a modified version of Urist's protocol was used to defat and demineralize the bone [*4*]. A frozen diaphyseal cortical section of bovine femur weighing approximately 50 g was sectioned using a band saw. The femur section was then cut into pieces approximately 1 x 1 cm with the thickness dimension (between the periosteum and endosteum) variable due to the off-centered position of the marrow cavity. After rinsing in absolute ethanol, the pieces were frozen. Several frozen pieces were loaded into a water-cooled grinding mill (Bel-Art Products; Pequannock, NJ). The pieces were ground, and fragments were sieved using a tissue sieve system (PGC Scientifics; Frederick, MD). Sieves with 10- and 20-mesh screens were used to collect fragments with particle sizes in the range of 0.86 – 1.91 mm. Grinding of the frozen bone into fragments was completed before proceeding with defatting and demineralization. The femur section yielded a total of about 20 mL of bone fragments in the desired size range.

The bone fragments were transferred to a glass petri dish for the defatting procedure, and 60 mL of a defatting solution consisting of chloroform and methanol (3:1) was added to the petri dish. The fragments were defatted for a two-hour period; thus, the petri dish was covered to inhibit evaporation of the solvent. After two hours, the excess solution was pipetted to a waste container, and 60 mL of fresh defatting solution was added for another two-hour cycle. The defatting solution was removed, and the fragments were washed in 20 mL of absolute ethanol and then dried in 20 mL of acetone. Excess ethanol and acetone were pipetted to a waste container after each 10-minute soak. Subsequently, the fragments were transferred to a 250 mL glass bottle to begin the demineralization procedure.

Approximately 200 mL of 0.5 *N* HCl was added to the bottle, and the acid/fragment mixture was stirred at room temperature for four consecutive 40-minute cycles, followed by subsequent cycles of 24 and 16 hours. The mixture was stirred to promote equal demineralization on all surfaces of the DBM fragments and to discourage the precipitate from settling on fragment surfaces. At the end of each acid-washing cycle, HCl was removed and replaced with fresh HCl until the endpoint was reached.

Following each cycle, HCl was retained and immediately tested by the chemical method in order to determine endpoint of demineralization. Specifically, 5 mL of 5% (v/v) ammonium hydroxide and 5 mL of 5% (v/v) ammonium oxalate were added to 5 mL of the used HCl to precipitate calcium oxalate [*23*]. Images of the precipitates were obtained with a digital camera.

When the HCl was replaced at the end of each cycle, approximately 0.5 mL of fragments was removed and rinsed thoroughly with distilled water to neutralize the remaining HCl. Fragments from all cycles and mineralized positive control fragments were separately collected for radiography and stereomicroscopy analysis to evaluate endpoint of demineralization. A mineralized ground cross-section of bone was also used as an additional control for radiography to ensure that the X-ray film was developed properly. Using a Torrex 120D X-ray cabinet (EG&G Astrophysics Research; Long Beach, CA), fragments from each cycle were subjected to X-rays at 1 mA and 55 kV for 5 seconds. Individual radiographs were acquired using X-ray film and an automatic film processor (Kodak; Rochester, NY). The radiographs were placed on an X-ray view box, and photographs were obtained using a digital camera.

For the stereomicroscopy method, a stereomicroscope (Meiji Techno America; San Jose, CA) with a color digital camera (Diagnostic Instruments; Sterling Heights, MI) was used, and digital images of fragments from each cycle were captured using image acquisition software (Diagnostic Instruments; Sterling Heights, MI). As in the other two methods, photographs were obtained using the same camera and software settings for picture-to-picture consistency.

Results

Digital images illustrating the results of the three methods for determining endpoint of demineralization were acquired (Figure 1). The cumulative amount of demineralization time for the three methods is indicated beside each image.

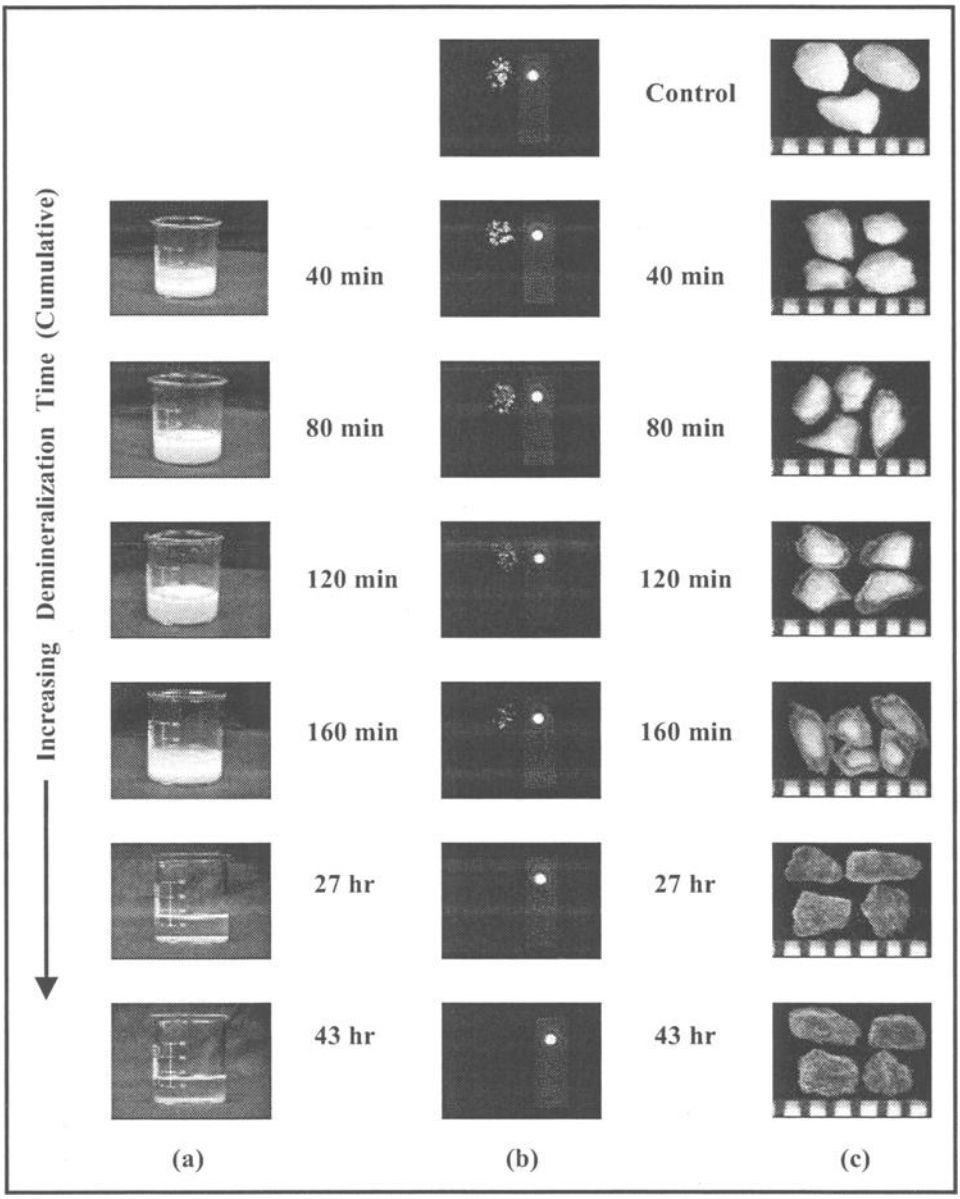

FIG. 1 – *Digital images to compare the feasibility of three tests in determining endpoint of demineralization. Cumulative demineralization time indicated for each method . (a) Chemical test results. (b) Radiography results. (c) Stereomicroscope results. The scale below the fragments in (c) is in millimeters.*

For the results of chemical testing on the used HCl (Figure 1a), the presence of a white calcium oxalate precipitate indicates that fresh HCl should be added and demineralization continued; otherwise, the endpoint has been reached if the precipitate is not observed [*14*]. The amount of precipitate appears to stay relatively constant between 40 and 160 minutes of demineralization time, but it decreases considerably between 160 minutes and 27 hours.

Radiographic images of the fragments are presented (Figure 1b) with the mineralized positive control fragments appearing in the top image. Radiopaque (white) areas in the radiographs indicate the presence of mineralized areas: the endpoint of demineralization occurs when the radiopaque areas are no longer observed. The white circle on the right of the fragments in each radiograph is the ground cross-section of mineralized bone used as an additional positive control. It is clearly evident that as demineralization time increases from 40 to 160 minutes, the radiopaque areas decrease in intensity and are completely absent by 27 hours.

Finally, the stereomicroscope images of the fragments are presented (Figure 1c). As in the radiographic images (Figure 1b), the mineralized positive control fragments appear in the top image. Bright areas in the fragments in the stereomicroscope images suggest mineralized areas are present. The stereomicroscope images illustrate the disappearance of a mineralized core in each DBM fragment as demineralization time increases from 40 to 160 minutes. The mineralized core disappears in each DBM fragment by 27 hours of demineralization time.

Discussion

When compared to the radiographs, images acquired via the stereomicroscope appear to accurately indicate the presence of mineralized tissue present at the end of each cycle. For the radiographs (Figure 1b), it is clearly evident that as demineralization time increases, the radiopaque areas decrease in intensity and are completely absent by 27 hours. The stereomicroscope images (Figure 1c) similarly illustrate the disappearance of a mineralized core in each DBM fragment over the same time period. By comparing the images, the endpoint of demineralization occurs between 160 minutes and 27 hours in both methods. While it would have been beneficial to obtain data during this broad time range to verify the exact endpoint, the results still provide a valuable comparison of the methods. In future studies with DBM, data will be collected during the time range of 160 minutes to 27 hours in order to determine the exact endpoint.

The demineralization behavior observed in the stereomicroscopic images is consistent with the theoretical model proposed by Lewandrowski and coworkers [*19*]. According to their study, demineralization of cortical bone with HCl occurs in a manner that fits a "classic shrinking-core reaction model" used for diffusion-limited processes in fluid-solid systems. The acid diffuses into the bone fragments along a moving reaction zone that divides the newly demineralized outer portion from the unreacted inner core. The shrinkage of the core is a function of the immersion time in

acid [*19*]. In a subsequent study, Squillace and coworkers validated Lewandrowski's model and determined that core shrinkage is also a function of acid agitation [*24*].

The comparison between the stereomicroscope and chemical methods is also favorable but not conclusive. While the radiography and stereomicroscope methods suggest an endpoint between 160 minutes and 27 hours, the photograph of the chemical test at 43 hours (Figure 1a) shows a slight precipitate of calcium oxalate. Demineralization was extended from 27 to 43 hours in an attempt to achieve confirmation of the endpoint with the chemical method. The amount of precipitate decreased considerably between 160 minutes and 27 hours. Due to the known accuracy of the radiographic method in determining the endpoint of demineralization [*15*] and its corresponding agreement with stereomicroscope images in this study, results of the chemical testing appear to be anomalous. This discrepancy may be due to insufficient rinsing of the fragments at the end of each cycle when the HCl was removed. Thus, a calcium residue may have accumulated on the bone fragments or the glassware over the course of the study. In future studies, the bone fragments and glass containers will be thoroughly rinsed between cycles.

A stereomicroscopy method appears to be equally effective in monitoring the degree of demineralization compared to conventional methods. Furthermore, each of the traditional methods has disadvantages. Radiography is an expensive and time-consuming method that requires a darkroom, an X-ray cabinet, film developer, film developing chemicals, and film [*14*]. The chemical method necessitates the purchase and handling of additional chemicals. Moreover, it must be performed often to obtain accurate results, and it becomes more time-consuming near the endpoint as the precipitate takes longer to form [*14*]. The only equipment required for the stereomicroscope method is a stereomicroscope, which is a standard piece of equipment in many clinical and research laboratories. The stereomicroscope method is also the least time-consuming method of those compared. It simply requires a rinse of the DBM fragments to remove the acid before the fragments are ready for a quick visual examination. Furthermore, it allows for a quick inspection of bone fragments having various particle sizes. Smaller fragments, which will demineralize faster, can be removed from the demineralizing agent before they become over-demineralized.

The *in vivo* performance of naturally-derived materials such as DBM is difficult to predict because of an inherent variability associated with patient age, gender, genetic characteristics, and health status. Additionally, numerous processing variables can affect the performance of DBM-based implants [*1*]. By developing a set of processing guidelines, the non-inherent variability can be limited. Without such guidelines, a cascade of compounding variability begins due to substrate variables such as the quantity of inductive factors, topography, surface charge, and surface chemistry. Variations in the substrate can then lead to changing cell responses in the form of unpredictable attachment, proliferation, matrix maturation, and mineralization. With various cell responses, the long-term viability of the TEMP is greatly affected, and predictability of an outcome becomes more difficult. Therefore, it is imperative that comprehensive standards be developed for DBM in TEMPs in order to protect patients' health and safety, provide legal protection for and instill confidence in the

medical staff, and lend credibility and marketability to the DBM product industry as well as the TEMP industry.

Conclusions

A stereomicroscope may be successfully used to determine the endpoint of demineralization with at least the same efficacy as radiographic or chemical methods. This cost-effective method may be invaluable to researchers in tissue engineering, clinicians specializing in reconstructive and orthopaedic surgeries, and histotechnologists in preparation of demineralized samples. Furthermore, the stereomicroscopic method may be an important part of a standard developed for monitoring and controlling the demineralization process for DBM used in TEMPs.

Acknowledgements

This work was funded through grants from the NSF and the AO ASIF Foundation, Switzerland. The authors thank Dr. Julie P. Martin of the Department of Bioengineering at Clemson University for her technical assistance.

References

[1] Russell, J. L. and Block, J. E., "Clinical Utility of Demineralized Bone Matrix for Osseous Defects, Arthrodesis, and Reconstruction: Impact of Processing Techniques and Study Methodology," *Orthopedics*, Vol. 22, No. 5, 1999, pp. 524-531; quiz 532-533.

[2] Urist, M. R., "Bone: Formation by Autoinduction," *Science*, Vol. 150, No. 698, 1965, pp. 893-899.

[3] Van de Putte, K. A. and Urist, M. R., "Osteogenesis in the Interior of Intramuscular Implants of Decalcified Bone Matrix," *Clinical Orthopaedics and Related Research*, Vol. 43, 1966, pp. 257-270.

[4] Urist, M. R., Silverman, B. F., Buring, K., Dubuc, F. L. and Rosenberg, J. M., "The Bone Induction Principle," *Clinical Orthopaedics and Related Research*, Vol. 53, 1967, pp. 243-283.

[5] Urist, M. R. and Strates, B. S., "Bone Morphogenetic Protein," *Journal of Dental Research*, Vol. 50, No. 6, 1971, pp. 1392-1406.

[6] Harakas, N. K., "Demineralized Bone-Matrix-Induced Osteogenesis," *Clinical Orthopaedics and Related Research*, Vol. 188, 1984, pp. 239-251.

[7] Glowacki, J. and Mulliken, J. B., "Demineralized Bone Implants," *Clinics in Plastic Surgery*, Vol. 12, No. 2, 1985, pp. 233-241.

[8] Tuli, S. M. and Singh, A. D., "The Osteoinductive Property of Decalcified Bone Matrix. An Experimental Study," *Journal of Bone and Joint Surgery (British)*, Vol. 60, No. 1, 1978, pp. 116-123.

[9] Einhorn, T. A., Lane, J. M., Burstein, A. H., Kopman, C. R. and Vigorita, V. J., "The Healing of Segmental Bone Defects Induced by Demineralized Bone Matrix. A Radiographic and Biomechanical Study," *Journal of Bone and Joint Surgery (American)*, Vol. 66, No. 2, 1984, pp. 274-279.

[10] Bolander, M. E. and Balian, G., "The Use of Demineralized Bone Matrix in the Repair of Segmental Defects. Augmentation with Extracted Matrix Proteins and a Comparison with Autologous Grafts," *Journal of Bone and Joint Surgery (American)*, Vol. 68, No. 8, 1986, pp. 1264-1274.

[11] Gepstein, R., Weiss, R. E. and Hallel, T., "Bridging Large Defects in Bone by Demineralized Bone Matrix in the Form of a Powder. A Radiographic, Histological, and Radioisotope-Uptake Study in Rats," *Journal of Bone and Joint Surgery (American)*, Vol. 69, No. 7, 1987, pp. 984-992.

[12] Dubuc, F. L. and Urist, M. R., "The Accessibility of the Bone Induction Principle in Surface-Decalcified Bone Implants," *Clinical Orthopaedics and Related Research*, Vol. 55, 1967, pp. 217-223.

[13] Urist, M. R. and Strates, B. S., "Bone Formation in Implants of Partially and Wholly Demineralized Bone Matrix. Including Observations on Acetone-Fixed Intra and Extracellular Proteins," *Clinical Orthopaedics and Related Research*, Vol. 71, 1970, pp. 271-278.

[14] Skinner, R. A., Hickmon, S. G., Lumpkin, C. K., Aronson, J. and Nicholas, R. W., "Decalcified Bone: Twenty Years of Successful Specimen Management," *Journal of Histotechnology*, Vol. 20, No. 3, 1997, pp. 267-277.

[15] Callis, G. and Sterchi, D., "Decalcification of Bone: Literature Review and Practical Study of Various Decalcifying Agents, Methods, and Their Effects on Bone Histology," *Journal of Histotechnology*, Vol. 21, No. 1, 1998, pp. 49-58.

[16] Sanderson, C., Radley, K. and Mayton, L., "Ethylenediaminetetraacetic Acid in Ammonium Hydroxide for Reducing Decalcification Time," *Biotechnic & Histochemistry*, Vol. 70, No. 1, 1995, pp. 12-18.

[17] Aitchison, G. U., "Use of a Faxitron X-Ray Cabinet for the Rapid Detection of the End-Point of Decalcification," *Medical Laboratory Sciences*, Vol. 36, No. 2, 1979, pp. 195-196.

[18] Rosen, A. D., "End-Point Determination in EDTA Decalcification Using Ammonium Oxalate," *Stain Technology*, Vol. 56, No. 1, 1981, pp. 48-49.

[19] Lewandrowski, K. U., Venugopalan, V., Tomford, W. W., Schomacker, K. T., Mankin, H. J. and Deutsch, T. F., "Kinetics of Cortical Bone Demineralization: Controlled Demineralization--a New Method for Modifying Cortical Bone Allografts," *Journal of Biomedical Materials Research*, Vol. 31, No. 3, 1996, pp. 365-372.

[20] Kotha, S. P., Walsh, W. R., Pan, Y. and Guzelsu, N., "Varying the Mechanical Properties of Bone Tissue by Changing the Amount of Its Structurally Effective Bone Mineral Content," *Bio-Medical Materials and Engineering*, Vol. 8, No. 5-6, 1998, pp. 321-334.

[21] Osbon, D. B., Lilly, G. E., Thompson, C. W. and Jost, T., "Bone Grafts with Surface Decalcified Allogeneic and Particulate Autologous Bone: Report of Cases," *Journal of Oral Surgery*, Vol. 35, No. 4, 1977, pp. 276-284.

[22] Urist, M. R., "Surface-Decalcified Allogeneic Bone (SDAB) Implants. A Preliminary Report of 10 Cases and 25 Comparable Operations with Undecalcified Lyophilized Bone Implants," *Clinical Orthopaedics and Related Research*, Vol. 56, 1968, pp. 37-50.

[23] Luna, L. G. and Gridley, M. F., *Manual of Histologic Staining Methods of the Armed Forces Institute of Pathology*. 3rd ed. Blakiston Division McGraw-Hill, New York, NY, 1968.

[24] Squillace, D. M. K., Summitt, M. C. and Bianchi, J. R. "Characterization of the Rate of Acid Demineralization of Human Tibial Bone -- a Cylindrical Model," *Transactions of the 27th Annual Meeting of the Society for Biomaterials*, 2001, pp. 141.

Chuck B. Thomas,[1] James F. Kellam,[2] and Karen J. L. Burg[1]

Comparative Study of Bone Cell Culture Methods for Tissue Engineering Applications

Reference: Thomas, C. B., Kellam, J. F., and Burg, K. J. L., "**Comparative Study of Bone Cell Culture Methods for Tissue Engineering Applications**," *Tissue Engineered Medical Products (TEMPs), ASTM STP 1452*, E. Schutte, G. L. Picciolo, and D. S. Kaplan, Eds., ASTM International, West Conshohocken, PA, 2004.

Abstract: Cells are used in bone tissue engineering applications to facilitate new bone formation in implants. Enzymatic digestion and marrow removal by either centrifugal force or syringe are three methods used to isolate the cells for culture, but each technique has benefits and drawbacks. This comparative study evaluated the effects of the three cell isolation techniques on the attachment, proliferation, and mineralization of rat bone cells. Cells were isolated, seeded, and cultured following standard protocols for each isolation method. Quantitative assays to determine metabolic activity, lactic acid production, glucose consumption, and amounts of intracellular protein, alkaline phosphatase activity, and extracellular calcium were performed. In addition, cell morphology and viability were examined qualitatively. The results indicate that the cell isolation method affects the attachment, proliferation, and type of tissue formed by cells cultured under identical conditions.

Keywords: tissue engineering, bone, osteoblasts, mesenchymal cells, cell culture

Introduction

In many tissue engineering research applications, cells are added to a natural or synthetic absorbable or degradable material *in vitro*, the cell/material composite is grown in the laboratory, and the product is implanted into the patient. As a result, cells are a necessary component in research and clinical testing of most tissue-engineered medical products (TEMPs). The success of many bone tissue-engineering products initially relies on the ability of osteoblasts to attach to the construct's surface. After attachment, the osteoblasts should proliferate and migrate on the construct surface, filling pores within the construct as the body begins to absorb the material. When the osteoblasts exit the proliferation phase, they must be able to produce a

[1] Graduate research assistant and assistant professor, respectively, Department of Bioengineering, Clemson University, 501 Rhodes Engineering Research Center, Clemson, SC 29634-0905.
[2] Vice Chairman, Department of Orthopaedic Research, Carolinas Medical Center, P.O. Box 32861, Charlotte, NC 28232-2861.

mineralized extracellular matrix. The osteoblasts must retain these functional characteristics throughout the process for a successful outcome.

Table 1 – *Cells in bone tissue engineering are derived from various species and methods.*

Species and Location	Cell Isolation Method	Cells Released	References
Rat calvaria	Enzymatic digestion	Osteoblasts	[1-5]
Rat femur	Flushing by syringe	Marrow cells	[6-8]
Rabbit tibia	Explants	Periosteal cells	[9]
Goat iliac crest	Marrow aspiration	Marrow cells	[8]
Rat femur and tibia	Flushing by syringe	Marrow cells	[10-12]
Rabbit femur	Marrow aspiration	Marrow cells	[13]

Due in part to the absence of standards, the bone-forming cells used in this research originate from a wide variety of species and cell isolation methods (Table 1). A specific example of this disparity is found in the culture of rat cells for use in bone tissue engineering. Rat bone cells are typically isolated using enzymatic digestion [*1-5*] or marrow removal [*6-8, 10-12*] techniques (Figure 1). In enzymatic digestion, the femur or calvaria of the rat is minced into fine pieces, and the small fragments are subjected to a series of collagenase/trypsin washes that release osteoblasts for culture. Alternatively, the marrow found in the intermedullary canal of the femur can be removed using syringe or centrifuge [*14*] techniques to release bone marrow cells that can be coaxed to differentiate into osteoblasts during culture.

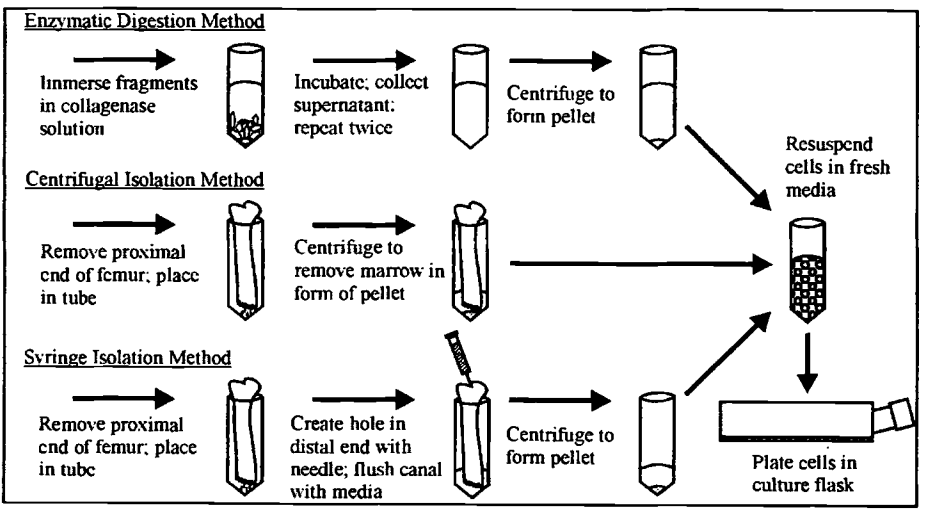

Figure 1 – *Schematic diagram illustrating the three cell isolation techniques.*

Bone-forming cells can be obtained from each of these methods, but depending on their attachment, proliferation, and mineralization characteristics, cells derived using one method may be better suited for a particular application than those derived using another. Osteoblasts and committed osteoprogenitor cells isolated via enzymatic techniques exhibit properties of bone that include characteristic morphology, synthesis of bone-related proteins, and calcification after 3-4 weeks in culture [*1-5*]. Collagenase used in enzymatic digestion, however, may harm the osteoblasts by removing proteins from the cell membrane, thereby affecting the osteoblasts' ability to attach and function normally. The damage can lower the yield of viable osteoblasts obtained, leading to a longer period of subculturing to achieve the high cell numbers required for seeding the product. As a further complication, extensive subculturing can lead to a reduction in the osteoblasts' phenotypic expression [*15*].

While enzymatic methods release cells that are more differentiated and committed to the osteoblast phenotype, cells obtained from the marrow of rat femur and tibia can be characterized as pluripotent, mesenchymal cells that form osteoblasts, chondrocytes, adipocytes, and other parenchymal cells [*16, 17*]. Under specific culture conditions, mesenchymal cells can be induced to develop into osteoprogenitor cells and osteoblasts [*18*]. Like cells isolated via enzymatic techniques, the cells obtained from marrow and cultured to form osteoblasts also exhibit properties of bone such as characteristic morphology, bone protein synthesis, and mineralization after several weeks of culture [*6-8, 10-12*]. The ability of marrow-derived mesenchymal cells, however, to proliferate and differentiate into the desired phenotype decreases with increasing donor age [*19, 20*]. An advantage of using marrow-derived cells in a tissue-engineered product is that autogenic cells can be retrieved percutaneously. If autologous cells are prepared by enzymatic digestion, the patient is required to have open surgery to harvest bone. Allogenic cells may also be used, but they pose the risk of disease transmission and immune rejection.

The purity of the cell population clearly depends on the cell isolation method, and this may affect the outcome of the cellular TEMP by altering cell proliferation time and the type of tissue formed. The advantages and disadvantages of each cell isolation method should be considered, and methods that are used to procure cells for TEMPs should be standardized in order to reduce variability between products. The objective of this study was to compare three common cell isolation methods to determine if significant differences exist in the cultured cells.

Materials and Methods

Cell Isolation, Culture, and Seeding

Osteoblasts were isolated from the femurs of three adult (90-day) male Sprague-Dawley rats using one of three methods: enzymatic digestion, centrifugal isolation, or syringe isolation.

Enzymatic Digestion – Osteoblasts were isolated by sequential collagenase digestions according to established protocols [*21, 22*]. Briefly, entire rat hind legs were collected and cleaned of large portions of extraneous soft tissue. The legs were rinsed and then temporarily stored (1-2 hours) in ice-cold, sterile Hank's Balanced Salt Solution (HBSS) supplemented with 1.0% Antibiotic-Antimycotic and 0.2% Fungizone (chemicals from Invitrogen; Carlsbad, CA). (HBSS with supplements will be referred to as HBSS-Complete or HBSS-C.) Each femur was then aseptically cleaned of all extraneous tissue, including cartilage at the epiphyses. The bones were fragmented into pieces approximately 2-3 mm in size with bone-cutting forceps and scalpels, and the fragments were collected in fresh HBSS-C. The fragments were vortexed vigorously, and the supernatant was removed to minimize the presence of erythrocytes in culture. Fragments from both femurs were added to 4 mL of 0.05% trypsin/0.02% ethylenediaminetetraacetic acid (EDTA) solution (Fisher; Pittsburgh, PA) in a centrifuge tube, and the mixture was placed in an incubator (5% carbon dioxide (CO_2)/95% air) for 10 minutes at 37 C. While the fragments were in the incubator, the digestive enzyme solution was made in a quantity forty times the volumetric amount of bone fragments to provide a sufficient supply for a series of digestive washes. The enzyme solution consisted of 0.1% type I collagenase (Worthington Biochemical; Lakewood, NJ) in phosphate-buffered saline (PBS) (Sigma; St. Louis, MO), and it was filter-sterilized through a 0.22μm cellulose acetate membrane filter unit (Corning; Acton, MA). After the incubation period, the trypsin/EDTA solution was discarded, and the enzyme solution was added in a quantity ten times the volumetric amount of bone fragments in the tube. The tube was returned to the incubator on an orbital shaker plate (IKA Works; Wilmington, NC) for 10 minutes (to facilitate access of the enzyme to the fragments) and vortexed. The resulting first supernatant was discarded since cells from it do not consistently develop into mineralized bone nodules [*21*]. Next, the same amount of enzyme solution was added, and the tube was placed in the incubator for 30 minutes. The tube was vortexed, and the second supernatant was collected in Dulbecco's Modified Eagle's Medium (DMEM) (Invitrogen; Carlsbad, CA) supplemented with 10% Fetal Bovine Serum (FBS) (BioWhittaker; Walkersville, MD), 1.0% Antibiotic-Antimycotic (Invitrogen; Carlsbad, CA), and 0.2% Fungizone (Invitrogen; Carlsbad, CA). (DMEM with supplements will be referred to as DMEM-Complete or DMEM-C.) The fragments were exposed to the enzyme solution for two additional 30-minute cycles in the incubator. After each incubation period, the tube was vortexed, and the third and fourth supernatants were collected in the same collection tube as the second supernatant. The collection tube was centrifuged at 1000 rpm for 5 minutes, and the supernatant was aspirated, leaving behind a cell pellet. The cell pellet was resuspended in DMEM-C, and the cells were plated in two T-25 flasks (Becton-Dickinson; Franklin Lakes, NJ). Cells were cultured in a 5% CO_2/95% air incubator at 37 C. Media changes were performed every 3-4 days with DMEM-C.

Centrifugal Isolation – Osteoblasts were isolated from rat femoral bone marrow using a centrifugal isolation technique described by Dobson and coworkers [*14*]. Rat

hind legs were collected, and soft tissue was removed as in the enzymatic isolation technique. The femurs were rinsed in fresh HBSS-C for 10 minutes. Proximal ends of the femurs were removed using sterile bone-cutting forceps, and each of the femurs was placed (proximal end down) in a sterilized polypropylene microcentrifuge tube. The tubes were centrifuged at 2000 rpm for approximately 60 seconds. Femurs were removed from each tube, and 1 mL of DMEM-C was added to the resulting marrow pellets. Then, using a sterile 20-gauge needle and 10 mL syringe (both from Becton-Dickinson; Franklin Lakes, NJ), the pellets were triturated in the media. The cell suspension was transferred to a centrifuge tube, and fresh DMEM-C was added to yield a total of 10 mL. The cells were plated in two T-25 flasks, and they were cultured using the same conditions as cells obtained from enzymatic digestion.

Syringe Isolation – A method described by Maniatopoulos and coworkers was used to obtain osteoblasts from rat bone marrow via syringe isolation [*18*]. Rat hind legs were collected and prepared in the same manner used for centrifugal isolation. The proximal end of the femurs were removed, and using a sterile 20-gauge needle and 10 mL syringe, a hole was created in the distal end of the femur to expose the intermedullary canal filled with marrow. A new, sterile 20-gauge needle with 5 mL DMEM-C in the syringe was inserted into the hole, and the marrow was flushed from the canal into a centrifuge tube. The flushing procedure was repeated twice with a new needle and 5 mL DMEM-C each time to give a total of 15 mL marrow/DMEM-C. A new needle was used to triturate the marrow in the DMEM-C. The subsequent cell suspension was then centrifuged at 1500 rpm for 5 minutes. After aspirating and discarding the supernatant, fresh DMEM-C was added to yield a total of 10 mL. The marrow pellet was then triturated with a pipet, and the cells were plated in two T-25 flasks. Cells were cultured under the same conditions as cells obtained from the other two methods.

Cell Seeding – Osteoblasts from passage 3 (centrifugal and syringe isolation) and passage 4 (enzymatic digestion) were seeded in 24-well tissue culture polystyrene plates (Corning; Acton, MA) at 7.6×10^4 cells/well (60% confluency). The osteoblasts were seeded in 1 mL mineralization media (DMEM-M) consisting of DMEM-C supplemented with 10 mM β–glycerophosphate (Sigma; St. Louis, MO), 50 μg/mL ascorbic acid (Sigma; St. Louis, MO), and 10^{-8} M dexamethasone (ICN Biomedicals; Costa Mesa, CA). The DMEM-M was changed every 3-4 days during the 24-day study.

Qualitative Microscopy: Cell Morphology and Viability

Cell Morphology – Cell morphology was assessed on days 1, 7, 10, 14, 17, 21, and 24 before assays or media changes were performed. Observations were made with an inverted microscope (Carl Zeiss; Thornwood, NY) in phase contrast mode. Images were obtained using image acquisition software (Diagnostic Instruments; Sterling

Heights, MI) with a color digital camera (Diagnostic Instruments; Sterling Heights, MI) attached to the inverted microscope.

Cell Viability – Cell viability was observed on days 1, 10, 17, and 24 using a LIVE/DEAD®[3] Viability/Cytotoxicity kit. The cells were fluorescently labeled using the calcein AM and ethidium homodimer dyes in the kit and following the manufacturer's protocol. Live cells retain a dye that produces bright green fluorescence (excitation and emission of 495 nm and 515 nm, respectively), while dead cells fluoresce a bright red (excitation of 495 nm and emission of 635 nm). Observations were made using the aforementioned microscope and a fluorescence filter set (Chroma Technology; Brattleboro, VT), and images were obtained using the same camera and software.

Quantitative Testing: Metabolic Activity, Lactic Acid and Glucose

Metabolic Activity – The metabolic activity of the cells was assessed on days 10, 17, and 24 using a CellTiter 96®[4] AQueous One Solution Cell Proliferation Assay. Two hundred microliters of reagent was added to each of the experimental and the acellular control wells (which contained DMEM-M only) in the 24-well plates. The samples were placed back in the incubator on a shaker plate for a period of two hours. After incubation, the samples were transferred in triplicate in 200 μL quantities to a 96-well plate (Corning; Acton, MA). Absorbance values were obtained immediately at 490 nm using a spectrophotometric reader (DYNEX Technologies; Chantilly, VA).

Lactic Acid and Glucose – The amounts of lactic acid and glucose present in the culture media were measured on days 1, 7, 10, 14, 17, 21, and 24 using a biochemistry analyzer (YSI; Yellow Springs, OH). One hundred microliters of media was removed from each of the experimental and acellular control wells before media changes were performed.

Quantitative Testing: Protein, Alkaline Phosphatase, and Extracellular Calcium

Assays were performed on cells obtained from days 10, 17, and 24 to confirm the presence of osteoblasts in culture. On each of the days, the wells of the 24-well plates containing the samples were rinsed twice gently with PBS, and deionized water was added. Deionized water was also added to acellular control wells after twice rinsing the empty wells with PBS. The plates were frozen at –80 C until all samples were collected and the assays were ready to be conducted. After three freeze/thaw cycles, the assays were performed and included: total intracellular protein (Pierce Biotechnology; Rockford, IL), alkaline phosphatase (ALP) (Sigma; St. Louis, MO), and extracellular calcium (Sigma; St. Louis, MO).

[3] Molecular Probes; Eugene, OR.
[4] Promega; Madison, WI.

Protein – Total intracellular protein was determined according to the manufacturer's protocol. The working reagent was added in 200 µL quantities to 25 µL of the cell lysate samples or the albumin standards in a 96-well plate. The albumin was mixed previously in defined amounts in order to produce a standard curve. The plate was gently agitated on a shaker plate for 30 seconds and incubated at 37 C for 30 minutes. After cooling to room temperature, absorbance values were recorded at 562 nm on a spectrophotometer previously described. The total intracellular protein was determined in order to normalize the results from the ALP and calcium assays.

Alkaline Phosphatase – The ALP assay was modified to incorporate 250 µL of the working reagent with 5 µL of the cell lysate in order to perform the test with 96-well plates. Once the lysate was added to the reagent, the mixture was incubated for 30 seconds at 37 C. Absorbance values were recorded every minute for 5 minutes at 410 nm on the spectrophotometric reader. The ALP activity was determined using the formulas provided in the protocol, and the activity was normalized with the total intracellular protein content. The results were reported in terms of µmol/min/mg protein.

Extracellular Calcium – Before the extracellular calcium was measured, it was extracted from the extracellular matrix using a method adapted from Webster and coworkers [*5*]. The acellular control wells and sample wells were treated with 500 µL of 0.5 N hydrochloric acid (HCl) and the plates were placed on an orbital shaker plate overnight at a temperature of 37 C. The extracellular matrix and the acid in each well were collected in centrifuge tubes that were spun at 1000 rpm for 5 minutes. Absorbance of the HCl supernatant samples and calcium standards was measured at 575 nm on a spectrophotometer previously described. Total extracellular calcium was determined using the formula provided in the manufacturer's protocol. The total extracellular calcium was normalized with the total intracellular protein content and was expressed in terms of µg/mg protein.

Statistical Analysis

All quantitative assays were performed in triplicate. Values presented are mean ± standard error of mean (SEM) (n = 3). Using SAS®[5] statistical software, two-factor analysis of variance (ANOVA) was conducted. The effects of cell isolation method and time were compared using Tukey's multiple comparison method. One-factor ANOVA was used to compare lactic acid production among cell isolation methods. The significance level for all comparisons was $p < 0.05$.

Results

Qualitative Microscopy

[5] SAS Institute; Cary, NC.

Cell Morphology – Light micrographs illustrate the cell morphologies observed as a result of the various cell isolation methods (Figure 2). No distinct changes were noticed in cell morphology between days 17 and 24 for any of the cell isolation methods. Cell morphology differences appeared, however, as a result of the cell isolation method used. Cells isolated using enzymatic digestion (Figures 2a and 2d) were fibroblast-like in appearance and formed a dense, continuous layer. Cells obtained from centrifugal isolation (Figures 2b and 2e) and syringe isolation (Figures 2c and 2f) had both spindle-shaped and polygonal morphologies. The marrow-derived cells were not confluent; instead, they appeared as colonies of cells that were interconnected more often than isolated. At some locations within these cell colonies, three-dimensional opaque regions were observed containing clumps of the polygonal cells.

Cell Viability – Fluorescence micrographs illustrate the results of cell viability testing on cells from the various isolation methods (Figure 3). Direct comparisons of cell viability between time points were not possible because the LIVE/DEAD® Viability/Cytotoxicity test is an endpoint assay. Enzymatically-isolated cells (Figures 3a and 3d) appeared as a dense layer of live cells as in the cell morphology examination. The marrow-derived cells from centrifugal isolation (Figures 3b and 3e) and syringe isolation (Figures 3c and 3f) appeared as clusters of live cells. Cells obtained from centrifugal isolation appeared to be clustered together in larger opaque colonies, and they appeared to be present in larger numbers than colonies from syringe isolation. A small number of dead cells were observed in cell populations derived from each of the isolation methods, but there appeared to be no substantial difference between methods.

Quantitative Testing

Metabolic Activity – The cells obtained by enzymatic digestion exhibited a significantly ($p < 0.05$) higher metabolic activity than cells from the other two isolation methods on days 10, 17, and 24 (Figure 4). The metabolic activity of cells from each isolation method declined as culture time increased with the activity on day 24 being significantly ($p < 0.05$) lower than on day 10.

Lactic Acid and Glucose – Enzymatically-isolated cells produced a significantly ($p < 0.05$) higher cumulative amount of lactic acid than the other two methods (Figure 5). Cells isolated by enzymatic digestion also consumed a significantly ($p < 0.05$) higher total amount of glucose (as evidenced by lower amounts of glucose remaining in the media) than the other methods (Figure 6). Data represents the cumulative amounts of lactic acid and glucose measured on days 1, 7, 10, 14, 17, 21, and 24 for all three

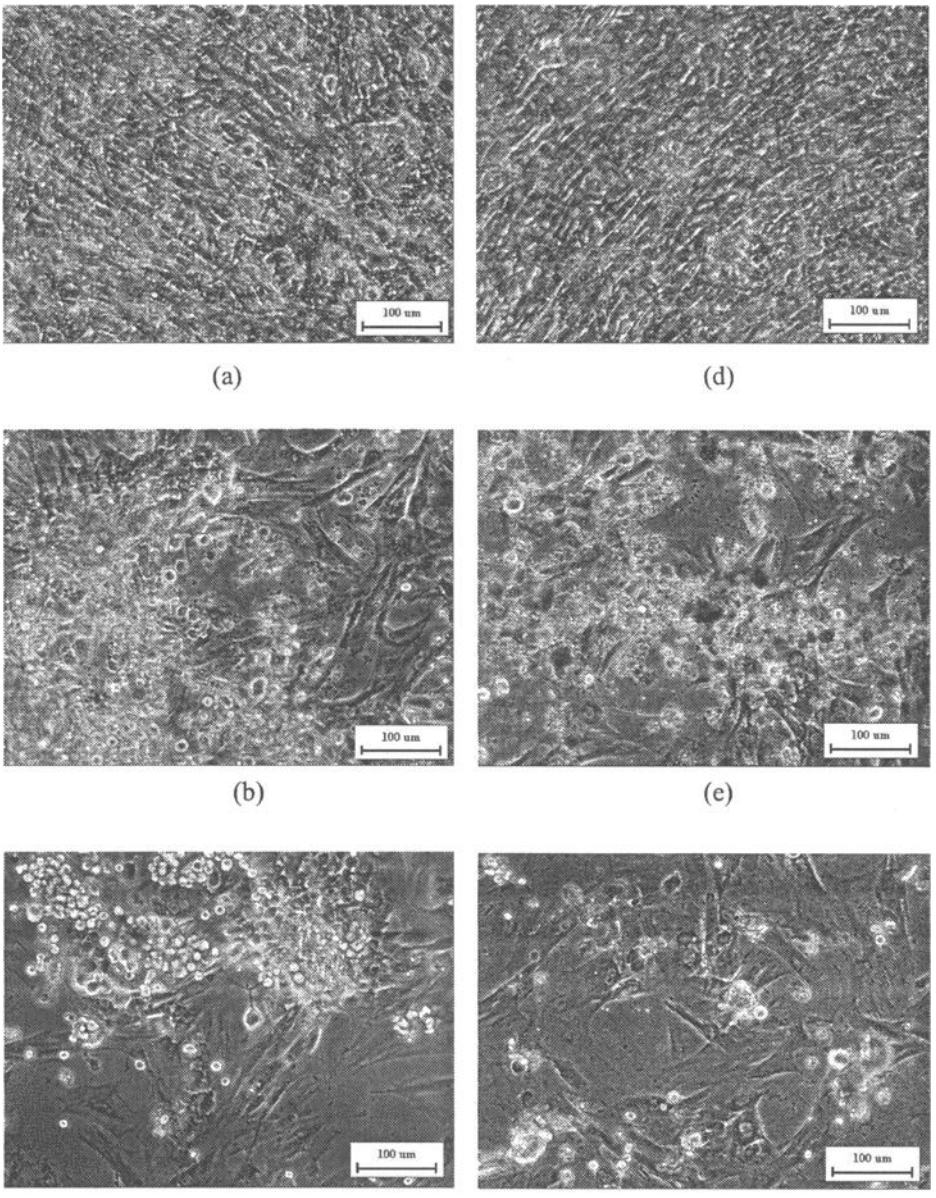

Figure 2 – *Light micrographs showing the effect of cell isolation method and time on cell morphology. (a) Day 17 - enzymatic (b) Day 17 - centrifugal (c) Day 17 - syringe (d) Day 24 - enzymatic (e) Day 24 - centrifugal (f) Day 24 - syringe. Original magnification is 200X.*

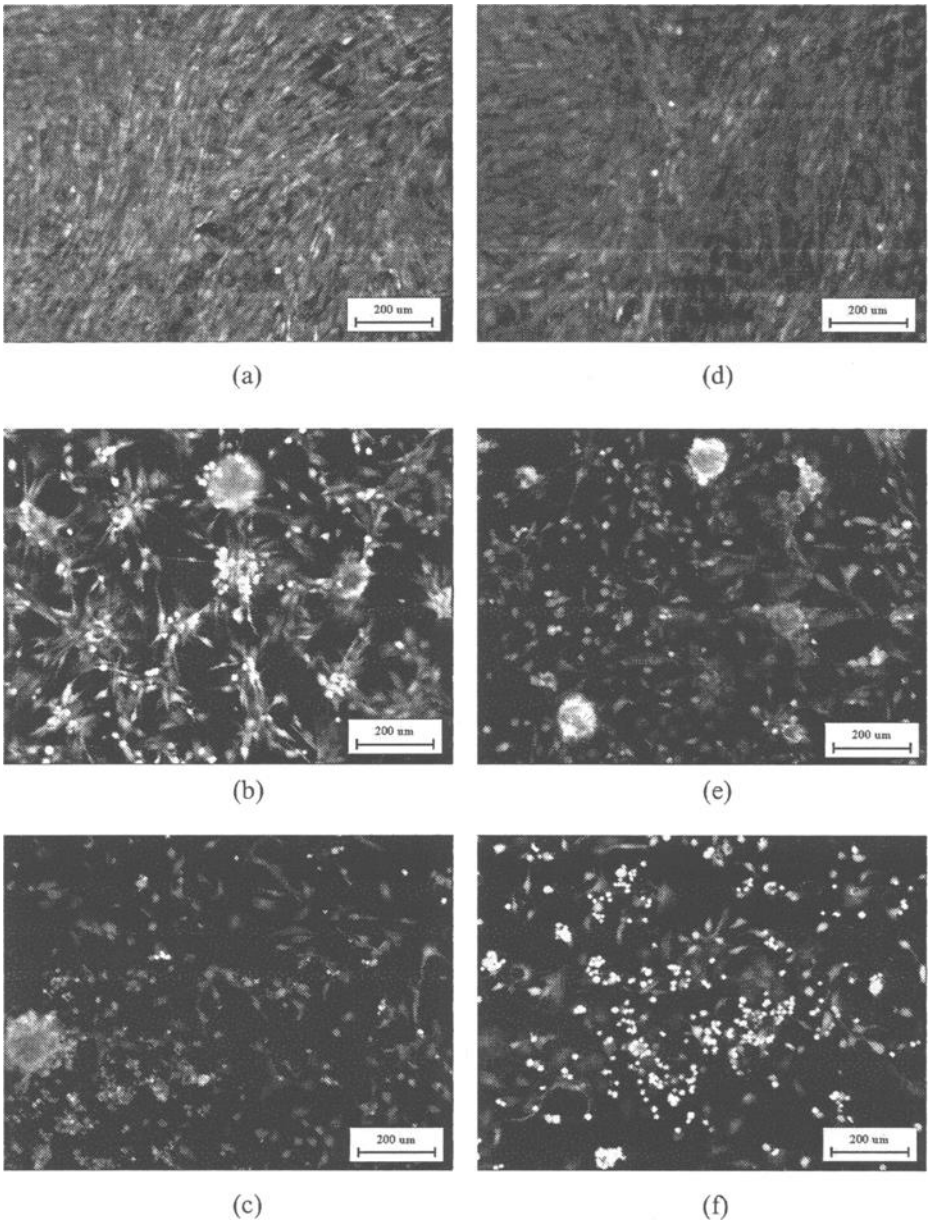

Figure 3 – *Fluorescence micrographs showing the effect of cell isolation method on cell viability. Images obtained after using LIVE/DEAD® Viability/Cytotoxicity kit. (a) Day 17 - enzymatic (b) Day 17 - centrifugal (c) Day 17 – syringe (d) Day 24 - enzymatic (e) Day 24 - centrifugal (f) Day 24 - syringe Original magnification is 100X.*

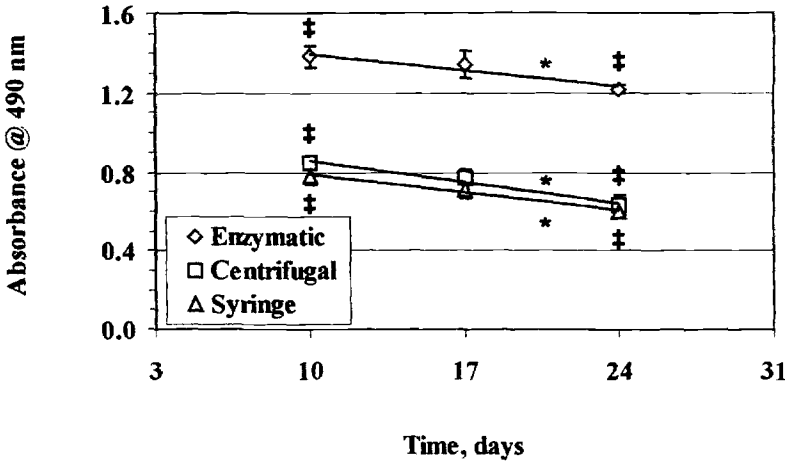

Figure 4 – *Metabolic activity as a function of time and cell isolation method. Each data point represents the mean of three values, and error bars denote SEM; * denotes difference ($p < 0.05$) in activity with respect to cell isolation method; ‡ denotes difference ($p < 0.05$) in activity with respect to time.*

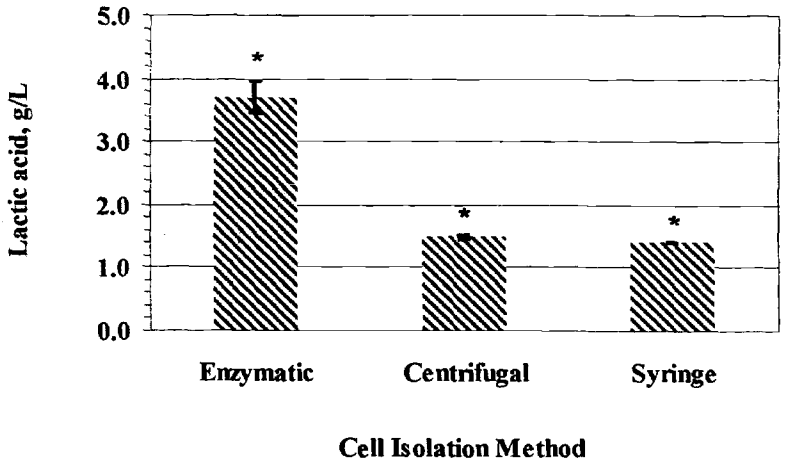

Figure 5 – *Lactic acid level as a function of cell isolation method. Each data point represents the mean of three values, and error bars denote SEM; * denotes difference ($p < 0.05$) in lactic acid level with respect to cell isolation method.*

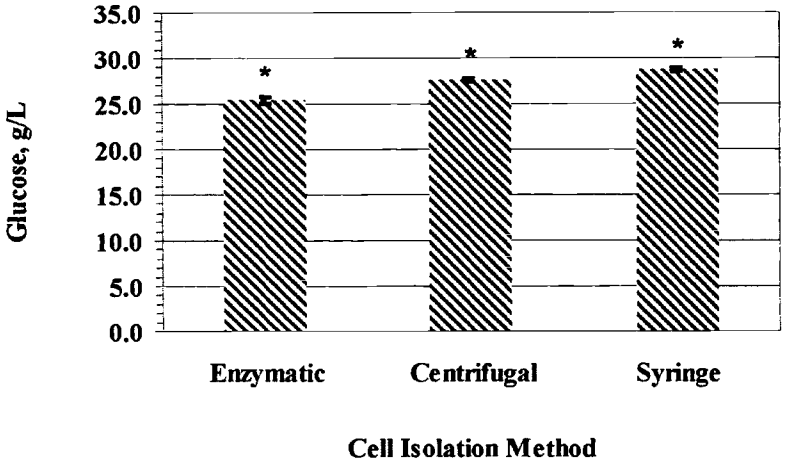

Figure 6 – *Glucose level as a function of cell isolation method. Each data point represents the mean of three values, and error bars denote SEM; * denotes difference ($p < 0.05$) in glucose level with respect to cell isolation method.*

methods. Lactic acid is a product of cellular anaerobic metabolism, and glucose is the primary energy source for cellular metabolism.

Protein – The cells obtained from enzymatic digestion contained a significantly ($p < 0.05$) higher amount of intracellular protein on days 10, 17, and 24 than cells isolated by the centrifugal and syringe techniques (Figure 7). The enzymatically-isolated cells contained less protein over time, with a significantly ($p < 0.05$) lower amount of protein on day 24 than on day 10. Cells isolated by the centrifugal and syringe methods showed no significant change ($p < 0.05$) in the quantity of intracellular protein during this time.

Alkaline Phosphatase – Syringe-isolated cells produced ALP activities that were significantly ($p < 0.05$) higher than found in centrifugally-isolated cells on days 10 and 17 and enzymatically-isolated cells on day 17 (Figure 8). On day 24, the ALP activity of centrifugally-isolated cells was significantly ($p < 0.05$) higher than cells isolated with the enzymatic method. No additional significant ($p < 0.05$) differences occurred between methods. The only significant ($p < 0.05$) increase in ALP activity between days 10 and 24 occurred in cells obtained by centrifugal isolation. Syringe- and enzymatically-isolated cells showed no significant change ($p < 0.05$) in ALP activity during this time period.

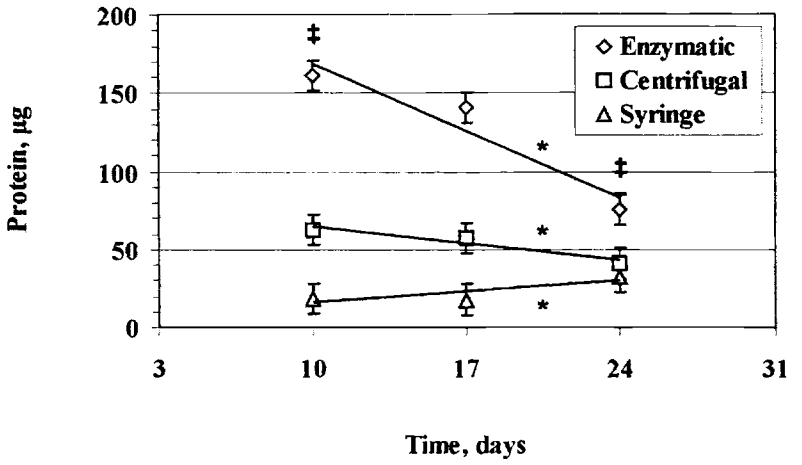

Figure 7 – *Intracellular protein level as a function of time and cell isolation method. Each data point represents the mean of three values, and error bars denote SEM; * denotes difference ($p < 0.05$) in protein level with respect to cell isolation method; ‡ denotes difference ($p < 0.05$) in protein level with respect to time.*

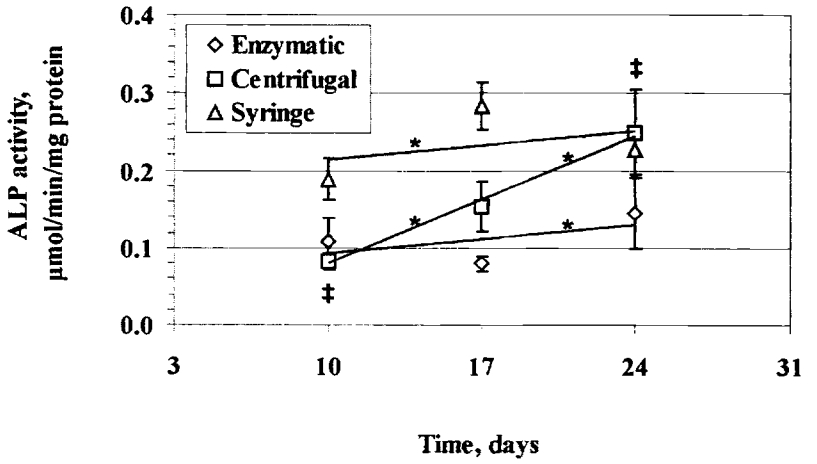

Figure 8 – *ALP activity as a function of time and cell isolation method. Each data point represents the mean of three values, and error bars denote SEM; * denotes difference ($p < 0.05$) in ALP activity with respect to cell isolation method; ‡ denotes difference ($p < 0.05$) in ALP activity with respect to time.*

Extracellular Calcium – Measurable amounts of extracellular calcium were not detected until assays were performed on day 17 (Figure 9). Enzymatically-isolated cells formed a significantly ($p < 0.05$) smaller amount of mineralized matrix (containing extracellular calcium) on days 17 and 24 than cells isolated by centrifugal and syringe methods. Additionally, the centrifugally-isolated cells produced a significantly ($p < 0.05$) smaller amount of mineralized matrix than the syringe-isolated cells did in this same time period. Between days 10 and 24, cells isolated from each of the three methods produced significantly ($p < 0.05$) greater amounts of mineralized matrix with increasing culture time.

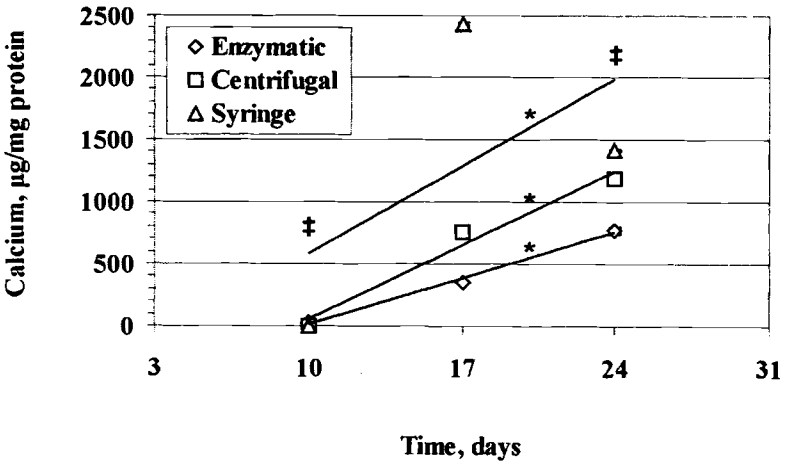

Figure 9 – *Extracellular calcium level as a function of time and cell isolation method. Each data point represents the mean of three values, and error bars denote SEM; * denotes difference ($p < 0.05$) in calcium level with respect to cell isolation method; ‡ denotes difference ($p < 0.05$) in calcium level with respect to time.*

Discussion

Bone-forming cells were characterized after being released using one of three cell isolation methods: enzymatic digestion, centrifugal isolation, or syringe isolation. Qualitative cell morphology and viability images suggest that cells from each of the isolation methods attached to tissue culture polystyrene substrates. Assays of metabolic activity, lactic acid and glucose levels, and intracellular protein levels indicate that the cells proliferated on the surface. The ALP assay showed that ALP, an active enzyme in the plasma membrane of osteoblasts [*16, 23, 24*], was present in each cell population. Finally, cells isolated by each technique produced mineralized matrix as shown by the results of the calcium assay. The temporal pattern observed, a down-regulation of intracellular protein and metabolic activity along with an increase in ALP

activity and extracellular calcium, agrees with the developmental sequence of osteoblasts proposed by Stein and coworkers [*16*]. The expression of ALP before mineralization indicates that it may be required to prepare the extracellular matrix for mineralization. The presence of extracellular calcium suggests that mineralization of the extracellular matrix is occurring. The calcium binds to inorganic phosphate in the form of crystals that are deposited between collagen fibrils.

Despite the general similarities in the cells cultured from the various isolation methods, statistically significant differences ($p < 0.05$) occurred in all of the quantitative tests performed. Qualitative microscopy also illustrated morphological differences in cells that were obtained from the three methods. Enzymatically-isolated cells produced the highest degree of metabolic activity, yielded the largest cumulative amount of lactic acid, consumed the largest cumulative amount of glucose, and contained the greatest amount of intracellular protein among the three isolation methods ($p < 0.05$ for each comparison). Cells isolated by enzymatic digestion also produced the lowest ($p < 0.05$) amounts of mineralized matrix (as measured by extracellular calcium) on days 17 and 24. Considering these results along with the fibroblast-like morphology observed for the enzymatically-isolated cells, it appears that the cells from this particular population exhibit a lower degree of osteoblast functional characteristics than the other two isolation methods.

One possibility for the reduced osteoblast function of the enzymatically-isolated cells is the use of collagenase in the isolation protocol. The collagenase can damage proteins in the cell membrane, affecting functionality of the cell [*15*]. An extensive amount of subculturing can affect the phenotypic markers; however, the cells were seeded at passage four, which is not considered extensive. In other studies, enzymatically-isolated cells from passage four have produced characteristic phenotypic markers [*2, 4*]. Although the enzymatically-isolated cells produced a mineralized matrix, the absence of nodules was conspicuous and is not consistent with the normal bone-like structures observed in previous research [*21*]; however, the cells used in that study were enzymatically-isolated from the calvaria of fetal (21-day) rats. The nodules' absence may be related to the low amount of ALP activity measured because intense ALP activity is often located around the perimeter of nodules [*21*]. Instead of nodules, the mineral phase may have been present as mineral plaque and less extensive mineral granules, as suggested by Williams and coworkers [*25*].

Centrifugally-isolated and syringe-isolated cells generated less metabolic activity, produced a smaller cumulative amount of lactic acid, consumed a smaller cumulative amount of glucose, and contained less intracellular protein than cells isolated enzymatically ($p < 0.05$ for each comparison). The marrow-derived cells also produced a higher ($p < 0.05$) amount of mineralized matrix on days 17 and 24. As in the culture of enzymatically-isolated bone cells, nodules are the normal bone-like structures formed in marrow cell cultures. Examination of cell morphology in the marrow-derived cells revealed the presence of dense cell clusters which have been previously characterized as nodules [*18*]. Maniatopoulos and coworkers found that cultures supplemented with dexamethasone and β-glycerophosphate formed mineralized nodules [*18*]. In the current study, the same supplements were used in the

culture media and nodules apparently formed. In view of the quantitative results and the apparent nodules formed, the marrow-derived cells follow the temporal pattern proposed by Stein and coworkers [*16*] more closely than enzymatically-isolated cells. Given the results from the intracellular protein and ALP assays, however, a definitive statement regarding the agreement between Stein and coworkers' temporal pattern [*16*] and this study cannot be made. While other signs of metabolic activity (metabolic activity, lactic acid produced, and glucose consumed) showed a decline ($p < 0.05$) with time, no change ($p < 0.05$) in intracellular protein was observed with time for the marrow-derived cells. For the syringe-isolated cells, no change ($p < 0.05$) in ALP activity occurred with time, but there was an increase ($p < 0.05$) in ALP activity in the centrifugally-isolated cells.

Future histological studies will be conducted to determine if mineralization actually occurs in the suspected nodules. Normal mineralization, dystrophic calcification with the presence of mineralized plaque, or a combination of the two could have taken place as previously described [*26*]; thus, alizarin red or von Kossa staining will be performed in future studies to determine how the mineralized tissue is organized. Additionally, assays to determine the presence of bone characteristic markers such as osteocalcin and type I collagen will be of interest. Measurements of intracellular protein, ALP, and extracellular calcium before day 10 and beyond day 24 will also be beneficial. This will allow for a determination of initial levels and verification that heavy mineralization occurs and ALP activity declines with extended culture times [*23*].

The outcome of cellular TEMPs is difficult to predict due to variations in cell behavior. Inherent differences in cells are caused by the age, gender, genetic characteristics, and health status of the patient from which the cells are retrieved. In this study, we varied a non-inherent factor, cell isolation method, to determine its role in affecting cell adhesion, proliferation, and the type of final tissue formed. Variations in cell behavior due to the methods of cell isolation and cell culture can be regulated by implementing a system of standard operating procedures. In addition to cell population characteristics, these standards should also consider the industrial and clinical feasibility and costs of processes associated with the culture of cells for use in TEMPs. For example, the time required for bone cells to proliferate and mineralize in sufficient quantities will affect the cost and efficacy of a clinically realistic product. Without cell retrieval standards, the outcome of cellular TEMPs will be highly variable, which will be detrimental to the TEMP industry and the field of tissue engineering.

Conclusions

Using a battery of biochemical assays, significant differences were observed between rat bone cells retrieved using three different accepted techniques. Cell proliferation of enzymatically-isolated cells was greater ($p < 0.05$) than that of marrow-derived cells as determined by assays of metabolic activity, lactic acid levels, and glucose levels. Mineralization of the extracellular matrix was greater ($p < 0.05$)

for marrow-derived cells than enzymatically-isolated cells as evidenced by an extracellular calcium assay. The results from these particular cell populations indicate that different characteristics of the bone-forming cells are obtained when the cells are cultured under the same conditions. The success of many TEMPs depends on the survival, proliferation, and differentiation of various cell types to form the appropriate tissue. Thus, standards are necessary for the treatment of cellular components in order to develop a framework of acceptable cellular characteristics for the many different applications of TEMPs and to reduce variability between products.

Acknowledgements

This work was funded through grants from the NSF and the AO ASIF Foundation, Switzerland. The authors thank Dr. Thomas Webster of Purdue University, Dr. Rena Bizios of Rensselaer Polytechnic Institute, Dr. Joel Bumgardner of Mississippi State University, Jason Burdick of the University of Colorado, and Dr. Julie Martin of Clemson University for their technical assistance. The authors also thank Aditya Chaubey and David Orr of Clemson University for their assistance with the cell isolation procedures and Dr. Larry Grimes of Clemson University for his assistance with the statistical analysis.

References

[1] Puleo, D. A., Holleran, L. A., Doremus, R. H. and Bizios, R., "Osteoblast Responses to Orthopedic Implant Materials in Vitro," *Journal of Biomedical Materials Research*, Vol. 25, No. 6, 1991, pp. 711-723.

[2] Ishaug, S. L., Yaszemski, M. J., Bizios, R. and Mikos, A. G., "Osteoblast Function on Synthetic Biodegradable Polymers," *Journal of Biomedical Materials Research*, Vol. 28, No. 12, 1994, pp. 1445-1453.

[3] Ishaug, S. L., Payne, R. G., Yaszemski, M. J., Aufdemorte, T. B., Bizios, R. and Mikos, A. G., "Osteoblast Migration on Poly(α-Hydroxy Esters)," *Biotechnology and Bioengineering*, Vol. 50, No. 4, 1996, pp. 443-451.

[4] Ishaug-Riley, S. L., Crane-Kruger, G. M., Yaszemski, M. J. and Mikos, A. G., "Three-Dimensional Culture of Rat Calvarial Osteoblasts in Porous Biodegradable Polymers," *Biomaterials*, Vol. 19, No. 15, 1998, pp. 1405-1412.

[5] Webster, T. J., Ergun, C., Doremus, R. H., Siegel, R. W. and Bizios, R., "Enhanced Functions of Osteoblasts on Nanophase Ceramics," *Biomaterials*, Vol. 21, No. 17, 2000, pp. 1803-1810.

[6] Ishaug, S. L., Crane, G. M., Miller, M. J., Yasko, A. W., Yaszemski, M. J. and Mikos, A. G., "Bone Formation by Three-Dimensional Stromal Osteoblast

Culture in Biodegradable Polymer Scaffolds," *Journal of Biomedical Materials Research*, Vol. 36, No. 1, 1997, pp. 17-28.

[7] Ishaug-Riley, S. L., Crane, G. M., Gurlek, A., Miller, M. J., Yasko, A. W., Yaszemski, M. J. and Mikos, A. G., "Ectopic Bone Formation by Marrow Stromal Osteoblast Transplantation Using Poly(Dl-Lactic-Co-Glycolic Acid) Foams Implanted into the Rat Mesentery," *Journal of Biomedical Materials Research*, Vol. 36, No. 1, 1997, pp. 1-8.

[8] De Bruijn, J. D., van den Brink, I., Mendes, S., Dekker, R., Bovell, Y. P. and van Blitterswijk, C. A., "Bone Induction by Implants Coated with Cultured Osteogenic Bone Marrow Cells," *Advances in Dental Research*, Vol. 13, 1999, pp. 74-81.

[9] Breitbart, A. S., Grande, D. A., Kessler, R., Ryaby, J. T., Fitzsimmons, R. J. and Grant, R. T., "Tissue Engineered Bone Repair of Calvarial Defects Using Cultured Periosteal Cells," *Plastic and Reconstructive Surgery*, Vol. 101, No. 3, 1998, pp. 567-574; discussion 575-566.

[10] Peter, S. J., Lu, L., Kim, D. J. and Mikos, A. G., "Marrow Stromal Osteoblast Function on a Poly(Propylene Fumarate)/Beta-Tricalcium Phosphate Biodegradable Orthopaedic Composite," *Biomaterials*, Vol. 21, No. 12, 2000, pp. 1207-1213.

[11] Goldstein, A. S., Juarez, T. M., Helmke, C. D., Gustin, M. C. and Mikos, A. G., "Effect of Convection on Osteoblastic Cell Growth and Function in Biodegradable Polymer Foam Scaffolds," *Biomaterials*, Vol. 22, No. 11, 2001, pp. 1279-1288.

[12] Lee, Y. M., Seol, Y. J., Lim, Y. T., Kim, S., Han, S. B., Rhyu, I. C., Baek, S. H., Heo, S. J., Choi, J. Y., Klokkevold, P. R. and Chung, C. P., "Tissue-Engineered Growth of Bone by Marrow Cell Transplantation Using Porous Calcium Metaphosphate Matrices," *Journal of Biomedical Materials Research*, Vol. 54, No. 2, 2001, pp. 216-223.

[13] Radice, M., Brun, P., Cortivo, R., Scapinelli, R., Battaliard, C. and Abatangelo, G., "Hyaluronan-Based Biopolymers as Delivery Vehicles for Bone-Marrow-Derived Mesenchymal Progenitors," *Journal of Biomedical Materials Research*, Vol. 50, No. 2, 2000, pp. 101-109.

[14] Dobson, K. R., Reading, L., Haberey, M., Marine, X. and Scutt, A., "Centrifugal Isolation of Bone Marrow from Bone: An Improved Method for the Recovery and Quantitation of Bone Marrow Osteoprogenitor Cells from Rat Tibiae and Femurae," *Calcified Tissue International*, Vol. 65, No. 5, 1999, pp. 411-413.

[15] Wong, G., "Isolation and Behavior of Isolated Bone-Forming Cells," *Bone, Vol 1: The Osteoblast and Osteocyte*, B. K. Hall, Ed., CRC Press, Boca Raton, FL, 1990, pp. 171-192.

[16] Stein, G. S., Lian, J. B. and Owen, T. A., "Relationship of Cell Growth to the Regulation of Tissue-Specific Gene Expression During Osteoblast Differentiation," *FASEB Journal*, Vol. 4, No. 13, 1990, pp. 3111-3123.

[17] Buttery, L. D. K., Bourne, S., Xynos, J. D., Wood, H., Hughes, F. J., Hughes, S. P. F., Episkopou, V. and Polak, J. M., "Differentiation of Osteoblasts and in Vitro Bone Formation from Murine Embryonic Stem Cells," *Tissue Engineering*, Vol. 7, No. 1, 2001, pp. 89-99.

[18] Maniatopoulos, C., Sodek, J. and Melcher, A. H., "Bone Formation in Vitro by Stromal Cells Obtained from Bone Marrow of Young Adult Rats," *Cell & Tissue Research*, Vol. 254, No. 2, 1988, pp. 317-330.

[19] Quarto, R., Thomas, D. and Liang, C. T., "Bone Progenitor Cell Deficits and the Age-Associated Decline in Bone Repair Capacity," *Calcified Tissue International*, Vol. 56, No. 2, 1995, pp. 123-129.

[20] D'Ippolito, G., Schiller, P. C., Ricordi, C., Roos, B. A. and Howard, G. A., "Age-Related Osteogenic Potential of Mesenchymal Stromal Stem Cells from Human Vertebral Bone Marrow," *Journal of Bone and Mineral Research*, Vol. 14, No. 7, 1999, pp. 1115-1122.

[21] Bellows, C. G., Aubin, J. E., Heersche, J. N. and Antosz, M. E., "Mineralized Bone Nodules Formed in Vitro from Enzymatically Released Rat Calvaria Cell Populations," *Calcified Tissue International*, Vol. 38, No. 3, 1986, pp. 143-154.

[22] Gray, C., Boyde, A. and Jones, S., "The Isolation, Culture, and Functional Assay of Osteoclasts and Osteoblasts," *Cell Biology: A Laboratory Handbook*, J. E. Celis, Ed., Academic Press, San Diego, CA, 1998, pp. 142-148.

[23] Lian, J. B. and Stein, G. S., "Concepts of Osteoblast Growth and Differentiation: Basis for Modulation of Bone Cell Development and Tissue Formation," *Critical Reviews in Oral Biology & Medicine*, Vol. 3, No. 3, 1992, pp. 269-305.

[24] Stein, G. S. and Lian, J. B., "Molecular Mechanisms Mediating Proliferation/Differentiation Interrelationships During Progressive Development of the Osteoblast Phenotype," *Endocrine Reviews*, Vol. 14, No. 4, 1993, pp. 424-442.

[25] Williams, D. C., Boder, G. B., Toomey, R. E., Paul, D. C., Hillman, C. C., Jr., King, K. L., Van Frank, R. M. and Johnston, C. C., Jr., "Mineralization and Metabolic Response in Serially Passaged Adult Rat Bone Cells," *Calcified Tissue International*, Vol. 30, No. 3, 1980, pp. 233-246.

[26] Howlett, C. R., Cave, J., Williamson, M., Farmer, J., Ali, S. Y., Bab, I. and Owen, M. E., "Mineralization in in Vitro Cultures of Rabbit Marrow Stromal Cells," *Clinical Orthopaedics and Related Research*, Vol. 213, 1986, pp. 251-263.

Guigen Zhang[1] and Jeremy L. Gilbert[2]

A New Method for Real-Time and In-Situ Characterization of the Mechanical and Material Properties of Biological Tissue Constructs

Reference: Zhang, G. and Gilbert, J. L., "**A New Method for Real-Time and In-Situ Characterization of the Mechanical and Material Properties of Biological Tissue Constructs,**" *Tissue Engineered Medical Products (TEMPs), ASTM STP 1452*, E. Schutte, G. L. Picciolo, and D. S. Kaplan, Eds., ASTM International, West Conshohocken, PA, 2004.

Abstract: To capture the transient, nonlinear and time-dependent characteristics of the mechanical and material properties of biomaterials and biological tissue constructs, we developed a real-time based evaluation method. This method measures the paired transient stress and strain as a function of time for a given material, and calculates instantaneously its complex modulus measurements as a function of frequency. Because the measured complex moduli contain not only the mechanical properties (magnitude of the modulus curves) but also the material characteristics (shape of the modulus curves), this method allows us to link directly the mechanical properties to the material characteristics in a real-time and in-situ manner. The significance of this capability is that the changes in both mechanical property and material structure can be correlated repeatedly during the growing or aggregating processes of the biological tissues or constructs.

Keywords: Biomaterials, biological tissue constructs, viscoelastic, material characteristics, mechanical property, complex moduli, Fast Fourier Transform, tissue engineering

[1]Assistant Professor, Faculty of Engineering, Department of Biological and Agricultural Engineering, Driftmier Engineering Center, University of Georgia, Athens, GA, 30602.
[2]Professor, Department of Bioengineering and Neuroscience, Syracuse University, Syracuse, NY, 13244.

Introduction

In the last decade, we have seen a drastic development of technologies for organ replacement and repair as a direct result of the integration of engineering principles and life sciences. For instance, tissue engineering – the field that applies the methods of interdisciplinary engineering and life sciences toward the development of biological substitutes and constructs - has demonstrated many promising ways to augment, replace and restore, partially or completely, various organs and tissues as well as their functions by combining synthetic and living components in appropriate configurations and environmental conditions [1-5]. And nanotechnology - the study and manufacturing of structures and devices with dimensions at the size of a molecule or smaller - has already revealed a very broad spectrum of opportunities for developing new and novel materials, biopolymer composites, nanocomposites, self-assembled biomaterials and nano-constructs. As we go down this path to seek ways to develop biological constructs from the bottom up (e.g., micro/nano-scale self-assembled materials and tissue constructs) to meet the health care challenges in the twenty first century, we have come to realize the importance of quantifying as well as being able to control the mechanical integrity of these biological constructs and materials. In many cases, the mechanical integrity of the biological constructs dictates their functional success.

To develop biological constructs with desired mechanical integrity requires not only the ability to create a dynamic in-vitro environment with histo-appropriate mechanical forces to guide the formation of desired microarchitecture of the developing constructs, but also the ability to quantify their mechanical properties and structural characteristics in-situ. So far, there have been many studies of mechanically induced responses on cellular and structural levels [2, 6-32], and these studies have helped elucidate the underlying mechanisms and provided pivotal knowledge toward understanding the linkage between the mechanical forces and the biochemical and molecular responses [9, 13-19, 33-34]. But, there is a lack of appropriate techniques to quantify the mechanical properties and material characteristics of these materials and constructs. The main reason is that for these new breeds of materials, the classic approach dealing with materials [25-37] from two separated angles (*materials science:* dealing with the microscopic and macroscopic structures of the materials; and *materials engineering:* dealing with the mechanical properties of the materials) is no longer pertinent. Instead, a new and integrated approach with the consideration of the relations between the material's assembly or formation process, microstructure, and mechanical properties is necessary so that the mechanical integrity of these biological constructs or materials can be evaluated as molecules or self-assembly processing aggregate, or as tissues grow.

To take on this challenge, we have advanced our previous study [38] and developed a new technique. This new development is capable of capturing the transient, nonlinear and time-dependent mechanical and material characteristics of biomaterials and biological or engineered constructs. This development is based on high-speed sensing and data acquisition, digital signal processing, Fourier transform and other fundamental engineering principles. It will have a significant impact toward many frontiers of sciences and engineering, including characterizing the biological constructs and materials, understanding the material formation on a micro/nano-scale, correlating the molecular self-assembly and aggregation to its mechanical integrity, monitoring the structural and

mechanical properties of engineered tissue constructs as they grow, and guiding the engineered tissue constructs to form desired microarchitecture and attain appropriate mechanical integrity.

Analytical Development

In this study, we seek an integrated approach for evaluating the mechanical properties and the material characteristics. This integrated approach allows us to consider the mechanical properties and the material's assembly/formation process as well as its microstructure. Contrary to conventional ways of considering materials either as elastic solids or viscous liquids, we consider all materials as viscoelastic systems, so the time-dependent nature of the materials will be inherently considered.

For a *known* viscoelastic material model (represented by two springs and a dashpot as depicted in Fig. 1; this model is commonly used to describe bone structures [39]) its governing differential equilibrium equation can be expressed as

$$\frac{d\sigma(t)}{dt} + \frac{E_1 + E_2}{\eta}\sigma(t) = E_1\frac{d\varepsilon(t)}{dt} + \frac{E_1E_2}{\eta}\varepsilon(t). \tag{1}$$

Where E_1, E_2, and η are material constants of the components, $\sigma(t)$ and $\varepsilon(t)$ are time-transient stress and strain. To solve this differential equation and obtain the time-dependent mechanical properties and material characteristics of this viscoelastic material, we apply Laplace transform to Eq.1 and derive

$$\sigma(s)\ [s + \frac{E_1 + E_2}{\eta}] = \varepsilon(s)\ [sE_1 + \frac{E_1E_2}{\eta}]. \tag{2}$$

Here s is Laplace variable. Rearranging Eq.2 and letting $s=i\varpi$ (i is the complex symbol, $i = \sqrt{-1}$), we have

$$\frac{\sigma(s)}{\varepsilon(s)} = \frac{s\eta E_1 + E_1E_2}{s\eta + E_1 + E_2}\Big|_{s=i\varpi} = \frac{\sigma(i\varpi)}{\varepsilon(i\varpi)} = \frac{i\varpi\eta E_1 + E_1E_2}{i\varpi\eta + E_1 + E_2} = E^*(i\varpi). \tag{3}$$

The complex variable $E^*(i\varpi)$ (also known as complex modulus) obtained in Eq.3 represents the time-dependent system characteristics of the viscoelastic material. The real part of this complex modulus (or, storage modulus) defines the elastic property of the material, and the imaginary part (or, loss modulus) governs the viscous property of the material.

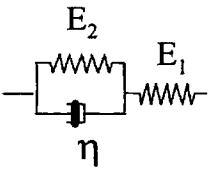

FIG. 1 — *This schematic shows a three-element (two springs and a dashpot) model representing a viscoelastic solid material.*

The step of letting $s = i\varpi$ indicates that we can obtain the same result as in Eq.3 by performing Fourier transform to Eq.2 instead of Laplace, thus $\sigma(i\varpi)$ and $\varepsilon(i\varpi)$ are Fourier transformations of $\sigma(t)$ and $\varepsilon(t)$, respectively. The benefit of performing Fourier transform is that it allows us to take advantage of the Fast Fourier Transform

(FFT) algorithms in this new development, thus paving the way for us to perform real-time and high-speed characterization of various materials.

Let us now consider an *unknown* time-dependent material system. In analogous to dealing with a linear electronic system (where the output response $y(t)$ is expressed in convolution of the input stimulus $x(t)$ and the system impulse response function $h(t)$ as $y(t) = x(t) \otimes h(t)$), we consider the relationship between the input strain and output stress in the same manner. For a given strain input $\varepsilon(t)$, its stress output $\sigma(t)$ is expressed as

$$\sigma(t) = \varepsilon(t) \otimes h(t). \tag{4}$$

Where $h(t)$ is the system impulse response function of the material. By applying Fourier transform to Eq.4 and rearranging it, we have

$$H(i\varpi) = \frac{\sigma(i\varpi)}{\varepsilon(i\varpi)}. \tag{5}$$

Here $H(i\varpi)$ - the Fourier transformed function of $h(t)$ - represents the system characteristics (mechanical, material and structural). Comparing Eq.5 to Eq.3, it is clear that $H(i\varpi)$ is essentially the same variable as the $E^*(i\varpi)$ - the complex modulus of the material.

This analytical development indicates that the mechanical properties and material characteristics of an *unknown* viscoelastic material can be obtained without any aprior assumption regarding its viscoelastic structure, such as using the three-element model to represent bone structures. This advancement is certainly important, because in reality we usually have no prior knowledge about the material structure.

With this analysis, the complex modulus of a material can be determined by the following steps. First, apply a strain stimulus in time-domain and measure the transient stress response; second, perform FFT to the paired time-based stress and strain measurements to obtain the frequency-based measurements in complex forms; third, take the ratio of the FFTed stress to strain to calculate the complex modulus as a function of frequency.

Testing Machine Development

To put this analysis to practical applications, we modified the design of our previously developed apparatus [34, 40] and developed a new testing machine capable of providing adequate sensitivity and high-speed to apply strain stimuli and measure stress responses, along with other delicate tasks. Fig. 2 shows a schematic view and a picture of the newly developed machine system. This system consists of four parts: a host computer for operation control; an electronic control unit for providing power, actuation, sensing, and data acquisition; a mechanical loading device; and a culture chamber for in-vitro testing.

To provide both ramp and cyclic actuations, we used a linear stage (1 inch travel) driven by a DC actuator and a piezo stage (up to 400μm travel and 0-100Hz capacity). A loading assembly (a T-shape structure with two linear voltage differential transformers - LVDT) was fabricated using a double-cantilever design. This assembly was then attached to the piezo-stage, so the bodies of LVDT1 and LVDT2 will move with the stages. The double-cantilever design is to provide adequate stiffness and sufficient compliance. The

adequate stiffness is for delivering loads, and the sufficient compliance is for allowing biological specimens to deform and adjust. With this design, we will be able to measure the force and deformation separately but simultaneously, so that the inherent machine compliance will be accounted for automatically.

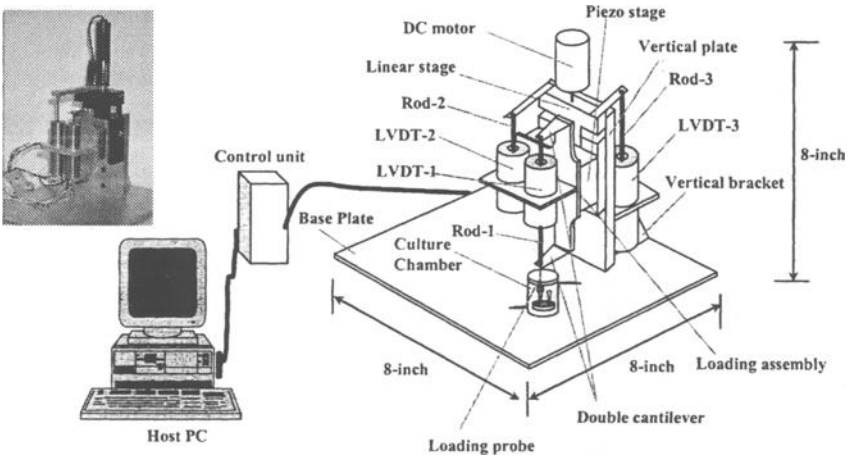

FIG. 2 — *A schematic view of the micromechanical system developed. Left top inset: A picture showing the actual mechanical unit.*

With the loading assembly, the load (P) is measured through the deflection of the cantilevers (Δ) by: $P = k\Delta$, where k is the stiffness of the cantilevers. When the loading assembly is driven up (or down) by D_{Total} to stretch (or compress) a specimen, the specimen will deform by D_S, and the cantilevers will deflect downward (or upward) by Δ. The specimen deformation is then determined as $D_S = D_{Total} - \Delta$ (see Fig. 3).

When actuation is driven by the piezo-stage, LVDT1 will register $\Delta = \alpha_1 V_{LVDT1}$, LVDT2 register $D_{Total} = \alpha_2 V_{LVDT2}$, and their difference measure $D_S = \alpha_2 V_{LVDT2} - \alpha_1 V_{LVDT1}$. When actuation is driven by the linear motor, LVDT2 will be idle, LVDT1 register $\Delta = \alpha_1 V_{LVDT1}$, LVDT3 register $D_{Total} = \alpha_3 V_{LVDT3}$, and their difference measure $D_S = \alpha_3 V_{LVDT3} - \alpha_1 V_{LVDT1}$. Here α_1, α_2 and α_3 are displacement calibration factors for LVDT1, LVDT2 and LVDT3, respectively.

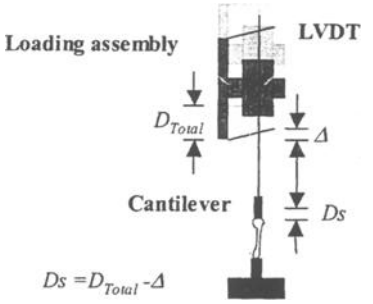

FIG. 3 — *A close view showing the detail design of the double-cantilever loading assembly and its working mechanism.*

For computer operations control, an A/D-D/A board (PCI-MIO-16E-1, 1.25MS/sec, National Instruments) was used, and an operating program along with a user-interface was developed (LabWindows CVI, National Instruments).

Numerical Implementation

As discussed above, letting $s = i\varpi$ equates, theoretically, Laplace transform to Fourier transform. Numerically, however, performing Fourier transform does not produce the expected result. Consider the case of a unit-step function. The Laplace transformed function of the unit-step function should be $1/s$, or $1/i\varpi$ when $s = i\varpi$, but discrete Fourier transform treats the unit step function as a DC signal and thus resolves it into an impulse at zero frequency. This is so because numerically Fourier transform is performed in discrete manner.

For $f(t)$ in $t \in (-T/2, T/2)$, its Fourier transform $F(i\varpi) = \int_{-T/2}^{T/2} f(t)e^{-i\varpi t}dt$ is calculated by the value of $f(t)$ at each discrete sampling point $f(j)$ $(j = 0,1,...N-1)$

$$F(i\varpi_k) = \sum_{j=0}^{N-1} f(j)e^{-i2\pi kj/N} = \sum_{j=0}^{N-1} f(j)\cos(\frac{2kj\pi}{N}) - i\sum_{j=0}^{N-1} f(j)\sin(\frac{2kj\pi}{N}). \quad (6)$$

Here N is the total number of samples, and k is an integer and varies from 0 to $N/2-1$ due to the Nyquist limit. When $f(t)$ is a unit step function, the discrete values will be $f(j) = 1$ $(j = 0,1,...N-1)$. Substituting these values into Eq.6, one has: $F(i\varpi_k) = N$ when $k = 0$, and $F(i\varpi_k) = 0$ when $0 < k < N/2$. Obviously the result is an impulse of magnitude of N at zero frequency. To overcome this, one solution is to use a numerical Laplace algorithm to handle the transform. But doing this, we would lose the advantage an FFT algorithm could provide: high speed and real time processing capability. An ideal solution should still be an FFT based transform.

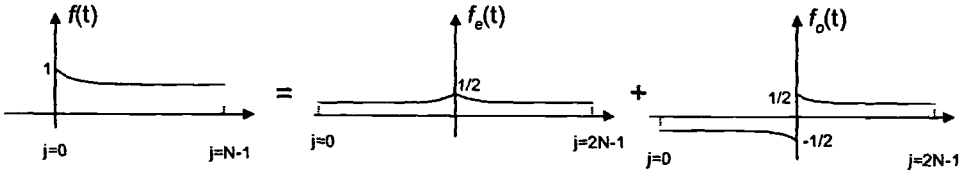

FIG. 4 — *A function can be expressed as the sum of an even and odd function.*

To seek such solution, we further explored the even and odd symmetry of FFT, and found that when a step function (or a relaxation function) is expressed as the sum of an even and an odd function, as depicted in Fig. 4, the FFT algorithm will be able to produce the expected transform.

For a given array of size N, $f(j)$ $(j = 0,1,...N-1)$, an equivalent one of size $2N$ is constructed, $f'(j) = f_e(j) + f_o(j)$ $(j = 0,1,...2N-1)$. $f_e(j)$ and $f_o(j)$ are even and odd arrays: $f_e(j) = f_e(2N-j-1) = f(j)/2$ and $f_o(j) = -f_o(2N-j-1) = -f(j)/2$ for $j = 0,1,...N-1$. Then, by performing FFT to $f'(j)$ one derives the transformation as expected

$$F(i\varpi_k) = \sum_{j=0}^{2N-1} f'(j)\cos(\frac{2kj\pi}{2N}) + i\sum_{j=0}^{2N-1} f'(j)\sin(\frac{kj\pi}{2N})$$
$$= \sum_{m=0}^{N-1} f(m)\cos(\frac{2km\pi}{N}) + i\sum_{m=0}^{N-1} f(m)\sin(\frac{k(2m+1)\pi}{N}) \quad (7)$$

Expressing the given array $f(j)$ into its equivalent $f'(j)$ does not need any new information in time-domain. Nor does it alter the upper frequency limit because of the same amount (N) zeros generated in frequency-domain.

Using this numerical development, we calculated the complex modulus measurements based on the obtained stress and strain measurements in time-domain

$$E^*(i\varpi_k) = \frac{\sigma(i\varpi_k)}{\varepsilon(i\varpi_k)} = \frac{\sum_{m=0}^{N-1}\sigma(m)\cos(\frac{2km\pi}{N}) + i\sum_{m=0}^{N-1}\sigma(m)\sin(\frac{k(2m+1)\pi}{N})}{\sum_{m=0}^{N-1}\varepsilon(m)\cos(\frac{2km\pi}{N}) + i\sum_{m=0}^{N-1}\varepsilon(m)\sin(\frac{k(2m+1)\pi}{N})}. \quad (8)$$

To complete the numerical implementation, we incorporated the above developments along with the FFT algorithm into the operating computer program such that testing, data acquisition and calculation can be performed and completed in real-time.

Solutions for Linear and Nonlinear Viscoelastic Materials

To demonstrate the validity of the developed analysis, we examined two examples: a linear and nonlinear relaxation models. For the linear model, we used the case given in Eq.1. We first applied a step strain stimulus $\varepsilon(t)$ with the rising portion (to mimic the actual loading) to Eq.1 and solved for its stress response $\sigma(t)$ (Fig. 5-left). We then performed FFT to the paired arrays, and obtained $\sigma(i\varpi)$ and $\varepsilon(i\varpi)$ in frequency-domain. The FFTed stress and strain in frequency-domain were plotted in Fig. 5-right, where Re[] and Im[] represent the real and imaginary parts, respectively. Finally, we calculated the ratio $\sigma(i\varpi)/\varepsilon(i\varpi)$ as the complex modulus measurements.

Fig. 6 shows the variation of complex moduli with frequency: storage modulus (upper dotted curve) and loss modulus (lower dotted curve), along with the theoretical solutions (solid curves) obtained from Eq.3. Obviously the two sets of results are in good agreement despite the fact that a non-ideal step strain stimulus was used. We also found that a better match of the two results can be achieved by decreasing the sampling interval in time-domain.

For the nonlinear model, we considered a nonlinear relaxation $\sigma(t) = e^{-\frac{t^2}{4}} + \frac{1}{2}$ in response to $\varepsilon(t) = 1$. We first derived the theoretical solution for the complex modulus for this nonlinear model

$$E^*(i\varpi) = 2\varpi^2 e^{-\varpi^2}\int_0^{\varpi} e^{u^2}du + i\sqrt{\pi}\varpi e^{-\varpi^2}. \quad (9)$$

Then, we generated two arrays in time-domain: $\sigma(j) = e^{-\frac{j^2}{4}} + 0.5$ and $\varepsilon(j) = 1$ for $j = 0,1,...N-1$. By performing FFT to the paired arrays and calculating their ratio in frequency-domain, we obtained the complex modulus measurements. Fig. 7 shows the

variation of the complex moduli with frequency for the nonlinear viscoelastic model: storage modulus (upper dotted curve) and loss modulus (lower dotted curve), along with the theoretical solutions (solid curves) obtained from Eq.9.

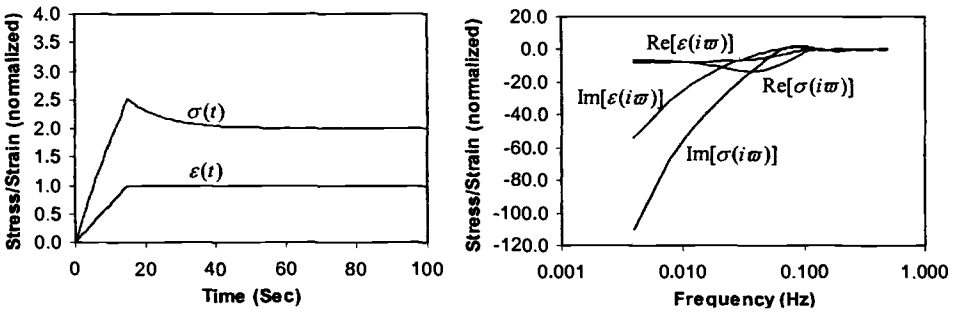

FIG. 5 — *Left: A paired stress and strain arrays in time-domain obtained based on Eq.1 representing a linear viscoelastic material. Right: FFT results of the complex stress and strain in frequency-domain.*

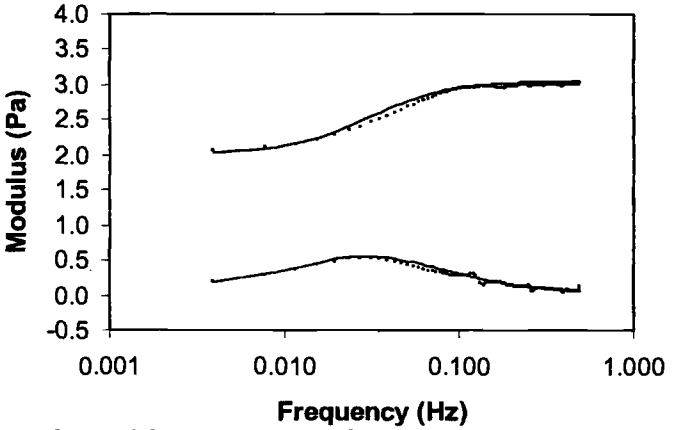

Fig. 6 — *Complex modulus measurements for the linear viscoelastic material: upper curves - storage modulus; lower curves - loss modulus. Also, solid curves are theoretical solutions from Eq.3, and dotted curves are measured/transformed results.*

The close agreement between the two sets of solutions for this nonlinear example suggests that the developed method, though linear based, is also applicable to nonlinear materials. In general, a nonlinear phenomenon can be closely represented by a series of linear approximations when the sequential interval is sufficiently small (e.g., use of Riemann sums of linear segments to integrate nonlinear curves). Obviously, this rule holds true here as well. The difference between the two sets of results, as we noticed, decreases as the time-domain sampling interval decreases. Thus, we believe when the time interval is sufficiently small, the linear based evaluation method developed here is able to evaluate nonlinear systems.

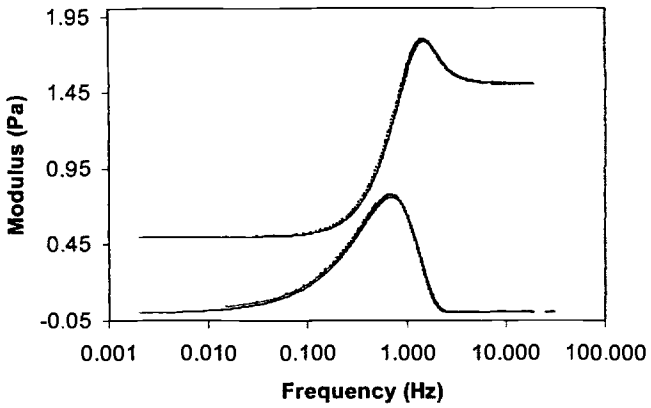

FIG. 7 — *Complex modulus measurements for the nonlinear viscoelastic material: upper curves - storage modulus; lower curves - loss modulus. Also, solid curves are theoretical solutions from Eq.9, and dotted curves are measured/transformed results.*

Experimental Evaluation of Living Bone Tissues

With this new real-time evaluation method we evaluated biological tissues in-vitro by using week-old mouse tibiae as living specimens. Week-old (five to seven days old) mice were used due to their rapid growing stage. Tibiae were removed from the mice following an approved protocol [41]. To focus on bone structure, we further removed the cartilage layers from the two ends of each tibia. To keep bones alive, we conditioned the bones in culture medium, DMEM containing 15% heat-inactivated horse serum and buffered with HEPES, immediately after dissection. A total of four mice were used in this study.

After immersing the bone specimens into the culture chamber (see Fig. 2) we applied a step displacement loading (with the rising portion, of course) to the specimens, and measured the transient force responses. In each test, the force and displacement were measured in time. Following the loading, FFT and complex modulus calculation were performed immediately, and the complex moduli measurements were calculated.

Fig. 8 shows four force curves (three were from seven-day-old mice and one from five-day-old) versus time. Despite their age difference, these bones were subjected to the same amount of displacement loading. All these curves possess decaying nature, but the rate of decaying is different between the two age groups. The transient force response of the younger bone decays much faster compared to the older ones. This fact indicates that in response to the same mechanical input, bone tissues may sense different levels of forces due to their structural differences.

Fig. 9 shows the obtained complex modulus measurement for the bone tissues. The upper curves are for storage modulus, and the lower curves are for loss modulus. Of all these bones, the seven-day-old bones showed similar material properties, while the five-day-old showed a much weaker elastic property and a higher viscous loss.

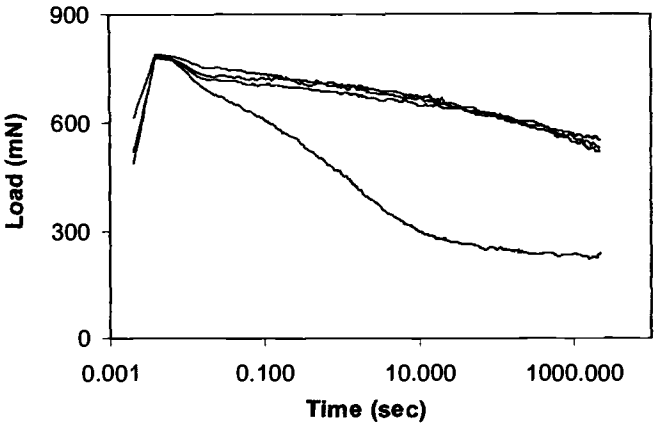

FIG. 8 — *These four measured curves represent the transient force response of each bone specimen in response to the step displacement loading. The upper three curves were from seven-day-old mice and the lower one was from five-day-old.*

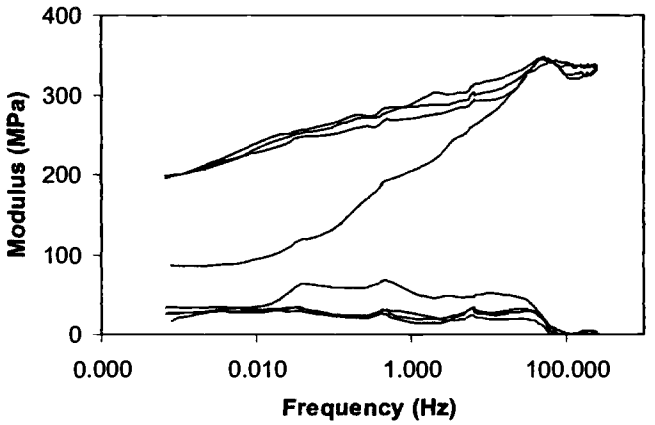

FIG. 9 — *Storage and loss moduli measurements obtained from the in vitro testing. The upper four curves are for storage modulus and lower four for loss modulus. The one with low storage modulus and high loss modulus was from the five-day-old mouse and the rest were from seven-day-old mice.*

Discussion

With the developed analysis along with its experimental and numerical implementation, we have demonstrated the following. We can directly measure material properties (elastic and viscoelastic) without any aprior assumption regarding the material structure. This advancement is of significant importance, because in reality we usually have no prior knowledge about the material structure. With the use of high-speed data acquisition and FFT, measurements of complex moduli can be obtained in a real-time and in-situ manner. It should be noted that the use of numerical transformation and calculation in this method does not make it anything less than an experiment-based method. As we know, in most testing procedures we rely on the measured raw data to

calculate the intended measurements. For instance, we calculate the elastic modulus by using the measured stress and strain values. The only difference is that in the current method calculation is done continuously, rather than discretely as in most other test procedures.

Because the measured complex moduli contain not only the mechanical properties (magnitude of the modulus curves) but also the material characteristics (shape of the modulus curves), this method allows establishing direct links between the mechanical properties and material characteristics in real-time and in-situ. Changes in magnitude (mechanical property) and in shape (material structure) in the complex moduli curves can be measured and correlated, repeatedly, during the growing or aggregating processes of the biological tissues or constructs.

This method is applicable to linear and nonlinear materials due to the available high-speed data acquisition. It requires paired stimulus-response measurements (i.e., stress and strain) for resolving property measurements, so that the machine compliance (existing in all testing systems) will be accounted for automatically.

Because of the use of FFT in this method, the measured material properties in frequency domain will have an upper frequency limit set by the Nyquist frequency (f_{upper} $=½\, f_{sampling}$). Thus, to push the upper limit, one needs to increase the sampling frequency (or decrease the sampling interval). The upper limit for the sampling frequency is most likely controlled by the current hardware limit in data acquisition (1MHz for the current system). The lower frequency limit is determined by the time duration (t_{test}) of the test ($f_{lower}=1/t_{test}$). For material property at a much low frequency, one needs to perform the test over an extended period of time. For the materials we are interested in, a frequency range from 0.001 to 1000Hz will suffice. This makes the time duration around 1000sec, and the max sampling rate about 2kHz.

With today's advanced sensing, computing technologies, and digital signal processing microchips (to handle FFT), this method can be further advanced into micro-scale real-time and in-situ and multiple dimensional evaluations.

Conclusions

With this method, the mechanical properties and material characteristics of biological tissues and constructs can be measured without making any aprior assumption regarding their structures. Direct links between the mechanical properties and material characteristics can be established in real-time and in-situ, so that changes in both the mechanical properties and material characteristics can be correlated, repeatedly, during the growing or aggregating processes of the biological tissues or constructs. This method is applicable not only to linear viscoelastic but also to nonlinear viscoelastic materials. The use of paired stress and strain transient measurements for resolving property measurements will automatically account for the machine compliance which exists in all testing systems.

Acknowledgement

This work is partially supported by NIH ES85431, R45326, and the University of Georgia Research Foundation.

References

1. Fuchs, J. R., Nasseri, B. A. and Vacanti, J. P., "Tissue engineering: A 21st century solution to surgical reconstruction," *Annals Thorac Surgery*, 72, 2001, 577-591.
2. Grodzinsky, A. J., Levenston, M. E., Jin, M. and Frank, E. H., "Cartilage tissue remodeling in response to mechanical forces," *Annul Review of Biomedical Engineering, Vol.2*, 2000, 691-713.
3. Marler, J. J., Upton, J., Langer, R. and Vacanti, J. P., "Transplantation of cells in matrices for tissue regeneration," *Advanced Drug Delivery Review*, 33, 1988, 165-182.
4. Nerem, E. M. and Seliktar, D., "Vascular tissue engineering." *Annul Review of Biomedical Engineering, 3*, 2001, 225-243.
5. Whitesides, G. M., Ostuni, E., Takayama, S., Jiang, X., Ingber, D. E., "Soft lithography in biology and biochemistry," *Annul Review of Biomedical Engineering*, 3, 2001, 335-373.
6. Bachrach, N. M., Valhmu, W. B., Stazzone, E., Raeliffe, A., Lai, W. M., Mow, V. C., "Changes in Proteoglycan Systhesis of Chondrocytes in Articular Cartilage Are Associated with the Time- Dependent Changes in Their Mechanical Environment," *Journal of Biomechanics*, 28(12), 1995, 1561-1569.
7. Berger, R., Delamarche, E., Lang, H. P., Gerber, C., Gimzewski, J. K., Meyer, E., Guntherodt, H. J., "Surface stress in the self-assembly of alkanethiols on gold," *Science*, Vol. 276, June 1997, 27.
8. Burger, E. H. and Veldhuijzen, J. P., "Influence of Mechanical Factors on Bone Formation, Resorption and Growth in vitro," Hall Ed., *Bone-Bone Growth*, CRC Press, Melbourne, Vol.7, 1993, 37-56.
9. Burger, E. H., Klein-Nulend, J. and Veldhuijzen, J. P., "Mechanical Stress and Osteogenesis in vitro," *Journal of Bone & Mineral Research*, 7(Supplement 2), 1992, S397-S401.
10. Cowin, S. C., "Bone Stress Adaptation Models," *Trans. ASME*, 115, 1993, 528-534.
11. Cowin, S. C., Moss-Salentijn, L. and Moss, M. L., "Candidates for the Mechanosensory System in Bone," *Jounal of Biomechanical Engineering*, 113, 1991, 191-197.
12. Dallas, S. L., Zaman, G., Pead, M. J. and Lanyon, L. E., "Early Strain Related Changes in Cultured Embryonic Chick Tibiotarsi Parallel Those Associated with Adaptive Modeling in vivo," *Journal of Bone & Mineral Research*, 8(3), 1993, 251-259.
13. Devlin, H. and Ferguson, M. W., "Alveolar ridge resorption and mandibular atrophy. A review of the role of local and systemic factors," [Review]. *British Dental Journal*, 170, 1991, 101-104.
14. Flieger, J., Karachalios, T., Khaldi, L., Raptou, P. and Lyritis, G., "Mechanical stimulation in the form of vibration prevents postmenopausal bone loss in ovariectomized rats," *Calcified Tissue International*, 63, 1998, 510-514.
15. Harter, L. V., Hruska, K. A. and Duncan, R. A., "Human Osteoblast-Like Cells Respond to Mechanical Strain with Increased Bone Matrix Protein Production," *Endocrinology*, Vol.136, No.2, 1995, 528-535.

16. Judex, S., Gross, T.S. and Zernicke, R.F., "Strain gradients correlate with sites of exercise-induced bone-forming surfaces in the adult skeleton," *Journal of Bone & Mineral Research*, 12, 1997, 1737-1745.
17. Klein-Nulend, J., Semeins, C. M., Veldhuijzen, J. P. and Burger, E. H., "Effect of Mechanical Stimulation on the Production of Soluble Bone Factors in Cultured Fetal Mouse Calvariae," *Cell Tissue Research,* 271, 1993, 513-517.
18. Lanyon, E. L., "Using Functional Loading to Influence Bone Mass and Architecture: Objectives, Mechanisms, and Relationship With Estrogen of the Mechanically Adaptive Process in Bone," *Bone*, 18, Suppl 1, 1996, 37S-43S
19. Lanyon, L. E., "Control of Bone Architecture by Functional Load Bearing," *Journal of Bone & Mineral Research,* 7, 1992, S369-S375.
20. Meena, D. J., Suh, J-K., Marui, T. and Woo, S. L-Y., "Interspecies Variation of Compressive Biomechanical Properties of the Meniscus," *Journal Biomedical Materials Research,* 29, 1995, 823-828.
21. Mow, V. C, Kwan, M. K, Lai, W. M. and Holmes, M. H., "A Finite Deformation Theory for Nonlinearity Permeable Soft Hydrated Biological Tissues," *Ch20 in Frontiers in Biomechanics,* Schmid-Schonbein GW, Woo S L-Y, and Zweifach BW, (Eds) Springer-Verlag, New York, 1986.
22. Mow, V. C., Kuei, S. C., Lai, W. M. and Armstrong, C. G., "Biphasic Creep and Stress Relaxation of Articular Cartilage in Compression: Theory and Experiments," *Journal of Biomechanical Engineering,* 102, 1980, 73-84.
23. Mow, V. C, Bachrach, N. M., Setton, L. A. and Guilak, F., "Stress, Strain, Pressure and Flow Fields in Articular Cartilage and Chondrocytes," *Ch20 in Cell Mechanics and Cellular Engineering,* Mow VC, Guilak F, Tran-Son-Tay R and Hochmuth RM, (Eds) Springer-Verlag, New York, 1994.
24. Pead, M. J., Suswillo, R., Skerry, T. M., Vedi, S. S. and Lanyon, L. E., "Increased 3H-uridine Levels in Osteocytes Following a Single Short Period of Dynamic Loading in vivo," *Calcified Tissue International,* 43, 1988, 92-96.
25. Raab-Cullen, D. M., Thiede, M. A., Petersen, D. N., Kimmel, D. B. and Recker, R. I., "Mechanical Loading Stimulates Changes in Periosteal Gene Expression," *Calcified Tissue International*, 55, 1994, 473-478.
26. Rawlinson, S. C. F., El-Haj, A. J., Minter, S. L., Tavares, I. A., Bennet, A. and Lanyon, L. E., "Load-Related Increase in Prostaglandin Production in vitro - A Possible Role For Prostacyclin in Adaptive Remodeling?" *Journal of Bone & Mineral Research*, 6, 1991, 1345-1351.
27. Rawlinson, S. C. F., Mosley, J. R., Suswillo, R. F. L., Pitsillides, A. and Lanyon, L.E., "Calvarial and Limb Bone Cells in Organ and Monolayer Culture Do Not Show the Same Early Responses to Dynamic Mechanical Strain," *Journal of Bone & Mineral Research,* 10 (8), 1995, 1225-1232.
28. Rubin CT and Lanyon LE, "Regulation of Bone Mass by Mechanical Strain Magnitude," *Calcified Tissue International,* 37, 1985, 411-417.
29. Rubin, C. T. and Lanyon, L. E., "Regulation of Bone Formation by Applied Dynamic Loads," *Journal of Bone & Joint Surgery,* 66A, 1984, 397-402.
30. Sennerby, L., Carlsson, G.E., Bergman, B. and Warfvinge, J., "Mandibular bone resorption in patients treated with tissue-integrated prostheses and in complete-denture wearers," *Acta Odontologica Scandinavica,* 46, 1988, 135-140.

31. Vandenburgh, H. H., "Mechanical Forces and Their Second Messengers in Stimulating Cell Growth in vitro," *American Journal of Physiology*, 262, 1992, R350-R355.
32. Wyatt, C.C., "The effect of prosthodontic treatment on alveolar bone loss: a review of the literature," [Review] *Journal of Prosthetic Dentistry*, 80, 1998, 362-366.
33. Gilbert, J. L., Kunnel, J., Zhang, G., Stern, P. H., "Strain Dependent Non-Linear Viscoelastic Micromechanics and Biological Response of Viable Week-Old Mouse Tibia," *Transactions of the Society For Biomaterial*, 1999, 532.
34. Zhang, G., Stern, P. H., Lautenschlager, E. P. and Gilbert. J. L., "In Vitro Micromechanical Behavior of Viable Neonatal Mouse Tibia," *Transactions of the 5th World Biomaterials Congress*, Toronto, Canada, May, 1996, II-392.
35. Rosen, S. L., "Fundamental Principles of Polymeric Materials," John Wiley & Sons, NY, 1992.
36. Ferry, J., "Viscoelastic properties of polymers," John Wiley & Sons, 1980.
37. Findley, W. N., Lai, J. S. and Onaran, K., "Creep and Relaxation of Nonlinear Viscoelastic Materials," Dover Publications, Inc., New York, 1989.
38. Gilbert, J. L. and Dong, D. R., "A Numerical Time-Frequency Transform Technique for the Determination of the Complex Modulus of Composite and Polymeric Biomaterials from Transient Time Based Experiments," *ASTM STP 1173*, 1994, 225-244.
39. Fung, Y. C., "Biomechanics, Mechanical Properties of Living Tissues," Springer-Verlag, NY, 1993.
40. Zhang, G., Stern, P. H., Gilbert, J. L., "A novel technique for evaluating viscoelastic complex properties of biomaterials," *Transactions of the Society For Biomaterial*, 2002, 311.
41. Animal Care and Use Assurance A2932-01, Northwestern University ACUC, 1999.

What Standards Exist and What Standards Are Needed?

Michael Dornish[1] and Arne Dessen[2]

Alginate and Chitosan Standards for Tissue Engineered Medical Products

Reference: Dornish, M. and Dessen, A., **"Alginate and Chitosan Standards for Tissue Engineered Medical Products,"** *Tissue Engineered Medical Products (TEMPs), ASTM STP 1452,* E. Schutte, G. L. Picciolo and D S. Kaplan, Eds., ASTM International, West Conshohocken, PA, 2004.

Abstract: More often than not users of biopolymers obtain their starting materials from a chemical supply company. Documentation is often lacking and the user is not aware of the fact that a biopolymer's functionality in an application is inherently linked to its characteristics. As a manufacturer of ultrapure biopolymers we have often heard the comment that "your biopolymer didn't work!" More often than not, however, the functional properties of the polymer were not appropriate for the intended use. Variability in naturally occurring biopolymers can lead to failed formulations. Alginate and chitosan are biopolymers that may be used in TEMPs. Derived from natural sources, these materials are particularly complex, and thus exhibit significant variability. Consequently, in order to understand the full range of their properties there is a need for accurate characterization of these materials. The development of standards for such TEMP starting materials is necessary to ensure product uniformity, enable more complete and precise characterization and to inform both users and manufacturers of the relationships among composition, functional properties and utility. This can only lead to more successful TEMP formulations.

Keywords: Alginate, chitosan, F 2064, F 2103, encapsulation, scaffolds, biopolymers

Introduction

In the emerging arena of tissue engineering and directed drug delivery there is a need for excipients and structural materials that possess specific functionality. For example, scaffolds and matrices for tissue engineering must promote cell growth and demonstrate biocompatibility, whether they are intended to be biodegradable or permanent. Alginate and chitosan have shown interesting potential as scaffolds in tissue engineered medical products [1,2], drug-containing materials for depot delivery [3,4], and encapsulating matrix for immobilization of living cells [5]. These are diverse applications that require unique functionality. In some cases, these materials have not

[1] VP, Research and Development, FMC BioPolymer AS/NovaMatrix, Gaustadalleen 21, N-0349 Oslo, Norway.
[2] Business Director, FMC BioPolymer AS, Tomtegate 36, N-3002 Drammen, Norway.

been characterized sufficiently for these applications and incorrect formulations have been chosen. There is, therefore, a need for guidance in the characterization of these materials in order to ensure uniformity and consistency in the development and manufacture of Tissue Engineered Medical Products (TEMPs). The purpose of this paper is to describe the diversity of properties that alginate and chitosan offer to the developers of TEMPs, depending on the choice of a wide variety of compositions and structures. In doing so, the authors aim to demonstrate that guidance on the characterization of TEMP starting materials, through standards development, is a key component of successful TEMP development.

Alginate is used in a variety of products, ranging from technically simple applications (*e.g.* viscosity enhancement) to advanced biomedical applications (*e.g.* controlled drug delivery from immobilized living cells). Chitosan is also used widely: from water purification (*e.g.* flocculation) [6,7], to dietary supplementation (*e.g.* fat binding) [8,9], to nasal drug delivery (*e.g.* transepithelial drug enhancement), a number of which are in various stage of clinical trials [10-12]. Commodity alginates are well known to the medical device and pharmaceutical industries as material for wound dressings [13-15], anti-reflux remedies [16,17], and a tablet excipient [18]. The purity level and the current means of manufacture and low level of characterization make it difficult to believe that commodity alginates will find a use in implantable devices and drug formulations for parenteral administration.

Table 1 summarizes the functional properties that are possible by varying the composition and structure of alginate and chitosan, as well as their relative benefits and potential applications. As indicated in Table 1, chitosan and alginate have been identified as two of several polymeric materials that possess suitable properties for tissue engineering applications [19-21]. It is expected, however, that ultrapure materials, made in accordance with current Good Manufacturing Practice (cGMP) and ISO Quality Management Systems – Requirements (ISO 9001:2000) quality guidelines, will be required for TEMPs, similar to other implantable devices and parenteral drug formulations based on these biopolymers. In addition to numerous other polymeric materials, alginate and chitosan are materials possessing significant qualities useful for tissue engineering and tissue-engineered medical products [19-21]. Excellent reviews of tissue engineering principles and applications using polymers and biopolymers are available [22-24], as well as examples of the use of ultrapure alginates inside the human body [25,26].

Table 1 - *Characteristics and functionality of alginate and chitosan in biomedical and pharmaceutical applications*
(- = little utility, + = some utility, ++ = good utility, +++ = very good utility)

Characteristics	Functional Properties	Advantages	Application	Relative utility	
				Alginate	Chitosan
Molecular weight	Viscosity	Thickening	Suspensions	+++	++
		Film-forming	Coatings	++	++
Composition and Sequence	Cross-linking	Gelling	Encapsulation Immobilization	+++	++
	Biological activity	Immune modulation	Immune stimulation	+++	+
		Opening tight junctions	Enhanced drug delivery	-	+++
Dissociation, pKa	Solubility	Solutions, pastes	Anti-reflux	+++	-
			Drug Delivery	+++	+++
	Precipitation	Fibers, films	Wound dressings Tissue Engineering scaffolds	+++	+++
	Swelling capability	Absorption	Tablet disintegration	+++	++
Polyion	Cation/anion affinity	Chelation	Drug/metal binding	++	++
Electrolyte		Charge density	Bioadhesion	+	+++

Alginate

Alginate is a carbohydrate, like sugar and cellulose. Much like cellulose is in trees, alginate is the structural polymer in marine algae. Alginate is a non-branched copolymer composed of two monomers, ß-D-mannuronic acid (M) and its C-5 epimer α-L-guluronic acid (G), linked by 1→4 glycoside bonds. It has been found that alginate is composed of M- and G-monomers joined together in a block-wise fashion. This implies that three types of sequential blocks may be found in the alginate molecule: homopolymeric M-blocks (M-M-M), homopolymeric G-blocks (G-G-G), and heteropolymeric, alternating MG-blocks (G-M-G-M) (Figure 1).

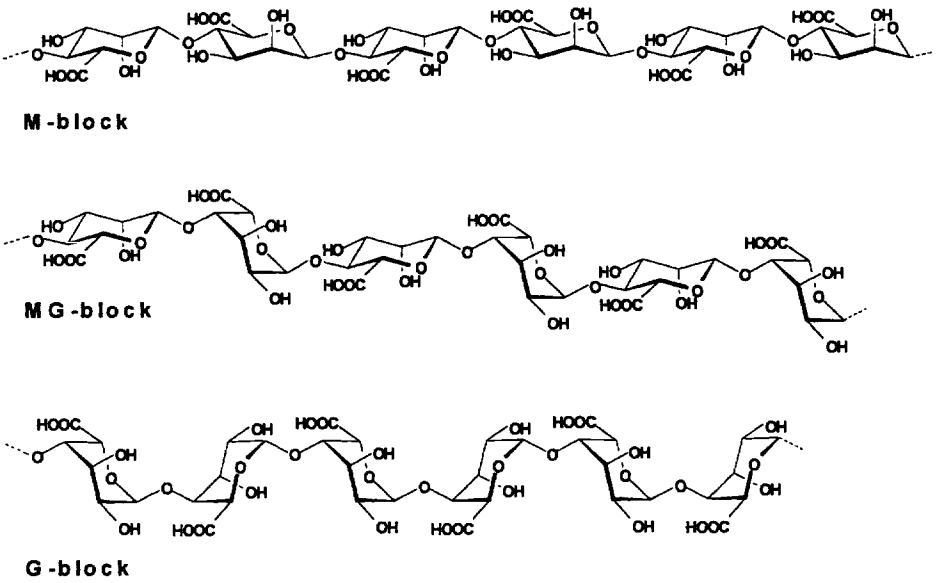

Figure 1 – *Sequential structures in alginate*

The relative amounts of the two uronic acid monomers and the sequential arrangement of them along the polymer chain vary widely, depending on the origin of the alginate. Table 2 lists the composition and sequential structure of alginate from several marine algae. As can be seen, the fraction of guluronate (F_G), the fraction of mannuronate (F_M), and the fraction of alternating sequences (F_{MGM}) vary widely in the various algae species. While at first the diversity in sequential structure may be viewed as a dilemma, variations in G-content, M-content, and G-block size can, in fact, impart different functional properties to alginate-containing TEMPs. Of practical importance, as will be discussed below, is the average number of guluronate monomers in a G-block ($N_{G>1}$).

Table 2 – *Composition and sequential parameters for algal alginates*

Alginate source	F_G	F_M	F_{GG}	F_{MM}	F_{GM}	F_{GGG}	F_{MGM}	$N_{G>1}$
Durv. antarctica	0.32	0.68	0.16	0.51	0.17	0.11	0.12	4
Asco. nodosum	0.39	0.61	0.23	0.46	0.16	0.17	0.09	5
Less. nigrescens	0.41	0.59	0.22	0.40	0.19	0.17	0.14	6
L. digitata	0.41	0.59	0.25	0.43	0.16	0.20	0.11	6
M. pyrifera	0.42	0.58	0.20	0.37	0.21	0.16	0.17	6
L. hyperborea leaf	0.49	0.51	0.31	0.32	0.19	0.25	0.13	8
L. hyperborea stem	0.63	0.37	0.52	0.26	0.11	0.48	0.07	15

"BioStructures" of Alginate

"BioStructures" made of ultrapure alginate may take various forms such as aqueous solutions, pastes, cross-linked gels, and solid structures such as membranes, fibers, non-woven felts, rods and tubes. The functionality of the "BioStructure" will depend upon both the innate characteristics of the alginate from which it is manufactured, as well as the way it is processed.

Innate Characteristics of Alginate – Composition, sequential structure, molecular weight, and molecular conformation are the key characteristics that determine the properties and functionality of alginate. The composition and sequential structure can be determined by high-resolution ^{1}H- and ^{13}C-NMR. Molecular weight can be determined by more than one method. The most common methods are based upon intrinsic viscosity (Mark-Houwink-Sakurada equation) and size-exclusion chromatography with light scattering measurement. In addition to average molecular weight, expressed as the number average and the weight average, the ratio between the two, referred to as the polydispersity index, is often used to describe the molecular weight distribution within an alginate product.

Functional Properties of alginate – While the innate characteristics represent parameters that describe how the polymer is composed (*i.e.* its physical-chemical characteristics), functional properties, such as these listed below, are parameters that describe how the polymer performs.

Solutions - The rheological properties of a pure alginate solution are depend strongly on the Mw of the alginate, while the sequential composition may play only a minor role, such as with viscosity. It is well known that adding other components to the solution may vary the properties of the solution dramatically. Most commonly, cations are added to increase the ionic strength or physical-chemical interactions with the alginate. The former results in changes in molecular conformation of the alginate; the latter increases the apparent viscosity. Sequential composition may also play an important role in chemical interactions with cations.

Cross-Linked Gels - The uniqueness of alginate as an immobilizing agent in biomedical applications rests in its ability to form heat-stable gels that can develop and set at room temperature. Alginate forms instantaneous gels with most di- and multivalent cations. Monovalent cations and Mg^{2+} ions do not induce gelation, while ions like Ba^{2+} and Sr^{2+} will produce stronger alginate gels than Ca^{2+}. The cross-linking capacity of an alginate depends on the innate characteristics of the alginate such as G content and number of consecutive G's in the G-blocks. The gelling occurs when divalent cations participate in the inter-chain binding between G-blocks, giving rise to a three dimensional network. Figure 2 schematically depicts the binding zone between the G-blocks that is often described by an "egg box" model. In general terms, an increase in both G-content (measured as $N_{G>1}$) and molecular weight will give a stronger gel [27,28]. Cross-linking of a G-rich alginate forms a stronger and more ridged gel, while an M-rich gel is typically weaker.

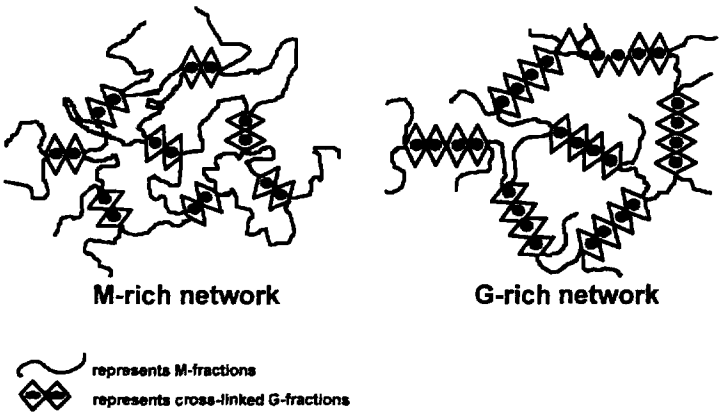

Figure 2 – *Alginate gel structure*

The effect of G-block size on gel strength can be visualized by comparing G-rich versus M-rich alginate gels (0.5% alginate in water gelled with calcium chloride). In Figure 3, LVG denotes an alginate with a high G content, while LVM is an M-rich alginate. Note that the gel made from the M-rich alginate collapses on itself, displaying a less rigid gel network. Moreover, the gel made from the G alginate shows greater gel strength (data not shown).

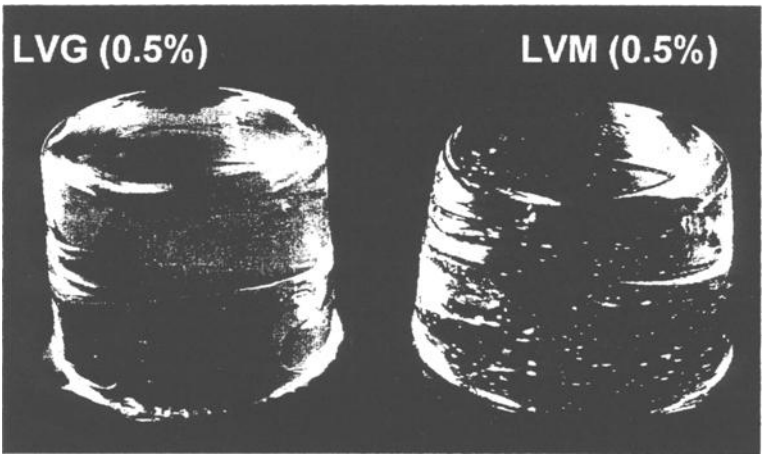

Figure 3 – *Calcium cross-linked alginate gels*

Scaffolds, Bolts, Rods and Tubes - Alginate BioStructures in the form of solid bolts and tubes can be made by extrusion from a thick alginate solution or an alginate paste followed by drying. The morphology and strength of these "biostructures" depend on molecular weight and composition. For example, the scanning electron micrographs shown in Figure 4 compare the morphology of an extruded bolt made from high Mw (A) versus low Mw (B) G-rich alginate. Note the differences in surface structure as well as internal pore structure. Consistent with higher gel strengths using G-rich alginates, bolts composed of G-rich alginate require a greater force to break.

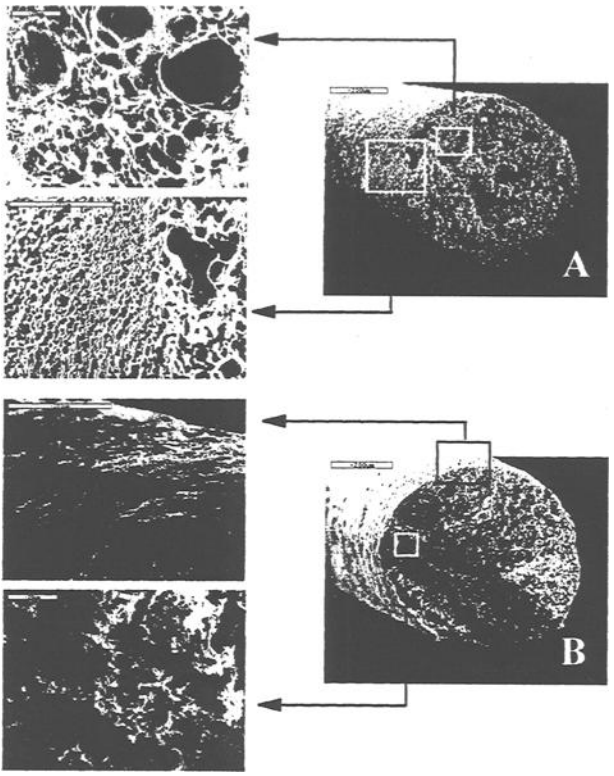

Figure 4 – *Alginate bolts extruded from (A) PRONOVA™ MVG and PROTANAL™[3] LFR 5/60 sodium alginate*

Chitosan

Chitosan is a polycationic polysaccharide derived from crustacean shells by deacetylation of naturally occurring chitin. Like alginate, chitosan is also a linear, unbranched, polymer that is composed of glucosamine and *N*-acetylglucosamine monomers linked in a ß-(1→4) manner (Figure 5). Unlike alginate, however, following

[3] PRONOVA™ and PROTANAL™ are trademarks of FMC BioPolymer AS, Drammen, Norway.

deacetylation of chitin there is a random distribution of glucosamine units along the polymer chain [29,30]. The ratio between glucosamine and *N*-acetylglucosamine is referred to as the degree of deacetylation. In solution, chitosan salts carry a positive charge through protonization of the free amino group on glucosamine. Reactivity with negatively charged molecules is a direct function of the positive charge density of chitosan. The cationic nature of chitosan gives this polymer a bioadhesive property [19,31,32].

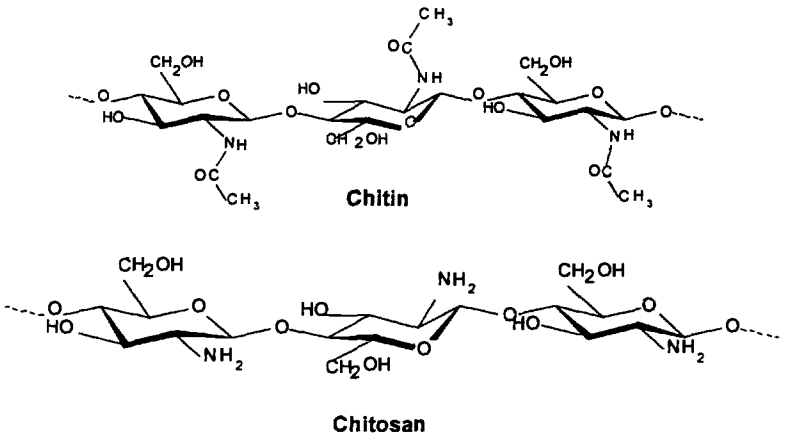

Figure 5 – *Chemical structure of chitin and chitosan*

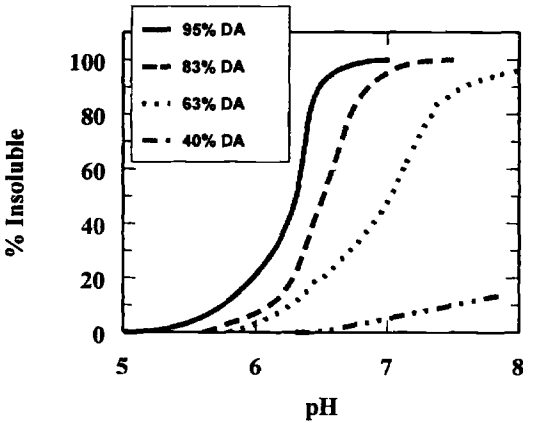

Figure 6 – *Solubility of chitosan with varying degrees of deacetylation.*

Solubility

In addition to affecting the bioadhesiveness of chitosan, the degree of deacetylation also affects its solubility. Figure 6 represents the solubility (measured as precipitation

or % insoluble material) of chitosan relative to pH of the solution. For example, a chitosan of 95% deacetylation would be completely soluble at pH 5 but totally insoluble at pH 6.5. A chitosan of lower degree of deacetylation, for instance 63%, would be slightly soluble at pH 7, while chitosan of 40% deacetylation would remain in solution at pH 7 [33].

Biological Effect

One of the important properties of chitosan for drug delivery applications (*e.g.* nasal drug delivery) is its ability to induce transient opening of tight junctions in an epithelial cell layer. This has been shown to depend on molecular weight and degree of deacetylation [34].

Regulatory Issues

In order to assist in the development of alginate- or chitosan-containing applications, two American Society for Testing and Materials (ASTM International) standards have been approved recently. They are entitled the ASTM Standard Guide for Characterization and Testing of Alginates as Starting Materials Intended for Use in Biomedical and Tissue-Engineered Medical Product Applications (F 2064) and ASTM Standard Guide for Characterization and Testing of Chitosan Salts as Starting Materials Intended for Use in Biomedical and Tissue-Engineered Medical Product Applications (F 2103). These Guides are meant to provide information as to what parameters (both analytical and regulatory) need to be addressed either by the biopolymer supplier or the developer when using alginate or chitosan in pharmaceutical and biomedical applications, such as TEMPs [35]. When alginate or chitosan are to be used for applications inside the body, as an implantable device or for parenteral administration of drugs, strict requirements of manufacture, characterization and purity will have to be met for the biomaterial. Common to both ASTM guides is the following:

Documentation

Alginate and chitosan for use in biomedical and pharmaceutical applications and in Tissue Engineered Medical Products (TEMPs) should ideally be documented in Drug Master Files (DMF) to which end users may obtain a letter of cross-reference from suppliers. Such Drug Master Files should be submitted to the US FDA and to other regulatory authorities, both national and international.

Impurity Levels

The term impurity relates to the presence of extraneous substances and materials in a biopolymer sample. Impurities can arise from the presence of other biopolymer salts (for example, calcium alginate or alginic acid in the sodium alginate material), or low molecular weight material present in a sample of high molecular weight (*i.e.* a broad polydispersity), could constitute an impurity. The major impurities of concern include the following:

Endotoxin - The endotoxin level in alginate or chitosan will be critical if they are intended to be implanted. Endotoxin levels must be below 5 EU/kg of body weight for all implantable devices.

Protein - Residual protein in alginate and chitosan could cause allergic reactions such as hypersensitivity. The biopolymer supplier should demonstrate protein removal and protein quantitative methods of satisfactory sensitivity.

Heavy Metals - The marine source of both alginate and chitosan means that heavy metals, such as lead and mercury, may be present. Biopolymers must be shown to contain acceptable quantities of these contaminants.

Microbiological Burden - The presence of bacteria, yeast and mold are also impurities that can arise in processed material. The presence of bacteria may also contribute to the presence of endotoxins.

Safety and Toxicology

The safety of alginate and chitosan in biomedical and pharmaceutical applications and in Tissue-Engineered Medical Products should be established according to current guidelines such as Biological evaluation of medical devices (ISO 10993) and ASTM Standard Practice for Selecting Generic Biological Test Methods for Materials and Devices (F 748). Preclinical safety studies specific to the clinical application under consideration must also be done in accordance with 21CFR312. Sodium alginate is listed on the list of materials Affirmed Generally Recognized as Safe (GRAS) by the US Food and Drug Administration (FDA) (21CFR184.1724). This permits sodium alginate (but not other salts such as magnesium) to be used in foods as a thickener or gelling agent. That sodium alginate is listed on the GRAS list does not indicate approval for the use of alginate in pharmaceutical and/or biomedical applications.

Conclusions

Alginate and chitosan are two biopolymers that are used in numerous industrial, controlled release and tissue engineering applications. It is clear that these biopolymers present a diversity of functional properties that depend strongly on composition, structure, molecular weight, and purity. Figure 7 summarizes this relationship for alginate and chitosan, and demonstrates that consistent and precise characterization of these materials is key to applications like TEMP development. The development of industry standards, such as the ASTM Guides for alginate (F 2064) and chitosan (F2103) enable reproducible characterization, good starting material selection and formulation, and precise regulatory documentation. The development of additional standards for starting materials is an important activity that will benefit both users and manufacturers alike.

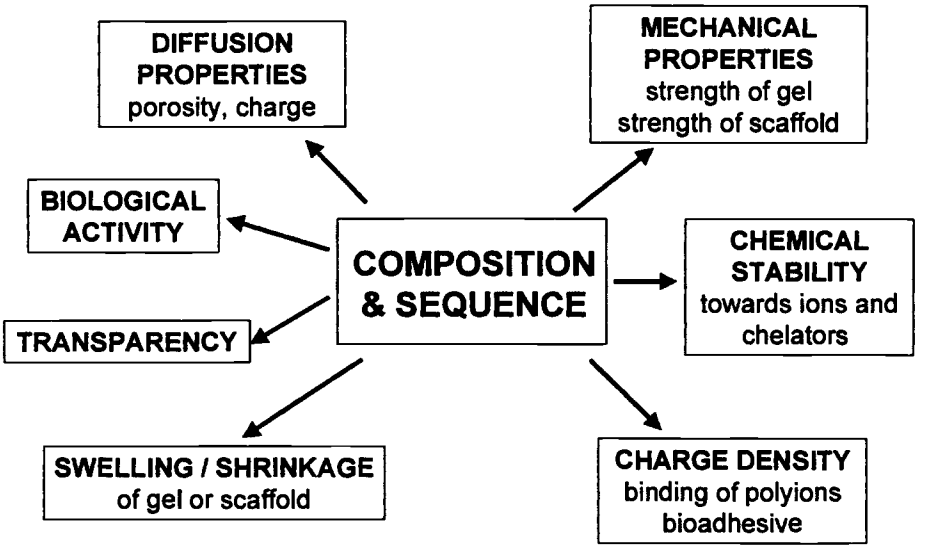

Figure 7 – *Structure-function correlation for alginate and chitosan*

References

[1] Kim, B. S., Bacz, C. E. and Atala, A., "Biomaterials for Tissue Engineering," *World Journal of Urology,* Vol. 18, 2000, pp. 2-9.

[2] Rowley, J. A., Madlambayan, G. and Mooney, D. J., "Alginate Hydrogels as Synthetic Extracellular Matrix Materials," *Biomaterials*, Vol. 20, 1999, pp. 45-53.

[3] Miyazaki, S., Kubo, W. and Attwood, D., "Oral Sustained Delivery of Theophylline Using in-situ Gelation of Sodium Alginate," *Journal of Controlled Release*, Vol. 67, 2000, pp. 275-280.

[4] Ramdas, M. *et al.*, "Alginate Encapsulated Bioadhesive Chitosan Microspheres for Intestinal Drug Delivery," *Journal of Biomaterial Applications,* Vol. 13, 1999, pp. 290-296

[5] Uludag, H., DeVos, P. and Tresco, P.A., "Technology of Mammalian Cell Encapsulation," *Advances in Drug Delivery Reviews,* Vol. 42, 2000, pp. 29-64.

[6] Struszczyk, H., Kivekas, O., and Niekraszewicz, A., "Some Modern Applications of New Chitosan Forms," *Advances in Chitin Science*, Vol. 1, 1996, pp. 482-489.

[7] Ramos, V. M., *et al.*, "Waste Water Treatment with Chitosan in a Paper Recycling Plant," *Advances in Chitin Science*, Vol. 2, 1997, pp. 853-857.

[8] Muzzarelli, R. A. A., "Recent Results in the Oral Administration of Chitosan." In *Chitosan* per os*: from dietary supplement to drug carrier*, R. A. A. Muzzarelli, Ed., Atec, Grottammare, Italy, 2000, pp. 3-40.

[9] Maezaki, Y., *et al.*, "Hypocholestrolemic Effect of Chitosan in Adult Males," *Bioscience Biotechnology Biochemistry*, Vol. 57, 1993, pp. 1439-1444.

[10] Dornish, M., Skaugrud, Ø., Illum, L., and Davis, S.S., "Nasal Drug Delivery with PROTASAN," *Advances in Chitin Science*, Vol. 2, 1997, pp. 694-697.

[11] Skaugrud, Ø., "Drug delivery systems with alginate and chitosan," *Royal Society of Chemistry*, Vol. 161, 1995, pp. 96-107.

[12] Illum, L., Farraj, N. F., and Davis, S. S., "Chitosan as a Novel Nasal Delivery System for Peptide Drugs," *Pharmaceutical Research*, Vol. 11, 1994, pp. 1186-1189.

[13] Thomas, S., "Alginate Dressings in Surgery and Wound Management - Part 1," *Journal of Wound Care*, Vol. 9, 2000, pp. 56-60.

[14] Thomas, S., "Alginate Dressings in Surgery and Wound Management: Part 2," *Journal of Wound Care* 9, 2000, pp. 115-119.

[15] Thomas, S., "Alginate Dressings in Surgery and Wound Management: Part 3," *Journal of Wound Care* 9, 2000, pp. 163-166.

[16] Hagstam, H., "Alginates and Heartburn - Evaluation of a Medicine with a Mechanical Mode of Action," In *Gums and stabilizers in the food industry*, G. O. Phillips, Ed., Elsevier,, Amsterdam, The Netherlands, 1986, pp. 363-370.

[17] Mandel, K.G., Daggy, B. G., Brodie, D. A. and Jacoby, H.I., "Review Article: Alginate-Raft Formulations in the Treatment of Heartburn and Acid Reflux," *Alimentary Pharmacology Therapeutics*, Vol. 14, 2000, pp. 669-690.

[18] Onsøyen, E., "Hydration Induced Swelling of Alginate Based Matrix Tablets at GI-Tract pH Conditions," In *Excipients and delivery systems for pharmaceutical formulations*, D. R. Karse and R. A. Stephenson, Eds., The Royal Society of Chemistry, Cambridge, UK, 1995, pp. 108-122.

[19] Skaugrud, Ø., Hagen, A., Borgersen, B. and Dornish, M., "Biomedical and Pharmaceutical Applications of Alginate and Chitosan," *Biotechnology and Genetic Engineering Reviews*, Vol. 16, 1999, pp. 23-40.

[20] Shapiro, L. and Cohen, S., "Novel Alginate Sponges for Cell Culture and Transplantation," *Biomaterials*, Vol. 18, 1997, pp. 583-590.

[21] Madihally, S. V. and Matthew, H. W., "Porous Chitosan Scaffolds for Tissue Engineering," *Biomaterials*, Vol. 20, 1999, pp. 1133-1142.

[22] *Principles of Tissue Engineering*, R. P. Lanza, R. Langer and J. Vacanti, Eds., Academic Press, San Diego, CA 92191-4495, 2000.

[23] *Tissue Engineering and Biodegradable Equivalents*, K-U. Lewandrowski, D. L. Wise, D. J. Trantolo, J. E. Gressen, M. J. Yaszemski and D. E. Altobelli, Eds., Marcell Dekker, Inc., Basel, Switzerland, 2002.

[24] *Methods of Tissue Engineering*, A. Atala and R. P. Lanza, Eds., Academic Press, San Diego, CA 92191-4495, 2001.

[25] Soon-Shiong, P. *et al.*, "Insulin Independence in a Type I Diabetic Patient after Encapsulated Islet Transplantation," *Lancet*, Vol. 343, 1994, pp. 950-951.

[26] Diamond, D. A. and Caldamone, A. A., "Endoscopic Correction of Vesicoureteral Reflux in Children Using Autologous Chondrocytes: Preliminary Results," *Journal of Urology*, Vol. 162, 1999, pp. 1185-1188.

[27] Smidsrød, O. and Skjåk-Bræk, G., "Alginate as Immobilization Matrix for Cells," *Trends in Biotechnology*, Vol. 8, 1990, pp. 71-78.

[28] Smidsrød, O. and Draget, K .I., "Chemistry and Physical Properties of Alginates," *Carbohydrates in Europe*, Vol. 14, 1996, pp. 6-13.

[29] Vårum, K. M., Anthonsen, M. W., Ottøy, M. H., Grasdalen, H., and Smidsrød, O., "Chemical Composition and Sequences in Chitosans Determined by High-Field Proton and Carbon N.M.R. Spectroscopy – Relation to Solubility," In *Advances in Chitin and Chitosan*, C. J. Brine, P. A. Sandford and J. P. Zikakis, Eds., Elsevier Applied Science, London, UK, 1992, pp. 127-136.

[30] Ottøy, M. H., Vårum, K. M. and Smidsrød, O., "Distribution of Chemical Composition in Heterogeneously Deacetylated Chitosans," *Advances in Chitin Science*, Vol. 12, 1996, pp. 317-324.

[31] Allan, G. G., *et al.*, "Biomedical Applications of Chitin and Chitosan," In *Chitin, Chitosan and Related Enzymes*, J. P. Zikakis, Ed., Academic Press, Inc., New York, NY, 1984, pp. 119-133.

[32] Li, Q., Dunn, E. T., Grandmaison, E. W. and Goosen, M. F. A., "Applications and Properties of Chitosan," *Journal of Bioactive and Compatible Polymers*, Vol. 7, 1992, pp. 370-397.

[33] Vårum, K. M., Ottøy, M. H. And Smidsrød, O., "Water-Solubility of Partially *N*-acetylated Chitosans as a Function of pH. Effect of Chemical Composition and Depolymerisation," *Carbohydrate Polymers,* Vol. 25, 1994, pp. 65-70.

[34] Holme, H.K., Hagen, A. and Dornish, M., "Influence of Chitosans on Permeability of Human Intestinal Epithelial (Caco-2) Cells: The Effect of Molecular Weight, Degree of Deacetylation and Exposure Time," *Advances in Chitin Science*, Vol. 4, 2000, pp. 259-265.

[35] Dornish, M., Kaplan, D. and Skaugrud, Ø., "Standards and Guidelines for Biopolymers in Tissue-Engineered Medical Products," *Annals of the New York Academy of Sciences*, Vol. 944, 2001, pp. 388-307.

Thomas J. Porter,[1] Suman Rathore,[1] Jason Rouse,[1] and Mary Denton[2]

Biomolecules in Tissue Engineered Medical Products (TEMPs): A Case Study of Recombinant Human Bone Morphogenetic Protein-2 (rhBMP-2)

Reference: Porter, T.J., Rathore, S., Rouse, J., and Denton, M., **"Biomolecules in Tissue Engineered Medical Products (TEMPs): A Case Study of Recombinant Human Bone Morphogenetic Protein-2 (rhBMP-2),"** *Tissue Engineered Medical Products (TEMPS), ASTM STP 1452,* E. Schutte, G. L. Picciolo, and D. S. Kaplan, Eds., ASTM International, West Conshohocken, PA, 2004.

Abstract: rhBMP-2 is an osteoinductive protein that, when administered locally, results in the induction of new bone tissue at the site of implantation. The osteoinductive properties of rhBMP-2 first were demonstrated by implantation at ectopic (nonbony) sites in rodents. BMPs are the only protein factors known to induce new, ectopic bone. rhBMP-2/Absorbable Collagen Sponge (ACS) is a TEMP that combines rhBMP-2 with a matrix for implantation. rhBMP-2/ACS is used in long bone fracture repair and spinal fusion. The development of rhBMP-2 protein as the active ingredient in the rhBMP-2/ACS product is summarized. Four aspects of rhBMP-2 development are covered: protein structural characterization, functional characterization, purity analysis and design of comparability studies to support changes in the manufacturing process. Topics discussed include rhBMP-2 as a "biologic" and as a constituent of a combination TEMP. The lessons learned during the development of rhBMP-2/ACS may allow general insight into the development of future standards for TEMPs that contain biologically active proteins.

Keywords: Recombinant Bone Morphogenetic Protein, Absorbable Collagen Sponge, rhBMP-2, rhBMP-2/ACS, biologic, fracture repair, osteoinductive

[1] Senior Scientist, Scientist and Lab Head, respectively, Department of Characterization and Analytical Development, Wyeth BioPharma, 1 Burtt Road, Andover, MA, 01810.

[2] Principal Scientist, Department of Biopharmaceutical Analysis, Wyeth BioPharma, 1 Burtt Road, Andover, MA, 01810.

Introduction

Bone morphogenetic proteins were initially isolated from bovine bone based upon their ability to induce cartilage and bone in a rat ectopic assay system [1]. BMPs are the only protein factors known to induce new, ectopic bone. The activity of bone extracts was used to identify and clone a family of genes known as the BMPs (or GDFs, growth and differentiation factors), members of the multigene TGF-β superfamily of growth and differentiation factors [2]. Proteins in this superfamily share seven conserved cysteines and have varying degrees of sequence homology with each other. The cDNA for human BMP-2 was cloned and expressed in Chinese hamster ovary (CHO) cells. CHO cells efficiently glycosylate the protein and process the large precursor molecule by removal of the signal peptide from prepro rhBMP-2 followed by removal of the propeptide region (Fig. 1) [3].

The processed, active protein is a disulfide-linked dimer that resembles natural BMP-2 derived from bovine bone. The purified protein has two NH_2-termini resulting from differential cellular processing, starting at either Thr^{266} or Gln^{283}. Gln^{283} spontaneously cyclizes to pyroglutamate in aqueous medium [4]. These three NH_2-terminal isoforms, designated T266, Q283 and <Q283, form six covalent dimers (Fig. 1).

rhBMP-2 is produced commercially using the CHO expression system. rhBMP-2 is purified from the conditioned cell culture medium by a series of three chromatography columns, a virus-retaining membrane filtration step and multiple 0.2 μm filtration steps. Finally, the protein is formulated and then stored at –80 °C. The bulk protein is further processed at a fill/finish facility and filled into vials at the appropriate dosage strength.

The general clinical application of rhBMP-2 is osteoinduction. Examples include spinal fusion and long bone fracture repair [5, 6]. While application of rhBMP-2 alone is sufficient for osteoinduction [7], an implantable matrix is required to facilitate surgical delivery and retention of rhBMP-2 at the surgical site. Numerous bioerodable matrices were characterized in combination with rhBMP-2 in preclinical models of bone repair with the goal of selecting a matrix suitable for the intended clinical use of rhBMP-2. Matrices tested include synthetic polymers, polysaccharides and collagen [8, 9, 10]. Bovine type I collagen was found to be compatible with rhBMP-2 and has a long, safe history of use in humans. When crosslinked, as it is in ACS (produced by Integra LifeSciences Corporation, 311C Enterprise Drive, Plainsboro, NJ 08536), collagen is cohesive, tissue adherent and can be folded and shaped. Based on these characteristics, ACS was chosen as the matrix for rhBMP-2.

rhBMP-2/ACS is supplied in a kit that contains all components necessary to prepare the implant: a vial of lyophilized rhBMP-2, a vial of Water for Injection for reconstitution of rhBMP-2, the ACS, and a syringe with needle. At the time of surgery, surgeons prepare rhBMP-2/ACS by reconstituting the lyophilized rhBMP-2 with Water for Injection, and then uniformly applying this rhBMP-2 solution to the matrix (Fig. 2). The wetted sponge is then implanted at the skeletal site where bone induction is desired.

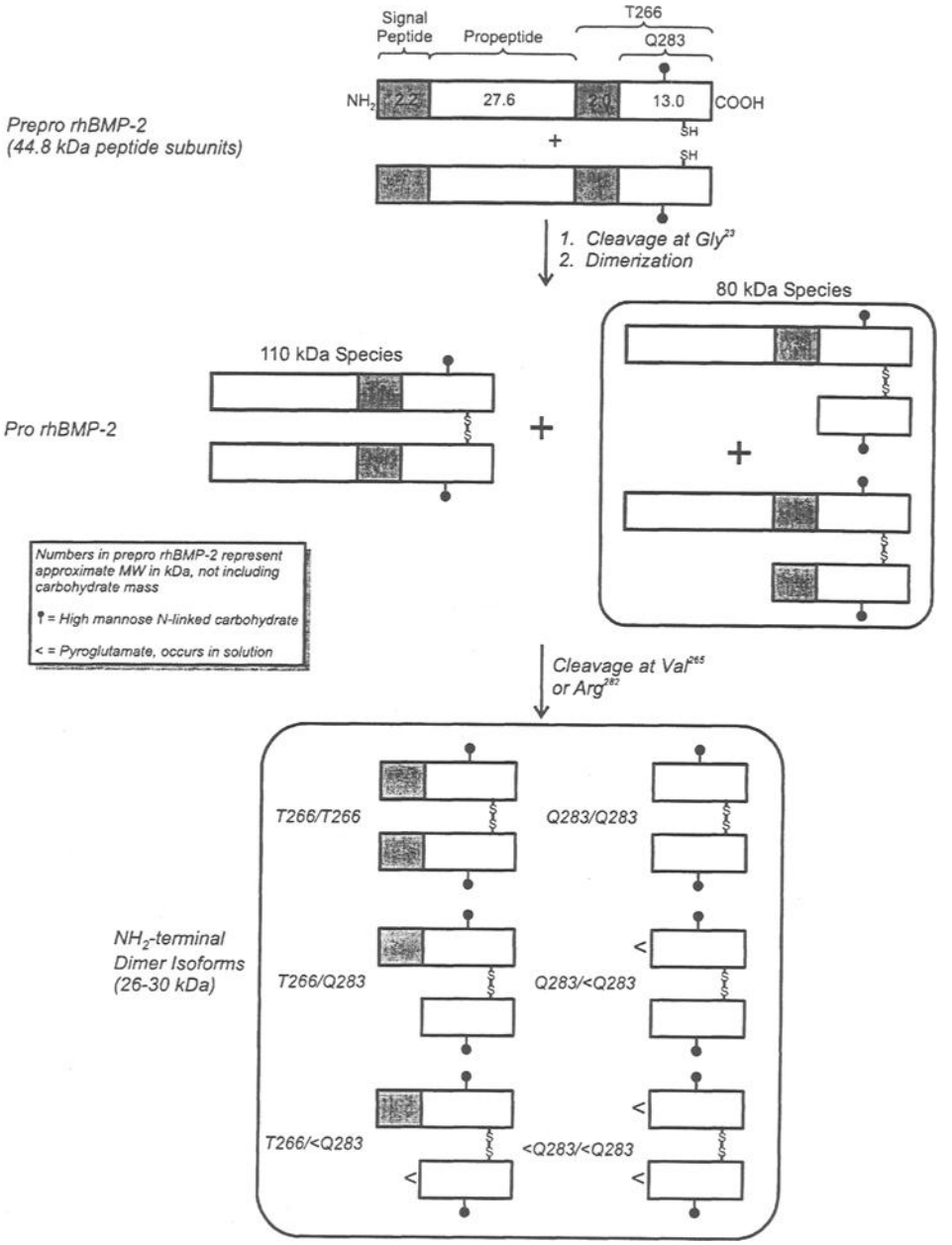

Fig. 1— *Cellular Processing of Prepro rhBMP-2.*

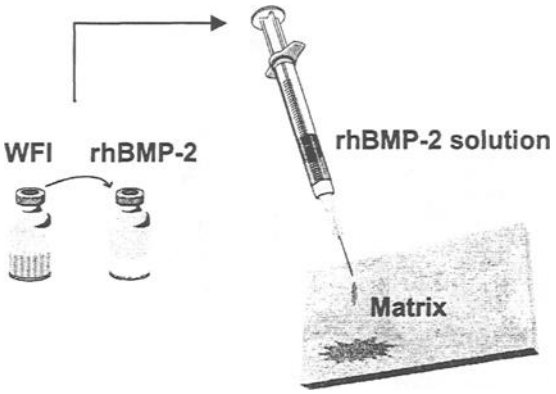

Fig. 2 — *rhBMP-2/ACS Product Preparation.*

rhBMP-2/ACS achieves osteoinduction by a pharmacologic mechanism of action attributable to rhBMP-2. rhBMP-2 binds to receptors on the surface of mesenchymal cells and causes these cells to differentiate into cartilage- and bone-forming cells. These differentiated cells form trabecular bone as the ACS is degraded, with vascular invasion evident at the same time [11]. The bone formation process develops from the outside of the implant towards the center until the entire rhBMP-2/ACS implant is replaced by bone.

The following discussion focuses on the development of the rhBMP-2 component of the rhBMP-2/ACS product. Characterization and assay development for rhBMP-2 were, for the most part, typical of those activities associated with a parenteral protein biologic. However, the final product contains both rhBMP-2 and ACS. Additional characterization of rhBMP-2 in combination with ACS was needed to assure proper functioning of the entire implantable product.

Materials and Methods

rhBMP-2

rhBMP-2 test samples were derived from protein batches produced at Wyeth BioPharma (Andover MA or Cambridge MA). The protein concentration of these samples was typically 3-8 mg/mL in in various formulation buffers.

High Performance Liquid Chromatography (HPLC)

All protein and peptide HPLC separations were carried out on HPLC systems from Waters Corporation using Vydac, Pharmacia, Phenomenex or Tosoh HPLC columns.

For the peptide map, rhBMP-2 was reduced with dithiothreitol and alkylated with iodoacetic acid. The reduced and alkylated protein was desalted and buffer exchanged into endoproteinase Asp-N digestion buffer by gel filtration and digested at 37 C for 90 min. The reaction was quenched with trifluoroacetic acid and peptides were injected onto

a Tosoh Super ODS C18 column. Solvent A was 6 mM trifluoroacetic acid (TFA) and 4 mM heptafluorobutyric acid (HFBA) in water, solvent B was 95% acetonitrile, 5% water, 6 mM TFA, 4 mM HFBA. Peptide separation occurred between 11% and 55% solvent B.

Carbohydrate Removal

High mannose-type N-linked glycans were removed from the protein by endoglycosidase H (Endo H) treatment. rhBMP-2 (100 μg) was treated with Endo H (10 milliunits, Oxford Glycosystems) overnight at 37 °C at pH 6.5 in a histidine, arginine buffer. Extent of glycan removal was judged by SDS-PAGE.

Mass Spectrometry (MS)

Intact protein mass was determined by online liquid chromatography/MS (LC-MS) with separation on a microbore phenyl reversed phase (RP)-HPLC column followed by MS with electrospray ionization on a hybrid quadrupole time-of-flight mass spectrometer (Micromass Q-TOF). Peptide masses were obtained by LC-MS with separation on a C18 RP-HPLC column followed by electrospray ionization MS on a ThermoFinnigan LCQ instrument.

Bioassays

The *in vitro* W-20 bioassay was performed as described in ASTM standard F2131-02. The *in vivo* Use Test was performed as described in [12].

Results and Discussion

Protein Primary Structure and Posttranslational Modifications

The structure of the purified protein was characterized by Edman degradation, mass spectrometry and various chromatographic techniques. The complete protein sequence of mature rhBMP-2 in drug substance was determined by LC-MS of the peptide map to be identical to that predicted from the nucleotide sequence of the cDNA (Figs. 3 and 4, Table 1).

rhBMP-2 contains a single N-glycosylation site per subunit at Asn^{338}, which is occupied. The N-linked oligosaccharides present at this site were characterized by 1H nuclear magnetic resonance and carbohydrate fingerprinting and determined to be high mannose structures, containing between 5 and 9 mannose residues. No O-linked oligosaccharides were found. The mixture of intact protein isoforms overlaid with carbohydrate heterogeneity was well resolved by electrospray ionization hybrid quadrupole time-of-flight (ESI Q-TOF) MS (the mass accuracy of the instrument is better than 0.005%). All expected glycoforms of each NH_2-terminal isoform were found in drug substance. The mass data for all species were consistent with results obtained from the LC-MS analysis of the peptide map for the glycopeptides and NH_2-terminal isoform-related peptides (Fig. 5 and Table 2). All observed masses for the dimer agreed with the expected masses with 0.004% mass accuracy and no unexpected masses were observed.

```
  1  M V A G T R C L L A L L L P Q V L L G G A A G | L V
 26  P E L G R | R K F A A A S S G R P S S Q P S D E V L
 51  S E F E L R L L S M F G L K Q R P T P S R D A V V
 76  P P Y M L D L Y R R H S G Q P G S P A P D H R L E
101  R A A S R A N T V R S F H H E E S L E E L P E T S
126  G K T T R R F F F N L S S I P T E E F I T S A E L
151  Q V F R E Q M Q D A L G N N S S F H H R I N I Y E
176  I I K P A T A N S K F P V T R L L D T R L V N Q N
201  A S R W E S F D V T P A V M R W T A Q G H A N H G
226  F V V E V A H L E E K Q G V S K R H V R I S R S L
251  H Q D E H S W S Q I R P L L V

266  T F G H D G K G H P L H K R E K R Q A K H K Q R K

291  R L K S S C K R H P L Y V D F S D V G W N D W I V

316  A P P G Y H A F Y C H G E C P F P L A D H L N S T
          *

341  N H A I V Q T L V N S V N S K I P K A C C V P T E

366  L S A I S M L Y L D E N E K V V L K N Y Q D M V V

391  E G C G C R
```

| = Signal peptide cleavage site ↑ = NH_2-terminal processing sites

I = Internal cleavage of propeptide * = Proline hydroxylation site

_____ = N-linked glycosylation consensus site

Fig. 3 — *Primary Sequence of rhBMP-2.*

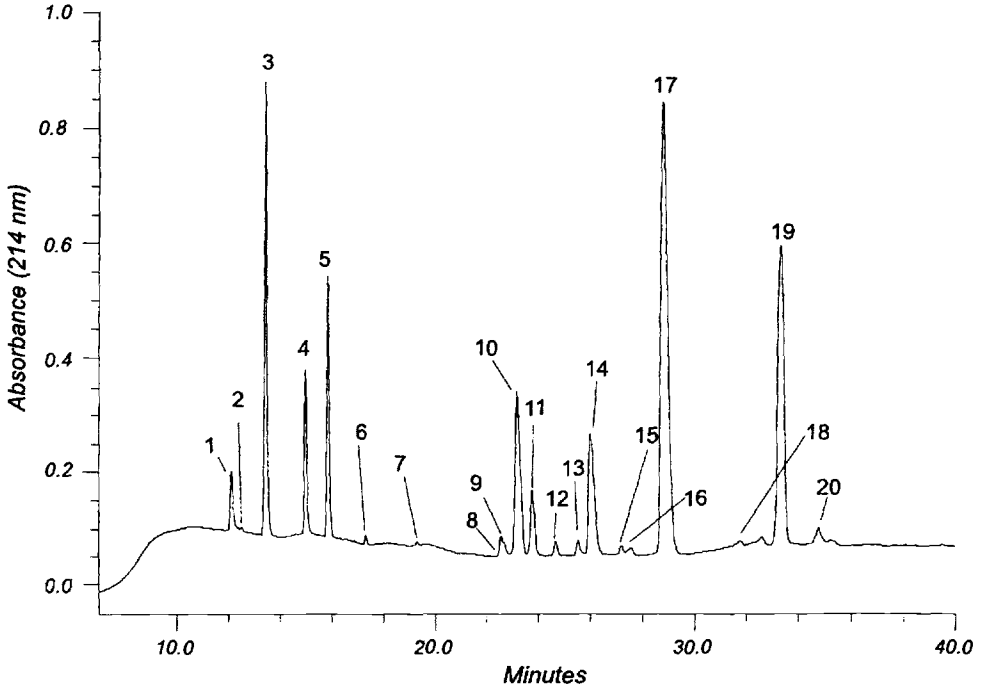

Fig. 4 — *Asp-N Peptide Map of rhBMP-2.*
A representative peptide map of rhBMP-2. The mapping procedure is described in the Materials and Methods section.

Table 1—*Identification of rhBMP-2 Peptides by Mass Spectrometry.*

Peak Number	Identity	Theoretical Mass[1]	Observed Mass
1	T266-H269	460.2	460.1
2	Modified D387-R396[2]	1199.4	1199.8
3	D307-N311	589.2	589.1
4	D387-R396	1183.4	1183.5
5	D375-Q386	1477.7	1477.9
6	D270-R279	1143.6	1143.7
7	T266-R279	1585.8	1585.8
8	D312-G327	1889.8	1889.9
9	<Q283-V303	2633.1	2632.4
10	<Q283-S306	2982.5	2982.2
11	Q283-S306	2999.5	2999.2
12	E280-S306	3413.0	3412.6
13	D270-V303	4189.9	4189.3

Table 1—*Identification of rhBMP-2 Peptides by Mass Spectrometry.*

Peak Number	Identity	Theoretical Mass[1]	Observed Mass
14	D270-S306	4539.2	4539.8
15	Modified T266-S306[3]	4981.7	4982.2
16	Modified D312-A334[4]	2723.0	2722.8
17	D312-A334	2707.0	2706.4
18	Modified D335-L374[5]		
	+ (2 GlcNAc, 5 Man)	5675.2	5674.1
	+ (2 GlcNAc, 6 Man)	5837.4	5836.0
	+ (2 GlcNAc, 7 Man)	5999.5	5998.4
	+ (2 GlcNAc, 8 Man)	6161.2	6160.8
	+ (2 GlcNAc, 9 Man)	6323.8	6324.3
19	D335-L374		
	+ (2 GlcNAc, 5 Man)	5659.2	5658.7
	+ (2 GlcNAc, 6 Man)	5821.4	5821.3
	+ (2 GlcNAc, 7 Man)	5983.5	5982.4
	+ (2 GlcNAc, 8 Man)	6145.6	6144.8
	+ (2 GlcNAc, 9 Man)	6307.8	6307.5
20	Modified D312-L374[6] and under digested rhBMP-2		
	+ (2 GlcNAc, 5 Man)	8348.2	8350.7
	+ (2 GlcNAc, 6 Man)	8510.4	8508.0
	+ (2 GlcNAc, 7 Man)	8672.5	8671.0
	+ (2 GlcNAc, 8 Man)	8834.7	8833.7
	+ (2 GlcNAc, 9 Man)	8996.8	8994.4

[1] Masses less than 2000 Da are monoisotopic values, masses greater than 2000 Da are average values, and all masses are nonprotonated values. Masses calculated using Masslynx V 3.4.

[2] Modification is consistent with methionine sulfoxide at position 388 based upon fragmentation pattern in the mass spectrometer.

[3] Modification is consistent with isoAsp^{270} based on mass analysis, NH_2-terminal sequencing and Asp-N selectivity.

[4] Hydroxyproline^{318} based on mass analysis, NH_2-terminal sequencing and amino acid analysis.

[5] Modification is consistent with methionine sulfoxide at position 371 based upon fragmentation pattern in the mass spectrometer.

[6] Modification is consistent with isoAsp^{335} based on mass analysis and Asp-N selectivity.

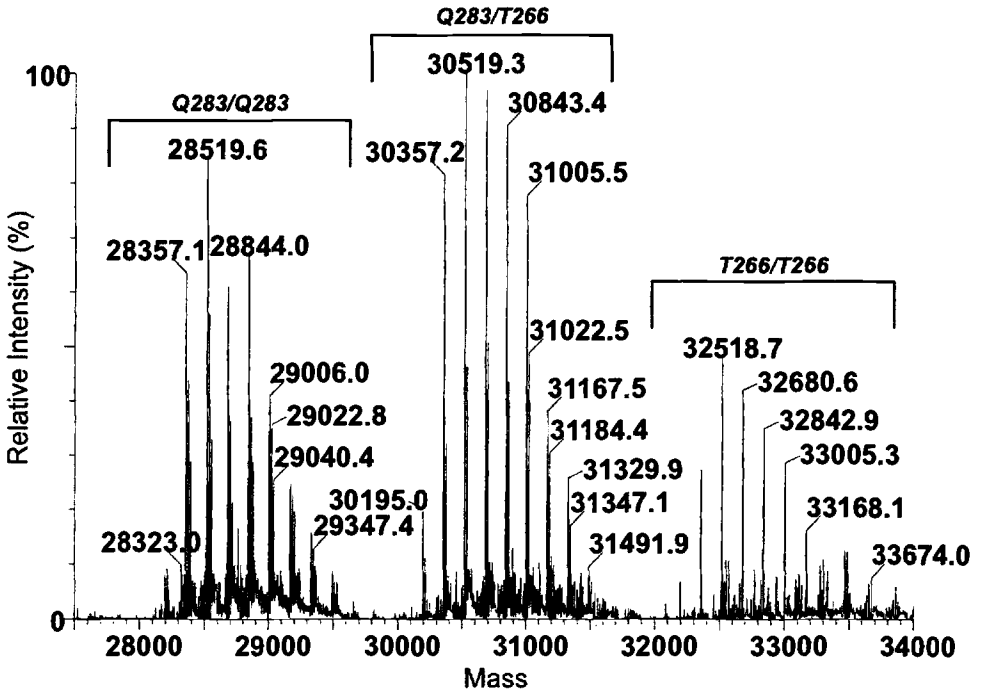

Fig. 5 — *Intact Protein Molecular Mass.*

rhBMP-2 covalent dimer was purified from dissociable dimer by phenyl RP-HPLC. The covalent dimer fraction was dried by rotary evaporation and redissolved in methanol:H_2O (1:1) to approximately 10 pmol/μL. The sample was analyzed by electrospray ionization on a hybrid quadrupole time-of-flight mass spectrometer (Micromass Q-TOF) by direct infusion in 2% formic acid (5 μL/min). The capillary voltage was 3000 V and the cone voltage was 50 V. The mass axis was externally calibrated with NaI. Chemical background was subtracted from the spectrum and the complex, multiply-charged signals were deconvoluted into zero-charge molecular weight spectra with Maximum Entropy software from Micromass (using 1 Da/channel resolution). The dimer subunits are indicated above the brackets. All Q283-containing dimers also contain <Q283.

Table 2—*Mass of Selected Glycoforms of rhBMP-2 Covalent Dimer.*[1]

Isoform	Expected Mass (Da, Avg.)	Observed Mass (Da, Avg.)	Difference (%)
<Q283/<Q283, 5/5 Mannose[2]	28,195.7	28,194.6	0.0039
<Q283/<Q283, 6/6 Mannose	28,520.0	28,519.6	0.0014
<Q283/<Q283, 7/7 Mannose	28,844.3	28,844.0	0.0010
<Q283/<Q283, 8/8 Mannose	29,168.6	29,168.0	0.0021
<Q283/<Q283, 9/9 Mannose	29,492.9	29,492.9	0.0000
<Q283/Q283, 5/5 Mannose	28,212.7	28,212.5	0.0007
<Q283/Q283, 6/6 Mannose	28,537.0	28,536.3	0.0025
<Q283/Q283, 7/7 Mannose	28,861.3	28,861.0	0.0010
<Q283/Q283, 8/8 Mannose	29,185.6	29,184.7	0.0031
<Q283/Q283, 9/9 Mannose	29,509.9	29,508.7	0.0041
Q283/Q283, 5/5 Mannose	28,229.8	28,229.0	0.0028
Q283/Q283, 6/6 Mannose	28,554.1	28,553.3	0.0028
Q283/Q283, 7/7 Mannose	28,878.4	28,877.9	0.0017
Q283/Q283, 8/8 Mannose	29,202.6	29,202.3	0.0010
Q283/Q283, 9/9 Mannose	29,526.9	29,528.0	0.0037
<Q283/T266, 5/5 Mannose	30,195.0	30,195.0	0.0000
<Q283/T266, 6/6 Mannose	30,519.3	30,519.3	0.0000
<Q283/T266, 7/7 Mannose	30,843.6	30,843.4	0.0006
<Q283/T266, 8/8 Mannose	31,167.8	31,167.5	0.0010
<Q283/T266, 9/9 Mannose	31,492.1	31,491.9	0.0006
Q283/T266, 5/5 Mannose	30,212.0	30,211.5	0.0017
Q283/T266, 6/6 Mannose	30,536.3	30,536.5	0.0007
Q283/T266, 7/7 Mannose	30,860.6	30,860.6	0.0000
Q283/T266, 8/8 Mannose	31,184.9	31,184.4	0.0016
Q283/T266, 9/9 Mannose	31,509.2	31,509.1	0.0003
T266/T266, 5/5 Mannose	32,194.2	32,194.1	0.0003
T266/T266, 6/6 Mannose	32,518.5	32,518.7	0.0006
T266/T266, 7/7 Mannose	32,842.8	32,842.9	0.0003
T266/T266, 8/8 Mannose	33,167.1	33,168.1	0.0030
T266 /T266, 9/9 Mannose	33,491.4	Not Detected	—

[1] Average mass is shown for selected glycoforms of the six protein dimer isoforms. The expected mass (avg) values were calculated with the program PAWS (2000.04.10) for NT (Proteometrics, NY, NY).

[2] The values represent the number of mannose residues on each subunit, only the masses for the dimers having identical glycans on each subunit are shown, other combinations are present, see Fig. 5.

Impact of the Collagen Matrix on rhBMP-2 Structure

rhBMP-2 solution is applied to the collagen sponge prior to surgical implantation. To allow flexibility in surgical schedules, it was necessary to have a window of time after product preparation and before implantation. The structural integrity and in vitro bioactivity of the rhBMP-2 component of the product is well characterized and is controlled by release testing. However, this testing does not assess the effect of contact with the ACS on the rhBMP-2 structure and activity.

An experiment was performed to determine whether the ACS had an impact on the structural integrity of the incorporated rhBMP-2 over the desired pre-surgery time window of the product after wetting. rhBMP-2 was separately combined with three different lots of ACS and incubated for 3.5 h at room temperature. This time period is 1 h 15 m beyond the maximum time limit for the pre-implantation period after the rhBMP-2 and the ACS are combined in the operating room. The rhBMP-2/ACS samples were extracted with citrate buffer. The collagen remained insoluble under these conditions, allowing peptide map characterization of rhBMP-2 (Fig. 6). Recovery of rhBMP-2 was 81% ±1% of the loaded protein, and no significant changes in the peptide map profile were found, suggesting that rhBMP-2 structure is not altered by extended contact with the ACS.

Biological Activity

Description of Bioassays- Two bioassays were employed in development of rhBMP-2, the in vitro W-20 assay and the in vivo Use Test (rat ectopic assay).

The W-20 assay is based upon rhBMP-2 dose-dependent receptor-mediated gene induction of alkaline phosphatase in the mouse W-20 stromal cell line [13, F2131-02]. This assay is a release test for rhBMP-2 drug substance and vialed protein and it is also used as the assay that defines the World Health Organization's International Unit of rhBMP-2 activity. The biological activity of each sample is determined relative to a reference standard with an assigned potency.

The rat ectopic implant model is a classic assay system for bone morphogenetic protein activity [14]. This assay has been modified and standardized for testing of rhBMP-2/ACS, and the assay is called the Use Test. It has been utilized during development of the product as a release assay for rhBMP-2/ACS product, and for assessing stability. It demonstrates that rhBMP-2/ACS has its intended activity, i.e., the local induction of bone. For each test, the rhBMP-2 component is diluted to 0.1 mg/mL and combined with an appropriately sized ACS section. Ten samples are implanted subcutaneously into five rats (bilateral implants). In addition, two negative control implants, buffer/ACS, are implanted into a rat. After 14 days, the implants are removed and processed for histology and scored for bone content. The amount of induced bone present in a section is assessed using a scoring scale of 0 (no bone present) to 5 (all of the implant is bone). The amount of bone formation is determined as the total area of bone including bone marrow that has been induced.

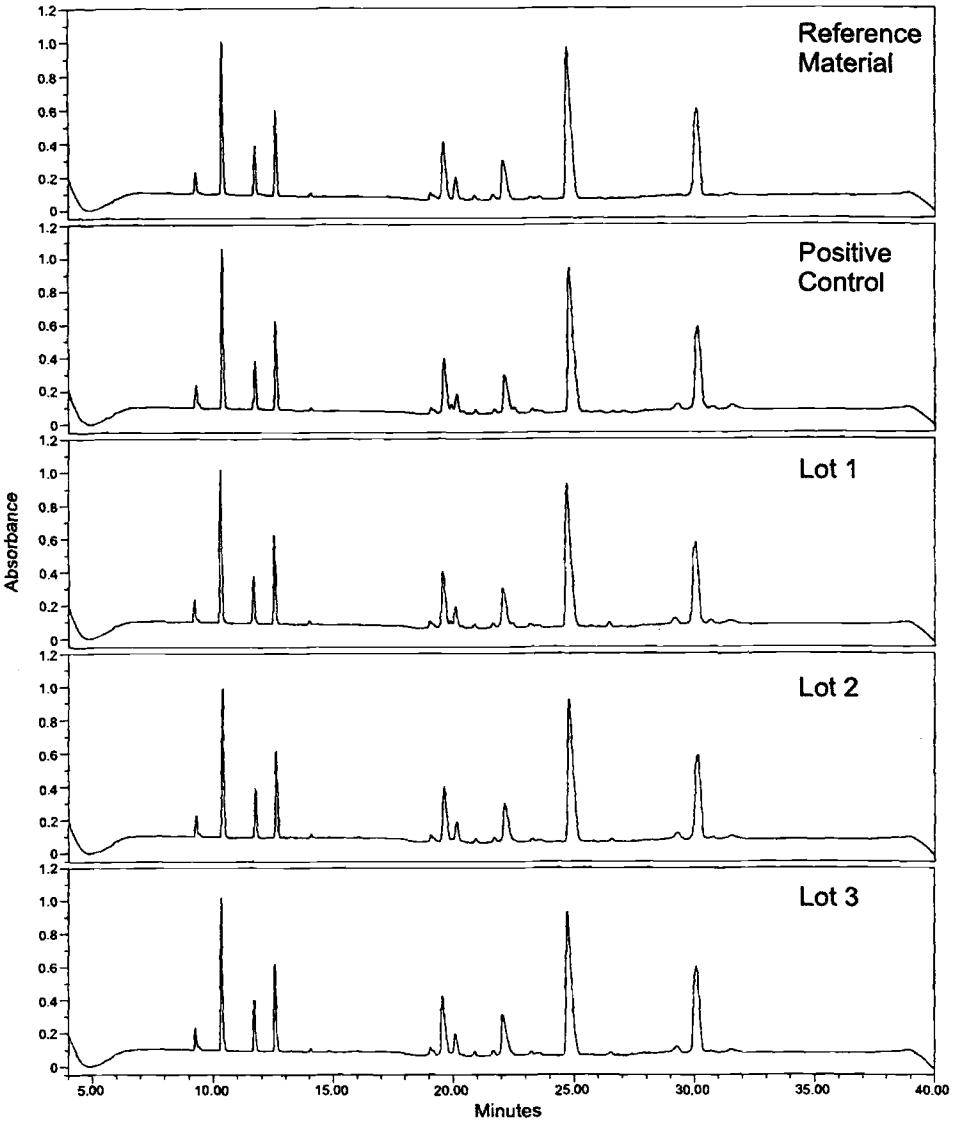

Fig. 6 — *Peptide Maps of rhBMP-2 Extracted from rhBMP-2/ACS*

rhBMP-2 positive control (citrate treated) and rhBMP-2 extracted from rhBMP-2/ACS (three lots of ACS as indicated) with citrate were desalted by C4 RP-HPLC, dried to dryness by vacuum centrifugation and subjected to Asp-N peptide mapping.

Biological Activity of Protein Isoforms- It was important to determine whether the major product isoforms were active for process consistency reasons. If one or more of the isoforms were found to be inactive, the purification process would have been modified to reduce or eliminate those species. The six NH_2-terminal isoforms were isolated and tested for biological activity in vitro and in vivo. Isoforms were purified by cation exchange chromatography. Tables 3 and 4 show the activity results. T266-containing isoforms had lower activity than the Q283 forms in vitro, but had similar activity to that of the Q283 forms in vivo.

Table 3—*In Vitro Bioactivity of NH_2-Terminal Dimer Isoforms (W-20 Bioassay).*

Sample	Specific Activity ± SD[1] (U_{WHO}/mg x 10^{-5})
Control[2]	5.2 ± 0.4
<Q283/<Q283	7.4 ± 1.2
<Q283/Q283	6.8 ± 0.7
Q283/Q283	6.2 ± 0.4
<Q283/T266	4.2 ± 0.3
Q283/T266	3.8 ± 0.3
T266/T266	2.7 ± 0.2

[1] Standard deviation reflects bioassay variability, does not include protein concentration assay variability.

[2] Unfractionated drug substance.

Table 4—*In Vivo Bioactivity of NH_2-Terminal Dimer Isoforms (Use Test).*

Protein	Dose (mg/mL)	Bone Score ± SD[1]
Control[2]	0.01	1.3 ± 1.2
	0.03	2.6 ± 1.9
	0.10	3.2 ± 1.3
<Q283/<Q283	0.01	1.3 ± 1.4
	0.03	4.0 ± 0.9
	0.10	3.4 ± 0.9
<Q283/Q283	0.01	1.2 ± 1.1
	0.03	4.4 ± 0.9
	0.10	3.4 ± 0.9
Q283/Q283	0.01	0.0 ± 0.0
	0.03	2.7 ± 1.5
	0.10	3.2 ± 0.4
<Q283/T266	0.01	2.0 ± 1.4

Table 4—*In Vivo Bioactivity of NH_2-Terminal Dimer Isoforms (Use Test).*

Protein	Dose (mg/mL)	Bone Score ± SD[1]
	0.03	2.5 ± 2.1
	0.10	3.8 ± 1.0
Q283/T266	0.01	1.7 ± 1.7
	0.03	3.4 ± 1.6
	0.10	3.4 ± 1.0
T266/T266	0.01	1.0 ± 0.9
	0.03	2.4 ± 0.5
	0.10	3.6 ± 0.9

[1] Rat ectopic bone scoring system described in text; ACS was used as the matrix.

[2] Unfractionated rhBMP-2.

Given these activity results, all NH_2-terminal isoforms were considered appropriate for inclusion in the rhBMP-2/ACS implantable product.

Although the N-linked glycosylation site is fully occupied as judged by the retention time and mass of the glycosylated peptide in the peptide map, it was important to determine the role of the carbohydrate in biological activity. A production process failure might result in unglycosylated protein in the drug substance. Since un- or underglycosylated species were not found in rhBMP-2 batches, rhBMP-2 was enzymatically demannosylated by Endo H treatment. This treatment resulted in protein with the high mannose glycan trimmed back to one N-acetylglucosamine. Removal of the mannose did not have a significant effect on either *in vitro* or *in vivo* activity (Tables 5 and 6).

Table 5 — *In Vitro Bioactivity of Endo H-treated rhBMP-2 (W-20 Bioassay).*

Sample[1]	Specific Activity ± SD (U_{WHO}/mg x 10^{-5})[2]
Contol	4.2 ± 0.6
Endo H-Treated	4.0 ± 0.0

[1] rhBMP-2 was treated with Endo H as described in Materials and Methods. Deglycosylated rhBMP-2 was purified from Endo H by cation exchange HPLC and C4 RP-HPLC. Control rhBMP-2 was taken through the same procedure without the addition of enzyme.

[2] The error shown is the standard error of the mean of duplicate determinations.

Table 6 — *In Vivo Bioactivity of Deglycosylated rhBMP-2 (Use Test).*[1]

Sample[2]	Dose (mg/mL)	Bone Score ± SD[3]
Control	0.01	1.3 ± 1.2
	0.03	2.6 ± 1.9
	0.10	3.2 ± 1.3
Endo H-Treated	0.01	2.5 ± 0.8
	0.03	2.8 ± 1.2
	0.10	1.7 ± 0.8

[1] See reference [12] for a description of the rat ectopic bone-forming assay (Use Test).
[2] Samples prepared as described in Table 5.
[3] Rat ectopic bone scoring system described in the text; ACS was used as the matrix.

These data indicate that the glycan does not play a significant role in rhBMP-2 biological activity.

Correlation of In Vitro and In Vivo Bioassays- The W-20 cell-based in vitro bioassay was determined to be a relevant indicator of biological activity based upon the correlation of rhBMP-2 activity in this assay with ectopic bone forming activity of rhBMP-2 in the in vivo Use Test.

The shape of the dose response curve in the Use Test, like many *in vivo* bioassays, is nonlinear and extremely steep. Nevertheless, because the Use Test assesses bone formation, which is the desired clinical outcome of implantation of rhBMP-2/ACS, the test is considered to be a useful characterization assay. Although the W-20 bioassay does not measure bone formation, it does measure specific induction of alkaline phosphatase (ALP) by rhBMP-2, one of the events on the differentiation pathway to osteoblasts. Detection of bone-specific ALP related to bone formation has clinical relevance. The measurement of ALP from a patient's serum has been used clinically as a surrogate marker to monitor therapies that stimulate bone formation [15]. The imprecision of the Use Test rules out an exact correlation of the Use Test and the W-20 bioassay, however, a general correlation was established that shows that the W-20 bioassay is a relevant surrogate for the Use Test.

The assays were compared by assessing the relative response of the each to rhBMP-2 with intentionally reduced activity. Chemical oxidation of rhBMP-2 with peracetic acid results in specific oxidation of the two methionine residues in each subunit of the rhBMP-2 dimer and decreased in vitro bioactivity. The protein was still dimeric as shown by SDS-PAGE analysis, and no significant differences other than oxidation at methionine was detected in the protein's covalent structure by peptide mapping and mass spectrometry. Characterization of the oxidized protein with near ultraviolet circular dichroism (near UV CD) and tryptophan fluorescence indicated that the tryptophan environment is disrupted [16]. Both methionine residues are near each other in space and are also close to the only two tryptophan residues in the protein. All of these amino acid residues reside in the hydrophobic finger-helix receptor-binding pocket on rhBMP-2.

This pocket interacts with the phenylalanine "knob" on the BMP Type I receptor (specifically BMPRIA) [17].

BMPRIA has been shown by Northern blot analysis to be expressed at a high level in the W-20 cell line as well as many other tissues, and therefore the BMP-2/BMPRIA structural information supports the relevance of the use of rhBMP-2 oxidized at the methionine residues as a tool to compare the in vitro and in vivo assays. Protein with different degrees of oxidation at the methionine residues was prepared and tested in both the W-20 bioassay and the Use Test. rhBMP-2 fully oxidized at both methionine residues was virtually inactive in both the W-20 bioassay and the Use Test (Table 7).

Table 7—*In Vitro and In Vivo Activity of Oxidized rhBMP-2.*[1]

		Specific Activity (U_{WHO}/mg x 10^{-5} ± SD)[2]			
			Oxidation Level (%)[3]		
Assay		**Control**	**62%**	**87%**	**100%**
W-20		5.4 ± 0.6	3.3 ± 0.3	0.9 ± 0.05	0.2 ± 0.01
Use Test		**Bone Score[4] ± SD**			
	% Oxidized				
	rhBMP-2 Dose (mg/mL)	**Control**	**62%**	**87%**	**100%**
	0.01	2.2 ± 1.8	0.9 ± 1.0	0.0	0.0
	0.03	3.6 ± 1.7	1.0 ± 1.3	1.3 ± 2.3	0.0
	0.10	4.1 ± 1.2	3.8 ± 1.7	2.4 ± 2.6	0.0
	0.30	–	–	–	0.0
	1.00	–	–	–	0.0

[1] rhBMP-2 active substance was oxidized with peracetic acid, then desalted by RP-HPLC. Protein was dried by vacuum centrifugation and reconstituted in formulation buffer. The control was incubated without peracetic acid, and was desalted and reconstituted in formulation buffer.

[2] Standard deviation reflects bioassay variability, does not include protein concentration assay variability.

[3] The % oxidation was determined from the peptide map, and is expressed as overall oxidation of the D335-L374 and D387-R396 peptides.

[4] Bone Score, on a scale of 0-5.

The activity in the W-20 bioassay decreased as the level of oxidation increased. This was also the case in the Use Test; the protein with intermediate levels of oxidation (62% and 87%) had lower activities than the control, but this difference is most striking at the lowest dose, 0.01 mg/mL.

Taken together, the structural information and activity data suggest that a single receptor binding domain on rhBMP-2 is responsible for both in vitro and in vivo activity and that the W-20 bioassay is a relevant predictor of bone-forming activity of rhBMP-2. The W-20 assay is used as an rhBMP-2 release assay. The Use Test remains in place as a characterization test, but is not used for product release.

Impact of the Collagen Matrix on rhBMP-2 Biological Activity- In addition to the determination of effect of the ACS matrix on rhBMP-2 structure (see above), the impact of contact with the ACS on the intrinsic bioactivity of rhBMP-2 was also investigated. rhBMP-2 is the active ingredient in the rhBMP-2/ACS. Although the rhBMP-2/ACS combination is active and induces bone growth, it was not known if the ACS partially inactivates the rhBMP-2.

rhBMP-2 was soak-loaded onto ACS, incubated and extracted as described above (*Impact of the Collagen Matrix on rhBMP-2 Structure*). The extracted rhBMP-2 was tested for bioactivity in the W-20 assay. There was no significant effect of the ACS on activity (Table 8).

Table 8—*In Vitro Bioactivity of rhBMP-2 After Extraction from rhBMP-2/ACS.*

	Specific Activity	
Sample[1]	**U_{WHO}/mg x 10^{-5}**	**% of Positive Control**
Positive Control	4.5	100
Extract 1	3.9	88
Extract 2	3.1	68
Extract 3	4.0	89
Extract Average (RSD)	3.7 (14.5%)	81 (14.5%)

[1]Each extract # corresponds to a different lot of ACS.

Purity Analysis

Impurities encountered during purification of recombinant protein pharmaceuticals may include adventitious viruses and bacteria, host cell-derived proteins and DNA, process-derived contaminants such as cell culture additives (e.g. methotrexate and insulin) and product-related impurities, such as incompletely processed product species. The rhBMP-2 process was designed to remove all of these potential impurities. In most cases, the ability of the purification process to remove these impurities routinely allowed for "validation of removal" studies to substitute for batch-to-batch release assays on the protein. However, general tests for protein purity were implemented in development and remain in place as commercial release assays to ensure that potential process failures that might result in unacceptable levels of impurities in the protein batches are detected. These tests include RP-HPLC, sodium dodecyl sulfate polyacrylamide gel electrophoresis (SDS-PAGE) and size exclusion HPLC (SE-HPLC).

The RP-HPLC assay can resolve propeptide, the 80 kDa and 110 kDa pro species and dissociable dimer from the main covalent dimer product species (see Fig. 1). This assay can also detect host cell protein. SDS-PAGE is a general test for protein impurities. Two types of SDS-PAGE are performed as release assays: SDS-PAGE with Coomassie Blue stain and SDS-PAGE with silver stain. The latter test is run with a bovine serum albumin control loaded at 1% of the weight of the product to serve as a semi-quantitative measure of potential protein impurities. SE-HPLC can detect and quantitate high molecular weight rhBMP-2 species that can result from self-association of the protein.

Comparability Studies

The overall goal of comparability studies is to demonstrate biochemically and non-clinically the similarity between product produced with a current production process and that produced with a newly developed production process. If successful, a comparability program may allow clinical or commercial use of product produced with the new process without clinical trials.

The rhBMP-2 production process underwent improvements during clinical development. The goal of the initial comparability program for rhBMP-2 drug substance was to demonstrate comparability between material employed in early clinical trials (produced with an earlier process) and material that would supply commercial launch (produced with an improved process). Subsequent comparability programs will focus on a comparison of initial commercial drug substance and that produced with a larger scale, more economic process.

The comparability program to support active substance process improvements was comprehensive in scope and included extensive studies of the manufacturing process and the rhBMP-2 protein. The process assessment included comparison of impurity removal capacity of the processes and comparison of results of in-process testing, such as degree of cell lysis and product yield at each step. Protein testing included a comparison of release assay results from testing of the rhBMP-2 produced with the clinical and commercial processes. Due to material limitations, three batches from each process were compared side-by-side. Future comparability programs will compare the dataset generated during testing of multiple commercial batches with data from testing of multiple batches produced with a scaled up process.

Additional characterization was also performed in a side-by-side manner on three batches produced by each process. This characterization included more involved studies that are not routinely performed for product release, such as LC-MS of the peptide map, intact molecular mass analysis and near UV CD, forced degradation and non-clinical testing.

All results indicated that the drug substance produced with the commercial process was comparable to that produced with the clinical process. All masses detected during mass analyses of the peptides or the intact protein were expected. The higher order structure of the proteins was also comparable as determined by near UV CD. A side-by-side forced degradation study was carried out. rhBMP-2 is a stable protein in its recommended storage conditions (-80 °C for bulk protein and room temperature for protein in single use vials). To compare the degradation pathways of rhBMP-2 produced by both processes, drug substance samples were stressed at 37-40 °C for one week. These conditions resulted in expected chemical changes to the protein. The primary degradation pathways observed for rhBMP-2 in liquid at 37-40 °C were isoAsp formation at two Asp residues and increased cyclization of the NH_2-terminal Gln. A low level of HMW species also formed. Despite these structural changes, no loss of bioactivity was detected, and the results indicated that the protein produced by the commercial and clinical processes were comparable.

Non-clinical functional comparability studies included a comparison of the clinical and commercial rhBMP-2 in the Use Test and in an implant pharmacokinetic model in rats. As in the other characterization studies, three batches from each process were compared in a side-by-side manner in both studies. The bone-forming results and

pharmacokinetic parameters were not sigificantly different and the two drug substances were judged to be comparable.

Regulatory Pathway

After negotiations with FDA and the EMEA following the marketing applications, rhBMP-2/ACS was approved in the European Union (EU) and in the United States for orthopedic trauma and spinal fusion, respectively. Table 9 shows the different regulatory pathways for the product.

Table 9—*Regulatory Pathway for rhBMP-2/ACS.*

Topic	US	EU
Product classification	Combination product = device	Integral product = Medicinal product
Reviewers	CDRH lead reviewer CBER consult	Rapporteur- Dutch Co-rapporteur- Finns
Review of ACS component	Licensed medical device, cross reference of manufacturing and quality sections sufficient	ACS a CE-marked, licensed medical device, but in rhBMP-2/ACS, the ACS considered an excipient. CPMP questions relavant to excipient quality
Product indication	Spinal fusion (Wyeth/Medtronic Sofomar Danek)	Orthopedic trauma (Wyeth)
Product name	Infuse	InductOs
Comparability of clinical vs. commercial production process	Focus on vialed protein lyophilization equivalency from site-to-site, no other issues	No issues

Lessons learned

There were multiple lessons learned during the development and approval process for rhBMP-2/ACS. For drug substance development, these include:

- Although an improved manufacturing process may consistently eliminate or significantly reduce undesirable species in the protein that were present in clinical trial material, the release assays should be configured to detect these species. This provides added assurance that an aberrant manufacturing run would be identified during testing of the product.

- An adequate supply of protein produced by earlier processes should be reserved for comparability studies. This would allow side-by-side comparison of old and new drug substance with contemporary release assays and characterization methods. Particularly important are protein batches that were employed in preclinical toxicology and early clinical trials.

- Protein degradation products, such as oxidized and deamidated protein, should be generated and tested in all assays during early assay development. This would avoid reconfiguraton of the assay to resolve these species later in development.

- Determination of the solubility profile of the protein with respect to ionic strength and pH will allow a better understanding of the protein/formulation and protein/matrix relationship.

- Major protein isoforms should be isolated and characterized both in vitro and in vivo early in purification process development. Information from these activities will allow adjustment of the purification process to yield appropriate product species.

- Correlation of the output of an in vitro bioassay to that of a relevant in vivo assay may allow the exclusive use of the in vitro bioassay for lot release. This will simplify product release testing.

Acknowledgments

The authors would like to acknowledge the contributions of Susan Abbatiello, Mary Lou Bell, John Champagne, Nancy Folk, Daniel Haq, Lisa Housianitis, Steve Koza, Yin Luo, Tatjana Matejic, Kristine McCarthy, Randy Morin, Russell Palmer, Bernardo Perez-Ramirez, Rod Riedel, Rachael Sorensen, John Steckert, Tom Last, John Wozney and Marcia Young.

References

[1] Urist M.R., "Bone Formation by Autoinduction," *Science,* Vol. 150, 1965, pp. 893–899.

[2] Wozney J.M., Rosen V., Celeste A.J., Mitsock L.M., Whitters M.J., Kriz R.W., Hewick R.M., Wang E.A., "Novel Regulators of Bone Formation: Molecular Clones and Activities," *Science*, Vol. 242, 1988, pp. 1528–1534.

[3] Israel D.I., Nove J., Kerns K.M., Moutsatsos I.K., Kaufman R.J., "Expression and Characterization of Bone Morphogenetic Protein-2 in Chinese Hamster Ovary Cells," *Growth Factors*; Vol. 7, 1992, pp. 139-150.

[4] Fukawa H., "Changes of Glutamine-Peptides on Heating in Aqueous Media," *Journal of the Chemical Society of Japan*, Vol. 88, 1967, pp. 459–463.

[5] Kleeman T.J., Ahn U.M., Talbot-Kleeman A., "Laparoscopic Anterior Lumbar Interbody Fusion with rhBMP-2: A Prospective Study of Clinical And Radiographic Outcomes," *Spine*, Vol. 26, 2001, pp. 2751-2756.

[6] Riedel G.E., Valentin-Opran A., "Clinical Evaluation of rhBMP-2/ACS in Orthopedic Trauma: a Progress Report," *Orthopedics*, Vol. 22, 1999, pp. 663-665.

[7] Wang E.A., Rosen V., D'Alessandro J.S., Bauday, M., Cordes, P., Harada, T., Israel, D.I., Hewick, R.M., Kerns, K.M., LaPan, P., Luxenburg, D.P., McQuaid, D., Moutsatsos, I.K., Nove, J., and Wozney, J.M., "Recombinant Human Bone Morphogenetic Protein Induces Bone Formation," *Proceedings of the National Academy of Science USA*, Vol. 87, 1990, pp. 2220–2224.

[8] Seeherman H., Wozney J., Li R., "Bone Morphogenetic Protein Delivery Systems," *Spine*, Vol. 27 (16 Suppl 1), 2002, pp. S16-S23.

[9] Uludag H., Gao, T., Porter, T.J., Friess, W., Wozney, J.M.., "Delivery Systems for BMPs: Factors Contributing to Protein Retention at an Application Site," *Journal of Bone and Joint Surgery,* Vol. 83-A, Part 2, Supplement 1, 2001, pp. S128-S135.

[10] Gao T.J., Kousinioris N.A., Wozney J.M., Winn S., Uludag H., "Synthetic Thermoreversible Polymers are Compatible with Osteoinductive Activity of Recombinant Human Bone Morphogenetic Protein 2," *Tissue Engineering.*, Vol. 8, 2002, pp. 429-440.

[11] Helm G., Anderson D.G., Andersson G.B., Boden S.D., Damien C., Ebara S., Lane J.M., McKay B., Sandhu H.S., Seeherman H., Wozney J., "Summary Statement: Bone Morphogenetic Proteins: Basic Science," *Spine* Vol. 27 (16 Suppl 1), 2002, p. S9.

[12] Uludag, H., D'Augusta, D., Golden, J., Li, J., Timony, G., Riedel, R., Wozney, J., "Implantation of Recombinant Human Bone Morphogenetic Proteins with Biomaterial Carriers: a Correlation Between Protein Pharmacokinetics and Osteoinduction in The Rat Ectopic Model," *Journal of Biomedical Materials Research*, Vol. 50, 2000, pp. 227–238.

[13] Thies R.S., Bauduy M., Ashton B., Kurtzberg L., Wozney J.M., Rosen V.,

"Recombinant Human Bone Morphogenetic Protein-2 Induces Osteoblastic Differentiation in W-20-17 Stromal Cells," *Endocrinology*, Vol. 180, 1992, pp. 1318–1324.

[14] Urist, M.R. in "Bone Morphogenetic Proteins: Biology, Biochemistry and Reconstructive Surgery," ed. Lindholm, T.S., R.G. Landes Co. and Academic Press, Inc., 1996, pp. 7-27.

[15] Kress B.C., "Bone Alkaline Phosphatase: Methods of Quantitation and Clinical Utility," *Journal of Clinical Ligand Assay,* Vol. 21, 1998, pp. 139–148.

[16] Porter, T.J., "Chemical Oxidation of Recombinant Human Factor IX and Recombinant Human Bone Morphogenetic Protein-2: Characterization of the Oxidized Proteins," IBC conference on The Impact of Post-Translational Modifications on Protein Therapeutics, May 8-10, 2002, San Diego CA

[17] Kirsch T., Sebald W., Dreyer M.K., "Crystal Structure Of The BMP-2 BRIA Ectodomain Complex," *Nature Structural Biology*, Vol. 7, 2000, pp. 492–496.

David S. Kaplan[1]

Development of Standards for the Characterization of Natural Materials Used in Tissue Engineered Medical Products (TEMPs)

Reference: Kaplan, D. S., **"Development of Standards for the Characterization of Natural Materials Used in Tissue Engineered Medical Products (TEMPs),"** *Tissue Engineered Medical Products (TEMPs), ASTM STP STP 1452*, E. Schutte, G. L. Picciolo, and D. S. Kaplan , Eds., ASTM International, West Conshohocken, PA, 2004.

Abstract: ASTM Committee on F4 Medical and Surgical Materials and Devices, Division IV, Tissue Engineered Medical Products (TEMPs), Biomaterials and Biomolecules for TEMPs Subcommittee (F4.42) has been developing standards for characterizing natural materials used in TEMPs. Natural materials include alginate, chitosan, collagen and hyaluronate. These materials support cell growth and differentiation on TEMPs substrates and scaffolds. Natural materials have been used in a variety of applications, including encapsulation, cell seeding, development of "memory" biomaterials, as well as degradable scaffolds, growth factor/nucleic acid delivery vehicles, and as a carrier to improve product handling characteristics. These materials have typically been very poorly characterized as to their chemical, physical and biological properties. This has resulted in variability in the products produced from these starting materials. The development of Standard Guides and Test Methods for characterizing natural materials is anticipated to reduce the variability of these starting materials and to aid in the assessment of the safety of the subsequent TEMPs.

Three Standard Guides for characterizing the natural materials that are used as starting materials in the production of TEMPs have been developed and approved as ASTM standard guides. The first guide deals with Alginate, while the second guide deals with Chitosan and Chitosan salts. A third guide was recently approved for the characterization of Type I collagen used for surgical implants and substrates for TEMPs. Standard test methods are under development for the use of ^{1}H-NMR to determine the molecular weight of alginate and the degree of deacetylation of chitosan.

Planned future documents will include guides to characterize additional types of collagen and hyaluronate, as well as the development of additional standard test methods for characterizing the natural materials.

[1] Natural biological materials characterization and test method development, FDA, Center for Devices and Radiological Health, Office of Science and Technology, 12725 Twinbrook Parkway, Rockville, MD 20852.

Keywords: natural materials, characterization, standards, TEMPs, biomaterials

Introduction

The biomedical and pharmaceutical industries are continually testing materials that may serve as scaffold materials for tissue engineered medical products (TEMPs). One such class of materials that is showing great promise is natural materials, which include materials such as alginate, chitosan, collagen and hyaluronate. The natural materials have shown potential for use as scaffolds (chondrogenesis using ionically crosslinked chondroitin sulfate A and chitosan; various tissues including bone, liver, neural, skin and vascular [1, 2, 3]; cultured skin substitutes [4]), cell seeding (chondrocytes, cardiac myocytes, [1]), drug delivery [3] and as an encapsulating matrix for immobilization of living cells (e.g., immunoisolation of pancreatic islets by semipermeable and biocompatible membrane, "bioartificial pancreas" [4]).

These materials appear to have excellent biocompatibility and immunogenicity properties when properly purified and may be amenable to cellular remodeling during the process of tissue formation. The degradation products of these materials are natural compounds that can be harmlessly excreted by the body. Naturally-derived materials must be isolated from human, animal or plant tissue. This typically results in a high cost and large batch-to-batch variations [2].

Poor characterization of these materials has often resulted in variability in the products produced from these starting materials. To ensure the functionality of these biopolymers in an application, they must be fully characterized as to their physical, chemical and biological properties. There is a need for standard guides and test methods to characterize these materials to reduce the variability of these starting materials and to aid in the assessment of the safety of the subsequent TEMPs. This paper describes the current activities for developing standards derived from natural materials for TEMPs. The need for additional standards for natural materials and the types of standards which may be required, will also be addressed.

Natural Material Standards: Approved or under Development

Standard Guides

The TE Biomaterials subcommittee has three published standards, ones for the characterization of alginate, chitosan and Type I collagen. The purpose of the three guides is to identify key parameters relevant for the functionality and characterization of these materials. It is important to note that these standards are guides, and do not require the user to use any of the methods outlined in the document. The documents outline tests of varying sensitivities and specificities and provide the user with references to decide which, if any, of the tests listed is appropriate for the application. The three documents are identified below, along with the salient features of these documents.

ASTM Standard Guide for Characterization and Testing of Alginates as Starting Materials Intended for Use in Biomedical and Tissue-Engineered Medical Product Applications (F2064-00).

ASTM Standard Guide for Characterization and Testing of Chitosan Salts as Starting Materials Intended for Use in Biomedical and Tissue-Engineered Medical Product Applications (F2103-01).

ASTM Standard Guide for Characterization of Type I Collagen as a Starting Material for Surgical Implants and Substrates for Tissue Engineered Medical Products (TEMPs) (F2212-02).

In order to assist the user in determining the applicability of these documents to the user's application, the documents define the significance and use of these materials and specify any forms of the materials which would be excluded from the techniques listed in the Standard Guide. An extensive description of the physical and chemical methods for characterizing the respective starting material is included, along with relevant terminology for characterizing the respective starting materials.

Extensive coverage is also provided with regard to microbiological safety where methods are outlined for sterilization, and the determination of endotoxin levels (bioburden) of the starting material. Currently accepted methods for verifying absence of adventitious agents are also outlined, including: sourcing, viral clearance and Transmissible Spongiform Encephalopathy (TSE).

Safety and Toxicology data, including biocompatibility and immunogenicity, are provided from sources such as International Conference on Harmonization, national and international standards and FDA Guidance Documents and Points to Consider, as well as the Code of Federal Regulations (CFR).

Standard Test Methods

Two standard test methods currently under development will assist the user in characterizing the alginate and chitosan used as the starting materials. These test methods are expected to be balloted at the subcommittee level Fall 2002. The methods are listed below.

ASTM Draft Standard Test Method for Determining the Chemical Composition and Sequence in Alginate by ^{1}H NMR (Z8713Z).

ASTM Draft Standard Test Method for Determining the Degree of Deacetylation in Chitosan Salts by ^{1}H NMR (Z8762Z).

Natural Material Standards: Future

The field of tissue engineering is evolving rapidly. The standards developed must not hinder or restrain the technological developments in the field. It is anticipated that natural materials will play an increasingly important role in the newly developing TEMPs constructs. With these concepts in mind, the following activities are anticipated with regard to natural materials.

A new task group has recently been formed to prepare a standard guide for characterizing hyaluronic acid. The document title is "Standard Guide for

Characterization and Testing of Hyaluronic Acid as Starting Materials Intended for Use in Biomedical and Tissue-Engineered Medical Product Applications (TEMPs)". This guide is expected to follow the format outlined above for the standard guides. In the area of collagen, it is anticipated that additional guides will be prepared for other collagen Types that are relevant to TEMPs.

As the field of tissue engineering matures and various classes of tissue engineered constructs become available, this subcommittee plans to develop standard specifications for the TEMPs constructs. These standards, with the associated sensitivities/specificities and precision values for the tests, will aid users in preparing well-characterized constructs and may provide assistance, depending on the standard, in the assessment of safety for the constructs.

With the availability of gene-splicing technology, additional standards for natural materials prepared wholly, or in part, from gene-manipulated raw natural materials may be required. Additional test methods may be required to ensure the biochemical, physiological, toxicological, immunological and immunogenic properties of these materials. Working with the Microbiological Safety/Adventitious agents subcommittee, methods need to be specified to ensure that the materials are free from adventitious agents.

Our goal in deciding which standards are appropriate for a given application is to ask the question: What information does the user need to know how to determine the safety of the TEMPs construct? The basic information required is the physical, biochemical, immunological, immunogenetic, toxicological and microbiological safety data to characterize the material. Although the technology may change, this core information will always be required. There may be more information required, at least initially, until the process or technique is verified and accepted. Future standards development will rely on these guiding principles and will be an evolving process, just as the scientific field of tissue engineering is ever evolving.

References

[1] Atala, A. and Lanza, R. P., Eds., in: *Methods of Tissue Engineering*, Academic Press, New York, 2002.

[2] Lanza, R. P., Langer, R. and Chick, W. L., Eds., in: *Principles of Tissue Engineering*, Academic Press, San Diego, 1997.

[3] Patrick, C., W., Mikos, A., G. and McIntire, L. V., Eds,. in: *Frontiers in Tissue Engineering*, Pergamon Press, New York, 1998.

[4] Morgan, J. R. and Yarmush, M. L., Eds., in: *Methods in Molecular Medicine: Tissue Engineering Methods and Protocols*, Humana Press, New Jersey, 1999.

Gail Sofer[1]

Microbiological Safety and Adventitious Agents Standards for TEMPS

Reference: Sofer, G., **"Microbiological Safety and Adventitious Agents Standards for TEMPS,"** *Tissue Engineered Medical Products (TEMPs), ASTM STP 1452,* E. Schutte, G. L. Picciolo, and D. S. Kaplan, Eds., ASTM International, West Conshohocken, PA, 2004.

Abstract: Microbiological contamination and adventitious virus contamination can be introduced into TEMPs from source materials, such as cells, cell culture media, scaffolds, and growth factors. Contamination can occur during isolation and expansion of cells, production of scaffolds and growth factors, and product manufacturing. Contamination may also arise during storage due to the inability to use sufficiently stringent preservation and storage methods without destroying the TEMPs' function.

Standard safety testing for pathogens may not be suitable for TEMPs. New rapid microbiological detection methods and PCR assays for mycoplasma and virus may enable preliminary product release. Cleaning and sanitization of equipment can be validated using a combination of traditional and new, more rapid methods. When there are significant processing steps, clearance studies can provide a further assurance of freedom from unwanted adventitious agents.

Keywords: adventitious agents, biological safety, TEMPs, virus, microorganisms, testing methods, assays

Introduction

The successful use of TEMPs depends on providing patients with safe and efficacious products. The safety of TEMPs is ensured, in part, by delivering products that are free from adventitious agents. Freedom from adventitious agents can be achieved by assessing the risks and their sources, controlling the manufacturing process, and employing sufficiently sensitive, validated testing methods. The complexity and biological properties of TEMPs, however, make this a unique challenge.

The Risks

Adventitious agents that may cause adverse patient reactions include bacteria, fungi, viruses, transmissible spongiform encephalopathies (TSEs), mycoplasma, and parasitic organisms. There may also be as yet unidentified biological agents that pose unknown risks. Adventitious agents may be associated with scaffolds, growth factors, cell

[1] Director Regulatory Services, BioReliance, 14920 Broschart Road, Rockville, MD 20850.

culture media, cells, tissues, or other components of the TEMPs. Donor screening is essential for controlling the risks. Contamination with adventitious agents can occur during isolation and expansion of cells, production of scaffolds and growth factors, and final product manufacturing. Adventitious agents may be introduced during processing—from the environment, operators, processing materials, and even equipment that has not been properly decontaminated.

Process Control

Control of the manufacturing process is essential for ensuring freedom from adventitious agents. Reagent and water quality and compliance with current good manufacturing practices (cGMPs) are critical elements. All materials should be made according to GMPs, with the assurance that the water quality and the reagents are suitable for production of human therapeutics. However, this is often problematic when dealing with novel technologies for which materials suitably screened for the absence of adventitious agents are unavailable. Testing of these research grade materials for adventitious agents is essential to ensure patient safety. Operator training in GMPs and the assurance that the environment is suitable for the degree of closure of the processing equipment are two additional steps that prevent introduction of adventitious agents into intermediate and final products. The use of newer technologies such as isolators may be beneficial to provide further environmental control. The sensitivity of in-process and final product analytical methods should be sufficient to provide confidence that any risks from adventitious agents are controlled.

Some of the components of TEMPs need rapid processing to preserve viability. This need plus the complex biological nature of these components makes process validation even more critical than for well characterized products. Process validation can enhance confidence in the capability of the process to produce final products free of adventitious agents. Cleaning and decontamination/sanitization validation is essential.

Validation of Decontamination/Sanitization/Cleaning

Regardless of whether the facility is dedicated to one product or used for multiple products, it is essential to ensure that no adventitious agents remain on processing equipment. Manufacturers of chemicals and devices that inactivate bacteria, viruses, and other potentially harmful agents often have extensive databases on the effectiveness of their products. It is, however, essential to evaluate the capability of the chosen method under conditions of use. The ability of the operators to prepare solutions consistently and apply them and to operate equipment is part of the validation effort, which leads to a high degree of confidence in the safety of products that will subsequently be processed in the same environment.

Assay methods and sampling techniques may not be sufficiently sensitive to achieve the desired level of confidence in adventitious agent inactivation. An additional approach is to perform validation using cut-out pieces of equipment. (These are called coupons, and they can often be obtained from the manufacturer of the equipment.) Using proper safety controls and trained personnel, the coupons can be spiked with adventitious agents in the presence and/or absence of product. It can be shown that under the extremes of

operating conditions (i.e., worst case), the selected method is sufficiently robust to provide the necessary level of inactivation.

When performing spiking studies, proper controls must be implemented. In addition to positive and negative controls, recovery from the coupon is also assayed to prevent an overestimation of the degree of inactivation that can be achieved by a given method. With spiking studies such as those described here, we have been able to determine the effectiveness of commercially available sanitizing agents, either alone or in combination with isopropanol, for inactivating viruses and bacteria. In one study, it was found that of the three agents evaluated, only one was sufficiently effective to inactivate adenovirus without the addition of isopropanol.[2]

Testing

Table 1—*Testing of TEMPs Summarized from FDA Approval Letters.*

Test	Product A	Product B	Product C
48-h sterility	FP		
14-day sterility	FP	FP	FP
Bacteria, fungi, yeast	CB, RM		CB, RM
Mycoplasma	FP, CB, RM	FP, RM	FP, CB, RM
Endotoxin		FP, RM	
In vitro virus	CB		
In vivo virus	CB		
EM (electron microscopy)	CB		
RT (reverse transcriptase)	CB		
Retroviruses	RM	CB, RM	
HIV-1 &-2	CB	CB	CB
HTLV-1 and -2	CB	CB	CB
HBV	CB	CB	CB
HCV	CB	CB	
CMV	CB		
EBV	CB	CB	CB
HHV-6	CB		CB
Syphilis (Treponema)		CB	
Virus screen, general	RM	RM	RM

FP: final product, CB: cell bank, RM: raw materials

Testing programs are designed commensurate with potential risks from adventitious agents. The programs are often quite complex and multi-tiered. Selection, implementation, and validation of testing methods are unique challenges for TEMPs, given the nature of the biological components that may require rapid release to ensure viability and functionality. Depending on the manufacturing scheme, clearance studies may add further confidence in the safety of TEMPs.

[2] Dr. Jeri Ann Boose, BioReliance, Personal Communication, 2002.

Testing Programs

Table 1 illustrates testing that has been described in U.S. Food and Drug Administration (FDA)approval letters for three different TEMPs. Raw material testing is a critical component of the testing program. Depending on the source of the material, assays may include those for sterility, mycoplasma, endotoxin, and both endogenous and adventitious viruses. For TEMPS that incorporate cells that are banked (i.e., master and working cell banks) or products made by those cells, cell bank testing is an important component in ensuring freedom from adventitious agents. For cell banks, testing of both master cell bank (MCB) and working cell bank (WCB) is necessary. ICH (International Conference on Harmonization) guidelines, although not directly applied to TEMPs, provide further relevant information for establishing cell bank testing programs [1,2]. The source, history (e.g., potential previous exposure to adventitious agents), purity, identity, and stability of the cells dictate what type of testing methods are applied. Final product testing is often restricted due to product viability and resulting short shelflives.

Testing Methods

Standard safety testing methods often take too long for viable intermediate and final product release. Administration of product and then later treating patients after release of the testing results is clearly not ideal. New technologies are enabling rapid testing that allows for significant levels of confidence in the safety of TEMPs. Some examples comparing traditional methods with newer technologies that might be applicable to TEMPs are presented below.

Sterility Tests

The USP (U.S. Pharmacopoeia) sterility tests were not designed for TEMPs. As described in the USP-NF <1046> 1st supplement, automated sterility testing methods that rely on colorimetric detection or continuous monitoring may be accepted if they are validated. A PDA (Parenteral Drug Association) Technical Report describes approaches for evaluation, validation, and implementation of new microbiological testing methods. [3] This approach has been applied for at least one such method, called Scan RDI. This technology detects viable microbial cells, and does not require an extended incubation period. It has been applied to both process water and detection of microbial contaminants in animal cell culture processes. [4,5]

Mycoplasma

PCR has been applied to myoplasma testing. An ATCC (American Type Culture Collection) newsletter compared PCR to the traditional Hoechst staining and direct culture methods (both broth and agar). [6] As discussed in the article, there are four species of mycoplasma that constitute 85% of the mycoplasmas that infect cells in culture. The PCR(polymerase chain reaction) methods are capable of picking up these species, and it would appear that applying this method to TEMPs can enhance patient safety.

Virus

PCR has been used for detection and quantitation of retroviral particles in licensed biotechnological products. PCR assays for human viruses such as HIV, HTLV, SV-40, BK/JC, hepatitis, and herpes viruses are available, and are generally performed by contract testing laboratories. The precision of these assays is high compared to infectivity assays. Equally, if perhaps not more, important is the rapid turnaround time for obtaining data that can provide a level of confidence in the safety of TEMPs. A comparison of the precision of an infectivity assay with a quantitative PCR assay is shown in Table 2.

Assay Validation

Each assay used to ensure freedom from adventitious biological agents must be validated. These assays need to be tested with the individual test article to ensure there is no inhibition that would lead to false negative results. Further information on assay validation is available in the relevant ICH documents. [7,8]

Table 2—*Comparison of Precision of MuLV Infectivity and QRT-PCR Assays.*

	$TCID_{50}$	QRT-PCR
Average	5.34×10^7 (16 results)	3.78×10^9 (15 results)
Standard deviation	4.54×10^7	2.97×10^8
% CV	84.9	7.86

Clearance Studies

The processing steps used to prepare components and final product TEMPs may remove and/or inactivate adventitious agents. Duplicating a process step at a smaller scale may be necessary. Once the scale-down is validated, various adventitious agents are spiked into the process and their clearance determined. As with the decontamination and cleaning studies, there are many controls that must be performed to ensure confidence in the data. The spike is titered before addition to a sample, after addition to a sample, and after the process step. Spiking has been performed for mycoplasma, viruses, and TSEs. Combining PCR and infectivity assays can show both inactivation and removal. For TSEs, the Western blot enables relatively rapid screening to determine where clearance might occur in the process.

ASTM F4.45 Status

Since it is evident that the development of standards for both the screening and removal of adventitious agents will be an ongoing process, the ASTM Biological Safety for TEMPs Subcommittee F04.45 has already been established, along with an internet-based discussion group to facilitate ongoing discussion of this subject. The web based discussion group entitled "astmsafetytemps" can be located directly at http://groups.yahoo.com/group/astmsafetytemps, with participation by new members both welcomed and encouraged. Relevant existing, worldwide documents have been posted and can be downloaded by all members. The group is preparing a guide that will address the risks, their sources, testing strategies, and testing methods. References to existing documents will be included in the guide as we work to harmonize our efforts with those of other organizations addressing the safety of TEMPs by ensuring freedom from adventitious agents.

References

[1] ICH Harmonized Tripartite Guideline, "Derivation and Characterisation of Cell Substrates Used for Production of Biotechnological/Biological Products," http://www.ich.org/, 1997.

[2] ICH Harmonized Tripartite Guideline, "Viral Safety Evaluation of Biotechnology Products Derived from Cell Lines of Human or Animal Origin," http://www.ich.org/, 1997.

[3] PDA Technical Report No. 33, "Evaluation, Validation, and Implementation of New Microbiological Testing Methods," *PDA Journal of Pharmaceutical Science and Technology*, Vol.54, No.3, 2002, Supplement.

[4] Costanzo, S. P.,Borazjani, R. N., and McCormick, P. J., "Validation of the Scan RDI for Routine Microbiological Analysis of Process Water," *PDA Journal of Pharmaceutical Science and Technology*, Vol. 56, No. 4, 2002, pp 206-219.

[5] Onadipe, A. and Ulvedal, K., "A Method for the Rapid Detection of Microbial Contaminants in Animal Cell Culture Processes," *PDA Journal of Pharmaceutical Science and Technology*, Vol. 55, No. 6, 2002, pp 337-345.

[6] Ikonomi, P. and Polayes, D., "Detecting Mycoplasma in Cell Cultures using the ATCC Mycoplasma Detection Kit" *ATCC Connection*, Vol. 22, No. 1, 2002, pp1-6.

[7] ICH Harmonized Tripartite Guideline, "Text on Validation of Analytical Procedures" http://www.ich.org/, 1994.

[8] ICH Harmonized Tripartite Guideline, "Validation of Analytical Procedures: Methodology," http://www.ich.org/, 1996.

Lance Stover[1] and Allison Hubel[1]

Standards Used in Meeting Requirements for a Model Pre-Market Approval (PMA) of a Neural Guidance Conduit

Reference: Stover, L. and Hubel, A., "**Standards Used in Meeting Requirements for a Model Pre-Market Approval (PMA) of a Neural Guidance Conduit,**" *Tissue Engineered Medical Products (TEMPs), ASTM STP 1452*, E. Schutte, G. L. Picciolo, and D. S. Kaplan, Eds., ASTM International, West Conshohocken, PA, 2004.

Abstract: A hypothetical neural guidance conduit, 'InnervTube,' employing autologous denatured muscle is presented in the form of a PMA as an example of how existing standards for tissue engineered medical products are used in product testing and evaluation. The performance requirements that determine the specific device characteristics are defined, along with a proposed method of manufacture, use, and control. Alternatives, contraindications, and preliminary in-situ and in-vitro results garnered from the literature are presented.

Keywords: neural guidance conduit, pre-market approval, standards testing

Introduction

As an exercise in demonstrating the extensive use of standards in the conception, development, and production of a tissue engineered medical product (TEMP), a hypothetical neural guidance conduit (NGC) called 'InnervTube' has been contrived. Its proposed design, method of use, and means of production are presented below as though it were to be submitted to the FDA in Pre-Market Approval (PMA) form.

Indications for Use

InnervTube is indicated for repair of peripheral nerve discontinuities in which the gap to be spanned is less than 10 mm. Since effective repair is impeded by fibrosis, gross infection, constriction, and tension in the nerve [1], the use of InnervTube is indicated only in the absence of these conditions at the site. InnervTube is designed to accommodate nerves having a diameter between 0.7 mm and 3.2 mm. Although there is little hope for peripheral nerve repair beyond two years following injury, there is no

[1] Student and Assistant Professor, respectively, Department of Laboratory Medicine and Pathology, University of Minnesota, Minneapolis, MN, 55455.

definitive time scale beyond which nerve repair cannot be attempted [2]. Obviously, however, the conditions preferred for optimal outcome include minimal local inflammation, minimal fibrotic incursion, and relatively cleanly severed nerve stumps, all of which suggest time intervals between injury and repair that is measured on the scale of hours rather than days.

Device Description

General Description

InnervTube is a porous, biodegradable poly(L-lactic acid) (PLLA) nerve guidance conduit containing denatured muscle tissue for nerve regeneration. It is a single use, temporary, absorbable implant. It is a mechanically flexible tube resistant to radially compressive forces from adjacent tissues, yet having tensile strength sufficient to hold microsutures.

Dimensions

Because the optimal internal diameter of a Neural Guidance Conduit (NGC) should be two and a half to three times that of the nerve to be repaired [3], InnervTube is available in internal diameters of 2, 5, and 8 mm. It is 12 mm long. The wall thickness of the tube is at least 0.5 mm, giving overall outer diameters of at least 3, 6, and 9 mm, respectively. The tube is packaged within an inner pouch to provide a sterile barrier against moisture and gas. The inner pouch is, in turn, sealed inside an outer pouch that protects the inner pouch sterility and the product against physical damage. Similarly, the denaturing solutions are packaged in a multi-chambered bag designed to protect against degradation, maintain sterility, provide a means of inspection, and facilitate the proper processing sequence.

Design

The theory of operation is outlined by Hudson in his general description of the nerve guidance channel: "Guidance channels help direct axons sprouting from the regenerating [proximal] end, provide a conduit for diffusion of neurotropic and neurotrophic factors secreted by the damaged nerve stumps, and minimize infiltration of fibrous tissue" [4]. Hudson goes on to state that there are principally three properties that the guides should possess, namely 1) they can be readily formed into conduits of the desired diameter; 2) they should require little effort to implant; and 3) they must be sterilizable. Unlike other NGCs, however, the InnervTube aims to enhance the natural regeneration process by taking advantage of its unique construction: the InnervTube has an increased porosity that is intended to increase vascularization, thereby accelerating healing; and, upon final on-site assembly, it will contain autologous, denatured muscle in the guide channel. This design aspect is intended to overcome the typical disadvantage of competing guides that employ a polymeric tube alone, namely that of providing cell matrix interaction. Among these interactions are those primary to the extracellular matrix

(ECM): tissue strength, the ability to bind water and growth factors, and provision of ligands for cell attachment [5]. Additionally, the insertion of denatured muscle tissue will provide for an increased margin of safety against premature conduit collapse during in-vitro and in-vivo degradation, previously identified as a failure mode for other types of NGCs [6,7]. PLLA is the polymer of choice for several reasons: 1) PLLA conduits are ten times stronger and stiffer than 75:25 poly (lactic-glycolic) acid (PLGA) conduits of similar pore morphology over an eight-week in vitro degradation period [8]. This was deemed necessary because for improved vascularization, a highly porous tube is desired, thereby necessitating a stronger material. 2) Semi-crystalline PLLA is preferred where mechanical strength, pliability, and toughness are required, especially for sutures [9,10]. 3) Conduits having the desired properties can be readily formed using a defined manufacturing process [8,11]. 4) PLLA has a relatively high glass transition temperature (Tg) that provides margin against creep at body temperatures [9]. 5) PLLA degrades through a hydrolytic process and is ultimately eliminated from the body via respiration [12]. 6) The relatively slow degradation rate of PLLA compared to other polymers and copolymers is acceptable because the volume of material (considering both device:body and material:device ratios) introduced was small. 7) There is an existing protocol [ASTM Specification for Virgin Poly (L-Lactic Acid) Resin for Surgical Implants, F1925-99] for specifying the virgin PLLA resin; this is beneficial in the control of material entering the manufacturing process. 8) There is an existing standard [ASTM In Vitro Degradation Testing of Poly (L-Lactid Acid] Resin and Fabricated Form for Surgical Implants (F1635-95)) for in-vitro testing of PLLA degradation that will also be beneficial in manufacturing control.

Method of Manufacture

As shown diagrammatically below (Figure 1), the process for forming the porous InnervTube is as follows.

1. The virgin PLLA resin is manufactured into a composite wafer with sodium chloride (NaCl) crystals using a solvent casting technique [11]. Briefly, the polymer is dissolved in methylene chloride (CH_2Cl_2) and the sized salt particles (150 – 300 μm) are added to achieve a saltweight fraction of 90%. The resulting dispersion is cast into a glass container. Because the salt is insoluble in methylene chloride, when the solvent evaporates, the polymer and salt remain bound together in a 'wafer-like' form.
2. Pieces of the wafer are cut and fit into the extrusion tool in which the heating (250 °C at 25 °C•min^{-1}, temperature equilibration (480 s), and the extrusion is performed (~130MPa for 10 mm•s^{-1} rate).
3. The extrusion is cut to the appropriate length using a diamond wheel saw.
4. Following a brief cooling (~1 hour), the tube is immersed in water for 24 hours to leach out the salt.
5. Drying occurs in a vacuum (13.3 Pa) for 24 hours.
6. Sterilization is performed using an RF, oxygen plasma system (240 s at 100 W). This method was selected over the more traditional ethylene oxide (EtO) procedure due to the excessive shrinkage (~50%) and stiffness induced by EtO. Similarly, irradiation was discounted as it has been shown to significantly change the mechanical properties

of PLGA scaffolds, specifically increasing the brittleness [13]. Conversely, low temperature plasmas have been shown to have a negligible effect upon the shear strength, bending strength, modulus, glass transition temperature, and crystallinity while providing effective sterilization. Additionally, a plasma process is short, is pyrogen free, has no effect on material dimensions, has minimal carcinogenic by-products, and suffers no material disposal problems [14].

7. Packaging occurs in a sterile environment and is guided by the ASTM Practice for Packaging of Plastics (D3892).

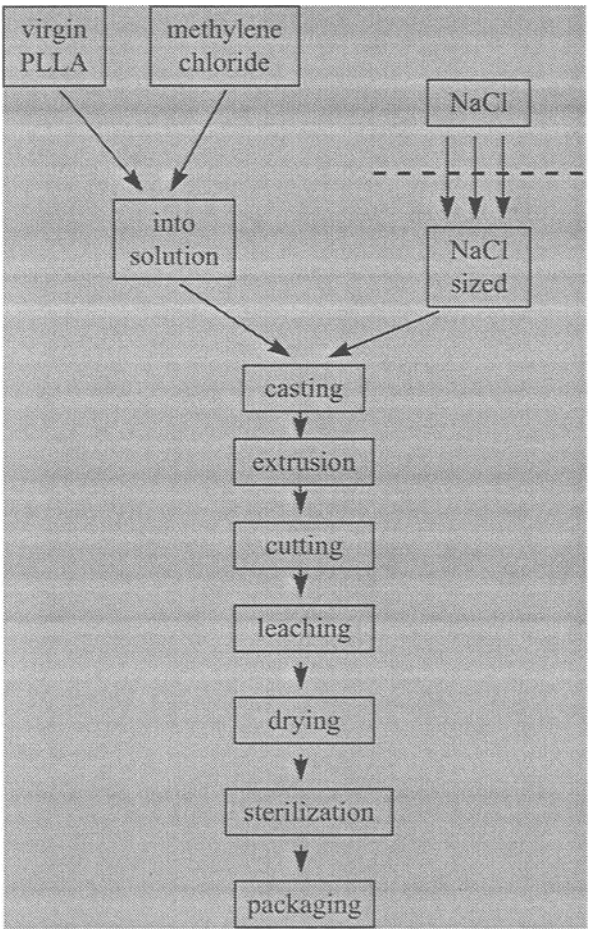

Figure 1 - *Process flow for InnervTube formation.*

Method of Use

Because InnervTube is intended to be used with autologous, modified muscle tissue, preparation for the use of InnervTube consists primarily of site selection and

harvest of a muscle biopsy section followed by 'assembly' of the modified tissue into the tube. As the intent is to enhance the body's regenerative power, it is advantageous to replicate the original structure. Namely, the design takes advantage of the finding that skeletal muscles with fibers arrayed in parallel have an oriented matrix of basement membrane tubes anatomically similar to that of peripheral nerve [15,16]. The functional application of this finding is that the tubular matrix of the modified muscle should be aligned with the direction of the nerve funiculi; this configuration results in more rapid regeneration [17]. Therefore, site selection should be directed towards anatomical locations having conditions of highly parallel muscle fibers, relatively remote from the area to be repaired, free from local infection, and relatively easily accessed for biopsy. Norris has demonstrated success with muscle autografts in humans using tissue taken from the inferior border of the pectoralis major in the anterior axillary fold [18]; this should be a consideration.

As described by Meek [6] and Glasby [17], preparation of the modified, denatured muscle tissue is as follows

1. Pin out the excised muscle tissue on a sterile polymer backing and immerse in liquid nitrogen until thermal equilibrium is attained. Subsequent thawing is accomplished in sterile, deionized, demineralized water.
2. Trim the tissue to form the graft size appropriate for the selected size of InnervTube. The graft should be slightly smaller at its widest point than the inner diameter of the InnervTube. Trim the graft to a length such that the graft is approximately 1.5 mm shorter than the nerve gap to be repaired.
3. Transfer the 16% acetic acid (CH_3COOH) solution from its package into a sterile petri dish and immerse the graft in the sterile solution at room temperature for 1 hour.
4. Remove the graft from solution, putting it into another sterile petri dish and placing it under vacuum at 1 kPa for 1 hour.
5. Transfer the in 0.1 M phosphate buffered saline (PBS) from its package into another sterile petri dish. Remove the graft from vacuum and place it in the PBS solution for 1 hour.
6. Inspect one end of the graft using light microscopy at 1500 to 2000X magnification. The extracellular matrix (ECM) should appear 'open' as shown below (Figure 2).

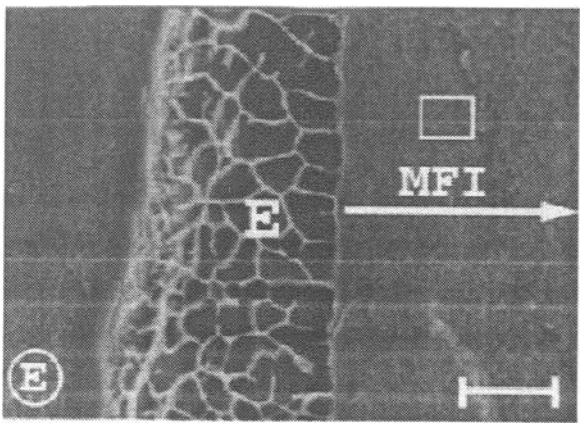

Figure 2 - *Micrograph of denatured muscle tissue. E, extracellular matrix; MFI, myofibrils. The bar corresponds to 4.5 μm [6].*

7. Carefully insert the graft into the tube such that it is recessed equidistantly into the tube at each end. Take care not to crush the graft.
8. Anchor the graft into the tube with a single suture in the middle using 10-0 degradable suture material.

An epineural approach is recommended for the surgical procedure. Making sure there is minimal tension in the nerve, the nerve stump ends should be inserted into the tube. Two to three sutures should be made by passing the suture through the tube and epineurium only, using 8-0 to 10-0 degradable suture material [2, 19].

Contraindications

The use of InnervTube is contraindicated for the following populations: patients under four years of age as the rate of normal growth may overtake the breakdown of the device; pregnant or lactating females may exhibit an abnormal healing response due to hormonal variation; patients previously treated with immunosuppressive agents, radiation, or chemotherapy within the past three months as these therapies may interfere with the normal healing response.

The use of InnervTube is also contraindicated for patients having the following medical conditions: patients having any type of autoimmune disorder; patients with hemophilia or other related blood clotting disorders; patients with either systemic infection or infection local to either the repair or donor sites; patients in which the nerve gap to be closed is greater than 10 mm long or in which the nerve diameter is greater than 3.2 mm; patients in which the site to be repaired requires the InnervTube to flex more than 30 degrees over its length [10]; patients in which the nerve to be repaired has been severed for more than two years; patients in which the site of repair contains excessive scarring or exhibits signs of chronic inflammation.

There may be other drug or therapeutic factors that contraindicate the use of InnervTube. Specifically, the attending physician should consider those treatments that affect the overall wound healing response of the patient. The physician is encouraged to contact the manufacturer with questions about the suitability for any specific application. Clinical signs of infection (pain, edema, drainage, odor, warmth, unexplained fever) may indicate removal of the device, depending upon severity of the local condition as well as the overall health of the patient.

Alternative Practices and Procedures

Presently the nerve autograft is the 'gold standard' against which other therapies are judged. It is indicated for use over a relatively wide set of separation conditions (gap length, nerve diameter), largely related to donor site nerve viability. Up to this point, however, nerve regeneration has met with variable success and functional recovery is rarely complete. Additionally there is the significant complication of donor site morbidity along with the realization that advances in microsurgery techniques will likely not improve clinical outcomes [4]. Another alternative is direct suture repair: the surgical realignment of individual nerve fascicles (i.e. primary neurorrhapy). This has been a viable alternative for nerve restoration for those cases in which the gaps to be closed can be done so with a minimum of tension. This has been performed since the 1960s and has demonstrated success on par with the autograft techniques [8].

There are three nerve guidance channels currently commercially available in the market; all have inherent limitations. Common to all is that the ends of nerves to be resected must be in proximity, whether by increasing tension, by interspersing autologous nerve sections, or by maintaining proximity through flexion. With the current standard of the nerve autograft, there is also the significant detriment of selecting a donor site that will likely cause serious functional debilitation following the procedure.

The InnervTube approach, however, relieves the restriction of proximity as well as eliminates the problem of nerve donor site morbidity. It is also an improvement over existing NGCs on the market as it employs native tissue to encourage rapid migration, proliferation, matrix remodeling, and ultimately, the re-establishment of functionality.

Potential Adverse Effects

As with any surgical procedure there exists the possibility of significant adverse effects, including death, as a result of factors that may or may not be directly related to the use of InnervTube. Some of these include surgical complications, anesthesiological complications, infection, pain, loss of sense to part or all of a limb, loss of motor control to part or all of a limb, and over- or under-sensitization.

Summary of Preclinical Data

In-Vitro Data

The following parameters have been deemed essential, either by the manufacturer or in accordance with recommendations of ASTM standards, to the proper function of InnervTube. Therefore, the associated data has been collected in demonstration of the physical safety of the design and construction of InnervTube.

Mechanical testing of the tensile strength of the tube was guided by the ASTM Standard Test Method for Tensile Properties of Plastics (D638-00) and ASTM Standard Test Method for In Vitro Testing of Poly (L-lactic Acid) Resin and Fabricated Form for Surgical Implants (F1635-95). Slight variation from standard D638-00, principally related to fixturing the ends of the tube with paraffin into aluminum tubes, was judged to have a negligible effect on the test outcome. The testing of ten tubes was performed at 37 °C after eight weeks in buffered PBS (changed regularly to maintain pH = 7.4 +/- 0.2). The mean (standard deviation) modulus was 62 MPa (15 Mpa), the tensile strength at failure was 0.2 MPa (0.06 MPa), and the tensile strain at failure was 0.005 mm/mm (0.0015 mm/mm). There was no statistical difference between the original modulus of 80 Mpa, while there were statistical differences between both the original tensile strength (= 1.0 MPa) and the original tensile strain (= 0.24 mm/mm) [8].

Again in accordance with F1635 and ASTM Standard Test Method for Molecular Weight Averages and Molecular Weight Distribution of Polystyrene by High Performance Size-Exclusion Chromatography (D5296-97), gel permeation chromatography was used instead of Dilute Solution Viscosity to determine the molecular weight of the samples. The samples were dissolved in chloroform and five measurements were made at a weekly time point over eight weeks. At eight weeks the tubes had an average (sigma) molecular weight of 14 500 Da (1 000 Da) or slightly less than half of their original MW of 32 000 Da (1 500 Da) [8].

Mercury intrusion porosimetry, as described in ASTM Standard Test Method for Interior Porosity of Poly (Vinyl Chloride) (PVC) Resins by Mercury Intrusion Porosimetry (D2873), was used to determine both the porosity and pore size distribution. The pore diameter distribution was obtained as described by Winslow [20]. Using the manufacturing process as described above, porosities of 82% (+/- 1%) and pore diameters of 20 μm (+/-2 μm) were measured [8].

Differential scanning calorimetry was used to determine the glass transition temperature (T_g) and the intrinsic degree of crystallinity [11]. After eight weeks in PBS the T_g decreased from 54.5 °C (0.5 °C) to 29.0 °C (2.2 °C). The relative percentage of crystallinity increased from 5.2% (0.4%) to 11.5% (0.7%) however, due to the preferred degradation of the amorphous phase regions [8].

Based upon the results shown above, we believe that the InnervTube will mechanically function as intended upon implantation, and continue to function while the wound heals. Furthermore, based upon the initial molecular weight, monomer concentration, and crystallinity, we project that under normal physiological conditions, the InnervTube will have completely degraded in approximately 48 weeks [12, 21].

In accordance with ASTM Standard Practice for Selecting Generic Biological Test Methods for Materials and Devices (F748-98), the following applicable tests are indicated for an implanted device that will reside in the body for longer than one month and principally contact tissue and tissue fluid.

Cytotoxicity was assessed under ASTM Standard Practice for Direct Contact Cell Culture Evaluation of Materials for Medical Devices (F813-83). Using cell line L929, cell cultures were grown and test and control specimens were placed in direct contact with the cell layer. Under microscopic examination, no malformation, sloughing, degeneration, lysis, or moderate reduction of the cell layer density was observed for either the test or control specimens.

Implantation effects were assessed under ASTM Standard Practice for Assessment of Compatibility of Biomaterials for Surgical Implants with Respect to Effect of Materials on Muscle and Bone (F981-99). Briefly, ten Fischer 344 rats were implanted in the gluteal muscles with InnervTube (as manufactured) and USP Negative Control Plastic having the same dimensions, one on either side of the body. Following sacrifice and implant retrieval after 90 days, the tissue response was scored according to the standard. The overall response of the tissues using a paired t-test was statistically not different and the average rating of both was '0: No reaction'.

Genotoxicity was assessed under contract with an external, independent laboratory. Using ASTM Standard Guide for Performing the Mouse Lymphoma Assay for Mammalian Cell Mutagenicity (E1280-97), the laboratory chose to use 'relative total growth' (RTG) of cells in culture as the measure of response. Although there is no single test available to test all types of mutagens, the laboratory found that under its evaluations, saline solutions extracted from PLLA were non-mutagenic when compared with control saline and solutions extracted from other known implantable materials.

Carcinogenicity was assessed under ASTM Standard Guide for Performance of Lifetime Bioassay for the Tumerogenic Potential of Implant Materials (F1439) by an external, independent laboratory. Fischer 344 rats, both male and female, were used. Implantation of InnervTube was performed in the gluteal muscle on one side, while the same procedure without actual implantation was done on the corresponding gluteal on the other side. Contrary to the recommended two year duration, the study was terminated after one year after the laboratory could find no significant differences in the blood chemistries or histology of tissues of animals sacrificed and examined at 90, 180, 270, and 360 days.

Pyrogenicity was assessed by an external, independent laboratory using a USP rabbit test. It found no evidence of pyrogenicity attributable to the implantation of InnervTube manufactured of PLLA when compared against the USP Negative Control Plastic.

Sensitization was assessed using ASTM Standard Practice for Testing Guinea Pigs for Contact Allergens: Guinea Pig Maximization Test (F720-81). Using a saline extraction liquid as described by ASTM Practice for Extraction of Medical Plastics (F619), Hartley Strain guinea pigs were tested for topical response and intradermal injection response. Scoring for erythema and edema was '0' in all ten cases, classifying the response as 'no different than control'.

Intracutaneous irritation and sytemic toxicity was assessed using ASTM Standard Practice for Evaluating Material Extracts by Intracutaneous Injection in the Rabbit (F749-98). A saline extract was prepared (F619) and injected intracutaneously. Examination after 24, 48, and 72 hours showed no evidence of tissue reaction (edema, erythema, or

necrosis) at either the test or control sites. Similar intravenous injection of the extract produced no signs of system toxicity in the 72-hour period.

Immunotoxicity was assessed based on ASTM Standard Practice for Selecting Tests for Determining the Propensity of Materials to Cause Immunotoxicity (F1905-98) and ASTM Standard Practice for Evaluation of Immune Responses in Biocompatibility Testing Using ELISA Tests, Lymphocyte Proliferation, and Cell Migration (F1906-98). The testing was divided into two areas: humoral immunity and cell mediated immunity. Enzyme linked immunoassay (ELISA) techniques were used to gauge the humoral response; following the protocol described in F1905, section 5, results of the optical density measurements made on the test serum samples (fetal calf) showed no elevations or depressions outside two standard deviations from the control. Similarly, conforming to the protocols given by sections 8.1, 8.2, and 8.3 in F1905, we concluded the following: a) no difference in lymphocyte transformation (test for presence of division stimulation cytokine in FCS); b) no difference in leukocyte migration using rabbit blood; c) no difference in macrophage migration using rabbit lung.

The degradation of PLA has been extensively studied, both in vivo and in vitro. Numerous studies have been published on the biocompatibility, biodegradation, and bioresorption of PLLA [22-24]. It is generally accepted that it degrades via hydolysis into the monomer L-lactate, which can be metabolized in the liver to carbon dioxide and water. Based on this research and the data above, we believe InnervTube is safe to use as a temporary, bioresorbable implant when used as prescribed.

In-Vivo Data

Evans et al. demonstrated the efficacy of PLLA conduits using a rat model [25]. Briefly, conduits were fabricated, largely similar to the methods described above. The sciatic nerves of Sprague Dawley rats were severed and the conduits were implanted. Control specimens were prepared similarly and received nerve isografts from donor animals. Histological assessment at 16 weeks demonstrated axonal growth and tissue advancement through the entire conduit. Additionally it was noted that along with firmly adherent muscle on the outside indicating tissue incorporation, vascularization, and polymer degradation, there were blood vessels traversing the conduit. Cross-sectional measurements of nerve fiber density near the distal nerve, while not equal to the control at 6 weeks, were equivalent at 16 weeks. Axonal density at the distal nerve was less for the conduit at both 6 and 16 weeks. Functional assessment using walking track analysis [26, 27] was performed monthly through 16 weeks and demonstrated functional recovery indicating muscle reinnervation. Similar studies involving multilumen channels (some of which were seeded with autologous Schwann cells) more closely resembling the morphology of InnervTube, have demonstrated comparable results [10, 28].

Based on this data we believe that InnervTube is an effective therapy when used as prescribed.

Good Manufacturing Processes

Standard Operating Procedures (SOPs) shall be written to cover a variety of functions including material acceptance criteria, inspection methods, test methods, specific processing instructions, cleanroom operation, maintenance, material tracking, glassware handling, training, and others. At a minimum they should include the purpose for the SOP, methods and/or validating steps, the author, the date, a revision, and an approval record.

Training, testing, and approval are required prior to unsupervised work on product to be released or tools affecting product to be released. Training shall be conducted per SOP by either the originator or someone already certified on the process or function to be performed. Training, testing, and certification for the muscle tissue preparation process can be performed either on-site or at the customer's location. This will be done using a mouse model in conformance with standard lab practices.

Quality is to be controlled via two potentially competing functions: 1) Ongoing development of a capable process aiming for high yields. This will entail developing process transfer functions relating the various process parameters to final product specification and implementing Standard Process Control (SPC) techniques to monitor process parameters. These activities reside in the 'Manufacturing' department. 2) Highly capable inspection and verification processes. This will require an understanding of both the product and the potential failure modes that might arise through processing. This function is to reside in the 'Releasing' department.

Inputs Requiring Control

Virgin Poly (L-Lactic Acid) Resin: The material coming in powder or small (maximum diameter <= 10 μm) bead form shall be qualified according to a Standard Operating Procedure (SOP) derived from ASTM Standard Specification for Virgin Poly (L-Lactic Acid) Resin for Surgical Implants (F1925-99). Specifically, the following batch properties must be confirmed: a) Homopolymer of L-lactide with a density between 1.20 and 1.28 g/cm3as measured by gas chromatography (GC); b) Weight average molecular mass between 30,000 Da and 35,000 Da as measured by gel permeation chromatography (GPC), (ASTM D3536); c) Residual solvents in less than the following amounts (test methods in parentheses): monomers < 0.1% to accommodate molding (GC), water < 0.5% (Karl-Fischer titration), tin <200 ppm (AA spectroscopy), lead <300 ppm (Method 231 of U.S. Pharmacopeia), and sulfated ash ,0.1% (ignition test @ 700 °C). Verification and validation should be demonstrated by vendor for each batch along with periodic sampling in-house and tracking via SOP.

Methylene chloride, liquid nitrogen: The material shall be medical grade with purity verified and validated by the vendor. Upon in-house arrival, purity sampling qualification shall be completed by absorption spectrum analysis and/or residual analysis as appropriate. Tracking shall be completed per the SOP.

Sodium chloride: The material shall be of medical grade with a specified granule sizing between 150 and 300 μm (diameter). Random sizing samples shall be drawn by batch

and measured with a calibrated microscope. All methods, analyses, reports, and tracking should be followed per the appropriate SOP.
Sizing sieve, extrusion tool: The dimensions and materials comprising the tool shall be specified in the design drawing. Verification shall be provided by the vendor and will be verified by acceptance measurements made at random locations on each sieve. The methods of operation, analysis, reporting, and tracking shall be described by the appropriate SOP.
Diamond saw, vacuum oven, plasma system: Conformance of each tool to specification criteria shall be determined during a formal tool acceptance protocol. Performance shall be verified after each repair or periodic maintenance procedure per SOP unique to each tool. Maintenance shall be tracked using an in-house tracking system per SOP.

Processing

Maintenance of equipment is to be done on a periodic, scheduled basis under control independent of the production control. There are to be documented processes for each maintenance procedure developed jointly with the equipment manufacturer and/or designer. Equipment that is 'down' for any reason should be clearly labeled to prevent production of potentially defective product. Maintenance staff is to be trained and certified on each tool and/or procedure for which they are responsible. These procedures are to be found in an approved SOP and made available to 'Releasing' personnel along with the records of training and maintenance.

In-line processes shall be controlled using accepted SPC techniques such as control charting and 'alarm' flagging. Actions resulting from an 'out-of-control' condition shall be clearly identified and recorded. The SOP for any particular process should contain functional information relating process variables to product specification (e.g., extrusion temperature to pore diameter) along with a flow chart of potential failures and responses. This shall be updated as process learning occurs. Each process shall record and track its critical parameters against process capability (e.g., C_{pk} number or similar). Ancillary processes (e.g., cleaning subsequent to cutting) shall be controlled under the primary process. Inspection processes must include a gage study in the SOP demonstrating capability. All processes are to be performed in conformance with the environmental protocol and associated training SOPs: e.g., glassware handling, chemical handling/disposal, cleanroom practices, etc.

Outputs to be Monitored

Tubes fashioned from three points in the extrusion batch (beginning, end, and random middle) are to be tracked through the manufacturing process and tested at the end for conformance to product release criteria. The following parameters are critical to product quality and performance. Testing is to be performed by inspectors certified for each measurement. SOPs cover details of testing methods, reporting, tracking, and corrective action(s). Inspectors shall verify completeness, accuracy, and correct processing as reported on lot tracking system.

Relative crystallinity shall be between 4.5% and 5.9% (Differential scanning calorimetry [SOP]).

Porosity shall be between 78% and 86% (mercury intrusion porisometry [SOP]).

Tensile modulus shall be greater than 35 MPa (modified ASTM standard apparatus as described in SOP).

Length shall be 12 mm +/- 0.10 mm (calibrated microscope [SOP]).

Inner diameter shall be 2.05 mm +/- 0.05 mm or 5.05 mm +/-0.05 mm or 8.05 mm +/-0.05 mm, depending upon size application (calibrated microscope [SOP]).

Cracking, shattering, or contamination shall be cause for rejection according to final inspection SOP (visual, SEM [SOP]).

Lots that meet these inspection criteria and have approved lot records may be released. Final shipment out of the facility must have an authorizing shipment statement signed by the director of the 'Releasing' department. This statement shall include, at a minimum, the lot/batch identification, the date of final inspection, the identification of the final inspector, and the authorizing signatures and date. The 'Production' department may only tally as 'completed product', those lots that have met the final releasing criteria and have been approved as such by the 'Releasing' department. Inspected samples from each lot shall be retained per SOP.

Discussion and Conclusions

Through a hypothetical PMA construction we have evaluated the appropriateness of using available standards in the design, testing, and production phases of a neural guidance conduit. As the purpose of standards is to provide common methodologies, criteria, and reporting structures, it is evident that there are a number of existing standards that serve their purpose very well, especially in the area of test methods. However, it is less obvious how the further use of existing standards could be used in the design phase. Nevertheless, there are a few possibilities that are, to various extents, already in use in the field of design engineering in industrial settings. In particular there are methods that are based upon rigorous control of transfer functions between customer requirements and product specifications (e.g., so-called 'Six Sigma' –type disciplines) and methods that are aimed at design failure risk management (e.g., 'Failure Mode and Effects Analysis'). Common to these tools is the recognition that there is some means of quantifying the robustness of a design through statistical methods. This may present an opportunity in the future to apply the use of standards to the design phase, potentially relieving some of the bottlenecks in FDA regulatory approval.

References

[1] Sunderland, S., "Rate of Regeneration in Human Peripheral Nerves: Analysis of Interval between Injury and Onset of Recovery," *Archives of Neurology and Psychiatry*, 1947;58:251–295.

[2] Rand, R. W., *Microneurosurgery*, St. Louis, The C. V. Mosley Co., 1985.

[3] Ducker, T. B., Hayes, G. J., "Experimental Improvements in the Use of Silastic Cuffs for Peripheral Nerve Repair," *Journal of Neurosurgery*, 1968;28:582–7.

[4] Hudson, T. W., Evans, G. R. D., Schmidt, C. E., "Engineering Strategies for Peripheral Nerve Repair," *The Orthopedic Clinics of North America*, Jul 2000; 31(3):485–497.

[5] Hubel, A., "BMEn 5041 Tissue Engineering Course Lecture," University of Minnesota, 1 Oct., 2001.

[6] Meek, M. F., et al., "Evaluation of Several Techniques to Modify Denatured Muscle Tissue to Obtain a Scaffold for Peripheral Nerve Regeneration," *Biomaterials*, 1999;20:401–8.

[7] Meek, M. F., et al., "Peripheral Nerve Regeneration and Functional Nerve Recovery after Reconstruction with a Thin–walled Biodegradable Poly (DL–lactide–caprolactone) Nerve Guide," *Cells and Materials*, 1997;7:53–62.

[8] Widmer, M. S., et al., "Manufacture of Porous Biodegradable Polymer Conduits by an Extrusion Process for Guided Tissue Regeneration," *Biomaterials*, 1998;19:1945–55.

[9] Engelberg, I., Kohn, "Physico–mechanical Properties of Degradable Polymers used in Medical Applications: A Comparative Study," *Biomaterials*, 1991;12:292–304.

[10] Hadlock, T., et al., "A Tissue Engineered Conduit for Peripheral Nerve Repair," *Archives of Otolaryngology Head and Neck Surgery*, 1998;124:1081–1086.

[11] Mikos, A. G., Thorsen, A. J., Czerwonka, L. A., Bao, Y., Langer, R., Winslow, D. N., and Vacanti, J. P., "Preparation and Characterization of Poly (L–lactic acid) Foams," *Polymer*, 1994;35:1068–77.

[12] Nakamura, T., et al., "Bioabsorption of Polylactides with Different Molecular Properties," *Journal of Biomedical Materials Research*, 1989;23:1115–1130.

[13] Holy, C. E., et al., "Optimizing the Sterilization of PLGA Scaffolds for use in Tissue Engineering," *Biomaterials*, Jun 2001;22(1):25–31.

[14] Gogolewski, S., et al., "Sterility, Mechanical Properties, and Molecular Stability of Polylactide Internal Fixation Devices Treated with Low-temperature Plasmas," *Journal of Biomedical Materials Research*, 1996;32:227–235.

[15] Ide, C., "Nerve Regeneration through the Basal Lamina Scaffold of the Skeletal Muscle," *Neuroscience Research*, 1984;1:379–91.

[16] Ide, C., et al., "Schwann Cell Basal Lamina and Nerve Regeneration," *Brain Research*, 1983;288:61–75.

[17] Glasby, M. A., et al., "Degenerated Muscle Grafts used for Peripheral Nerve Repair in Primates," *Journal of Hand Surgery*, Oct 1986; 11B(3):347–351.

[18] Norris, R. W., et al., "Peripheral Nerve Repair in Humans using Muscle Autografts," *Journal of Bone and Joint Surgery*, Aug 1998; 70-B(4):530–533.

[19] Seddon, H., *Surgical Disorders of the Peripheral Nerves*, Baltimore, The Williams and Wilkins Co., 1972.

[20] Winslow, D. N., "Advances in Experimental Techniques for Mercury Intrusion Porisometry," *Surface and Colloid Science*, Matjevic, E., Good, R. J., editors, Plenum Press, New York, 1984:259–82.

[21] Chawla, A. S., Chang, T. M. S., "In–vivo Degradation of Poly (lactic acid) of Different Molecular Weights," *Biomaterials Medical Devices and Artificial Organs*, 1985–86; 13(3&4):153–162.

[22] Brady, J. M., et al., "Resorption Rate, Route of Elimination and Ultra Structure of the Implant Site of Polylactic Acid in the Abdominal Wall of the Rat," *Journal of Biomedical Materials Research*, 1973; 7:155–166.

[23] Cutright, D. E., et al., "Degradation Rates of Polymers and Copolymers of Polylactic and Polyglycolic Acids," *Oral Surgery Oral Medicine and Oral Pathology*, 1974; 37:142–152.

[24] Leenslag, J. W., et al., "Resorbable Materials of Poly (L–lactide), VII: In vivo and in vitro Degradation," *Biomaterials*, 1987; 8:311–314.

[25] Evans, G. R. D., et al., "In vivo Evaluation of Poly (L–lactic acid) Porous Conduits for Peripheral Nerve Regeneration," *Biomaterials*, 1999; 20:1109–15.

[26] Hare, G. M. T, et al., "Walking Track Analysis: A Long–term Assessment of Peripheral Nerve Recovery," *Plastic Reconstructive Surgery*, 1986;42:805–20.

[27] de Medinaceli, L., et al., "An Index of the Functional Condition of Rat Sciatic Nerve Based on Measurements Made from Walking Tracks," *Experimental Neurology*, 1982;77:634–643.

[28] Ansselin, A. D., et al., "An Alternative to Nerve Grafts in Peripheral Nerve Repair: Nerve Guides Seeded with Adult Schwann Cells," *Acta Chururgica Austriaca*, 1998; 30(Supplement 147):19–24.

John R. Walsh,[1] Michael J. Taylor,[1] and Kelvin G. M. Brockbank[1]

Storage and Transport Issues for Tissue Engineered Medical Products

Reference: Walsh, J. R., Taylor, M. J., and Brockbank, K. G. M., "**Storage and Transport Issues for Tissue Engineered Medical Products,**" *Tissue Engineered Medical Products (TEMPs), ASTM STP1452,* E. Schutte, G. L. Picciolo, and D. S. Kaplan, Eds., ASTM International, West Conshohocken, PA, 2004.

Abstract: A prominent barrier to widespread commercialization of tissue engineered medical products (TEMPs) is the development of storage and transport technologies to maintain high product viability and integrity at point of use. Advances in biostabilization and low temperature biology have produced effective preservation technologies for cells and tissues in areas of hypothermic storage, cryopreservation by freezing and vitrification, and anhydrobiotic preservation. Preservation methods are anticipated to progress in step with development of TEMPs and may ultimately influence construct designs, as the final form of these products are determined. However, development of preservation methods is complex and requires optimization of several chemical and biophysical processes to achieve maximal viability and stability. The development of standards for materials and processes used in preserving TEMPs will be integral in ensuring final product quality and integrity pertaining to pre-process treatment, materials and containment systems, preservation processes, storage, transport, restoration and post-process treatment.

Keywords: tissue engineering, biopreservation, cryopreservation, vitrification, hypothermic storage, anhydrobiosis, freeze-drying, storage and transport technology, stabilization

Introduction

The rapid growth of tissue engineering has produced an enormous number of potential product benefits matched only by the number of technical challenges to be solved. Many tissue-engineered products are on the market with several more in development. Most of these products contain or will contain highly specialized cell components that will require

[1] Laboratory Director, Vice President of Research and Development, and Senior Vice President of Scientific, Clincal and Regulatory Affairs, respectively, Organ Recovery Systems, Inc., 701 East Bay Street, Suite 433, MSC 1119, Port City Center, Charleston, SC, 29403.

effective transport solutions, storage methods and devices to enable efficient product distribution and increase shelf life.

Advances in biostabilization and low temperature biology have produced high viability preservation technologies including hypothermic storage, cryopreservation by freezing and vitrification, as well as anhydrobiotic preservation. However, the development of preservation methods is not straightforward. The stabilization of biomaterials generally involves complex processes of coupled heat and mass transfer performed under non-equilibrium conditions in addition to concomitant biochemical transport. Process development requires the optimization of chemical and thermal treatments to achieve maximal survival and stability.

Tissue engineered medical products will be sensitive to many of the factors associated with preserving native tissues. Other characteristics of engineered products that will influence the preservation of TEMPs include cell type, extracellular matrix material composition, interaction between biological components and synthetic scaffolding as well as the compatibility of the process with the product configuration itself. It is expected that preservation methods will progress in step with the development of tissue engineered products and may ultimately affect design of the construct. Standards are required to define compatibility limitations of tissue-engineered products and the processes and materials used to preserve them. Several areas will require examination to determine if standards are necessary for issues related to pre-process treatment, materials and containment systems, preservation processes, storage, transport, restoration and post-process treatment.

Preservation Technologies

Several processes are available for effectively stabilizing biological materials with therapeutic levels of cellular viability and structural integrity. These processes are directly applicable to tissue engineered medical product preservation. The choice of process type will typically be the method that confers maximum viability. However, it is necessary to consider several factors, including, intended duration of storage, end-use specifications and manufacturing process capabilities before final selection.

Hypothermic Storage

Hypothermic storage is frequently used as a short-term preservation method to stabilize cells and tissues and is generally applied before therapeutic use or during the manufacturing process. Biological materials placed in hypothermic storage are suspended in liquid media and stored across a range of temperatures from just below normothermic (37°C) to above the equilibrium freezing point of the solution. Storage solution and temperature are optimized to maintain cellular stasis by providing essential biochemical components that satisfy metabolic requirements. Storage duration is a function of cell type, solution composition as well as storage temperature and is limited to periods from hours to days.

Cryopreservation

Cells and TEMPs can be stabilized by cryopreservation involving freezing of the liquid phase of the extracellular water or solidification of the entire system using a vitrification process. In both cases, materials are cooled below the equilibrium freezing point of the preservation solution in which there is a resultant solidification of the liquid components of the cells or tissues. Cryopreserved cells and TEMPs have negligible levels of metabolic activity at storage temperatures below the glass transition temperature.

Freezing - Cryopreservation by freezing involves the solidification of biological materials by the crystallization of water into ice. Simply freezing cells or tissues results in dead, nonfunctional materials. The process of freezing and thawing cells and complex tissues involves coupled processes of heat and mass transfer. Cryoprotective agents (CPAs) are added to ameliorate the damaging effects associated with ice formation by modulating intracellular water content during freezing and thawing. Maximum viability requires optimization of cooling and warming rates for precise control of the rate of ice crystal formation and cellular hydration events during freezing and thawing. Optimum parameter values for cryopreservation variables such as cooling and warming rates vary with cell and tissue types are determined with experimental studies.

Vitrification - An alternative to conventional freezing of living biological materials involves the solidification of samples without crystallization of water in a process called vitrification. Vitrification (derived from vitri, the Greek word for glass) is a kinetic process in which the suspending medium is cooled sufficiently to raise the solution viscosity greater than 10^{15} poise [1]. The process produces a glassy solid that visually appears to be ice-free, however, vitrified samples may contain microscopic amounts of crystalline water. Vitrification can be achieved by adjusting the solute concentration and cooling rate to form a glass and avoid the ubiquitous formation and growth of ice obtained in slow rate freezing. Vitrification can be applied to the stabilization of cells and tissue engineered products without the deleterious effects associated with ice crystallization.

Anhydrobiotic Preservation

A principle goal of cryopreservation is to inhibit water mobility within cells as part of the process in halting metabolic activity. This is achieved through the removal of water by crystallization in slow rate freezing processes and arrest of molecular translational motion in vitrification processes. Anhydrobiotic preservation methods achieve water immobilization in multi-step processes in which water is removed from the system of interest. This is accomplished by desiccation and freeze-drying (lyophilization). Desiccation is primarily used to remove liquid water by evaporation at temperatures above the equilibrium freezing point of the system. In freeze-drying (what is technically known as lyophilization), the system is first frozen to transform extracellular water into ice that is subsequently removed, first, by sublimation and then by desorption. Freeze drying has been used to preserve proteinaceous materials (pharmaceuticals), a variety of microorganisms and various biomaterials. When applied to biomaterials such as de-

mineralized bone, freeze-drying has been used primarily to preserve structure over cell viability. In general, freeze-drying can be readily applied to substances that are not damaged by freezing with the exception of mammalian cells that demonstrate extreme sensitivity to freeze-drying. Current research efforts are focused upon the development of novel techniques to permit cells and tissues to be anhydrobiotically preserved with therapeutic levels of cell survival.

Process Techniques

Biostabilization involves numerous phenomena of complex physico-chemical and biochemical processes that are typically governed by coupled nonlinear kinetic rate reactions in non-equilibrium states. Improved preservation systems can be obtained by understanding the many sub-processes involved in cell and tissue preservation. Determination of the key parameters and how they affect the specific cell or tissue is essential in selecting and developing preservation processes that maximize product viability and stability.

Pre-Process Issues

Material Selection - Packaging materials should be selected that are compatible with the selected preservation process. Tissue engineered products preserved under cryogenic conditions should use packaging and labeling with temperature ranges that extend from ambient to –196°C. Product tracking methods and identification systems used during preservation must conform to methods developed for the manufacturing process of the product. Product tracking should be carefully evaluated for materials stored in vapor-phase or liquid-phase nitrogen containment systems. Labeling for cryopreserved products should remain attached at the appropriate storage temperatures. Materials used in anhydrobiotic preservation are dense materials with low porosity to prevent moisture from entering the product container. Stability studies are recommended to ensure that these materials are not only compatible with standard use environments but account for non-ideal conditions in which the product may be used. Packaging and labeling previously certified for products at ambient temperatures should be re-certified for the range of temperatures and times encountered during the complete storage and use period.

Cell and Tissue Biophysical Characterization – Since biopreservation is primarily driven by coupled processes of heat and transfer, it is recommended that the biophysical parameters that govern the response of living cells and tissues to the stresses imposed by the selected stabilization process, are identified and characterized. Cells and tissues respond at specific rates to accommodate these stresses as they equilibrate with the extracellular environment. The parameters that govern the cellular and tissue level response are functions of the physical and biochemical properties of the cell or tissue. Variances in biophysical properties such as membrane permeability will have a first order effect upon how the cells respond to certain preservation processes. Cells maintained in slightly different culture conditions can exhibit considerable differences in cellular metabolism, membrane permeability and thus respond differently to a preservation protocol. Adherence to process control methods will assist in minimizing variances with

protocol outcome. Strict process control methods should be instituted from pre-process handling through the entire preservation process to minimize deviations and ensure product quality and integrity. Many factors can cause variations in cellular responses.

Preservation Solutions

Hypothermic Storage Solutions - Hypothermia works by directly controlling the extracellular environment of cells directly, and controlling the intracellular environment indirectly, during cold exposure and is largely achieved by appropriately applied hypothermic preservation solutions. Hypothermic solutions are designed to meet biophysical requirements with the essential biochemical components that meet the metabolic needs of the cell and prevent cell swelling typically observed during storage. To this end, specialized solutions have been designed for profound hypothermic temperatures (<15°C), as well as applications for moderate hypothermia (~25°C) [2-4].

Solutions may contain components specifically selected to: a) minimize cell and tissue swelling, b) maintain appropriate ionic balance, c) maintain a state of acidosis, d) remove or prevent the formation of free radicals, and e) provide substrates for the regeneration of high energy compounds and stimulate recovery upon rewarming and reperfusion. The optimum temperature and solution composition for the hypothermic storage of mammalian tissues is not well-established and therefore studies may be required to determine solution design and the range of temperatures to maintain viability and maximized storage duration capability. In the design and selection of temperature conditions, consideration should be applied to cases in which hypothermic storage is performed below the suspected membrane lipid phase transition zone (8-10°C). The thermotropic changes occurring within the membrane have been shown to affect cells in hypothermic storage [5-7].

Vehicle Solutions - Optimum control of the environment of cells during cryopreservation demands consideration of the chemical composition of the suspending medium used as a vehicle for the CPAs as temperature. Although conventional culture media are commonly used for this purpose, it should not be assumed that tissue culture medium is an ideal or optimum vehicle solution for exposure of cells at low temperatures. A variety of factors are known to influence the survival of cells during cryopreservation, but the role of the vehicle solution for the cryoprotective agents is often overlooked. It is generally assumed that conventional culture media used to nurture cells at physiological temperatures will also provide a suitable medium for exposure at low temperatures. However, it is now well-established in tissue and organ preservation that maintenance of the ionic and hydraulic balance in cells during hypothermia can be better controlled by using solutions designed to physically restrict these temperature-induced imbalances [2, 8], and can equally be applied to the choice of vehicle solution for adding and removing CPAs in a cryopreservation protocol.

Cryoprotective Agents – Cryoprotectants protect slowly frozen cells by one or more of the following mechanisms: suppression of high salt concentrations; reduction of cell shrinkage at a given temperature; reduction in the fraction of the solution frozen at a given temperature; and minimization of intracellular ice formation. A comparison of

chemicals with cryoprotectant properties reveals no common structural features. These chemicals are usually divided into two classes: 1) intracellular cryoprotectants with low molecular weights that permeate cells, and 2) extracellular cryoprotectants with relatively high molecular weights (typically greater than or equal to sucrose [342 daltons]) that do not penetrate cells. Intracellular cryoprotectants, such as glycerol and dimethyl sulfoxide at concentrations from 0.5 to 3 molar, are effective in minimizing cell damage in many slowly frozen biological systems. Combinations of cryoprotectants may result in additive or synergistic enhancement of cell survival [9, 10].

The addition and removal of cryoprotectants from cells imposes osmotic stresses that result in the coupled transport of water and cryoprotectants across the plasma membrane of the cell. The introduction of penetrating cryoprotective additives to isotonic suspending media results in a rapid efflux of water from cells and interstitial spaces followed by a slower influx of cryoprotectant and water. This coupled transport causes a characteristic "shrink/swell" response as the cell volume reaches a new osmotic equilibrium. During cryoprotectant removal, a similar but reverse process occurs when cryoprotectants are diluted from solutions containing cells and tissues. A rapid influx of water followed by a slower efflux of cryoprotectant and water occurs when cells are exposed to diluted solutions. This results in a typical "swell/shrink" response of the cell volume. For the case of non-penetrating cryoprotectants, cells respond osmotically by shrinking during cryoprotectant addition and swelling during cryoprotectant removal. Cryoprotectant addition and removal must be performed cautiously to avoid excessive volume excursion that can compromise membrane and cytoskeleton integrity and disrupt extracellular matrices resulting in lethal injury. Non-penetrating compounds can be used as osmotic buffers to lower the magnitude of volume changes during CPA addition and removal.

Although cryoprotective agents protect cells and tissues via several mechanisms, many protective compounds produce cytotoxic side effects. It is essential to evaluate a panel of compounds in the cell types of the specific application since cytotoxicity can be cell type dependent. For example, dimethyl sulfoxide may produce little or no toxic effects in one cell type yet cause lethal injury in another. Consequently, selection of cryoprotective agents for TEMPs with different cell types requires testing and optimization to balance toxicity concerns among the constituent cells within the construct.

In practice, cytotoxicity can be partially reduced by introducing cryoprotective agents of greater toxicity at lower temperatures prior to cryopreservation. The reduced temperature state slows down the metabolic uptake of many cryoprotectants and allows them to permeate into intracellular and interstitial spaces with reduced incidence of injury. Membrane permeability to water and CPA decreases exponentially with temperature, therefore addition and removal protocols require longer exposure times to permit sufficient cryoprotectant equilibration. The increased time results prolong CPA exposure that may increase the risk of toxic side effects. Additional testing may be necessary to establish low temperature exposure limits for cryoprotectants.

It is also recommended that cryoprotectants as well as vehicle solutions be evaluated with TEMPs that employ non-native and synthetic materials as scaffolding. A compatibility study of common scaffold materials and cryoprotectant compounds is currently nonexistent. Testing should be performed to determine if selected CPAs and

vehicle solutions could cause leaching of undesirable compounds from scaffolds or deteriorate materials that would alter the mechanical integrity of the scaffolding and change the desired specifications of the product at the point of use.

Controlled Rate Freezing

Controlled rate freezing before long-term storage maximizes viability for a wide variety of cells. The use of controlled rate freezing in cryopreservation permits greater process control and therefore raises consistency of product outcome. Many cells and tissues are frozen under controlled cooling at optimized rates from temperatures just above the equilibrium freezing point of the suspension solution to temperatures below the homogeneous nucleation point of water (-38°C). Following controlled cooling, specimens are generally transferred to cryogenic storage devices (-80°C to -196°C) for further cooling at uncontrolled rates. In practice, most cryopreserved samples are generally cooled to temperatures well below -40°C, i.e. -80°C, to reduce the risk of sample warming as they are transferred from the controlled rate freezing chamber to storage freezers. It should be noted that even though uniform cooling rates are effective for a variety of freezing applications nonuniform rates may need to be developed for some cells and tissues if adequate viability is not obtained.

Optimal cooling rates have been obtained for various mammalian cell types and range from 0.3°C to 10°C/min and are generally determined with experimental studies. Optimal slow cooling conditions typically result in some cell shrinkage (dehydration) without the formation of damaging quantities of intracellular ice. The tolerances for cell shrinkage and intracellular ice formation vary between cell and tissue types. The determination of optimal cooling rates for complex tissues typical of tissue engineered medical products often requires optimizing cooling rates for the different cell types within the construct to obtain maximum viability of the entire sample.

Controlled Seeding of Extracellular Ice – Cooling samples to their freezing point and beyond does not automatically result in freezing of the samples at the equilibrium freezing point. There is invariably a tendency for samples to under cool (often referred to as super cooling) to a varying degree that depends upon cooling rate, sample size and the presence of nucleating agents. The probability of intracellular ice formation is greatly enhanced with continued undercooling. A major reason for the use of control rate freezing equipment rather than simply placing samples in cold environments is that experience has shown that control of nucleation and the temperature compensation provided during controlled rate preservation for release of the latent heat of fusion results in improved post-freeze cell viability.

Since cooling rate is a major determinant of cell viability following cryopreservation, it has proved beneficial to avoid variable degrees of undercooling in multiple samples by deliberately inducing freezing (nucleation) at a point when the samples have cooled a few degrees below their equilibrium freezing point. In this way, a more uniform cooling profile can be achieved for multiple samples. Varieties of other methods have been employed to induce freezing including contact with a cold material, mechanical vibration, and rapid reduction of temperature until ice nucleation occurs. The latter approach is often employed in commercial controlled rate freezers. Since freezing is an exothermic process,

heat release (known as the heat of fusion or crystallization) during ice formation must be conducted away from the material that is being frozen to reduce undesired sample warming.

Vitrification

Although cryopreservation with freezing can provide high viability in most cell types and some tissues, it frequently produces sub-optimal preservation for larger, more complex tissues with multiple cell types. In these cases, vitrification has been used as a successful alternative by eliminating some of the problems encountered with freezing methods. Firstly, complete vitrification eliminates concerns for the known damaging effects of intra- and extracellular crystallization. Secondly, tissues cryopreserved by vitrification are exposed to less concentrated solutions of CPAs for shorter periods. For example, during a typical cryopreservation protocol involving slow freezing to -40°C, or -70°C, cells are exposed to solutions whose concentration increases gradually to 21.5 and 37.6 osmolal respectively. In contrast, cells dehydrated in vitrification solutions are exposed for much shorter periods of time to < 18 osmolal solution, although the temperature of exposure is higher [11]. Thirdly, unlike conventional procedures that employ freezing, vitrification does not require controlled cooling and warming at optimum rates - cooling and warming need only be rapid enough to prevent crystallization, and this can generally be achieved without the need for specialist equipment. It is widely anticipated therefore, that for many integrated multi-cellular tissues, vitrification may offer the only feasible means of achieving cryopreservation without ice damage, and for some tissues that appear to partially withstand cryopreservation by freezing, vitrification offers a number of practical advantages that will be attractive in tissue engineering, as indeed they have been for embryo banking [11].

Vitrification can be generally achieved with one of two approaches or a combination of both. The first approach employs cooling highly concentrated solutions (typically >50% w/w) that become sufficiently viscous at low temperatures to suppress crystallization rates. Typically, a vitrified material is considered solid when the viscosity reaches 10^{15} poise [1]. Vitrification can also be achieved by selecting sufficiently high cooling rates to prevent ice crystallization in relatively dilute solutions (<50% w/w). This approach generally produces a metastable state that is at risk of devitrifying (recrystallization) during warming and ice formation during warming is just as injurious as during cooling. Nevertheless, vitrification procedures have been developed by with this technique and have been shown to provide effective preservation for a number of cells, including monocytes, ova and early embryos and pancreatic islets [12-15].

A principle benefit of vitrification is the elimination of requisite studies to determine optimal cooling rates for tissues with multiple cell types. With vitrification, it is only necessary to cool solutions at critical rates in which a negligible fraction of the solution forms ice (typically < 0.2%) [16]. Vitrified materials have a similar rate requirement during heating when samples are rewarmed for subsequent use. During rewarming, it is required that heating occur at critical rates in which the amount of solution that devitrifies to ice upon rewarming is negligible (typically <0.5%) [17].

Development of optimum vitrification solutions requires selecting compounds with glass-forming tendencies and tolerable levels of toxicity at the levels required to achieve

vitrification. Due to the high total solute concentration within the solution, stepwise protocols should be used under low temperatures for the addition and removal of cryoprotectants to limit excessive volume excursions and lower the risk of toxic side effects.

Anhydrobiotic Preservation

Although freeze-drying technology has been used to process de-mineralized bone, the use of anhydrobiotic preservation methods to stabilize mammalian cells is emerging. Preservation technologies have been developed that maintain cell viability during drying and rehydration in small numbers (3-4%). Maximum viability via anhydrobiotic stabilization has been primarily achieved in non-nucleated cells such as red blood cells and platelets. Current efforts in several areas are focused upon the application of lyophilization technology to nucleated cells as well as tissue-level materials. As previously mentioned, the principle advantage of dry-stabilized materials is that the glass transition temperature of the product lies near or even above ambient temperatures. High glass transition temperatures permit storage and transport of biological materials to occur under ambient conditions with the use of special equipment. Although feasibility has been demonstrated, there are several significant technical hurdles to be overcome during the optimization of drying and subsequent rehydration.

It has been well-established in the development of pharmaceutical products that well planned freeze-drying formulations can maintain adequate physical and chemical stability of proteins during shipping and long-term storage, even at ambient temperatures. Experience has identified five criteria as a starting point for successful freeze-dried protein formulation (Table 1).

Table 1 - *Criteria for a Successful Lyophilized Protein Formulation*

• Protein unfolding inhibited during freezing and drying
• The glass transition temperature of the product is above the anticipated storage temperature
• The water content is relatively low (2% or less by mass)
• A stable cake structure is obtained (collapse and meltback are avoided)
• Steps are taken to minimize specific routes of product degradation (i.e., packaging sealed under nitrogen to reduce rate of oxidation)

Storage

For preserved cells and TEMPs, storage temperature is a determining factor of product shelf life. In most cases, lower storage temperatures provide longer viable storage periods. However, the preservation method and the intended duration of storage generally define the type of storage containment system. The storage temperature and duration for hypothermic materials is generally a function of the capacity of the hypothermic storage medium to maintain cellular stasis. For desiccated or freeze-dried materials it is required that the storage temperature is maintained below the glass

transition temperature of the material. The shelf life of freeze-dried materials is often the subject of many stability studies but is typically about months if not years.

Cryopreserved cells and tissues have been safely stored with mechanical freezing equipment at temperatures below –70°C for extended periods. Although many types of samples can be stored at -70°C for months or even years, the chemical reactions responsible for cellular deterioration are not completely halted at this temperature and therefore anaerobic metabolism continues albeit at a significantly slower pace. For increased shelf life, cooling below the glass transition temperature is recommended. The glass transition temperature, T_g, represents a point in which translational motion of all molecules becomes very slow or non existent. In a practical sense, the motion of water and solute molecules becomes effectively arrested causing ice nucleation and growth to cease.

For frozen products, short-term storage periods above the glass transition may not produce appreciable changes in cellular health. However, evidence shows that sample degradation can occur for extended periods at temperatures above the solution's glass transition temperature. For example, protein synthesis in heart valve leaflets is retained at normal levels for two years within the patient when stored at temperatures below -135°C, but is reduced after storage above -100°C [18]. Therefore, stability studies are recommended to ensure product quality does not fall below levels specified at the time of use.

Contrary to frozen cells and tissues, vitrified samples must be stored below the glass transition temperature since the range of ice nucleation of most vitrification solutions becomes significant a few degrees above T_g. For extended storage periods, it is suggested that cryopreserved cells and TEMPs are maintained well below the glass transition temperature [19, 20]. Vitrified materials stored at levels well below T_g should be handled with minimal vibration. Since vitrified materials are glassy solids, they have the potential to form cracks due to inherent thermal stresses in the material that formed during cooling, a problem most predominant in large volume samples [21]. The formation and the disappearance of cracks in experimental cryopreservation solutions depends on the interaction of several factors, in particular the mechanical properties of the material, the concentration of solute, the temperature gradients, the overall temperature, and the rate of temperature change [22-24]. Studies of frozen biological materials have also supported the presence of mechanical forces in cryopreserved tissues [25, 26]. Annealing processes can be applied to samples by briefly warming the material slightly above T_g to relieve these stresses and reduce the risks of cracking [27].

Cryogenic storage temperatures can be achieved with mechanical refrigeration (-80 to -150°C) or nitrogen systems using vapor (-140°C to -196°C) and liquid phases (-196°C). Unless required, storing materials within liquid nitrogen should be avoided. Caution should be used if rapid cooling with liquid nitrogen is used because immersion of tissues directly into liquid nitrogen for as little as 5 minutes may result in tissue fractures [28]. Although liquid phase storage offers a uniform temperature of -196°C, many packaging materials may leak and allow nitrogen to enter the package. Leakage of nitrogen into the containers creates a risk of contamination with freeze hardy microbes floating in the liquid phase nitrogen. Vapor phase storage can be used for non-liquid phase storage requirements. The principle disadvantage of vapor phase storage is a lack of a uniform temperature profile throughout the storage container. Raising liquid levels or adding

conductive material liner such as aluminum aids in reducing thermal gradients between the top and bottom of the container. Therefore it is important to fill nitrogen dewars with the maximum number of racks or containers. This combined with a temperature or fluid level monitoring procedure should minimize temperature fluctuations within the storage container. Storage procedures should include the use of temperature monitoring and audible alarm systems to provide thermal history information of preserved samples as well as provide alerts in the event of equipment failure. The alarm system should provide appropriate warning information well before product temperatures reach damaging levels to permit corrective intervention.

Transportation Issues

The transportation of preserved cells and TEMPs requires systems that are compatible with the storage temperature and duration requirements of the product and the original preservation method. Additional shipping time should be considered when shipping preserved materials to account for unexpected delays in transit systems. Consideration should be given when shipping hypothermically preserved materials that the packing material is not below the equilibrium freezing temperature of the storage solution to prevent inadvertent nucleation and freezing. Cryopreserved products stored at vapor or liquid phase nitrogen temperatures can be shipped with a nitrogen dry shipper. In all cases, the shipping container and samples should be inspected upon arrival to ensure that the sample and container are free of damage and that the thermal integrity of the sample area was maintained. Some form of temperature monitoring within the sample area during shipping is recommended to track the product's thermal history and should be part of an overall quality system. Additionally, adequate identification tags should be placed on every product container listed on the shipping inventory. All containers should be adequately packed to minimize excessive vibrations during handling.

Post-Preservation Treatment

Following preservation, cells and TEMPs are returned to normal physiological stasis to permit functional recovery with optimized protocols compatible with the method of preservation. Cryopreserved materials must be rewarmed sufficiently to preclude ice formation and recrystallization as well as thermal cracking. Frozen and vitrified materials are typically rewarmed to temperatures slightly above the equilibrium melting temperature of the solution at which point the cells and tissues may be returned to isotonic physiological solutions or body fluids following cryoprotectant removal. In practice, many cryopreserved cells and tissues are rapidly rewarmed to 0°C in a warm water bath and then placed on ice for CPA removal. Cryoprotectants are generally diluted using protocols designed to prevent excessive osmotic stresses. Placement on ice reduces the risk of cytotoxicity effects until CPA concentration is diluted to safe levels.

During rewarming, melting ice generates available water that dilutes the previously concentrated extracellular solution that creates an automatic osmotic imbalance with the intracellular compartment. This imbalance is corrected by water transport into the cell with a concomitant efflux of cryoprotectant. The process, which is temperature-dependent, continues until melting. The rate of water and cryoprotectant transport is

temperature-dependent and therefore increases as warming continues. Carefully selected warming rates can produce optimal cellular rehydration and minimize recrystallization effects during thawing. The interaction between cooling and warming rate can be more clearly seen by examining the fact that many cryopreservation processes are dependent upon thermal history. The state of the system at the initiation of rewarming is primarily a function of the cooling rate and the initial physicochemical state at the beginning of cooling. It is clear that cooling rate and warming rate cannot be optimized independently.

However, most protocols are developed without examining variations in warming rates. This typically occurs when protocols are optimized by studying different cooling rates with a constant warming rate conveniently obtained with the use of warm water baths that produce rapid rewarming. Once acceptable viability levels are obtained, little interest is given to evaluating warming rate. Extensive experimental studies may be required to determine the correct combination of cooling and heating rates to produce maximum cell survival rate. For example, the successful preservation of mammalian embryos was achieved only after it was discovered that slow warming was essential for survival [29]. Similarly, it is now known that red blood cells, which have traditionally been cryopreserved using rapid cooling and warming, can be successfully recovered after slow cooling in the presence of glycerol if they are also thawed slowly [30].

The rewarming of vitrified materials requires careful selection of heating rates sufficient to prevent significant thermal cracking, devitrification and recrystallization during heating. Carefully designed warming protocols are necessary to maximize product viability and structural integrity. Vitrified materials may require an initial slow warming step to relieve residual thermal stresses that developed during cooling. Dwell times in heating profiles above the glass transition should be brief to minimize the potential for devitrification and recrystallization phenomena. Devitrification is an occurrence of ice nucleation and subsequent growth that occurs when vitrified materials are slowly warmed through successive temperature ranges for maximum ice nucleation and optimal crystal growth. Rapid warming through these temperature regimes generally minimizes prominent effects of ice crystal damage.

Summary

Several issues related to biopreservation processes have been presented. Many of the techniques discussed have successfully been applied to a wide variety of cells and tissues. Manufacturers of TEMPs considering biostabilization methods as part of their product have an increasing number of preservation techniques available for evaluation. Determination of standards related to biopreservation will be integral in ensuring final product quality and integrity at the end-point of use.

References

[1] Franks, F., "The Properties of Aqueous Solutions at Subzero Temperatures," *Water: A Comprehensive Treatise, Vol. 7*, F. Franks, Ed., Plenum Press, NewYork, 1982.

[2] Taylor, M.J., Elrifai A.M., and Bailes, J.E., "Hypothermia in Relation to the Acceptable Limits of Ischemia for Bloodless Surgery," *Advances in Low*

Temperature Biology, Vol 3, P.L. Steponkus, Ed., JAI Press, London UK and Greenwich, CT, 1996, pp. 1-64.

[3] Taylor, M.J., US Patent Serial # 5,405,742. April, 1995.

[4] Taylor, M.J., "Biology of Cell Survival in the Cold" *Transplantation: Principles and Practice,* J.M. Dubernard and P. McMaster, Eds., Harwood Academic Publishers, Amsterdam, (In Press).

[5] Kruuv, J. and Lepock, J.R., "Factors Influencing Survival of Mammalian Cells Exposed to Hypothermia. VI. Effects of Prehypothermic Hypoxia Followed by Aerobic or Hypoxic Storage at Various Hypothermic Temperatures," *Cryobiology*, Vol. 35, 1995, pp. 191-198.

[6] Kruuv, J., Glofcheski, D.J. and Lepock, J.R., "Evidence for Two Modes of Hypothermic Damage in Five Cell Lines," *Cryobiology*, Vol. 32, 1995, pp. 182-190.

[7] Kruuv, J., "Survival of Mammalian Cells Exposed to Pure Hypothermia in Culture". *Advances in Molecular and Cell Biology, Vol. 19*, JAI Press. Greenwich CT, 1997, pp. 143-192.

[8] Taylor, M.J. and Hunt, C.J., "A New Preservation Solution for Storage of Corneas at Low Temperatures," *Current Eye Research*, Vol. 4, No. 9, 1985, pp. 963-973.

[9] Brockbank, K.G.M. and Smith, K.M., "Synergistic Interaction of Low-Molecular-Weight Poly-vinylpyrrolidones with Dimethyl Sulfoxide During Cell Preservation." *Transplant Proceedings.*, Vol. 25, 1993, pp. 3185.

[10] Brockbank, K.G.M., U.S. Patent 5,145,769, and Patent 5,158,867, 1992.

[11] Rall, W.F., "Factors Affecting the Survival of Mouse Embryos Cryopreserved by Vitrification," *Cryobiology*, Vol. 24, 1987, pp. 387-402.

[12] Fahy, G.M., "Vitrification," *Low Temperature Biotechnology: Emerging Applications and Engineering Contributions,* J.J. McGrath and K.R. Diller, Eds., American Society of Mechanical Engineers, New York, 1988, pp. 113-146.

[13] Jutte, N.H.P.M., Heyse, P., Jansen, H.G., Bruining, G.J. and Zeilmaker, G.H., "Vitrification of Mouse Islets of Langerhans: Comparison With a More Conventional Freezing Method," *Cryobiology*, Vol. 24, 1987, pp. 292-302.

[14] Jutte, N.H.P.M., Heyse, P., Jansen, H.G., Bruining, G.J. and Zeilmaker, G.H., "Vitrification of Human Islets of Langerhans," *Cryobiology*, Vol. 24, 1987, pp. 403-411.

[15] Van Wagtendonk-De Leeuw, A.M., Den Daas, J.H.G., Kruip, T.A.M. and Rall, W.F., "Comparison of the Efficacy of Conventional Slow Freezing and Rapid Cryopreservation Methods for Bovine Embryos," *Cryobiology* Vol. 32, 1995, pp. 157-167.

[16] Boutron, P., Mehl, P., Kaufmann, A., and Augibaud, P., "Glass Forming Tendency and Stability of the Amorphous Stat in Aqueous Solutions of Polyalcohols with Four Carbons. I Binary Systems Water-Polyalcohols," *Cryobiology*, Vol. 23, 1986, pp. 453-469.

[17] Boutron, P., and Mehl, P., "Theoretical Predictions of Devitrification Tendency: Determination of Critical Warming Rates Using Finite Expansions," *Cryobiology*, Vol. 27, 1990, pp. 359-377.

[18] Brockbank, K.G.M., Carpenter, J.F. and Dawson, P.E., "Effects of Storage Temperature on Viable Bioprosthetic Heart Valves," *Cryobiology*, Vol. 29, 1992 pp. 537.

[19] Karow, A.M., "Biophysical and Chemical Considerations in Cryopreservation," *Organ Preservation for Transplantation*, A.M. Karow and Pegg D.E., Eds., Dekker, New York, p. 113, 1981.

[20] Mazur, P., "Freezing of Living Cells: Mechanisms and Implications." *American Journal of Physiology*, 1984, pp. 247-125.

[21] Fahy, G.M., Saur, J.S., and Williams, R.J., "Physical Problems With the Vitrification of Large Biological Systems," *Cryobiology*, Vol. 27, 1990, pp. 492-510.

[22] Wolfinbarger, L., Adam, M., Lange, P., Hu, J.F., "Microfractures in Cryopreserved Heart Valves: Valve Submersion in Liquid Nitrogen Revisited," *Applications of Cryogenic Technology, Vol. 10*, Plenum Press, 1991, pp. 227-233.

[23] Kroener, C. and Luyet, B., "Discontinuous Change in Expansion Coefficient at the Glass Transition Temperature in Aqueous Solutions of Glycerol," *Biodynamica,* Vol. 10, 1966, pp. 41-45.

[24] Kroener, C. and Luyet, B., "Formation of Cracks During the Vitrification of Glycerol Solutions and Disappearance of the Cracks During Rewarming." *Biodynamica,* Vol. 10, 1966, pp. 47-51.

[25] Rubinsky, B., Lee, C., Bastacky, J. and Onik, G., "The Process of Freezing in the Liver and the Mechanisms of Damage." *Proceedings, CRYO 87, 24th Annual Meeting of the Society for Cryobiology*, 1987.

[26] Rajotte, R., Shnitka, T., Liburd, E., Dossetor, J. and Voss, W., "Histological Studies on Cultured Canine Heart Valves Recovered From -196°C." *Cryobiology* Vol. 14, 1977, pp. 15-22.

[27] Baudot, A., Boutron, P., and Descotes, J. L., "Physical Vitrification of Rabbit Aortas Without Any Fracture," *Proceedings, CRYO 2001, 38th Annual Meeting of the Society for Cryobiology*, 2001.

[28] Adam, M., Hu, J.F., Lange, P. and Wolfinbarger, L., "The Effect of Liquid Nitrogen Submersion on Cryopreserved Human Heart Valves." *Cryobiology*, Vol. 27, 1990, pp. 605-614.

[29] Whittingham, D.G., Leibo, S.P., Mazur, P., "Survival of Mouse Embryos Frozen to –196°C and –269°C," *Science*, Vol. 178, 1972, pp. 411-414.

[30] Miller, R.H., and Mazur, P., "Survival of Frozen –Thawed Human Red Cells as a Function of Cooling and Warming Velocities," *Cryobiology*, Vol. 13, 1976, pp. 404-414.

What Standards Are Used Globally and How by the Regulatory Bodies for Approvals?

Eliane Schutte[1]

The European Situation on Standards for Tissue Engineering Products

Reference: Schutte, E., "**The European Situation on Standards for Tissue Engineering Products,**" *Tissue Engineered Medical Products (TEMPs), ASTM STP 1452*, E. Schutte, G. L. Picciolo, and D. S. Kaplan, Eds., ASTM International, Wet Conshohocken, PA, 2004.

Abstract: Human tissue engineered medical products are not regulated on a European level. This means that, to date, various national approaches exist to regulation of Tissue Engineered Products in Europe. In general, diversity exists how these products should be regulated. Some Member States wait for the European Commission to take a position and fill in the gap of regulation. Other countries develop specific regulation on human tissue products, and use elements on tissue banking principles; other countries use the pharmaceutical approach, whereas others use the medical device regulation as a basis.

The industry favors a new regime based on a risk/ benefit based approach. The Directive should define essential requirements, and to demonstrate compliance to these requirements, harmonized standards should be used.

Recently, some new initiatives have started, concerning future harmonized European regulation, such as the draft Directive as "Setting high standards of quality and safety for the procurement, testing, processing, storage and distribution of human tissues and cells", in order to ensure a high level of human health protection. At the same time the European Commission solicited input for a framework to solve free trade amongst Member States.

Keywords: European regulatory framework, Tissue Engineered Medical Products, Draft Directive DG Sanco, DG Enterprise, EMEA, standards

Introduction

Although current medical technology can solve many clinical problems, it is clear that use of conventional hardware components cannot adequately substitute for complex human body parts. The tissue engineering technology offers a solution to existing clinical problems by using the human body's own regenerative capacity. Human cellular- and tissue-based products, developed with use of the tissue engineering technology, include

[1] MSc, Vice President Regulatory Affairs/ Operations, IsoTis NV, Prof. Bronkhorstlaan10 geb 10D, 3723 MB, Bilthoven, The Netherlands.

an array of medical products used for repair, reproduction, replacement or other therapeutic purposes.

Typical examples of tissue-engineered products are orthopedic prostheses (bone, cartilage), cardiovascular prostheses (heart valves, blood vessels, arteries), neurological tissue repair, skin repair, muscle repair, liver or pancreatic regeneration/prostheses, and prostheses for urinary tract.

Developments in the United States

With recent technology advances, regulators all over the world have become more concerned about the oversight of these products to protect recipients from transmission of communicable diseases.

The FDA acknowledged the unique nature of the tissue engineered products and adapted its regulatory scheme by combining expertise from two existing departments, Center for Biologic Evaluation and Research (CBER) and Center for Devices and Radiological Health (CDRH). In addition to existing regulation and classification FDA developed specific regulations for production and use of human tissues [1,2,3]:

- Establishment registration and product listing rule,
- Donor suitability; which defines screening and testing requirements for donors; and
- Good Tissue Practices.

Wild West Situation in the European Union

Currently, human tissue products are not regulated on an European level. According to article 1.5f of the Medical Device Directive (93/42/EEC), all products with a human component are excluded from the directive. Hence, many of these products also do not meet the definition of a medicinal product as defined in the medicinal directive 65/65/EEC. In the absence of clear regulation for these products, several initiatives in Europe have been prepared to define regulation.

In conclusion, to date, in Europe various national approaches to the regulation of human tissue products exist. Manufacturers of any human tissue product will have to ask for approval for each of the Member States.

Table 1 provides a short list of examples of how autologous tissue engineered products are regulated in various countries of the European Union.

Table 1—*Regulation of autologous tissue engineered products in Europe.*

Country	Current situation
The Netherlands	- Law on Quality and safety of human body materials passed the second chamber in the fall of 2002. - All produced human products need to be registered . Manufacturers will be inspected.
Germany	- Arznei Mittelgesetz (pharmaceutical regulation) - No market authorization required for autologous products; approval from the governmental state

	importing the product is required. GMP compliance certificate required.
Austria	- Arznei Mittelgesetz (pharmaceutical regulation). - Only registrations after GMP certificate.
Switzerland	- Local responsible clinician is required. - Approval from the Swiss authorities based on a product file.
France	- Life saving product can be on the market after approval. - Other products only after full clinical investigations.
Spain	- Import only via tissue banks. - The manufacturer must have a contract with a local tissue bank. - Spanish Transplantation Association called Organizacion Nacional Transplantation (ONT) shall give an approval based on the contract with the tissue bank and a product file.
Norway	- Import after approval from the Norwegian Board of Health on exceptional import.
UK	- Waiting for the EU to regulate these products. - Code of conduct for tissue banks is applicable to tissue banks in the UK. - First prove that it is not a pharmaceutical product.
Belgium	- Import via tissue banks.
Italy	- Currently developing legislation.

In some countries the product can only be imported via tissue banks. In other countries pharmaceutical regulation must be followed. In a third category of countries no regulations exist, but will be developed soon in absence of EU regulation.

Experience to launch a product in the European Union

The system in The Netherlands illustrates the difficulties experienced when a tissue engineered product is marketed within Europe. Due to absence of regulation in the Netherlands and no mandate by the Dutch authorities to inspect human tissue production sites, a trade barrier to Germany and Austria existed because both countries required a GMP compliance certificate. Some countries, such as Spain, require a tissue bank as an intermediate agency to take over responsibility for the product once human tissue is imported to the Spanish market. For autologous products this is purely an administrative route to the tissue bank. Other countries protect the market by arranging contracts with tissue banks and thereby protecting the local markets from outsiders. Some countries ask for clinical trials. In complete contrast to this is the situation of a growing number of hospital labs throughout Europe where culturing on a small-scale of human cells for human application is still allowed without any regulatory constraint.

The variations in regulation of these emerging therapies results in gaps and inconsistencies in regulation and creates confusion for the industry. It presents a very

difficult environment for consistent and safe development and marketing of human tissue products. [4]

A tremendous amount of time is spent by regulatory affairs departments to find out local regulation, find the appropriate regulators, submit separate files and keep up to date with the changing environment in every country. This vacuum and a potential pharmaceutical framework for all these products create a disadvantageous situation for the industry. The industry in Europe asked the European commission to act quickly for European Union wide development of regulation.
Although many initiatives are as of today ongoing, which will be discussed later in this document, no decision has yet been taken by the European Commission.

European Commission

The main Directorate-Generals (DGs), hat are involved with tissue products in Europe are the Health &Consumer protection Directorate-General (DG SANCO), responsible for consumer protection, and DG Enterprise, responsible for the putting products on the European Union market and solving trade barriers. Within the DG Enterprise two departments are concerned with Tissue Engineered Medical Products, DG Enterprise "F" is responsible for Pharmaceutical products and DG Enterprise "G" is responsible for Medical devices.

The following sequence of initiatives concerning Tissue Engineered Medical products (TEMPs) has been taken in Europe. The three most relevant documents will be explained in more detail.

1. The central authority for regulation of pharmaceuticals, the European Agency for the Evaluation of Medicinal Products (EMEA), committee for proprietary medicinal products (CPMP) developed a concept paper of that gives points to consider on the manufacture and quality control of human somatic cell therapy, May 2001 [5]
   This concept document was an initiative from the Biologics and Biotechnology Sector division within the central pharmaceutical regulatory authority. The paper proposes to define a different definition of pharmaceutical products and addresses the main points to consider for all human somatic cell therapies, including all tissue engineered medical products.

2. The European Commission DG Sanco Scientific committee (SCMPMD) provided an "Opinion on the State of the Art of Tissue Engineering" 2001 [6].
   The scientific committee of the DG Sanco in the European committee published this paper. The opinion provides a description of the scope of tissue engineering and related products, a summary of risk factors associated with the future use of tissue engineering techniques and a series of observations and eight recommendations concerning the desirability of regulatory intervention at the community level.
   The SCMPMD concludes that there could be a need for a specific legal framework, different from the medical devices and pharmaceutical products regulatory systems. According to the Scientific Committee, a medical technique should not be regarded as tissue engineering when it involves the isolation of cells from some appropriate donor and their delivery to the site of treatment with only minimal manipulation. As yet,

there is no agreed definition of human tissue engineering. The Scientific Committee suggests that tissue engineering is the "regeneration of biological tissue through the use of cells, with the aid of supporting structures and/or biomolecules." However, as the Committee states, there is a need to produce a scientifically valid and legally sustainable definition of tissue engineering and tissue engineered products in order to underpin a legislative framework and to provide a sound basis for demarcation, between tissue-engineered products on the one hand and medical devices, pharmaceutical products and cell therapy on the other.

3 The European Commission DG Sanco Proposed Directive on "Setting High Standards of Quality and Safety for the Donation, Procurement, Testing, Processing, Storage and Distribution of Human Tissues and Cells to Ensure a High Level of Human Protection in the Community," came out on 24 June 2002 [7].
During a meeting convened under the Portugese Presidency in Porto in June 2000, experts in the area of tissues and cells analysed the regulatory situation in Europe and concluded that there is an urgent need for an EC Directive on the safety and quality of these human substances. This draft Directive proposal establishes a framework of Community legislation to ensure a high level of quality and safety for human tissues and cells, while leaving fundamental decisions on the ethically problematic use of cells, such as embryonic stem cells, to Member States. Insofar as is possible under Article 152, it also addresses the health and rights of donors. With its comprehensive approach, establishing requirements ranging from accreditation and inspection of tissue establishments to the labelling of tissues and cells, this proposal represents a step forward in regulating tissues for application in and on the human body. This proposal from the DG Sanco is currently being reviewed at the Member States and in the EU Parliament. This draft directive covers tissue products, including traditional transplants, as well as some Tissue engineered Medical products, and sets standards for quality and safety. This intended regulation doesnot solve the part where the products are put on the market nor solves any trade barrier. The draft directive will be discussed in the following section.

4 Amendment of Directive 2001/83 of medicinal products Annex I, would modify the pharmaceutical directive (2001/83/EC]. This proposal would change the current definition on pharmaceutical products to include basically all TEMPs [8].
This proposal will be discussed at the next council of ministers on December 2, 2002. The current discussion is still focused on the question whether all TEMPs should be covered under this definition. The next revision also could very well address only the products, with a primary intended mode of action being the pharmacological, metabolic or immunologic action. This is consistent with the current demarcation between medical devices and pharmaceuticals.

5 European Commission DG Enterprise consultation document "Need for a legislative Framework for Human tissue engineering and Tissue-Engineering products," July 2002 [9].
This consultation document as prepared by DG Enterprise presents an addition to the SANCO draft Directive initiative on setting standards for quality and safety of human tissues and addresses tissue engineering products when they are not covered under the

pharmaceutical regime. It has suggestions for a regulatory regime in order to put products on the market in the European Union. This proposal, with 15 questions to the public, has been posted on the internet [9]. DG Enterprise has solicited feedback on this proposal.

As an overview, the proposed regulatory system for tissues and TEMPs could be visualized as illustrated in figure 1.

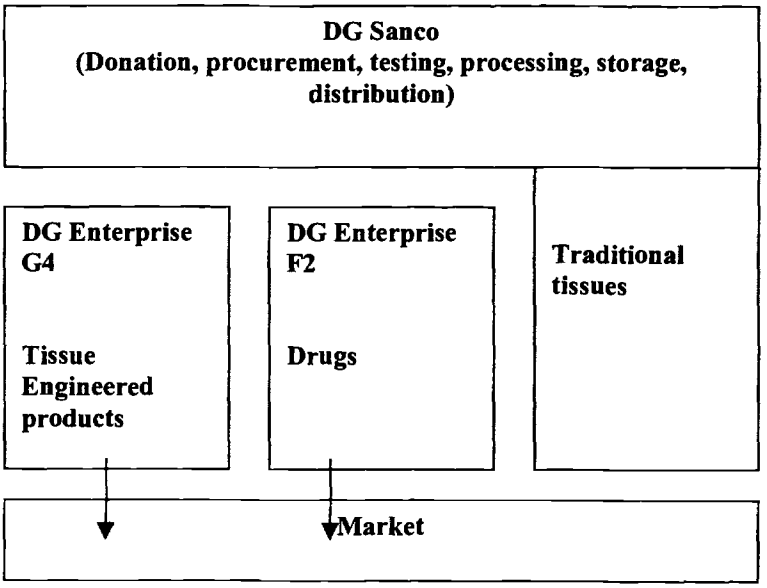

Figure 1 - *Schematic overview of proposed regulatory system.*

European Commission DG SANCO proposal for "Setting High Standards of Quality and Safety for the Donation, Procurement, Testing, Processing, Storage and Distribution of Human Tissues and Cells to Ensure a High Level of Human Protection in the Community," June 24, 2002 [7].

The scope of the directive is "donation, procurement and testing of human cells or tissues for application to the human body." The scope excludes organs, blood and blood products, and tissues and cells used as autograft within the same surgical procedure. It as well excludes autologous cells used for medicinal products such as immunotherapies, cellular cancer vaccines e.g. Furthermore, the proposed directive will apply to the "processing, preservation, storage and distribution of tissues and cells intended for transplantation." The proposed directive did not intend to cover the research using human tissues and cells, when not used to the human body.

It is important to note that article 2.1 states that for industrially manufactured products derived from tissues and cells, this directive applies only to donation, procurement and testing. The Directive proposes the following controls:

- Accreditation of Tissue Banks: All activities relating to the processing, preservation, storage and distribution of human tissues and cells for human transplantation can only be undertaken by accredited tissue banks.
- The Member States shall ensure that the competent authority organizes inspections and that the tissue bank carries out appropriate control measures. The interval between inspections shall not exceed two years.
- The import and export of human tissues and cells for transplantation shall be undertaken only through accredited tissue banks. There is in this clause no provision for ensuring free placing on the market within the European Union.
- Tissue establishments should take all necessary measurements to ensure all tissues can be traced from donor to recipient and visa versa.
- Serious adverse events shall be reported to the competent authority.
- Promotion and publicity activities to support the donation of human tissues and cells should receive prior approval of the competent authority and donation shall be encouraged to be carried out on a non-profit basis.
- Mandatory consent shall be obtained from the donor and recipients. All data, including genetic information, must be rendered anonymous so that the donor and the recipient are no longer identifiable.
- Specifications are set for donor testing for allogenic and autologous use.
- A responsible person should be appointed for ensuring proper testing of every unit of tissues and cells.
- Provisions for quality and safety in tissue processing cover general basic quality management aspects, such as quality system documentation and record keeping qualification of personnel, tissue and cell reception and tissue and cell processing, storage, labeling, user information and packaging, transport and distribution.
- Access to human tissues and cells shall be ensured by Member States without prejudice to the provisions in the force in Member States on the use of certain tissues and cells such as embryonic. This Directive does not prevent Member States from maintaining or introducing more stringent protective measures.
- Exchange of information, reports and penalties chapters cover aspects of identification and traceability, a single European coding system (to be defined). Penalties are applicable to violations.
- Furthermore the draft document includes seven very detailed annexes concerning:
- Requirements for the procurement of human tissues and cells,
- Quality management,
- Information to be provided on the donation of cells and/or tissues,
- Selection criteria for the donor of tissues and/or cells,
- Laboratory test required for donors,
- Cell and/or tissue procurement procedures and reception at the tissue bank, and
- Tissues and cell processing, preservation and distribution.

Commentary

The current draft directive does not clearly define its scope of application and the types of products to which it applies. Although the scope states that it excludes autologous cells used for medicinal products such as immunotherapies, and that for industrially manufactured products derived from tissues and cells (tissue engineering), only the donation, procurement and testing parts apply, it is still unclear which specific parts of these directives do apply.

The proposed directive is very much driven by traditional tissue banking practices and is for industry working with tissue engineering too light in its quality management requirements and too restrictive and prescriptive in defining procurement, processing and testing requirements and will be inappropriate for rapid innovation in this field.

Article 152 of the Treaty of Amsterdam, has provided the European Community (EC) with an opportunity, as well as an obligation, to implement binding measures laying down high standards of quality and safety for the use of blood, organs, and substances of human origin. This is the fundament of this draft Directive. This draft directive is not sufficient or adequate for placing products on the market. This is outside the remit of DG Sanco and beyond the authority conveyed by Article 152. The wider scope proposed for "transplants," covering a wide range of products, could remove the impetus for an Enterprise directive based on the single market. Because the DG Sanco directive does not (can not) address issues of placing products on the market, and does not cover the manufacture of tissue products, this leads to a potential for a continuing gap in the legislative framework for these products. Furthermore the Directive even states that this Directive doesnot prevent Member States from maintaining or introducing more stringent protective measures.

The Directive is mainly oriented to the allogeneic use of tissue and cells. Allogeneic and autologous products are treated in almost the same way, without any consideration on the different risks and health concerns posed. For some requirements, such as the accreditation of the procurement centers it is hindering industry to develop these technologies, because the success of the human tissue product often depends on the manner of tissue harvesting. Industry organizes its specific training for those involved in harvesting procedures. Accreditation of each new customer by an outside party unfamiliar with the specifics of the technology is significantly slowing down access to patients and is an unnecessary burden.

The draft proposal gives the impression of inherent inconsistencies. As an example; traceability from donor to recipient is mandatory but on the other hand data must also be rendered anonymous. It is unclear how these two conflicting requirements can be combined and implemented.

Nothing in the proposed Directive specifies how these requirements should be applied to tissue products. For example, will manufacturers of "unregulated" products currently on the market have to demonstrate that their procurement activities meet these requirements?

The proposal covers donation, procurement e.g., and distribution, but excludes aspects relating to the evidence of efficacy of the product.

European Commission DG Enterprise Consultation Document, "Need for a Legislative framework for Human Tissue Engineering and Tissue-Engineered Products," July 2002 [9].

This initiative from DG Enterprise presents a suggestion for a new approach to regulate tissue engineered products. The document solicits input on 15 questions regarding the new regulatory framework. The paper has been listed on the internet since July 2002 [9].

The document recognizes tissue engineering as a new and rapidly developing technology and that it differs from standard therapies in that the engineered products become integrated within the patient, affording a potentially permanent and specific cure of the disease, injury or impairment. It is acknowledged that this is an interdisciplinary field, which applies the principles of biology and engineering.

The introduction of the paper states that tissue engineering is far from having reached the maturity and the stability of the pharmaceutical and medical devices sectors and neither the development of knowledge and technologies nor the potential risks are fully foreseeable. The challenge for legislators is to strike the correct balance between the possibility for patients to gain rapid access to new and highly promising types of products, and appropriate guarantees on safety and quality. Different opinions have been expressed as to the scope of any legislation for tissue engineering. As indicated by the Commission's Scientific Committee on Medicinal Products and Medical Devices (SCMPMD), some tissue engineered products may be considered analogous to medical devices, but in many ways they are quite different. Similarly, some carry risks of the same types as are associated with pharmaceuticals (e.g., cell therapy products), but again are very different in other respects such as the mode of action, the intended use. The SCMPMD therefore concludes that there could be a need for a specific legal framework, different from the medical devices and pharmaceutical products regulatory systems. Another possibility might be to include a tissue engineering legislation in one of the existing legislative frameworks (pharmaceutical or medical devices).

The consultation document addresses various questions related to whether there should be a differentiated approach between different kinds of products and whether the Committee's suggestion for a new specific legal framework, different from the medical devices and pharmaceutical products regulatory systems, is the preferred option. The DG enterprise framework envisaged excludes gene therapy and proposes a third (new) legal framework in addition to the existing medical device and pharmaceutical regime, and covers:

- human organs produced by a process of bioengineering (BioOrgans), and
- tissues and cells, autologous and allogeneic, both non-viable and viable, and including combined tissue/non-tissue type products that have been substantially modified by treatments butt do not exert their effect through metabolic, pharmacological or immunological means.

It is proposed not to cover xenogeneic organs, tissues and cells as they are considered to be already covered by the medicinal product Directives.Questions are asked such as:

1) this idea is acceptable for legislative scheme, and
2) further borderlines need to be defined, for instance regarding cell therapy or stem

cells or whether the fact that cells have a metabolic pharmacological or immunological effect should be the only criteria relevant for legislative purposes.

The consultation document states that although there is a need for more detailed rules, the "new" legislative framework may have to be limited to fundamental issues in order to allow for technological progress. There is a need for further, substantiate the requirements. These may take the form of:

- Guidance documents compiled by authorities;
- Binding rules adopted by authorities, and
- Standards for voluntary application, compiled by the relevant European standards bodies (e.g., for the matrix).

In the consultation document, questions are asked whether there is a role for standardization or guidance by regulators and whether the provisions on clinical tests for new biological medicinal products (approval to start the clinical trials) are appropriate. If the proposal from DG Enterprise is received positively, there might be a role for standardization in the future regulatory regime.

Standardization in Europe

In case the DG Enterprise document does obtain sufficient positive feedback, a following step is to define regulatory systems in more detail. Standards may become a part of the overall regulatory system. This part provides a general overview on how standards are used in Europe and subsequently provides an overview of current thinking of areas for standardization for tissue engineered medical products.

Definition

Standardization is a mechanism by which interested parties establish, on the basis of a consensus, by means of an open and transparent procedure, technical specifications that are adopted as standards after a public enquiry and with which compliance is voluntary. The standards should be developed within a framework of recognized standards organization.

Benefits

In standards, agreements between parties are documented on the basis of consensus. Examples are requirements of a product, production process, tests that the product has to undergo etc. Standards are always developed with a specific purpose in mind. Standards are used as a support vehicle to comply with legal requirements, for certification or internal efficiency or marketing. Standardization, however, does not normally cover price agreements, market distribution or contact agreements.

Standardization and certification are related instruments, which are often used to encourage the market mechanism. For medical devices, standards have been developed and used for years in Europe. Normalization and certification are often related instruments, which are used to give a meaning to legislation. Standards are often part of self-regulation. If addressed well, innovation is possible. It can influence free trade and

influence quality levels of products. In the US standards are also used by regulators and are in these instances not voluntary.

The health care is a community sector in which the governments, national and international, chose to protect the public concerns within a legal framework. The Medical Device Directive is an example where the public concern is protected via regulation and is further developed via standards and partly required certification.

Medical Devices in Europe

An example of how this works in Europe is the medical device field. For commercial distribution, the product must meet "Essential Requirements" as described in the Medical Device Directive. This has been organized in specific rules with a specific responsibility for the manufacturer, government and notified body. The requirements of the specific rules are filled in by voluntary recognized norms and sometimes cover a mandatory certification.

Two main standardization institutes are important. One is CEN, whose aim is to harmonize standards and develop European Standards in the context of the 'new approach' of the European internal market. It addresses conformity assessment issues and European Standards (ENs).

The other is the ISO, the International Organization for Standardization and its aim is to harmonize standards and develop International Standards.
Not all requirements have been listed in the Medical Device Directive, just the requirements that relate to putting the product on the market. The standards, which are developed should not be design specific, but rather based on a horizontal basis with performance requirements. The standards give the manufacturer the possibility to address requirements where deemed applicable to the design, development and operation of the device on order to make solid, and sound choices. An example is biological evaluation standards as described in ISO 10993. These standards do not dictate what needs to be done; the choice depends on the situation and the complexity of the problems, such as the type of products, and duration and body contact of the product.

Tissue Engineered Medical Products and ISO/ CEN

Attempts to regulate medical technology product utilizing tissues or cells of human origin in Europe are not new. In the early 1990s it was planned to include the subject of medical devices utilizing human tissues in the draft Medical Device Directive (MDD), but due to a lack of agreement at Council level, the matter was excluded from the finally adopted MDD.

In absence of regulation, the industry and various existing standardization committees showed interest in the following subject areas:

- CEN/TC 285 *Non- active implants* and ISO/TC *150 Implants for surgery*. CEN/TC 285 and its ISO/TC 150 counterpart address both surgical implants and have both expressed interest in relation to various types of Tissue Engineered Implants.
- CEN/TC206 *Biological Evaluation of Medical devices* and ISO/TC194 *Biological evaluation of Medical devices*. CEN/TC 206 and its ISO /TC 194 counterpart both

are interested to address standards for Tissue Engineered Products from a biological safety perspective.

- CEN/TC 55 *Dentistry,* ISO/TC 106 and CEN/TC 170 *Optics and optical instruments,* ISO/TC 172 have potential interest in relation to dental and ophthalmic implants.
- ISO/TC 210 *Quality management and corresponding general aspects for medical devices* has expressed an interest in the area of human tissue products.
- CEN/TC 316 *Medical Devices utilizing tissues* covers today animal tissues used in medical devices and risk management has also expressed interests in this area

Currently, the CHef (CEN Healthcare Forum) is preparing a recommendation as to that tissue engineering is suitable for standardization. Suggestions for titles and scopes of the individual subjects have been defined. The recommendation has not been formalized, It was discussed that vertical standards of the type under preparation of ASTM F4 Division IV would be inappropriate in the European context. There would be a role for a limited number of horizontal standards in subject areas that would be difficult or inappropriate to cover in detailed future legislative texts. Following subjects would be listed as possible subjects:

- Quality systems,
- Biological safety,
- Risk management of tissue engineering,
- Microbiological safety,
- Terminology & definitions,
- Sourcing/inactivation,

In light of the current activities at the European Commission level it was decided by the management of CHef to wait further standardization actions until transparent regulatory principles are known.

Summary

This paper provided an overview of the current activities and initiatives at the European level to develop a harmonized regulatory framework for tissue engineered medical products. This paper is based on the most up-to-date information available today, but because activities are moving quickly, information could be outdated soon. Nevertheless, tissue engineered medical products will most likely have to comply with the requirements of donation, testing and procurement of the DG SANCO document. In addition, for putting the products on the EU market the products could still end up to be all regulated as medicinal products or it might be the case that for products that do not exert their effect through metabolic, pharmacological or immunological means, a third regime is applicable. The system of the third regime is currently on a very high level and no details of how this should function in practice are known. If a medicinal regime is chosen for these types of products, Europe will face a significant competitive disadvantage.
Today, the situation remains unclear. The compromise could win and as result a complex system could exist, possibly hindering future technology development.

References

[1] Federal register "Human Cells, Tissues, and Cellular and Tissue-Based Products; Establishment Registration and Listing; Final rule; delay of effective date," FDA, 1/21/2003.
http://www.fda.gov/cber/tissue/docs.htm

[2] Federal register "Suitability Determination for Donors of Human Cellular and Tissue-Based Products; Proposed Rule; reopening of comment period," FDA, 4/18/2000.
http://www.fda.gov/cber/tissue/docs.htm

[3] Federal register Current Good Tissue Practice for Manufacturers of Human Cellular and Tissue-Based Products; Inspection and Enforcement; Proposed Rule, FDA, 1/8/2001.
http://www.fda.gov/cber/tissue/docs.htm

[4] IAPM / Eucomed Taskforce," European Industry Position on Human Tissue Product Regulation," Brussels, 31 July 1999.
http://www.eucomed.be/

[5] EMEA, Committee for proprietary medicinal products (CPMP), "Points to consider on the manufacture and quality control of human somatic cell therapy," CPMP/BWP/41450/98, May 2001.

[6] European Commission, DG Sanco Scientific committee (SCMPMD),"opinion on the state of the art of tissue engineering," 2001.
http://europa.eu.int/comm/food/fs/sc/scmp/out37_en.pdf

[7] European Commission, DG SANCO Proposed Directive on "Setting High Standards of Quality and Safety for the Donation, Procurement, Testing, Processing, Storage and Distribution of Human Tissues and Cells to Ensure a High Level of Human Protection in the Community," Com (2002) 319 final, 24 June 2002.
http://europa.eu.int.comm/health/ph/othres/human_tissues/index_en.htm

[8] Working document on future revision of Annex 1; Analytical, Pharmatoxicological and Clinical Standards and Protocols in respect of the testing of Medicinal products to 2001/83/EC," 2001
http://pharmacors.eudra.org/F2/pharmacos/docs/Docs2002/april/2001_83an1.pdf.

[9] European Commission DG Enterprise consultation document "Need for a legislative framework for Human tissue engineering and tissue-engineering products, " July 2002.
http://europa.eu.int/comm/enterprise/consultations/list.htm

Robert E. Geertsma,[1] Marjon Kallewaard,[2] and Claes Wassenaar[1]

A European View on Risk Management Strategies for Tissue Engineered Medical Products (TEMPs)[3]

Reference: Geertsma, R. E., Kallewaard, M., and Wassenaar, C., "**A European View on Risk Management Strategies for Tissue Engineered Medical Products (TEMPs),**" *Tissue Engineered Medical Products (TEMPs), ASTM STP 1452*, E. Schutte, G. L. Picciolo, and D. S. Kaplan, Eds., ASTM International, West Conshohocken, PA, 2004.

Abstract: In order to guarantee the quality, safety and efficacy of Tissue Engineered Medical Products (TEMPs), the application of risk management strategies by all parties involved in the life cycle of TEMPs is of the utmost importance. Due to the novelty of TEMPs, their risks have not been clearly and completely identified yet. Extrapolation of experiences with related medical products indicates that the most important risks of TEMPs will relate to the transmission of disease, biocompatibility and efficacy. Many of the risk control measures included in current regulations and standards covering related product categories like medicinal products, blood (products) and medical devices are applicable in generic form to TEMPs. From a regulatory perspective control measures for TEMPs should be combined into a regulatory framework that is complementary to and connects with current European regulation on medical products. Decisions on risk acceptability should preferably be based on predefined standards. Development of internationally accepted standards is therefore essential.

Keywords: Tissue engineering, risk management

[1] Senior Scientists, Centre for Biological Medicines and Medical Technology, National Institute for Public Health and the Environment (RIVM), P.O. Box 1, NL-3720 BA BILTHOVEN, The Netherlands.
[2] Senior Scientist, Department for Health Services Research, National Institute for Public Health and the Environment (RIVM), P.O. Box 1, NL-3720 BA BILTHOVEN, The Netherlands.
[3] Adapted with permission from a previously published report: Wassenaar, C., Geertsma, R. E., and Kallewaard, M. "Tissue Engineered Medical Products (TEMPs): A Prelude to Risk Management," RIVM report 605148009, 2001.

Introduction

Health care technology is facilitated and supported by developments in various fields of science. In the last decade the combination of techniques that are derived from fields like (bio)material science, biochemistry, pharmacology and cellular physiology has produced new solutions for clinical problems and presents a promise for future products. One cluster of techniques is known as "tissue engineering" and has been defined as "the application of principles and methods of engineering and life sciences towards fundamental understanding of structure-function relationships in normal and pathological mammalian tissues and the development of biological substitutes to restore, maintain or improve tissue function" [1]. The products that arise from these techniques may provide an alternative to available therapies to replace damaged, injured or missing body tissues. Conventional therapies either face a limitation of supply and necessitate immunosuppression (transplantation), or do not completely replace all functions of a lost organ or tissue and often fail in the long-term (surgical reconstruction, drugs, mechanical devices). The theoretical possibilities of the concept of tissue engineering drives a large number of research and development programs that have resulted in an increase of knowledge relating to the control of cellular functions and in a growing industrial activity in this area [2]. These developments are expected to result in an increasing number of clinical applications in the coming decade [3].

From the wide range of innovative health care products that combine cellular elements with the traditional materials of construction we have defined a group, which we have labelled as "tissue engineered medical products" (TEMPs) as subject of this review. We have confined our scope to combination products that contain human cells or tissues. Consequently, TEMPs that contain xenogenic sources of cells are excluded. Some of the products under consideration are already available and some are being evaluated in clinical trials. Other products that are merely theoretical possibilities at this moment have also been included.

The combination of living cells with biomaterials in TEMPs creates products for which presently no pan-European regulation is in force [4], although the development of such regulation has recently been initiated. The European Commission and Member States have placed a high priority on developing proposals for a comprehensive regulatory framework for products containing human tissue. DG Sanco has initiated a work programme on the "Proposal for a Directive of the European Parliament and of the Council of setting standards of quality and safety for the donation, procurement, testing, process, storage and distribution of human tissues and cells" which primarily focuses on the donation, procurement and other activities of tissue banking practices. DG Enterprise is reviewing two specific definitions which could well widen the scope of the Medicinal Products Directive (2001/83/EC). DG Enterprise is also conducting an open consultation programme on the "Need for a legislative framework for human tissue engineering and tissue-engineered products".

It may be anticipated that many of the risks associated with TEMPs will be similar to those associated with medicines and medical devices, although new risks will emerge. Therefore, a review of the strategies for management of risks is deemed necessary for TEMPs. Before specific risk management measures can be determined, specific risks must be identified and evaluated. This paper reviews risk management strategies for

TEMPs. Such strategies are important both to manufacturers and to regulatory authorities, who are developing legislation in this area.

Methods

Various literature databases (e.g., Medline, Current Contents) were searched for relevant literature. The Internet was searched for additional information.

The resulting data were used for risk management purposes following the structure of "Medical-Devices- Risk Management - Application of risk management to medical devices" (EN-ISO 14971). Given the generic nature of the strategies described in this standard, it was deemed appropriate not only for the risks that can be related to the application of medical devices, but also of TEMPs. In EN-ISO 14971 the process of risk management is defined as the systematic application of management policies, procedures and practices to the tasks of analysing, evaluating and controlling risk. Risk management is described as a set of repeatable steps throughout the entire life cycle of medical devices, re-evaluation of all steps in this iterative process being essential. It includes the following important elements:

- risk analysis, i.e., basic product characterisation, description of the intended use of the device, identification of known and foreseeable hazards and estimation of their risks,
- evaluation of the identified risks,
- analysis of control options throughout the life cycle of a product, implementation of the selected control measures and evaluation of residual risks,
- a risk benefit analysis incorporating the results of the previous steps, and
- periodical re-evaluation of all previous steps, which incorporates all information available (including post-marketing information).

The primary user of risk management is the manufacturer, because it is this party that is placing the product on the market and therefore has the obligation to ensure quality, including safety. EN-ISO 14971 was designed as a framework to be applied by manufacturers for effective management of the risks associated with the application of medical devices. However, a systematic approach to analysis, evaluation and control of safety problems may also be of use to other parties such as health care facilities, regulatory authorities and researchers.

Risk Analysis

Basic Product Characterisation

TEMPs typically are a combination of three entities, i.e., isolated cells, an extracellular matrix (ECM) and signal molecules, such as growth factors.

The cells can be derived from autologous or allogenic sources. Theoretically, every cell of the body can serve as a source, but at this moment not every cell can be processed (e.g., kept in culture) to become part of a tissue engineered product. Cells can be harvested from embryos in their early stages of development up to adults. Evidently, the

role of the cells is to form a new tissue. The expression of the appropriate genes to develop and maintain the desired tissue-specific functions must be guaranteed in the final product.

The ECM serves three primary roles. First, it facilitates the localisation and delivery of cells in the body. Second, it defines and maintains a three-dimensional space for the formation of new tissues with appropriate structure. Third, it guides the development of new tissues with appropriate function. The ECM can consist of biodegradable, or non-degradable material, usually polymers. These materials can be synthetic, like poly-lactic acid, poly-glycolic acid, hydroxy apatite or isolated from natural sources, like collagen, hyaluronic acid, alginate. The interaction of the cells and the ECM is of great importance for the intended function of the final product.

Signal molecules serve as additional and essential stimuli in order to guide the cells towards their intended function. These signal molecules can be synthesised by the cells during their interaction with the ECM. They can also be isolated or synthesised and attached to the ECM before having contact with cells, or they can be added to the product in a final stage. Examples of signal molecules are Bone Morphogenetic Proteins (BMP), Transforming Growth Factor-ß, Angiogenic Factors, Epidermal Growth Factor, Nerve Growth Factor and Fibroblast Growth Factor [5,6].

Intended Use

The intended use of TEMPs is the treatment of the loss or malfunction of a tissue or an organ. TEMPs are intended to be used as implants or as extra-corporeal devices to be connected to the blood circulation of the patient. While extra-corporeal connection is usually for temporary support (e.g., liver support), the longevity of TEMPs after implantation can vary and will partly depend on the degradation characteristics (possibility and speed) of the matrix and the persistence of viable cells.

TEMPs are supposed to support or replace the functions of diseased tissues. Generally, two specific cell/tissue functions can be discerned: structural (skin, bone, cartilage, blood vessels) and metabolic (e.g., insulin synthesis and secretion). The level of interaction between the product and the tissue of the recipient can be local (providing a scaffold for cells) and/or systemic. Within the group of systemic TEMPs, a subset can be discerned of which the cells are encapsulated. This capsule not only functions as a means to deliver and localise the cells in the body but also as a semi-permeable barrier. The object of this strategy is to prevent immunological recognition and subsequent rejection phenomena while nutrients and cell products can be exchanged with the surrounding recipient tissues.

Hazard Identification

Publications and reports on adverse events with TEMPs are scarce, mainly because of limited clinical experience. Only a relatively small number of products have been available for a few years. Another explanation can be the absence of regulation for this class of products, which means absence of the obligation to report adverse events.

A number of hazards that are related to TEMPs are listed in Table 1a. Most of them are either theoretical or derived from experiences with transplantation of human tissues and organs, or the use of related medical products like medicinals and medical devices [7,8,9]. Additional, but more generally applicable (public health and/or occupational) hazards are, for example, absence of regulation on the safety of hazardous products, control measures themselves (e.g. false-negative HIV test results, virus inactivation steps introducing chemical residues).

Risk Estimation

Risk is defined as the combination of the probability of occurrence of harm and the severity of that harm. Several forms of 'potential harm' that are associated with the hazards in Table 1A are listed in Table 1b. As previously discussed, the clinical experience with adverse events of TEMPs in terms of frequency and severity of outcome is limited. Consequently, quantification of the magnitude of the various risks is very difficult at this moment. However, considering the (clinical) experience with related product groups like organ transplantation and biomaterials, it is foreseen that the most important risks are related to transmission of disease, biocompatibility and efficacy.

Transmission of disease is a significant risk carried by products containing living cells and tissues. Conventional sterilisation procedures cannot be used because they compromise the viability of cells and therefore the efficacy of the product. Biocompatibility relates to the dynamic interaction between the TEMP and the recipient: TEMP cells react to their (micro-) environment and the recipient's immune system reacts to the implant. These mechanisms will also affect efficacy. Efficacy can also be compromised by inconsistent quality of the final product. Manufacturing of TEMPs requires considerable control of cell culturing and processing techniques in order to produce TEMPs of consistent and high quality. An additional risk lies in the unfamiliarity of users with (these) new products, the indications/contraindications for use, clinical handling and complications.

Table 1 - *Hazards, potential harm and control measures related to TEMPs.**

	Part A **Hazard**	*Part B* **Potential Harm**	*Part C* **Control measures**
1	Microbial contamination of cells and/or matrix	• Local/systemic infection/immunogenic reaction/disease transmission, possibly also leading to malfunction	• Selection/screening of sources • Decontaminating measures • Sterility testing
2	Contamination of cells and/or matrix with viruses, parasites, TSE's	• local/systemic infection/disease transmission	• selection/screening of sources • inactivation/elimination processes • product quarantine procedures
3	Natural variation in cell characteristics (e.g. production of insulin)	• desired effect not achieved (under-/overtreatment)	• quality control of source materials
4	Variation in natural source materials (e.g. ratio's of types of collagen)	• desired effect not achieved	• quality control of source materials
	Part A **Hazard**	*Part B* **Potential Harm**	*Part C* **Control measures**
5	Contamination of cells/tissues for autologous use with allogenic cells	• disease transmission • immune-response/rejection leading to malfunction	• quality control of processing steps
6	Contamination with unwanted cell types	• desired effect not achieved • adverse effects	• cell-type specific culturing conditions
7	Endotoxin contamination	• pyrogenic reaction	• endotoxin testing
8	Reduced viability of cells	• desired effect not achieved	• viability testing
9	Altered gene expression by cells affecting intended synthesis	• desired effect not achieved • adverse effects	• RNA-testing
10	Tumourogenicity	• uncontrolled cell growth in product or systemically	• process monitoring
11	Processing residues	• toxic/immunologic effects	• processing/final product testing
12	Processing/manipulation: minimal vs. complex	• alteration of cellular function	• increasing level of quality control of processing and products from minimal to complex processing
13	Production time of (autologous) TEMPs	• deterioration of condition of patient	• Criteria for application

	Part A	*Part B*	*Part C*
	Hazard	**Potential Harm**	**Control measures**
14	Inadequate function of active/metabolic TEMP (e.g. releasing insulin)	• potential systemic effects	• follow-up
15	Heterologous intended use (e.g. cartilage cells around ureter), incompatibility of TEMP source cells and target tissue	• desired effect not achieved • adverse effects due to local tissue reaction	• increasing level of control as compared to homologous intended use • preclinical/clinical testing
16	Altered structural strength of ECM (e.g. membrane failure of encapsulated TEMPs)	• desired effect not achieved • overdose by massive release of entrapped substances • immune phenomena	• mechanical testing • testing of resorption speed
17	Histoincompatibility	• rejection, possibly leading to malfunction	• HLA matching • Immunosuppression
18	bio-incompatibility of (metabolites/components of) the biomaterial	• Adverse effects • cross reactions/auto-immune phenomena	• biocompatibility testing (e.g. cytotoxicity, mutagenicity, hemocompatibility)
19	Tumourogenicity	• neoplasm formation in recipient tissue	• follow-up
20	Altered resorption/diffusion	• desired effect not achieved • adverse effects due to accumulation of substances	• follow-up
21	Unanticipated hazards	• ?	• follow-up
22	Use-related hazards	• diverse	• labelling • training
23	Treatment hazards	• formation of scars • improper vascularization	• second treatment • use of collateral drugs

* nr. 1-4: sourcing phase; nr. 5-13: processing phase; nr. 14-22: post-marketing phase

Risk Evaluation

It should be decided for each identified hazard whether the magnitude of estimated risk(s) is acceptable, or requires the pursuit of risk reduction. However, while probabilities on the occurrence of adverse events can often be extremely remote, it is universally accepted that in all cases, zero risk is an unattainable goal. For instance, when using TEMPs in allogenic applications, the risk of transmission of disease cannot be fully eliminated without damage to the cellular functions. Therefore, the level of safety to be expected and achieved must be defined.

As with safety, the acceptability of risks is not an absolute concept. No fixed level of risk has been identified as acceptable in all cases and under every regulatory program. The acceptability of the risks depends on [10]:

- the probability of the occurrence of the hazard and the severity of the harm,
- the reversibility of the health effect,
- the (im)possibility of further risk reduction,
- the knowledge or familiarity of the risk,
- the fact whether the risk is voluntarily accepted or involuntarily imposed,
- the benefits of the risk imposing activity, and
- risks and benefits of any alternative.

Additionally, possible compensation for the exposure to the risk may also play a role when a decision has to be made on the acceptability of risk. Deciding on risk acceptability is an iterative process. Once new information becomes available, for example in the post-production phase, the acceptability of risk should be re-evaluated.

Risk evaluation can be based on predefined safety standards. Standards should specify requirements, which, if implemented, will indicate achievement of acceptability concerning particular kinds of TEMPs or particular risks [EN-ISO 14971, 2001]. The European Committee for Standardization (CEN) has set up a task group to determine the need for development of European standards related to tissue engineering. This group recommends the start of standardisation on horizontal subjects related to the field of TEMPs. Specifically the following subjects are mentioned: risk management, quality systems, biological safety, microbiological safety, and terminology. Several Technical Committees of ISO (International Standardization Organization) have set up a working group to monitor and review the developments in the area of tissue engineering, and to issue recommendations on working programmes if and when deemed necessary.

It is to be expected that a number of existing safety standards for medicinal products, medical devices and blood products can be used for TEMPs, or for their components after validation with respect to their applicability for TEMPs. An important issue in combining standards is whether it is allowed to add the results of separate safety evaluations of each of the different components of a product. The combination of components should also be safe. It is well-known, also for risks, that the combination can be more than the sum of the parts, which means that at least additional testing would be required.

Risk Control

Life Cycle of Products and Involved Parties

Throughout the life cycle of medical products one can discern several phases such as research and development, selection of source materials, manufacturing, product review, application, and follow-up. Inherent to 'high tech' medical products is the diversity of parties involved in customer-supplier relationships during these phases and the various roles they fulfil (see Table 2).

Briefly, the quality of the TEMP throughout its life cycle depends on the quality of and the interactions between the components, which are obtained from various establishments. The quality of processing and of the agreements between these parties are also relevant to the quality of the final product. The manufacturer should ensure the quality of the product throughout its lifecycle.

Table 2 - *Parties possibly involved and their roles during the life cycle of TEMPs.*

Role	Party
Sourcing	
Source of cellular components/tissues	Donor
Source of non-cellular components (signal molecules/matrix materials)	Supplier
Harvesting of cellular components/tissues	Manufacturer, laboratory, hospital
Processing	
Manipulation/storage of cells	Laboratory, bank, manufacturer
Construction of TEMPs	Manufacturer
Testing/Evaluation	
Pre-clinical evaluation	Manufacturer/Test house
Clinical evaluation	Manufacturer / CRO / Health care provider / recipient / Ethical review commission
Marketing authorisation	Competent Authority or designated body
Clinical application	
Application of TEMPs	Health care provider
Follow-up of TEMP-patient combination	Health care provider/recipient
Reporting adverse events	Health care provider, manufacturer, recipient

Control Measures

In order to limit the probability that the hazards identified in Table 1a might cause harm and to reduce the (severity of) possible consequences as described in Table 1b, control measures can be considered, as listed in Table 1C. These risk control measures should be considered throughout the life cycle of TEMPs. The party that is responsible for the application of control measures, most often being the manufacturer, should be clearly identified. Depending on the timing of the application and the instruments used, any party mentioned in Table 2 (or others) can be involved.

Control measures can be applied in any phase of the life cycle of the product. The production and pre-marketing phases may deserve special attention, as prevention still is

the mainstay of risk management. The post-marketing phase, however, is also important because the product is then used in daily practice, which generates useful experience.

Quality Systems - The methods of risk control can be focused on the people that provide the safety-critical services, on critical manufacturing processes, or on source materials. An integrated approach would be to require parties to implement a full Quality Assurance system. Additionally, specific systems (to be developed) that are unique to address the generic issues related to tissue engineering can be applied. It is now generally accepted that quality assurance systems (e.g., ISO 9000 series) are a prerequisite to assure that handling, processing and manufacturing result in products that meet applicable requirements and specifications. In the field of medicinal products, manufacturers, suppliers, blood banks and test laboratories have to comply with quality system requirements like Good Manufacturing Practices (GMP), Good Laboratory Practices (GLP) and other more general as well as more specific quality assurance standards. Reference to these standards is included in recommendations for blood and blood products [11], and in regulation for medical devices [12-14] and medicinal products [15]. With respect to the "products" that are processed by tissue banks, several organisations such as the American and the European Associations of Tissue Banks (AATB, EATB) have described their general standards, which can be appreciated as a form of Good Tissue Practices (GTP). An important element addressed by these quality assurance systems is the qualification and skills of staff, the "human factor". General quality systems like ISO 9000 require that personnel are competent, trained, qualified, skilled and experienced. It should be realised that the educational requirements for personnel apply to all who are somehow involved in the life cycle of a product, e.g., regulatory authorities, notified bodies, distributors, (hospital) purchasers and clinicians who apply the product. All these requirements can be expected also to be applicable for TEMPs.

Product Testing - An important set of control measures is formed by product testing. During the pre-marketing phase the safety aspects of any medical product can be evaluated by reviewing the results from pre-clinical studies as well as results from clinical investigations. Pre-clinical safety testing (in vitro/in vivo) generally focuses on physical and biological characteristics of the product and the interaction between (components of) the product and biological systems like cells or animals. Especially, mechanical, pharmacological, toxicological and immunological effects are important. For some product groups viral safety aspects are also relevant. Clinical testing focuses on performance and/or efficacy evaluation and safety evaluation in humans. In dealing with the phasing between pre-clinical and clinical studies, two issues need to be distinguished: 1) safety information from pre-clinical studies must warrant the start of clinical investigations in humans); 2) safety information from clinical and pre-clinical studies must warrant marketing of the product. In Europe recent regulation requires approval to start clinical trials with new biological medicinal products [16]. For medicinal products and medical devices the contents and phasing aspects of pre-clinical and clinical testing have been formulated in various standards.

Risk Classification - It is clear that all the aspects of the different risk control methods are closely interrelated and can be combined in various ways. Furthermore, different

review strategies can be applied for products in different groups that are classified according to the estimated magnitude of risk. This has been included for instance in the European regulation for medical devices and in the US in the FDA program "Proposed approach to regulation of cellular and tissue-based products" [17]. Several criteria for risk classification of medical products that include cells have already been proposed [17,18]. These criteria and additional ones are summarised in Table 3. The immuno-isolation potential applies to encapsulated TEMPs. Manipulation refers to a variety of techniques of handling cells, ranging from simple to complex, such as trimming, packing, controlled rate freezing, selection, culturing, stimulation, and incorporation of new genes. Homologous use refers to similarity in function between the source tissue of the cells and the tissue location after implantation. The potential for recovery applies to, e.g., products containing biodegradable materials.

Table 3 - *TEMP parameters relevant to risk classification.*

	Low Risk	High Risk
Cell Donor – Recipient combination	Autologous	Allogenic/hybrid
Immuno-isolation potential	High	Low
Manipulation of cells	Minimal	More than minimal
Natural cellular function vs. intended function	Homologous use	Non-homologous use
Action	Structural (local)	Metabolic (systemic)
Contact site*	Ext./s.c./i.m.	i.p./i.v./i.t.
Potential for recovery	Yes	No
Duration of exposure	Short	Long
Information regarding indications for use	Adequate	Insufficient
User (medical staff) skill/experience	High	Low

*ext.: external; s.c.: subcutaneously; i.m.: intramuscularly; i.p.: intraperitoneally (in the abdominal cavity); i.v.: intravenously; i.t.: intrathecally (in the central nervous system)

A similar kind of classification scheme has resulted in control measures of the FDA focused on source selection (donor screening), processing, clinical safety/efficacy, promotion/labelling, and monitoring (e.g., Post-Marketing Surveillance (PMS) - systems)/education. In Europe there is currently a debate on the question whether the new legislative system on human tissue products should be based on a risk classification.

Residual Risks

Earlier it was stated that a zero risk is not achievable. Standardised control measures cannot prohibit that the reduction of risks below certain limits may be hampered by technical constraints. An example is the technical impossibility to select organ donors with 100% freedom of viruses. Processing activities to reduce the risk of infection may also introduce new risks, for example, the adverse effects of residues from sterilants.

Furthermore, some potential (residual) risks may not be identified during the pre-marketing process. This can be a result of the limitations of the safety standards themselves or the ability to identify low occurrence events in clinical studies. During clinical studies, for example, only a limited group of people are exposed to a product, and often only a limited number of physicians participate. The patients form a highly selected and carefully screened group of people, which are closely monitored. Furthermore,

participating physicians often have special interest in the therapy under study and may receive extensive training for the purpose of the study. Because of these selection mechanisms the clinical study does not fully represent the clinical situation after market introduction of a therapy.

Finally, even the flawless and comprehensive application of standard control measures cannot prevent previously unknown risks to emerge after market introduction. An example is the discovery that the CJD agent was transmitted by human pituitary derived growth hormone.

Overall Risk Evaluation

During the process defined in the previous paragraphs, stakeholders identify each hazard, evaluate the risks, and implement and verify risk control measures one at a time. Next to that, there is a need to step back, add up all the individual residual risks, and decide on the acceptability of risks and the need and possibility for further risk reduction: the overall risk evaluation. It is possible that the overall residual risk can exceed the stakeholders' criteria for acceptable risk, even though individual risks do not. If a manufacturer judges the overall residual risk to be acceptable, the marketing phase can be entered. According to current regulation for most medical products, regulatory authorities or designated independent bodies (e.g. Notified Bodies) decide on the acceptability of the overall residual risk of the product by assessing the scientific evidence on safety and performance/efficacy as provided by the manufacturer. If the safety and performance/efficacy is deemed acceptable, market authorisation can be granted.

The existing regulatory frameworks for marketing authorisation of blood, medicinal products, medical devices and in-vitro diagnostics show differences. Authorisation schemes for these product groups also differ between the European Union (EU) and the United States (US).

For medicinal products, marketing authorisation is granted by regulatory authorities. Extensive files addressing quality, safety and efficacy of the product need to be submitted by the manufacturer to these bodies. In the United States this task is carried out by the FDA (CDER and CBER). In Europe different procedures can be followed depending on the nature of the product. In these procedures, the EMEA (European Agency for the Evaluation of Medicines), national Competent Authorities and Official Medicines Control Laboratories (OMCL) play active roles [15]. Biotechnological products are considered as high-risk products and are allowed only to be reviewed via a centralised procedure. If marketing authorisation is obtained through a national procedure in one Member State, the manufacturer can apply for marketing authorisation in other member states by a mutual recognition procedure. For certain medicinal products (e.g., derived from blood or human plasma) a batch release procedure is required [15]. Samples of each batch of the product need to be sent to an OMCL, where product specific safety and potency parameters are tested. Only after approval of the test results by the competent authority, is the manufacturer allowed to place the batch on the market.

For medical devices the USA-approach and the EU-approach differ considerably. In the USA a pre-marketing approval has to be obtained from the FDA (mostly CDRH, some products by CBER), very much like the system for medicinal products. In the EU manufacturers are required to place a CE-mark on the medical device thereby claiming

that the device complies with the Essential Requirements of the Medical Device Directive [13]. This Directive classifies products in four risk groups and requires the manufacturer to follow certain CE-conformity assessment procedures depending on the risk class. These procedures are combinations of requirements for the product and the manufacturer. Depending on the classification of the product, more detailed information has to be provided. Most of these procedures require the involvement of a so-called Notified Body (NB). NBs are commercial organisations, accredited by a competent authority, which test and/or review data with respect to the CE-conformity assessment. Specific NBs are designated for specific product groups. When medical devices form intrinsic combinations with medicinal products or stable derivatives of human blood or human plasma, the non-device constituents should be reviewed according to regulations for medicinal products [13,19]. CE-marked products are allowed to be marketed throughout the EEA.

In Europe, IVDs have to be CE-marked and the conformity assessment may require the involvement of a NB (specialised in IVDs), similar to the system for medical devices. Depending on the risk classification of the products a batch release procedure may be required. In contrast with the batch release procedure for certain medicines, for IVDs a NB instead of a Competent Authority is allowed to release batches.

For blood and blood products marketing authorisation is regulated at a national level in the various European countries.

US regulations require all manufacturers of human cellular and tissue-based products to register and list their products with the FDA [20]. It is proposed that they meet the standard regarding determination of donor suitability, and conform to GTP [21]. To this end the FDA may inspect facilities. Certain product groups (like having metabolic function, combining with devices) will be subject to current US regulations for biologics and/or medical devices. These manufacturers are required to apply for marketing authorisation [17].

Post-Marketing Issues

Post-Marketing Risk Assessment

Given the intended purpose of medical products, reliability is often a key issue. However, it is a theoretical entity rather than an estimate based on long-term (large-scale) field experience. Pre-marketing clinical studies only evaluate short-term safety issues and almost never detect rare (but serious) adverse events. Other problems that relate to product labelling (including instructions), user technique and skill and safety issues (durability, biocompatibility, toxicology and disease transmission) will often only be detected during the post-marketing phase. In addition, under normal conditions of long-term use the frequency of risks may be higher than expected. Hence, information that emerges during the post-marketing phase has to be fed back into the risk management cycle so it can be evaluated whether earlier decisions on risk acceptability need to be reconsidered.

Post-marketing surveillance is the key to post-marketing risk assessment. Surveillance has been defined as "the ongoing, systematic collection, analysis and

interpretation of health data essential to the planning, implementation and evaluation of public health practice, closely integrated with the timely dissemination of these data to those who need to know" [22]. Surveillance is manufacturers' but also public health officials' most important tool for monitoring the safety of products. Surveillance systems form the basis for recognising emerging (public health) problems that may require intervention. Two types of surveillance methods can be distinguished: passive and active surveillance.

Passive surveillance means that parties (hospital staff, laboratories, physicians and manufacturers) that might report essential data are provided with the appropriate instructions, while the collector awaits their reports and hopes that all reportable conditions will be reported. The information is evaluated as it comes in. For medical products mandatory and voluntary reporting systems may provide data to be used for passive surveillance. By law EU member states are obliged to have vigilance systems in place for medicinal products and medical devices [13,15]. With respect to mandatory reporting manufacturers and/or distributors in the EU are obliged to report to the regulatory authorities on product recalls and product related incidents that come to their attention and that led or might have led to serious adverse events. Regulatory authorities have an obligation to inform manufacturers about reportable incidents that are brought to their attention through other channels [13,15]. These requirements apply to all regulated medical products.

Active surveillance means that public health officials, manufacturers or researchers actively contact other stakeholders directly to gather data and actively search for information and/or even conduct post-approval studies, often on a periodic basis. There are several approaches to perform active surveillance, but none of them are part of current regulation for medical products. One approach is that of so-called sentinel sites [23]. By contracting representative sites where specific (kinds of) medical products are used it is hoped that surveillance can be optimised. Another approach can be the extension of data collection on patients, who participated during pre-marketing clinical investigation, within the first years of marketing [24]. The use of existing health care databases, like for example implant registries (see below), that combine usage data and event data may also be helpful.

The efficacy and quality of the post-marketing surveillance depends on 1) who has to report; 2) what needs to be reported where; 3) which methods are used to gather and analyse information and to evaluate risks. The Achilles heal of all passive surveillance systems is the total reliance on the alertness, willingness, and co-operation of users and health care professionals, the first to encounter adverse events. Training and education of organisations, and active information campaigns could stimulate this. Furthermore, it should be transparent for all parties what needs to be reported where. By using standard forms, like for example the MedWatch and MEDDEV forms the quality and usability of gathered information could be enhanced. Furthermore, reporting can be facilitated and enhanced by offering multiple ways to report, for example by phone, regular mail, fax and the Internet [25].

The surveillance method chosen has implications for completeness of the data and the validity of risk estimates. Given the drawbacks of passive surveillance, by which complete information on actual use and duration of use will hardly ever become available, long-term follow-up of TEMPs through active surveillance seems to be the

preferred surveillance method of choice, although it is far more costly, time consuming and labour-intensive than passive surveillance. Given the diversity and complexity of possible problems for TEMPs, evaluation of possible safety problems not only calls for a systematic, but also a multidisciplinary approach.

Post-Marketing Risk Control

Risk analysis and evaluation in the post-marketing situation is necessary to control the risks. Examples of additional control measures will be discussed briefly.

Traceability of medical products from the manufacturer to the ultimate user, the patient, is needed in case a potentially dangerous product has to be recalled. The simplest way to achieve this would be to hand out implant cards, which are filled out after implantation of a device and returned to the manufacturer. The ultimate method to ensure traceability would be to have registries identifying products, recipients and treatments. The usability of registries in relation to risk assessment depends on the information registered (e.g., implant/product-, patient- and procedure characteristics) and availability of follow-up information on registered patients. In case of mandatory registries it appears important to clearly designate the holder(s).

In the EU a so-called Periodic Safety Updates Report (PSUR) is required for each authorised medicinal product [26]. PSURs are a summary of the worldwide safety information available on a product like for example: adverse event reports, clinical studies, literature and other sources of data ,i.e., epidemiological databases.

The use of new high-risk technologies is often restricted by regulatory authorities to specific health care facilities/providers (like the transplantation of lungs and livers). However, the initiative to restrict the use of a certain product may also be taken by health care professionals. A recent example is the initiative of the Dutch Society for Vascular Surgery to restrict the use of vascular endoprostheses.

The periodical renewal of licenses for manufacturers, based on the safety information gathered in the earlier years of marketing may also be a way to control safety problems. Suspension of licenses, voluntary or non-voluntary recalls and voluntary or non-voluntary product withdrawals are ways to control risks post-marketing once they have emerged.

Discussion

New techniques like tissue engineering hold promise for medical therapy. In this paper we reviewed the risks that are known or foreseen to be associated with tissue engineered medical products and discussed the options for risk control. Apart from giving an overview of risk management strategies that may be useful to manufacturers, this paper may serve as background information for any regulatory structure.

At present, knowledge about the risks is fragmented and incomplete. Therefore, quantification of the risks is often impossible. However, it is possible to devise measures to control the identified risks. Products manufactured by tissue engineering are largely unregulated in the EU at this moment. The ideal way forward would be to negotiate for a suitable pan European framework to address the development of a firm and fair structure

to ensure the quality and safety of health care products from tissue engineering. Several EU member states have formulated, or will formulate national regulations. Presently, the European Commission has also realised the importance of regulation for this issue and has initiated the development of a comprehensive legislative system for human tissue products.

In describing the management of risks, the EN-ISO 14971 standard relies heavily on Deming's quality cycle: the iteration of Plan, Do, Check and Act. According to this circle, one has to: plan activities on relevant information, perform these activities according to the plan, take care of appropriate checks afterwards, evaluate the results of these checks and react to the findings by adapting the plan. In theory this strategy will result in a cycle of continuous improvement and elimination of ineffective activities. This concept is also relevant to all parties with regard to improving their strategies to control the safety of all (groups of) products available on the market.

The most important risks that can be foreseen at this moment (see Table 2) seem to be related to the transmission of disease, biocompatibility and efficacy. Control measures should therefore focus on these aspects. Given the diversity in tissues, matrix materials and signal-molecules, different TEMPs will certainly carry various combinations of risks, each varying in character and magnitude. Classification of products into risk groups can help in designing efficient control measures. Parameters relevant to this classification have already been put forward (Table 3) and may serve as a starting point for the development of a European system.

In addition to the development of a regulatory system, the development of standards should be encouraged, preferably on a world-wide scale. It is the "language" that enables discussion on and interpretation of product and process performance. The need for standards is increasing because some products are already available for clinical application and a large number is under development. Quality and safety standards should also describe the specifications that processes and/or products have to conform with. At this moment ASTM International has instituted specific workgroups for development of TEMP standards. Also, CEN has taken formal interest in TEMP developments. It is advisable for European, US and other international parties to communicate in order to establish widespread acceptance of new standards. Given the large diversity of possible products, a horizontal approach (standards applicable to a large number of products) is preferred over a vertical approach (standards for specific product groups). Guided by the identified major risks, the topics of standardisation should include donor selection criteria and methods for evaluation of safety and efficacy. With respect to donor selection criteria, guidelines from blood and tissue banks may serve as a starting point.

Already before the development of technical standards, new technologies will be discussed by the general public with regard to ethical aspects and perceived risks. The current discussion on xenotransplantation illustrates this process and reveals the strong commitment of several parties against and in support of this technique. The information that becomes apparent from these discussions is relevant to the determination of the level of safety that is expected by the general public. A structured study (interview/questionnaire) among the general public on the limits of acceptance for certain risks may generate additional information.

Standards for professional skills and conduct as well as for specific quality systems (e.g., Good Laboratory Practice) for laboratories or certain areas of industrial activity are just as important as product standards. Manufacturing TEMPs will be based upon highly sophisticated techniques, for which validated processing steps are mandatory to guarantee the safety of products. The capacity and skills of the organisations may be regulated by requiring implementation of general Quality Systems such as ISO 9000 and/or systems and standards more specific for the field of tissue engineering. These systems should address, e.g., staff skills (training), manufacturing/handling processes and products. Products and processing techniques should be characterised and documented. The regulatory authorities should conduct formal reviews to assure that these requirements (being in itself control measures) are implemented, are used as intended and that the results conform to relevant standards. The results of such reviews can be linked to granting licences for facilities for manufacturing, for marketing authorisation of products, or in case of health care providers, for the application of products.

In view of the complexity of TEMPs and the lack of experience in applying these products in humans, it is advisable to conduct a careful, formal and centralised review of the product characteristics before clinical testing as well as before introduction on the market. The results of these investigations should be documented in product files.

A formal review should focus on the results of the pre-clinical studies consisting of in vitro tests and animal tests of the new TEMP and/or its components. The contents of the file describing the product characteristics and performance need to be assessed according to pre-defined procedures. This review should lead to a decision on the suitability for clinical evaluation.

Aspects relating to a formal review as discussed for pre-clinical studies are also relevant for clinical studies. The results of these studies should indicate both the clinical safety and the efficacy of the product. Review of both pre-clinical and clinical results is needed to obtain marketing authorisation. For certain high-risk products, an additional batch release procedure (like for certain IVDs, vaccines and blood products) can be considered.

Once a product is on the market, an additional set of risks, namely use-related, also needs to be taken into account. When the Regulatory Authorities limit the number of centres that use TEMPs, risks could be controlled more easily. An alternative approach could be to let the professional organisations decide where clinical experience on new techniques/products will be collected. A limited number of staff is easier to train and because the frequency of application of TEMPs can be kept high, their expertise will remain on an adequate level more easily. Expertise and skills are not only relevant to first-time application, but also to handling of complications and adverse events. To support structural review of experiences, these centres could be required to incorporate their experiences with the new products in an Annual Quality Report. In any case, the review procedure of these reports should be transparent to all parties involved.

Postmarketing clinical experience is valuable in assessing the, mostly long-term, safety of TEMPs. Pre-marketing clinical studies involve only a limited number of patients over a limited period of time. Cells in TEMPs may maintain their function and interact with the recipient for a long time. It is therefore important to monitor the experience with TEMPS after marketing, preferably through long-term active surveillance, including a structured system of (mandatory) adverse event reporting,

accumulation of both the adverse events and use data, analysis and (periodic) review. The accumulation, analysis and review of the results of this system should preferably be centralised and performed by an independent party, i.e., neither manufacturer nor health care provider.

As a means to control and limit the consequences of possible adverse events caused by malfunctioning TEMPs, it is advisable to maintain a database system that registers the combination of TEMPs and recipient. This can be a central national system or a local (e.g., hospital, manufacturer) one, by documentation of a minimum set of data by health care professionals and manufacturers. The archive duration of these data should exceed ten years, as long-term effects may emerge after this period. An independent party should preferably keep the database (or the linking key), as the institutions involved (manufacturer and clinical centre) may have opposing interests. Privacy legislation will prohibit direct and full access by manufacturers and third parties to these databases.

Conclusions and Recommendations

- At present, the knowledge about risks related to TEMPs is fragmented and incomplete.
- The most important risks seem to be related to disease transmission, biocompatibility and efficacy.
- Given the risks of products that are produced by tissue engineering techniques it is necessary to develop a single, EU-wide system of regulation in Europe.
- This system should be tailored to the specific risks of TEMPs and should be complementary to and connect to existing European regulation for medical products.
- Control measures could be specified for TEMP subgroups that are stratified according to increasing risk.
- Evaluation of acceptability of individual risks should ideally be based on predefined standards. These should be formulated for tissue engineered products and should first aim at generic aspects of products (horizontal approach).
- General quality systems and GMP/GLP with additional specific requirements should be implemented by involved parties.
- Manufacturers should be subjected to a licensing system.
- Results of pre-clinical evaluation should be subject to formal review by an independent body before the onset of clinical evaluation.
- Marketing authorisation should be applied and should be based on a formal review of product/process characteristics (results of pre-clinical and clinical evaluation).
- Additional measures like batch release procedures or designated clinical centres could be considered.
- Some form of post-marketing surveillance should be installed, preferably including a structured system of (mandatory) adverse event reporting, accumulation of both the adverse events and use data, analysis and (periodic) review.
- Traceability of products to patients should be warranted.

Acknowledgment

Dr. Esther van Tienhoven is acknowledged for critically reviewing the manuscript.

References

[1] Skalak, R. and Fox, C., Eds., "Tissue engineering", *Proceedings of a workshop held at Granlibakken, Lake Tahoe, CA, Feb 26-29, 1988,* Liss, New York, NY; Liss; 1988.
[2] Lysaght, M. J. and Reyes, J., "The Growth of Tissue Engineering- Review", *Tissue Engineering,* Vol.7, 2001, pp. 485-493.
[3] Wassenaar, C. and Geertsma, R. E., "Tissue Engineered Medical Products (TEMPs): Historical Developments and Forecasts [in Dutch]", *RIVM report 605910 004,* RIVM, Bilthoven (NL), 2000.
[4] Jong, M. de, "The conundrum of products of human origin", *Regulatory Affairs Journal (Devices),* Vol. 8, 2000, pp. 283-293.
[5] Baldwin, S. P., Saltzman, W. M., "Materials for protein delivery in tissue engineering", *Advanced Drug Delivery Reviews,* Vol. 33, No. 1-2, 1998, pp. 71-86.
[6] Pollok, J. M., Vacanti, J. P., "Tissue engineering", *Seminars in pediatric surgery,* Vol. 5, No. 3, 1996, pp. 191-196.
[7] Gottesdiener, K. M., "Transplanted infections: donor-to-host transmission with the allograft", *Annals of internal medicine,* Vol. 110, No. 12, 1989, pp. 1001-1016.
[8] Patel, R., Paya, C. V., "Infections in solid-organ transplant recipients", *Clinical microbiology reviews,* Vol. 10, No. 1, 1997, pp. 86-124.
[9] Tienhoven, E. A. E. van, Geertsma, R. E., Wassenaar, C., and Jong, W.H. de, "Preclinical safety assessment of Tissue Engineered Medical Products (TEMPs)", *RIVM report 640080 002,* RIVM, Bilthoven (NL), 2001.
[10] Fischhoff, B., Bostrom, A., and Quadrel, M.J., "Risk perception and communication", *Annual review of public health,* Vol. 14, 1993, pp. 183-203.
[11] Council of the European Communities, "Recommendation No. R(95) 15 on the preparation, use and quality assurance of blood components".
[12] Council of the European Communities, "Directive 90/385/EEC of 20 june on the approximation of the laws of the Member States relating to active implantable medical devices", *Official Journal,* Vol. L189, 1990, pp. 17-36.
[13] Council of the European Communities, "Directive 93/42/EEC of 14 june 1993 concerning medical devices", *Official Journal,* Vol. L169, 1993, pp. 1-43.
[14] Council of the European Communities, "Directive 98/79/EC of the European Parliament and of the Council of 27 October 1998 on in vitro diagnostic devices", *Official Journal,* Vol. L331, 1998, pp. 1-37.
[15] Council of the European Communities, "Directive 2001/83/EC of the European Parliament and of the Council of 6 November 2001 on the Community code relating to medicinal products for human use", *Official Journal,* Vol. L311, 2001, pp. 67-128.
[16] Council of the European Communities, "Directive 2001/20/EC of the European Parliament and of the Council of 4 April 2001 on the approximation of the laws, regulations and administrative provisions of the Member States relating to the implementation of good clinical practice in the conduct of clinical trials on medicinal products for human use", *Official Journal,* Vol. L121, 2001, pp. 34-44.

[17] FDA, "Proposed approach to the regulation of cellular and tissue-based products", Rockville, MD, USA. 1997.
[18] Omstead, D. R., Baird, L. G., Christenson, L., Du Moulin, G., Tubo, R., Maxted, D. D., Davis, J., and Gentile, F. T., "Voluntary guidance for the development of tissue-engineered products", *Tissue Engineering*, Vol. 4, No. 3, 1998, pp. 239-266.
[19] Council of the European Communities, "Directive 2000/70/EC of the European Parliament and of the Council of 16 November 2000 amending Council Directive 93/42/EEC as regards medical devices incorporating stable derivates of human blood or human plasma", *Official Journal*, Vol. 313, 2000, pp. 22.
[20] FDA, "Human cells, tissues, and cellular and tissue-based products; Establishment registration and listing (final rule)", FDA, 21 CFR 207, 807, 1271, *Federal Register*, Vol. 66, No. 13, 2001, pp. 5447-5469.
[21] FDA, "Current Good Tissue Practice for manufacturers of human cellular and tissue-based products. Inspection and Enforcement (proposed rule)", FDA, 21 CFR 1271. *Federal Register*, Vol. 66, No. 5, 2001, pp. 1508-1559.
[22] Thacker, S. B., Berkelman, R. L., "Public health surveillance in the United States", *Epidemiologic reviews*, Vol. 10, 1988, pp. 164–190.
[23] FDA, Office of Surveillance and Biometrics, CDRH, "Final report of a study to evaluate the feasibility and effectiveness of a sentinel reporting system for adverse event reporting of medical device use in user", Rockville, MD USA, 1999.
[24] Friedman, M. A., Woodcock, J., Lumpkin, M. M., Shuren, J. E., Hass, A. E.; and Thompson, L., "The safety of newly approved medicines: do recent market removals mean there is a problem?", *JAMA the journal of the American Medical Association*, Vol. 281, 1999, pp. 1728-1734.
[25] ECRI, "Medical device problem reporting for the betterment of healthcare", *Health Devices*, Vol. 27, 1998, pp. 277-290.
[26] EMEA, "Clinical safety data management: period safety update reports for marketed drugs", *CPMP/ICH/ 288/95*, London, 1996.

Catherine O'Connell,[1] Peter E. Barker,[1] Michael Marino,[2] Patricia McAndrew,[2] Donald H. Atha,[1] Pawel Jaruga,[3] Mustafa Birincioglu,[4] and Henry Rodriguez[1]

Molecular Biomarkers Used to Detect Cellular/Genetic Damage in Tissue-Engineered Skin

Reference: O'Connell, C., Barker, P. E., Marino, M., McAndrew, P., Atha, D. H., Jaruga, P., Birincioglu, M., and Rodriguez, H., **"Molecular Biomarkers Used to Detect Cellular/Genetic Damage in Tissue-Engineered Skin,"** *Tissue Engineered Medical Products (TEMPs), ASTM STP 1452*, E. Schutte, G. L. Picciolo, and D. S. Kaplan, Eds., ASTM International, West Conshohocken, PA, 2004.

Abstract: In this study, tissue-engineered skin (TestSkin II) was obtained, separated into its two cellular layers (epidermis and dermis) and DNA was extracted. The first biomarker tested consisted of screening for DNA point mutations in exons 5 and 6 of the TP53 gene, the most commonly mutated gene in skin cancer. To ensure the accuracy of the results, two measurement technologies that incorporate internal calibration standards were used. It was shown that tissue-engineered skin did not contain mutations in this gene at the level of sensitivity of SSCP-capillary electrophoresis and Denaturing High Performance Liquid Chromatography. Results were compared to control cells (neonatal fibroblasts and neonatal keratinocytes) and fibroblasts that were obtained from a 55-year-old and 96-year-old human donor. The second set of biomarkers tested looked at the loss of the Y-chromosome. Using Fluorescent In Situ Hybridization technology, no detectable loss of Y-chromosome was found in the tissue-engineered skin and neonatal control cells. Y-chromosome loss was found in the fibroblasts from the 96-year-old donor. Biomarkers such as TP53 mutations and chromosome loss can provide the basis for an international reference standard of cellular biomarkers that can aid in the development and safety of tissue engineered medical products.

Keywords: TP53, CE-SSCP, DHPLC, Y-chromosome, biomarkers.

[1]Staff Scientist, Staff Scientist, Staff Scientist, and Staff Scientist, respectively, Chemical Science and Technology Laboratory, National Institute of Standards and Technology, 100 Bureau Drive, Mail Stop 831, Gaithersburg, MD 20899-8311.
[2]Transgenomic, Inc., 11 Firstfield Road, Suite E, Gaithersburg, MD 20878.
[3]Guest Researcher, University of Maryland, Baltimore County.
[4]Department of Pharmacology, Medical School, Inönü University, Malatya, Turkey.

Introduction

Tissue engineering is an emerging area of biotechnology that will provide replacement tissues for patients, as well as complex, functional biological systems for research and testing in the pharmaceutical industry. There are two forms of tissue engineering: one whereby cells are grown in culture and seeded onto a material, and in the other in which an implanted material induces a specific response such as tissue regeneration *in vivo*. The former approach is used to create skin substitutes, while the latter is used to accelerate nerve regeneration, for example.

The aim of the DNA Technologies Group tissue engineering program at the National Institute of Standards and Technology (NIST) is to identify cellular biomarkers and measurement technologies that could be used to assure that tissue-engineered skin products are free of genetic changes that could occur during the development phase. In this study, we looked at two potential biomarkers: (1) DNA point mutations in the TP53 gene, the most commonly mutated gene in skin cancer [1,2] and (2) loss of the Y-chromosome, a common occurrence in aging [3]. In the accompanying study presented at this meeting, oxidative damage to DNA by free radicals was also studied.

To examine the tissue engineered products for mutations in exons 5 and 6 of the TP53 gene, two measurement technologies that incorporate NIST internal calibration standards [4,5] were used. It was shown that tissue-engineered skin did not contain mutations in this gene at the level of sensitivity of single strand conformation polymorphism-capillary electrophoresis (CE-SSCP) and Denaturing High Performance Liquid Chromatography (DHPLC) analysis. Results were compared to control cells (neonatal fibroblasts and neonatal keratinocytes) and fibroblasts that have not gone through the tissue engineering process. These were obtained from a 55-year-old (YO) and 96-YO human donor. To examine these products for Y-chromosome loss, Fluorescent In Situ Hybridization (FISH) technology was used. No detectable level of Y-chromosome was found in the tissue-engineered skin and neonatal controls cells. Y-chromosome loss was found in the fibroblasts from the 96-YO donor as was to be expected. Biomarkers such as TP53 mutations and chromosome loss can provide the basis for an international reference standard of cellular biomarkers that can aid in the development and safety of tissue-engineered medical products.

Experimental Methods[4]

Cell Culture and DNA Isolation

Human dermal neonatal fibroblast cells (HDFn; Cascade Biologics, Portland, Oregon, Catalog Number C-004-25P) and fibroblasts obtained from a 55-YO and 96-YO donor

[4]Certain commercial equipment or materials are identified in this paper in order to specify adequately the experimental procedures. Such identification does not imply recommendation or endorsement by the National Institute of Standards and Technology, nor does it imply that the materials or equipment identified are necessarily the best available for the purpose.

(Coriell Cell Repositories, Camden, New Jersey, Catalog Numbers AG06287 and AG04059B, respectively) were cultured in Medium 106 supplemented with Low Serum Growth Supplement (LGGS) in the absence of antibiotics and antimycotics (Cascade Biologics, Portland, Oregon). Medium was aspirated off, and cells were rinsed with 20 mL of 1X PBS. Cells were detached by adding 3 mL trypsin/EDTA solution. Trypsin/EDTA solution was immediately removed and an aliquot of 3 mL of Trypsin neutralizer solution (Cascade Biologics, Portland, Oregon) was added to each flask. Human epidermal neonatal keratinocyte cells (HEKn; Cascade Biologics, Portland, Oregon, Catalog Number C-001-25P) were cultured in EpiLife medium supplemented with Human Keratinocyte Growth Supplement (HKGS) in the absence of antibiotics and antimycotics (Cascade Biologics, Portland, Oregon) and then treated as above. Normal male lymphocytes were donated by a volunteer. These were cultured for 72 hr in RPMI (80% v/v), 20% v/v fetal calf serum, 2 mM/L glutamine with penicillin-streptomycin (100 U; 100 μg/ml) at 37 °C with 5% CO_2.

DNA was isolated from cells using a blood and cell culture DNA kit (Qiagen, Valencia, CA). DNA was recovered by spooling, washed once in 70% ethanol, and then air-dried. DNA was dissolved in 10 mM sodium phosphate buffer at a concentration of 0.3 mg/mL and dialyzed against water for 18 h at 4 °C. Water outside the dialysis bags was changed three times during the course of the dialysis. Subsequently, DNA concentration was determined by UV spectroscopy. Aliquots of this solution containing 100 μg of DNA were dried under vacuum in a SpeedVac.

TestSkin II: Fibroblast/Keratinocyte Cell Layer Separation Followed by DNA Isolation

Separating Cell Layers - A TestSkin II disk (Organogenesis, Inc., Canton, MA) was placed in a 150 mm^2 sterile petri dish containing 35 mL 1x PBS and incubated at room temperature for 30 min in a cell culture hood. PBS was removed and replaced with 40 mL protease type X solution (0.5 mg/mL 1x PBS) and incubated at 37 °C for 2 h in a humidified cell culture incubator with 5% CO_2/95% air. Epidermal layer (keratinocytes; gray top layer) was gently separated from the dermal layer (fibroblasts; white bottom layer) using sterile forceps.

Separating Individual Cells and DNA Isolation - Epidermal layer was placed in a 50-mL polypropylene conical tube containing 40 mL trypsin-versene and incubated in a 37 °C water bath for 2 h. The dermal layer was placed in a 175-cm^2 T-flask containing 180 mL collagenase solution [60 mL collagenase (4.17 mg/mL H_2O) and 120 mL collagenase pre-mix (120 ml 1x PBS, 14 mL of 2.5% trypsin solution, 1 mL filtered 0.45% glucose solution)] and incubated at 37 °C in a humidified cell culture incubator with 5% CO_2/95% air for 2 h. Independently, each respective tube was agitated every 15 min. Cells were pelleted by centrifugation (1300 x g/4 °C for 5 min) and rinsed twice with 20 mL 1x PBS with centrifugation (1300 x g/4 °C for 5 min) between each rinse step. Cells were eventually suspended in 4 mL 1x PBS and counted using a cell culture hemocytometer. DNA was isolated from the cells using a blood and cell culture DNA kit (Qiagen, Valencia, CA).

Analysis of TP53 Status

Amplification of TP53 Exons 5 and 6 - PCR primers to amplify a region of the TP53 gene containing exons 5 to 6 have been previously described [4]. The 2 kilobase fragment was amplified in a 20 μL reaction volume containing the following: 250 ng genomic DNA, 1X PCR buffer H (Invitrogen, Carlsbad, CA), 500 nMol/L each primer, 2.0 mmol/L $MgCl_2$, 2.5 U *AmpliTaq Gold* DNA Polymerase, and 200 umol/L each dNTP. Thermal cycling conditions were as follows: pre-amplification denaturation: (1 cycle), 94 °C for 5 min; amplification (35 cycles): denaturation, 94 °C for 30 s; annealing, 66 °C for 30 s; elongation, 72 °C for 40 s; final elongation: (1 cycle), 72 °C for 7 min. A Perkin Elmer 9700 thermal cycler and was used for amplification.

Exon-Specific Amplification - For mutation detection, 1 μL of the 2 kilobase amplification products was reamplified with exon-specific fluorescent labeled PCR primers. NIST standard clones were used for both positive and negative exon specific controls at 50 ng per PCR reaction. 1 μL of a 1:10 dilution of these amplification products was analyzed by CE-SSCP. The exon-specific primers (cat. # 6398-1) were purchased from Clontech Laboratories (Palo Alto, CA). The fluorescent labeled primers labeled with FAM (5-carboxyfluorescein), 5' primer, and JOE (2', 7'-dimethoxy-4',5'-dichloro-6-carboxyfluorescein), 3' primer were provided by PE Biosystems. A Perkin Elmer 9700 thermal cycler and *GeneAmp* PCR core reagents (Perkin Elmer, Part No. N808-0009) were used for all amplifications. PCR reactions contained: 1X PCR buffer II, 500 nMol/L fluorescently labeled primers, 1.5 mMol/L $MgCl_2$, 2.5 units *AmpliTaq* DNA Polymerase, and 200 μMol/L each of dATP, dCTP, dGTP and dTTP. Thermal cycling conditions were as follows: pre-amplification denaturation: (1 cycle), 94 °C for 3 min; amplification (35 cycles): denaturation, 94 °C for 30 s; annealing, 66 ° C for 30 s; elongation, 72 °C for 40 s; final elongation: (1 cycle) 72 °C for 7 min.

CE-SSCP Analysis - Fluorescent-labeled PCR samples were prepared for electrophoresis by combining 10.5 μL deionized formamide with 0.5 μL 0.3 N NaOH, 1 μL of PCR sample (diluted 1:10) and 0.5 μL of GENESCAN-500 TAMRA (6-carboxy-tetramethyl - rhodamine) - labeled internal size standard. The mixture was heated for 2 min at 95 °C and chilled on ice. SSCP separations were performed using the Perkin Elmer/Applied Biosystems PRISM Model 310 Genetic Analyzer modified to evaluate mutations at sub-ambient temperatures. All separations were performed using the Perkin Elmer, Applied Biosystems GENESCAN capillary and polymer system (41 cm X 75 cm capillary, 3% GENESCAN polymer containing 10% glycerol in 1 X TBE). This capillary and polymer system was chosen because previous studies demonstrated its high resolution and reproducibility for the detection of sequence-induced mobility differences in double-stranded DNA fragments. Samples were electrokinetically injected (10 s, 3 KV) and separated at 10-13 KV. Data were collected and analyzed using Perkin Elmer/Applied Biosystems PRISM and GENESCAN software, version 2.0.2.

DHPLC Analysis - The samples were analyzed on the WAVE® 3500HT DNA Fragment Analysis System (Transgenomic, Inc. Omaha, Nebraska). The stationary phase consists of alkylated nonporous polystyrene-divinlybenzene particles, and the mobile phase consists of buffer (A) 0.1M triethylammonium acetate (TEAA), and (B) 0.1M TEAA; 25% acetonitrile (v/v). The PCR products were denatured for 4 minutes at 94 °C and cooled to room temperature at a rate of 1 °C/min. Ten to 20 µL of PCR products were applied to the DNASep preheated reverse phase column (Transgenomic Inc.) As previously, described, the temperature for optimal resolution of heteroduplex and homoduplex DNA detection was determined by analyzing the melting of a PCR fragment of each exon while the temperature was increased by 1 °C increments from 50° C until the fragment was completely melted [6]. The analysis temperature for each fragment was chosen as the temperature at which about ~75% of the DNA was present as an alpha helix [6]. The experimental DNA melting data was analyzed using Wavemaker software (Transgenomic, Inc.) included with the DHPLC analysis system.

Y-Chromosome Analysis

Cells were treated with hypotonic solutions, fixed, air dried, and slides were prepared using standard procedures [7]. Briefly, lymphocytes were treated with 75 mM KCl for 10 min at 37 °C, and keratinocytes and fibroblasts were treated with 24 mM Na_3Citrate for 20 min at 37 °C prior to fixation. Cells were collected from these hypotonic solutions by mild centrifugation, fixed (methanol:acetic acid, 3:1 v/v) and spun out of fresh, ice cold fixative three times before air-dried slides were prepared. FISH methods for the whole chromosome painting (WCP) Y SpectrumGreen probe were followed according to manufacturer's instructions (Vysis item #32 122024, Downers Grove, IL). Imaging by CCD has been described [8].

Results

DNA mutation can be measured by a variety of analytical techniques, which have their own advantages and drawbacks [9]. Most of these techniques scan for mutations within a region of the gene of interest. If mutations are found, the specific region involved can be sequenced. Alternatively, if hotspot regions for mutations are known and are not overly large, direct DNA sequencing may be used. A drawback for direct sequence analysis is its lack of sensitivity in detecting mixtures of wild type and mutant DNA (approximately 20% for automated fluorescent sequencing) and the presence of mutations spanning large regions of a gene. Two commonly used scanning techniques were used to search for DNA mutations within the hot spot regions of the TP53 gene: CE-SSCP and DHPLC analysis. NIST internal calibration standards were used to confirm analytical validity of the two systems. Fig. 1 is a representative picture of the results obtained in screening exons 5 and 6 of the TP53 gene using either CE-SSCP or DHPLC technology.

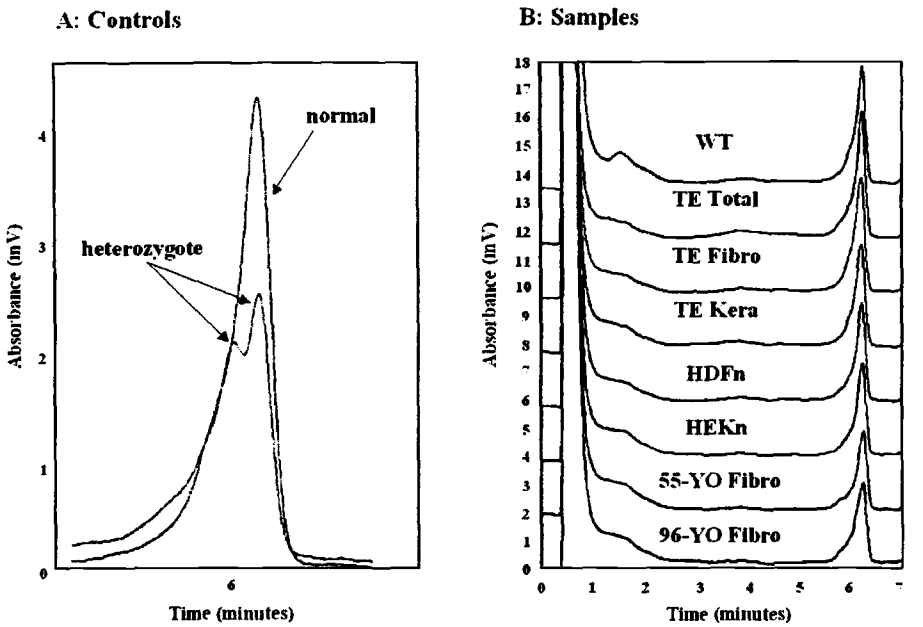

FIG. 1 — *Mutational analysis of TP53 exon 6 using DHPLC technology. WT is wild type p53, exon 6 control from NIST TP53 Standard Reference Material (in development); TE Total is TestSkin II keratinocyte DNA and fibroblast DNA combined into one sample material; TE Fibro is TestSkin II fibroblast DNA; TE Kera is TestSkin II keratinocyte DNA; HDFn is human dermal fibroblast neonatal control DNA; HEKn is human epidermal keratinocyte neonatal DNA; 55-YO is fibroblast DNA from fibroblast cells obtained from a 55-YO donor; 96-YO is fibroblast DNA obtained from a 96-YO donor.*

Specifically, Fig. 1 displays the results for mutational analysis of the TP53 exon 6 using DHPLC technology. Results indicate that mutations were not detected in either exon 5 or 6 of this gene in the tissue-engineered material. Mutations were also not detected in the DNAs from the control cells (normal neonatal keratinocyte and fibroblast primary cells), including that obtained from the 55-YO and 96-YO human donors.

To determine if the cells comprising the tissue-engineered skin material had undergone chromosome damage, loss of the Y-chromosome was measured. For background levels, the rates of Y-chromosome loss were estimated in control and aged fibroblasts (Table 1).

	% Cells with Y chromosome detected by FISH	Cells Scored
Age-Dependent Exp.		
Control PBL	100%	158
96-YO fibroblasts	92%	245
Tissue Culture Exp.		
Control PBL	100%	216
HDFn	100%	176
HEKn	100%	128
TestSkin II Exp.		
Control PBL	100%	150
TE Skin fibroblasts	100%	214
TE Skin keratinocytes	100%	160

Table 1 — *Y-Chromosome in Peripheral Blood Cultures, Fibroblasts and TE samples. Control PBL is peripheral blood lymphocyte cells; 96-YO fibroblasts is fibroblast cells obtained from a 96-YO donor; HDFn is human dermal fibroblast neonatal control cells; HEKn is human epidermal keratinocyte neonatal control cells; TE Skin fibroblasts is fibroblast cells obtained from TestSkin II; TE Skin keratinocytes is keratinocyte cells obtained from TestSkin II.*

In neonatal fibroblast cells, neonatal keratinocyte cells, and lymphocyte controls (peripheral blood), no loss of the Y-chromosome was detected. Y-chromosome loss in fibroblasts from the 96-YO donor was detected at a rate of 8%. No loss of the Y-chromosome was detected in the cells from the tissue-engineered skin material.

The National Institute of Standards and Technology is making a concerted effort to identify cellular biomarkers for the field of tissue-engineered medical products. These studies can provide the basis for an international reference standard of cellular biomarkers that can aid in the development and safety of tissue-engineered medical products.

References

[1] Hussain, S. P., Hofseth, L. J., and Harris, C. C., "Tumor suppressor genes: at the crossroads of molecular carcinogenesis, molecular epidemiology and human risk assessment," *Lung Cancer*, Vol. 34, Suppl. 2, 2001, pp. S7-15.

[2] Whittaker, S., "Molecular genetics of cutaneous lymphomas," *Annals of the New York Academy of Sciences*, Vol. 941, 2001, pp. 39-45.

[3] Stone, J. F. and Sandberg, A. A., "Sex chromosome aneuploidy and aging," *Mutation Research*, Vol. 338, 1995, pp. 107-113.

[4] O'Connell, C. D., Tian, J., Juhasz, A., Wenz, H. M., and Atha, D. H., "Development of standard reference materials for diagnosis of p53 mutations: analysis by slab gel

single strand conformation polymorphism," *Electrophoresis*, Vol. 19, 1998, pp. 164-171.

[5] Atha, D. H., Wenz, H. M., Morehead, H., Tian, J., and O'Connell, C. D., "Detection of p53 point mutations by single strand conformation polymorphism: analysis by capillary electrophoresis," *Electrophoresis*, Vol. 19, 1998, pp. 172-179.

[6] Keller, G., Hartmann, A., Mueller, J., and Hofler, H., "Denaturing high pressure liquid chromatography (DHPLC) for the analysis of somatic p53 mutations," *Laboratory Investigation,* Vol. 81, 2001, pp. 1735-1737.

[7] Barch, M. J., Knutsen, T., and Spurbeck, J. L., 1997, *The AGT Cytogenetics Laboratory Manual*, Lippincott-Raven Publishing, New York.

[8] Barker, P. E. and Schwab, M., "Junction mapping of translocation chromosomes by fluorescence *in situ* hybridization (FISH) and computer image analysis in human solid tumors," *Methods in Molecular Genetics*, Vol. 2, 1993, pp. 129-154.

[9] Cotton, R. G., "Methods in clinical molecular genetics," *European Journal of Pediatrics*, Vol. 159, 2000, pp. S179-S182.

Toshie Tsuchiya[1]

A Useful Marker for Evaluating the Safety and Efficacy of Tissue Engineered Products

Reference: Tsuchiya, T., **"A Useful Marker for Evaluating the Safety and Efficacy of Tissue Engineered Products,"** *Tissue Engineered Medical Products (TEMPS), ASTM STP 1452*, E. Schutte, G. L. Picciolo, and D. S. Kaplan, Eds., ASTM International, West Conshohocken, PA, 2004.

Abstract: We propose a survey of the function of the gap-junctional intercellular communication (GJIC) as a useful marker for evaluating the safety and efficacy of tissue-engineered products.

Keywords: Gap junction, Connexin43, normal human dermal fibroblast, bFGF, KGF, cell differentiation, tumor promotion.

Introduction

An in vitro system for evaluating the safety of tissue engineered products is convenient because of its rapidity and low cost consumption. On the basis of recent studies, intercellular channels called gap-junctions are considered to play an important role on the tumor-promotion stage during the tumorigenesis induced by biomaterials [1]. We demonstrate the significance of the intercellular communication during the neuronal cell differentiation and cytokine productions. From these results, we propose a survey of the function of the gap-junctional communication as a potentially useful marker for evaluating the safety and efficacy of tissue engineered products.

Increase in Gap-Junctional Intercellular Communications (GJIC) of Normal Human Dermal Fibroblasts (NHDF) on Surfaces Coated with High-Molecular-Weight Hyaluronic Acid

Normal cells and tissues have functional gap-junctions. Gap-junction are hydrophilic intercellular channels that allow intercellular passage of small molecules (up to 1 kDa). They are constructed from connexin proteins that form structures called connexons. Moreover, many substances, such as ions, sugars, nucleotides, amino acids, drugs, carcinogens, and so on, are small enough to move between cells though gap-junction channels. Gap junctions are important for coordinating the activities of electrically active cells, and they are thought to play many regulatory roles, such as growth control, developmental and differentiation processes, synchronization, and metabolic regulation. The aim of the study was to clarify the effect of hyaluronic acid (HA) on intercellular communication *via* gap junction.
Many investigators have demonstrated increases in cell migration, invasion, and

[1] Director, Division of Medical Devices, National Institute of Health Sciences, Kamiyoga 1-18-1, Setagaya-ku, Tokyo 158-8501, Japan.

proliferation by exposure to HA. It also has been reported [2] that HA in collagen gel culture enhances the proliferation and chondroitin 6-sulfate synthesis of chondrocytes while maintaining their phenotype. HA is involved in these process *via* cell-surface receptors, such as the receptor for HA-mediated motility (RHAMM) and CD44 glycoproteins [3]. Additionally, cellular behaviors such as adhesion, differentiation, and proliferation are greatly affected by surface properties such as receptor-ligand binding, hydrophilicity, roughness, charge, and morphology of the materials.

In this study, safety evaluation for HA was investigated using NHDF cells, which are known to express CD44 glycoproteins on their surface.

Normal human dermal fibroblast (NHDF) cells were used to detect differences in gap-junctional intercellular communication (GJIC) by hyaluronic acid (HA). HA is a linear polymer built from repeating disaccharide units that consists of N-acetyl-D-glucosamine and D-glucuronic acid linked by a β 1-4 glycosidic acid. The NHDF cells were cultured with different molecular weights (MW) of HA for four days. The rate of cell attachment in dishes coated with high-molecular-weight (HMW; 310 kDa or 800 kDa) HA at 2mg/dish were significantly reduced at an early time point compared with low-molecular-weight (LMW; 4.8 kDa or 48 kDa) HA with the same coating amounts. HA-coated surfaces were observed by atomic force microscopy (AFM) under air and showed that HA molecules ran parallel in the dish coated with LMW HA and had an aggregated island structure in the dish coated with HMW HA surfaces. The cell functions of GJIC were assayed by a scrape-loading dye transfer (SLDT) method using a dye solution of Lucifer yellow. Promotion of the dye transfer was clearly obtained in the cell monolayer grown on the surface coated with HMW HA. These results suggest that HMW HA promotes the function of GJIC in NHDF cells. In contrast, when HMW HA was added to the monolayer of NHDF cells, the functions of GJIC clearly were lowered in comparison with the cells grown in the control dish or with those grown on the surface of HMW HA. LMW HA showed tumor-promoting activities in two-stage Balb 3T3 cell transformation assay [4]. Therefore it is suggested that the MW size of HA and its application method may be important factors for generating biocompatible tissue-engineered products because of the manner in which the GJIC participates in cell differentiation and cell growth rate.

In this study [5], the cell adhesion and cell function of GJIC were compared on dishes treated with various molecular weights of HA. The extent of attachment of NHDF cells on the HA-coated surfaces decreased linearly proportional to the MW size of HA at an early time point in the culture.

The SLDT method was used to study the effects of HA on the GJIC of NHDF cells. The results indicate that NHDF cells on dishes coated with HA of HMW (800 kDa) promote GJIC. However, the addition of HMW HA showed the opposite effect. Nutrients that promote the formation of the gap junction, such as bFGF, EGF, and TGF-β, could be enveloped in the molecule of the coated HMW HA. In the case either of addition or coating of LMW HA, the inhibitory effect of gap formation was not observed. In conclusion, it is suggested that the selection of the MW of HA is an important factor in designing biocompatible artificial skins that retain and enhance the function of GJIC in NHDF cells.

Increase in Gap-Junctional Intercellular Communication (GJIC) by High Molecular Weight Hyaluronic Acid Associated with Fibroblast Growth Factor 2 and Keratinocyte Growth Factor Production in Normal Human Dermal Fibroblasts

Most normal cells within tissues have functional gap-junctional intercellular communication (GJIC).

The importance of GJIC makes it desirable to estimate gap-junction channel function by a rapid and reliable quantitative method. The scrape-loading dye transfer (SLDT) method [6], involving use of the fluorescent dye Lucifer yellow and published [6] as a rapid and relatively uncomplicated method for measuring intercellular communication, has by now become a routine assay for analyzing the effects of various reagents on GJIC.

Hyaluronic acid (HA) is a negatively charged glycosaminoglycan composed of repeated disaccarides of D-glucuronic acid and N-acetylglucosamine and is found in most types of extracellular in the mammalian body. By interaction with other matrix molecules, HA provides stability and elasticity to the extracellular matrix. HA has been implicated in biological processes such as cell adhesion and proliferation. HA-binding proteins such as CD44, and aggrecan, and versican have been implicated in structuring the extracellular matrix (ECM) by stabilizing large macromolecular aggregates. More importantly, it was suggested that the receptor for HA-mediated motility (RHAMM) regulates gap junction channel and connexin43 expression, possibly through its actions on focal adhesions and the associated cytoskeleton [7]. It also reported that HA can both promote [8] or inhibit cytokine expression depending on its molecular mass [9].

Fibroblast growth factors (FGFs) play multiple roles during development and in adult tissues as paracrine regulators of growth and differentiation. Furthermore, it was reported that stimulation of neurite growth correlated strongly with the amount of FGF-2 bound to surfaces coated with heparin, heparan sulfate, or HA [10]. Keratinocyte growth factor (KGF) is a member of the FGF family and is expressed almost exclusively by stromal cells from a variety of tissues, including the lung, skin, mammary gland, and prostate. KGF in vivo is a member of the heparin-binding FGF family and is a paracrine mediator of proliferation and differentiation of a wide variety of epithelial cells. KGF has also been shown to cause angiogenesis and repair after major damage.

The aim of the study was to explore the relationship between gap junction channel function and production of growth factors [8]. We investigate the effect of LMW HA and HMW HA on FGF-2 and KGF expression by NHDF cells in vitro, and gap-junctional channel function as estimated by the SLDT method, simultaneously.

The effects of different molecular weights of hyaluronic acid (HA), a major component of extracellular matrix, on gap-junctional intercellular communication (GJIC) in normal human dermal fibroblasts (NHDF cells) were investigated. NHDF cells were cultured for four days with different fibroblasts molecular weights of HA and then the extent of GJIC was assessed by the scrape-loading dye transfer method, using Lucifer yellow. The area of dye transfer [8], a quantitative indicator more than the dye migration distance [4,6], was greater in the dishes coated with HA than in those to which HA was added. Thus, NHDF cells cultured on surface coated with high molecular weight (HMW) HA (MW, 800 kDa) showed greatly enhanced GJIC.

Furthermore, another aim of this study was to evaluate the effects of different molecular weights of HA on the production of FGF-2 and KGF because both are important cytokines produced by NHDF cells. When FGF-2 and KGF cultured levels of cell extracts and media were determined by ELIZA, both levels were significantly enhanced when cells were grown on plates coated with HMW HA. This finding indicated that the function of gap-junction channels in NHDF cells grown on plates coated with HMW HA may promote the biosynthesis of growth factors such as FGF-2 and KGF [8].

A Useful Marker for Evaluating Tissue-Engineered Products: Gap-Junctional Communication for Assessment of the Tumor Promoting Action and Disruption of Cell Differentiation in Tissue Engineered Products

Disruption of gap-junctional communication has been implicated in tumor promotion as well as abnormal development. Tumor promoting chemicals, such as phorbolesters, have been reported to inhibit gap-junctional intercellular communication in vitro and in vivo. It has been assumed that tumor promoters induce suppression of initial cells from surrounding communicating normal cells, resulting in a clonal expansion of the initiated cells.

Many tumor cells exhibit aberrant cell contact-mediated intercellular communication, i.e., loss of gap-junctional communication among themselves or with surrounding normal cells. In tissue engineering areas, various kinds of chemicals and metallic ions are used as scaffolds and catalysts. One of the representative degradable materials is polylactic acid, which has been widely used in biomaterials. However, the tumorigenicity of poly-L-lactide (PLLA) film was reported via a rat two-year-implantation study [11]. PLLA has been applied in surgical devices, such as a bone plates, pins, and screw, for which a longer duration of mechanical toughness is required and supported by a slow degradation of high molecular weights of PLLA. Usually, it takes several years for the complete absorption of such kinds of PLLA into the tissues. However, the mechanisms of PLLA tumorigenicity in rats are unclear. We investigated the effects of poly-D, L-lactic acid (PDLA, MW. 5000), a commercial product and its monomers of L- and D-lactic acid on the gap-junctional intercellular communication (GJIC). GJIC is considered to be important in the neuronal functions, because neurons have the equipment of connexins, and germ-line mutations of the Cx32 gene have been reported to be responsible for X-linked Charcot-Marie-Tooth disease of the peripheral nervous system. Therefore, the effects of neuronal toxic metal ions such as Cd^{5+}, V^{5+}, and Zn^{2+} ions were surveyed using two assay systems, namely, rat neuronal cell differentiation and V79 metabolic cooperation to clarify the inhibitory action of these ions on the GJIC of rat midbrain cells and V79 cells, both cells have gap-junctions composed of connexin 43 (Cx43). Whether the connexins play an important role in neuronal cell differentiation or not, three kinds of metal ions were assayed and compared with its inhibitory potentials between cell differentiation and metabolic cooperation.

Metabolic cooperation is a form of intercellular communication in which the mutant phenotype of enzyme-deficient cells is corrected by normal cells or by different mutant cells. Thus, wild-type Chinese hamster V79 cells (6-thioguanin-sensitive (6-TGs)) reduce the recovery of 6-thioguanine-resistant cells (6-TGr) when they are cultured together at high densities through intercellular

communication (metabolic cooperation). Cooperation is inhibited by 12-O-tetradecanoyl phorbol-13-acetate (TPA) rescuing the 6-thioguanine-resistance cells. These results may be useful in the study of an aspect of the mechanism of tumor-promotion and in assaying for promoters.

Three metal ions induced inhibitory action on embryonic midbrain differentiation, and the disruption of the cell-cell communication by these metal ions possibly led to the inhibition of the differentiation of the midbrain cells. Next, some polymers and their oligomers used in the tissue engineering field have inhibitory activities on GJIC. One cause may be related to the different manufacturing process using various kinds of metallic catalysts. From the present results, the in vitro short-term test for estimating the function of GJIC is important and useful for the safety of tissue-engineered products, especially with regard to dedifferentiation [10].

A Strategy for the Suppression of Tumorigenesis Induced by Biomaterials: Restoration of Transformed Phenotype of Polyetherurethane-Induced Tumor Cells by Cx43 Transfection

Polyetherurethanes (PEUs) are used for implant applications because of their useful elastomeric properties and high tensile strength, lubricity, good abrasion resistance, and ease of handling. However, some kinds of PEUs are known to be unstable in the body and can induce tumors in rats. We have reported the tumorigenic potentials of these PEUs in vivo and in vitro [13]. For many years, foreign body carcinogenesis in rodent species has been recognized as a classic model of multistage endogenous tumorigenesis that requires half to two-thirds of the life span for tumor development. A number of studies have demonstrated that physical, not chemical, characteristics are responsible for this phenomenon and that a dose-dependent relationship is evident with respect to implant size and tumor frequency [14]. We have examined the potency of tumor-initiating and tumor-promoting activities of the PEUs. The promoting activities were considered to be stronger than the initiating activities [15]. Furthermore, inhibitory action of polyethylene's surface on gap-junctional intercellular communication (GJIC) has been detected [16,17]. Thus, different inhibitory potential of GJIC on the surface of the biomaterials, including PEUs, may likely be a key step in determining the tumorigenic potentials. PEU-components had inhibited GJIC in cultures of Balb/c 3T3 A31-1-1 cells and Chinese V79 fibroblasts. GJIC has long been postulated to play an important role in the maintenance of cell homeostasis and in the control of cell growth. Therefore, the loss of GJIC has been considered to cause aberrant development and tumor formation. Gap- junctions are formed by jux taposition of two hemichannels known as connexons, located on the surface of adjacent cells [18]. Each connexon consists of six connexin (Cx) molecules. Cx43 is the most widely expressed Cx type. Accumulating evidence indicates that loss or reduction of GJIC in malignant transformed cells or tumor cells closely correlates to transcriptional down-regulation of Cx genes and /or to aberrant localization of Cx proteins. Restoration of GJIC by transfection of Cx genes has been demonstrated to reverse the transformed phenotype of cancer cells [19].

To clarify a tumor promoting activity of PEU, we have established an U41 rat tumor cell line from malignant fibrous histiocytoma (MFHC) developed in the PEU film implanted sites. Function of GJIC in our cell line was assayed by the scrape-loading dye transfer method and the expression of Cx43 connexin was

examined either by western blotting or by reverse transcription-PCR (RT-PCR). Since the introduction of Cx43 gene overcame the GJIC function, poor GJIC development in U41 cells might be caused by a suppressed connexin expression. The Cx43 up-regulated stable transfectant showed rather controlled cell growth on contact inhibition, and revealed poor anchorage independent growth in soft agar [20].

Biomaterials such as polyetherurethanes (PEUs) are the scaffolding, which is indispensable for the development of the bio-artificial organs. However, PEUs can induce tumors in subcutaneous implantation sites in rats. We have shown that the different inhibitory potential of gap-junctional intercellular communication (GJIC) on the surface of the biomaterial, including PEUs, is a key step in determining the tumorigenic potentiality. Here we show that suppression of a gap-junctional protein connexin 43 (Cx43) plays an important role *in vivo* tumorigenesis induced by PEUs for the first time and that Cx43 transfection may be an effective strategy for preventing tumorigenesis induced by biomaterials [20]. The rat tumor cell line U41 is derived from tumors in the subcutaneous implantation of PEU films. The GJIC and the expression of Cx43 were suppressed in U41. The restoration of normal phenotype, such as reduction of growth rate, recovery of contact inhibition and loss of colony formation ability in soft agar, was achieved by Cx43 transfection. These results strongly suggest that suppression of Cx43 expression plays an important role in the development of rat malignant fibrous hisitiocytome (MFHC) caused by PEUs and that Cx43 transfection is effective for prevention of tumorigenesis induced by PEUs [20].

References

[1] Tsuchiya, T., and Nakamura, A., "A New Hypothesis of Tumorigenesis Induced by Biomaterials: Inhibitory Potentials of Intercellular Communication Play An Important Role on the Tumor-Promotion Stage," *J. Long. Term. Effects Med. Implants*, Vol. 5, 1995, pp.233-242.

[2] Kawasaki, K., Ochi, M., Uchio, Y., Adachi, N., and Matsusaki, M., "Hyaluronic Acid Enhances Proliferation and Chondroitin Sulfate Synthesis in Cultured Chondrocytes Embedded in Collagen Gels," *J Cell Physiol*, Vol. 179, 1999, pp. 142-148.

[3] Alaish, S. M., Yager, D. R., Diegelmann, R. F., and Cohen, I. K., "Hyaluronic Acid Metabolism in Keloid Fibroblasts," *J Pediatric Surg*, Vol. 30, 1995, pp. 949-952.

[4] Park, J., and Tsuchiya, T., "Tumor-Promoting Actibity of 48 kDa Molecular Mass Hyaluronic Acid," *Materials Transactions*, Vol. 43, 2002, pp. 3128-3130.

[5] Park, J. U., and Tsuchiya, T., "Increase in Gap-Junctional Intercellular Communications (GJIC) of Normal Human Dermal Fibroblasts (NHDF) on Surfaces Coated with High-Molecular-Weight Hyaluronic Acid (HMW HA)," *J Biomed Mater Res*, Vol. 60(4), 2002 pp.541-547.

[6] Trosko, J. E., Madhukar, B. V., and Chang, C. C., "Endogenous and Exogenous Modulation of Gap Junctional Intercellular communication: Toxicological and Pharmacological Implication," *Life Sci*,Vol. 53(1), 1993, pp. 1-19.

[7] Nagy, J. I., Hossain, M. Z., Lynn, B.D., Curpen, G. E., Yang S., and Turley, E. A., "Increased Connexin-43 and Gap junctional Communication Correlate

with Altered Phenotypic Characteristics of Cells Overexpressing the Receptor for Hyaluronic Acid-Mediated Motility," *Cell Growth Differ.*, Vol. 7(6), 1996, pp. 745-751.

[8] Park, J.U., and Tsuchiya, T., "Increase in Gap Junctional Intercellular Communication by High Molecular Weight Hyaluronic Acid Associated with Fibroblast Growth Factor 2 and Keratinocyte Growth Factor Production in Noemal Human Dermal Fibroblasts," *Tissue Engineering*. Vol. 8 No. 3, 2002, pp. 419-427.

[9] Neumann, A., Schinzel, R., Riederer, P. D., and Munch, G., "High Molecular Weight Hyaluronic Acid Inhibits Advanced Glycation End Product-Induced NF-kappaB Activation and Cytokine Expression," *FEBS Lett,* Vol. 25, 453(3), 1999, pp. 283-287.

[10] Walicke, P.A., "Interactions between Basic Fibroblast Growth Factor (FGF) and Glycosoaminoglycans in Promoting Neurite Outgrowth," *Exp Neurol*, Vol. 102(1), 1988, pp.144-8.

[11] Nakamura, T., Shimizu, Y., Okumura, N., Matsui, T., Hyon, S. H., and Shimamoto, T., "Tumorigenicity of Poly-L-lactide (PLLA) Plates Compared with Medical-Grade Polyethylene," *J Biomed Mater Res*, Vol. 28(1), 1994, pp.17-25.

[12] Tsuchiya, T., "A Useful Marker for Evaluating Tissue-Engineered Products: Gap-Junctional Communication for Assessment of the Tumor-Promoting Action and Disruption of Cell Differentiation in Tissue-Engineered Products," *J Biomater Sci Polym Ed*, Vol. 11(9), 2000, pp. 947-959.

[13] Tsuchiya, T., Hata, H., and Nakamura, A., "Studies on the Tumor-Promoting Activity of Biomaterials: Inhibition of Metabolic Cooperation by Polyetherurethane and Silicone," *J Biomed Mater Res*, Vol. 29(1), 1995, pp. 113-119.

[14] Schoen, F. J., "Biomaterial-Associated Infection, Neoplasia, and Calcification Clinicopathologic Features and Pathophysiologic concepts." *ASAIO Trans*, Vol. 33(1), 1987, pp. 8-18.

[15] Tsuchiya, T., Nakaoka, R., Degawa, H., and Nakamura, A., "Studies on the Mechanisms of Tumorigenesis Induced by Polyetherurethanes in Rats: Leachable and Biodegradable Oligomers Involving the Diphenyl Carbamate Structure Acted as an Initiator on the Transformation of Balb 3T3 Cells," *J Biomed Mater Res*, Vol. 31(3), 1996, pp.299-303.

[16] Nakaoka, R., Tsuchiya, T., Kato, K., Ikada, Y., and Nakamura, A., "Studies on Tumor-Promoting Activity of Polyethylene: Inhibitory Activity of Metabolic Cooperation on Polyethylene Surfaces is Markedly Decreased by Surface Modification with Collagen but not with RGDS Peptide," *J Biomed Mater Res*, Vol. 35(3), 1997, pp.391-397.

[17] Nakaoka, R., Tsuchiya, T., and Nakamura, A., "The Inhibitory Mechanism of Gap Junctional Intercellular Communication Induced by Polyethylene and the Restorative Effects by Surface Modification with Various Proteins," *J Biomed Mater Res*, Vol. 57(4), 2001, pp.567-574.

[18] Bennett, M. V., Barrio, L. C., Bargiello, T. A., Spray, D. C., Hertzberg, E., and Saez, J. C., "Gap Junctions: New Tools, New Answers, New Questions," *Neuron*, Vol. 6(3), 1991, pp.305-320.

[19] Huang, R. P., Fan, Y., Hossain, M. Z., Peng, A., Zeng, Z. L., and

Boynton, A. L., "Reversion of the Neoplastic Phenotype of Human Glioblastoma Cells by Connexin 43 (cx43),"*Cancer Res*, Vol. 58(22), 1998, pp.5089-5096.

[20] Ichikawa, A., and Tsuchiya, T., "A Strategy for the Suppression of Tumorigenesis Induced by Biomaterials: Restoration of Transformed Phenotype of Polyetherurethane-Induced Tumor Cells by Cx43 Transfection," *Cytotechnology*, Vol. 39, 2002, pp.1-8.

Author Index

Subject Index